I. NADPH REGENERATION SOURCES IN NON-GROWING, ENGINEERED *ESCHERICHIA COLI* CELLS
II. EVALUATION OF OLD AND NEW ALKENE REDUCTASES AS POTENTIAL BIOCATALYSTS

By

DESPINA BOUGIOUKOU

A DISSERTATION PRESENTED TO THE GRADUATE SCHOOL
OF THE UNIVERSITY OF FLORIDA IN PARTIAL FULFILLMENT
OF THE REQUIREMENTS FOR THE DEGREE OF
DOCTOR OF PHILOSOPHY

UNIVERSITY OF FLORIDA

2006

To my loving parents: Έμμα and Γιάννη.

TABLE OF CONTENTS

LIST OF TABLES

LIST OF FIGURES

Abstract of Dissertation Presented to the Graduate School
of the University of Florida in Partial Fulfillment of the
Requirements for the Degree of Doctor of Philosophy

I. NADPH REGENERATION SOURCES IN NON-GROWING, ENGINEERED *ESCHERICHIA COLI* CELLS
II. EVALUATION OF OLD AND NEW ALKENE REDUCTASES AS POTENTIAL BIOCATALYSTS

By

Despina Bougioukou
December 2006

Chair: Jon D. Stewart
Major Department: Chemistry

In the first part of this dissertation, an effort was made to define the pathways by which the NADPH is regenerated in *E. coli* cells under non-growing conditions. We used the reduction of ethyl acetoacetate by a *Saccharomyces cerevisiae* reductase (Gre2) overexpressed in *E. coli* as a model system and specifically deuterated glucose (C_1-d_1, C_3-d_1 or C_6-d_2) as isotopomer carbohydrate sources. Deuterium atoms originating at C_1, C_3 or C_6 of glucose are first transferred to $NADP^+$ and then appeared at the C_3 atom of ethyl-3-hydroxybutyrate, allowing us to measure the isotopic composition of the intracellular NADPH pool by GC/MS. In addition, we perturbed the NADP($H/^+$) levels of the host cell by environmental and genetic manipulation means and evaluated the effects of those perturbations on the productivity of the system under study. Our data showed that the NADPH sources present in *E. coli* cells under growing conditions are also active in non-dividing cells and most likely are not the limited factor for the maximum productivity of this particular biotransformation.

In the second part, a set of 15 genes encoding known and putative alkene reductases were successfully cloned by a rapid recombination technique and overexpressed as GST-fused proteins in *E. coli.* Their ability to reduce ca. 40 simple enones and enals was evaluated. This study uncovered subtle differences in substrate specificity among the distinct en-reductase subfamilies, as well as the function of a previously uncharacterized in *S. cerevisiae* gene product.

CHAPTER 1
UNCOVERING THE NADPH REGENERATION PATHWAYS IN ESCHERICHIA COLI: TOOLS AND METHODOLOGIES

If you're converting carbohydrate into triglyceride,
If you need pentose moieties to make nucleotide,
You'll find that Embden-Meyerhof is not the game to play
And you'll do your biosynthesis the pentose phosphate way
-The Pentose Phosphate Shunt Song, Author unknown[1]

Introduction

The reduced form of nicotinamide adenine dinucleotide phosphate, NADPH, plays a central role in fueling biosynthetic reactions and maintaining the redox potential necessary to protect cells against oxidative stress.[2] A careful inspection in the model-organism database for *Escherichia coli* K-12 (EcoCyc, version 10.0)[3] reveals five potential routes for NADPH formation. The exact location of each in the carbon central metabolism of *E. coli* is depicted in Figure 1-1. The pentose phosphate pathway (PP pathway) provides NADPH in two reactions catalyzed by glucose-6-phosphate dehydrogenase (zwf) and gluconate-6-phosphate dehydrogenase (gnd) respectively (Figure 1-2A); the tricarboxylic acid cycle (TCA) produces NADPH to a lesser extent by isocitrate dehydrogenase (icd, Figure 1-2B). In addition, an anaplerotic reaction catalyzed by the malate dehydrogenase (maeB, Figure 1-2C), as well as the membrane-bound pyridine nucleotide transhydrogenase (pntAB, Figure 1-2D), could serve as catalysts for the regeneration of NADPH. Even though the Embden-Meyerhof-Parnas (EMP) pathway is not directly involved in the NADPH synthesis, the branching points which connect it with the aforementioned pathways are of fundamental importance for control of NAPDH production. The efforts that have been made the last six decades

towards the identification and estimation of the partition of each NADPH-producing step to the overall NADPH pool in *E. coli* will be described.

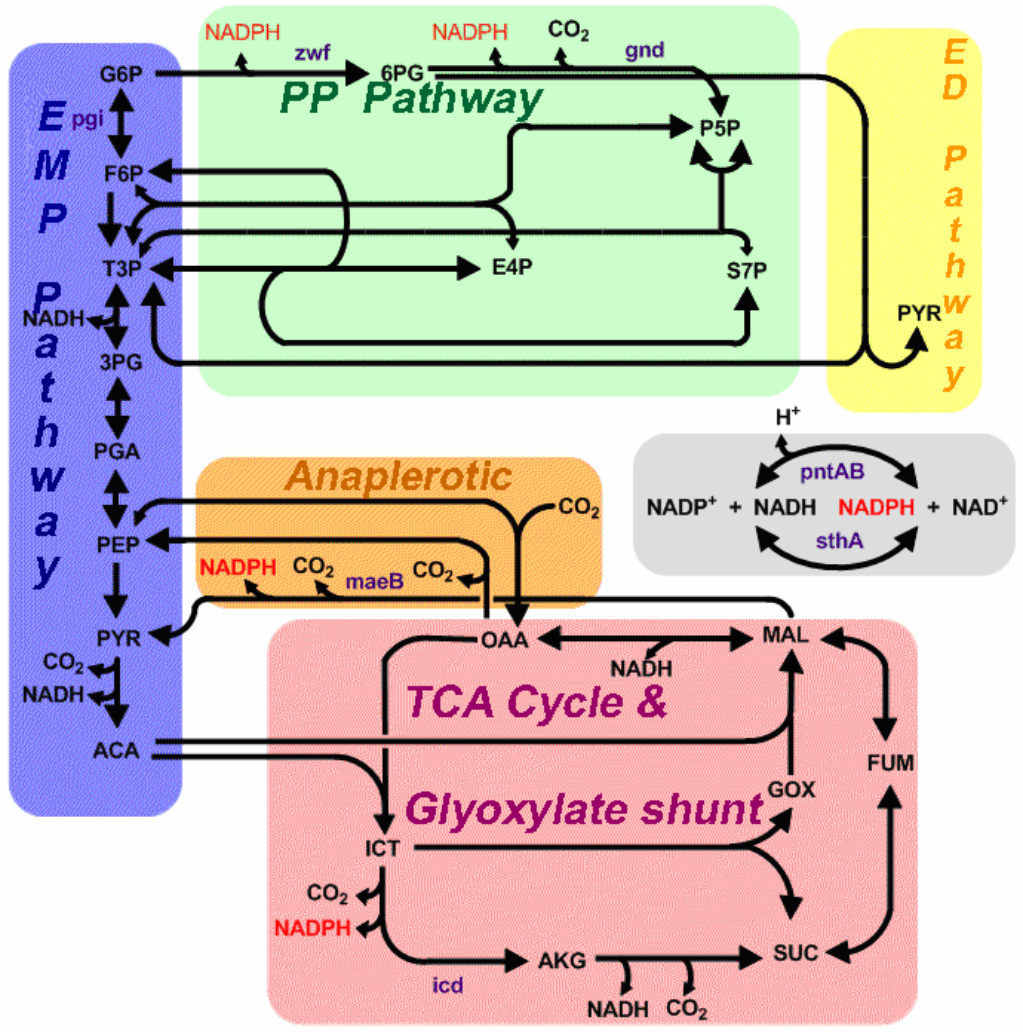

Figure 1-1. Overview of central metabolic pathways involved in NADPH formation in *E. coli*. Enzymes are indicated by their 3-letter code. Abbreviations: G6P, glucose-6-phosphate dehydrogenase; F6P, fructose-6-phosphate; 6PG, gluconate 6-phosphate; P5P, pentose 5-phosphate; E4P, erythrose 4-phosphate; S7P, sedoheptulose 7-phosphate; T3P, triose 3-phosphate; 3PG, glyceraldehyde 3-phosphate; PGA, 3-phosphoglycerate; PEP, phosphoenolpyruvate; PYR, pyruvate; ACA: acetyl coenzyme A; OAA, oxaloacetate; ICT, isocitrate; AKG, α-ketoglutarate; SUC, succinate; FUM, fumarate; MAL, malate; GOX, glyoxylate. Pgi, phosphogluconase isomerase; zwf, G6P dehydrogenase; gnd, 6PG, 6-phosphogluconate dehydrogenase; PntAB, membrane-bound transhydrogenase; sthA, soluble transhydrodenase; maeA, MAL dehydrogenase; icd, ICT dehydrogenase; PP pathway, pentose phosphate pathway; EMP, Embden-Meyerhof-Parnas pathway; ED pathway, Entner-Doudoroff pathway; TCA cycle, tricarboxylic acid cycle. (Adapted from references 60 and 50).

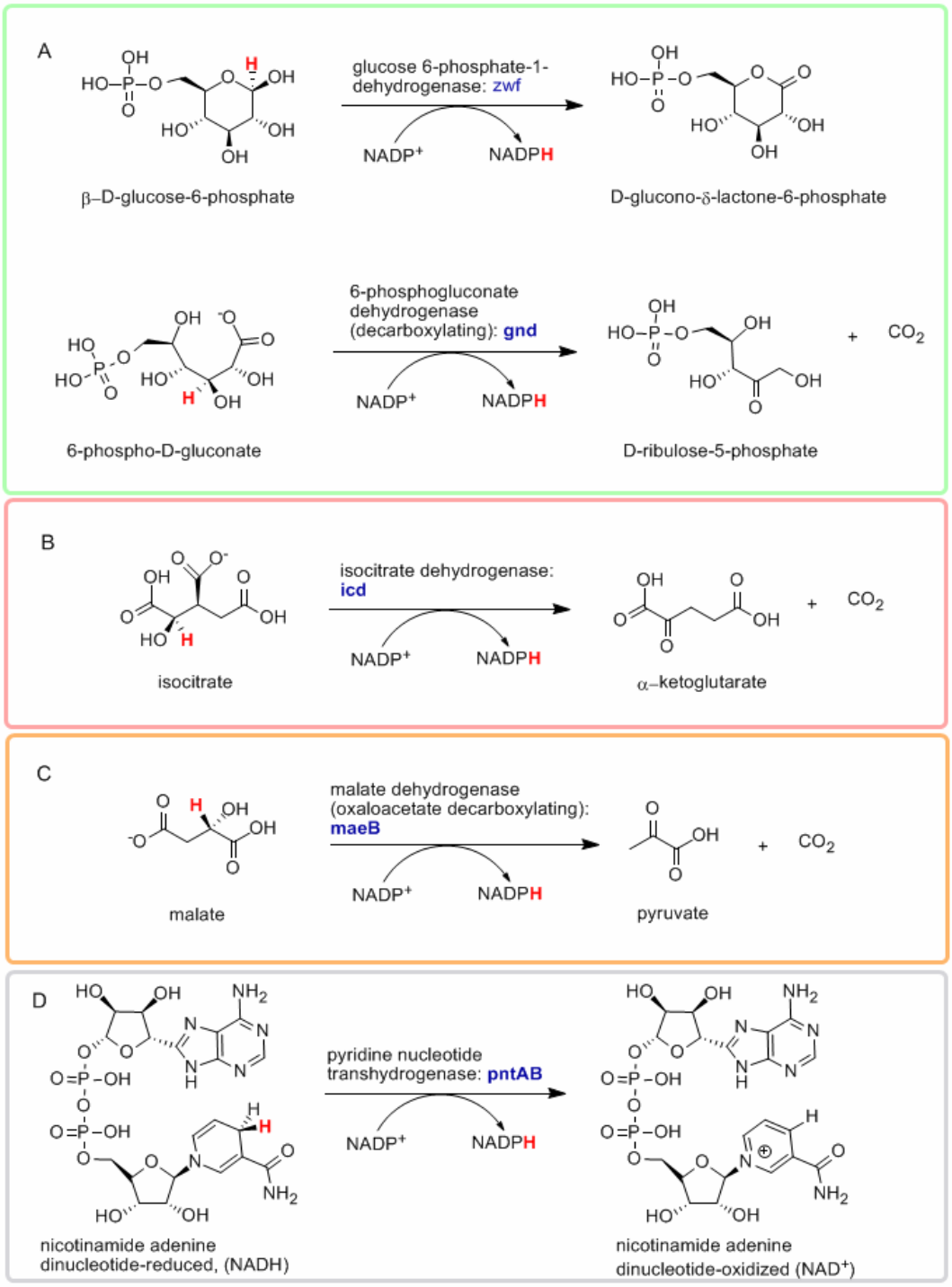

Figure 1-2. NADPH sources in *E. coli* metabolism. A) both Zwf and Gnd are belonging to the PPP, B) the Icd is a part of TCA cycle, C) MaeB participates in an anaplerotic reaction, and D) the PntAB catalyzes the reversible transfer of a hydride ion equivalent between NAD(H) and NADP(H).

The Past: Pentose Phosphate Pathway Partition

The PP pathway, also known as the hexose monophosphate shunt (HMS), can be considered as a metabolic scrambler for the cells. It is an alternative pathway for glucose metabolism that shunts some G6P away from the EMP glycolytic pathway (oxidative part) and returns parts of the diverted hexose carbons to the latter pathway as F6P and 3PG (non-oxidative part, Figure 1-3). The extent of the contribution of the PP pathway to glycolysis has been a subject of numerous investigations, as this pathway, among other functions, provides ribose-5-phosphate (R5P) which is needed for nucleic acid synthesis and reduces $NADP^+$ to NADPH, which is needed for amino acid and fatty acid synthesis as well as for the regeneration of glutathione, a key peptide in the antioxidant protection of the cells. In addition, recent studies[4] have shown that pathways involved in redox-metabolism also play an important role in biosynthesis of metabolites of industrial importance. Indeed, the knowledge of the PP pathway flux provides a basis for better understanding of the cell physiology and serves as a guide for directed improvements of performance of industrially exploited organisms.[5]

In classic isotope studies of metabolism, the fate of a label at a specific position of a substrate is 'traced' by examining the incorporation of the labeled atom into the end-products (e.g. CO_2) or intermediates (e.g. NADPH) of the investigated pathways. Different pathways, even though they utilize the same labeled substrate, produce end-products which are labeled at different positions and to different extents since distinct enzymes are participating in each of pathway. Thus, using the same substrate, in this particular case glucose, and labeling it at a different position (Figure 1-3 and Figure 1-4) each time, investigators estimated the percentage of glucose that is metabolized through the PP pathway. Their efforts are summarized in Table 1-1 and will be described in the following pages.

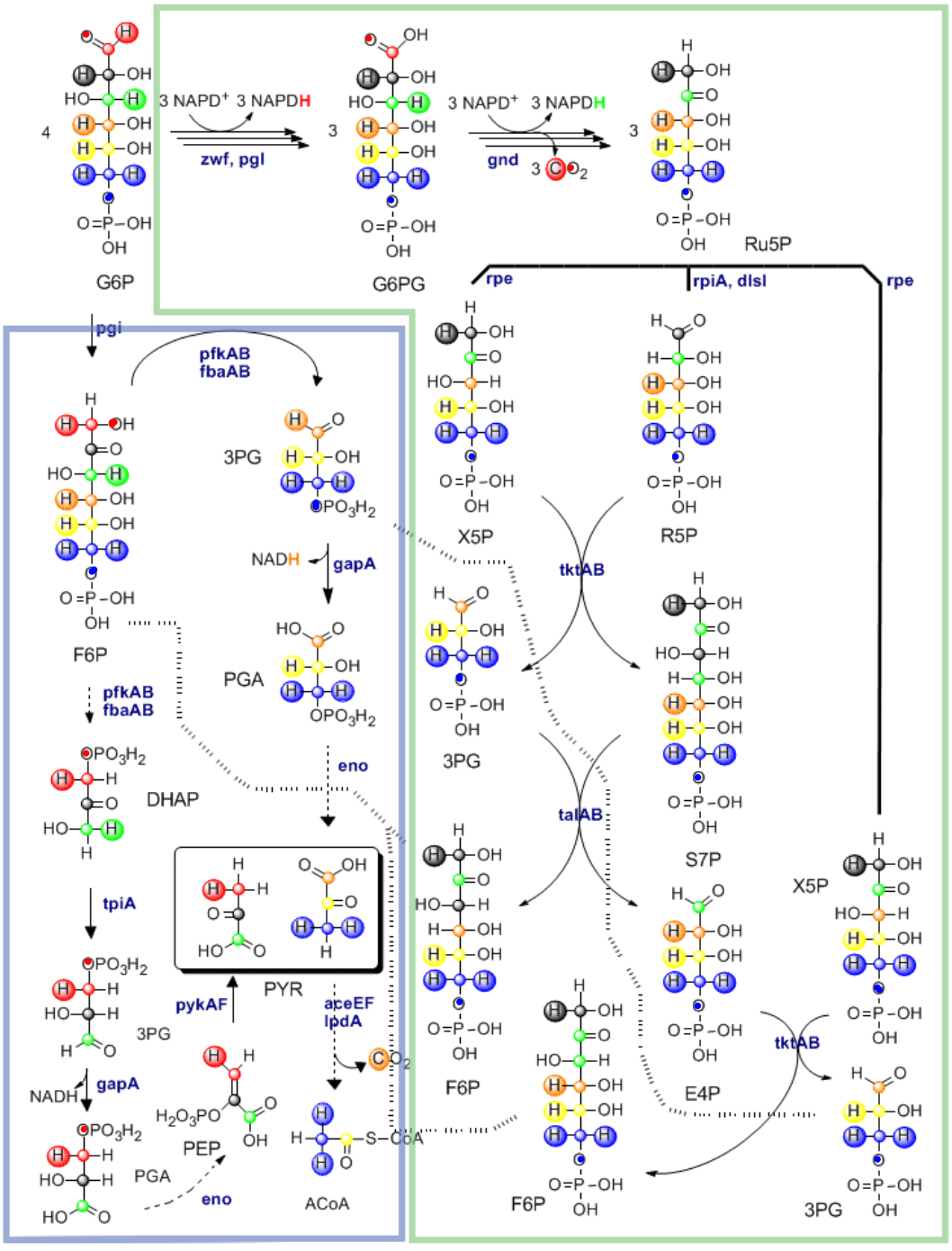

Figure 1-3. The fate of G6P, labeled in different positions, via EMP (blue frame) and PP (green frame) pathways. Enzymes are indicated by their 3-letter code. Dashed arrows indicate that more than one step is involved. Hashed lines indicate the branching points in between the two pathways (Adapted from references 2, 3 and 68)

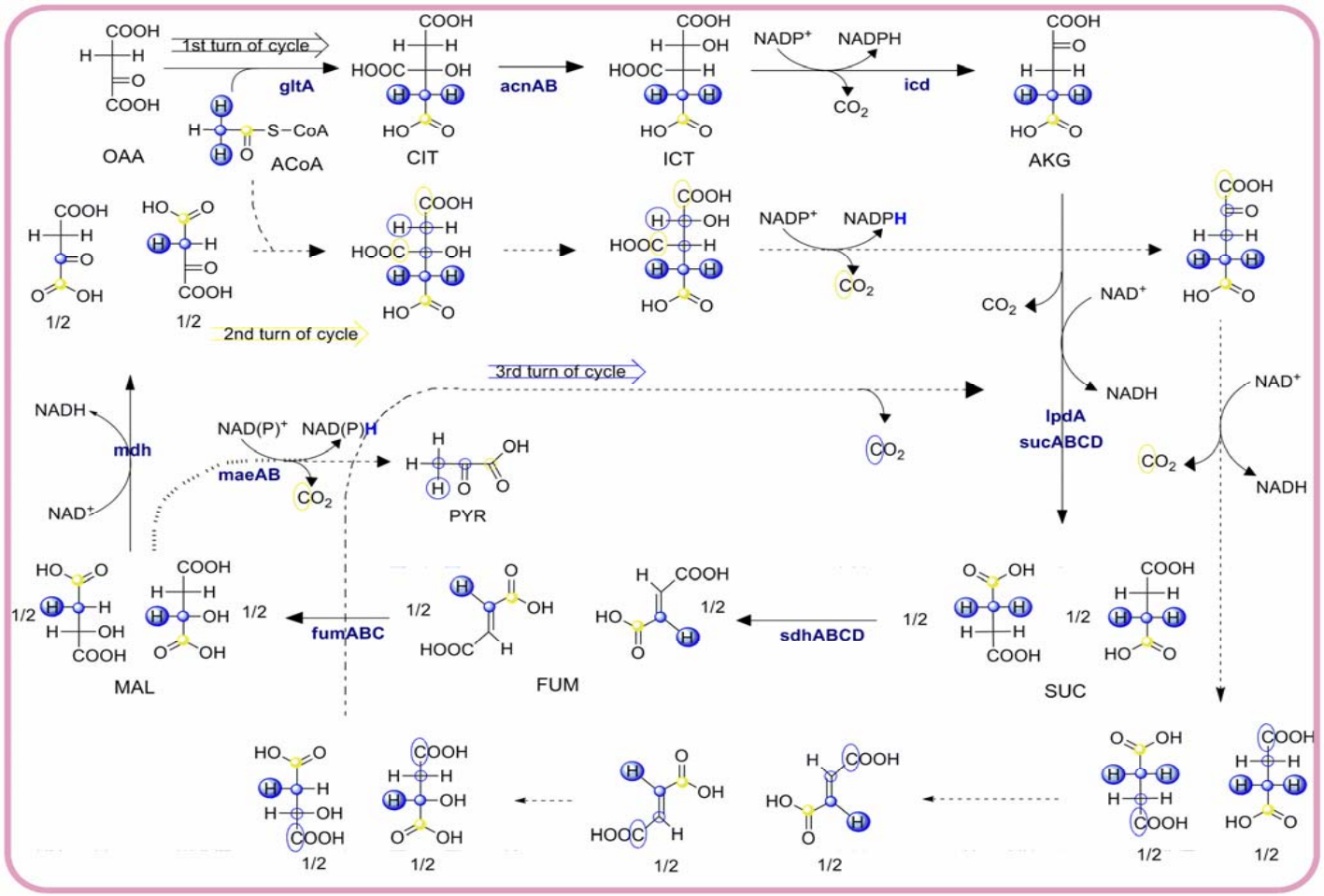

Figure 1-4. The fate of labeled ACoA in TCA cycle. Enzymes are indicated by their 3-letter code. Dashed arrows and lines indicate the fate of oxaloacetate acid (OAA) after the second and third turn of cycle. Hashed lines indicate the interconnection between the TCA cycle and the anaplelotic reaction catalyzed by maeA or maeB. Open cycles indicated partially labeled atoms (Adapted from references 3 and 24)

Table 1-1. Tabulation of glucose passage through the PP pathway.

Year (Ref.)	*E. coli* strain	Methods and Tools	Physiological conditions	PPP[a] (%)
1950 (6)	B	^{14}C-1glucose, $^{14}CO_2$ recovery measured	Growing cells	22-38
			Resting cells	<1
			Growing cells infected with T2 virus	6
1953 (7)	B	Activity of zwf and gnd in cell-free extracts	Exponential aerobic growth on glucose	40
1958 (8)	B	C^{14}-labeled glucose at 1 or 2 or 3 or 6 position, rediorespirometric measurements	Resting cells in media optimum for growth	28
1962 (9)	W	Glucose-1-O^{18} or glucose-6-O^{18} recovery of labeled CO_2	Rapid growth	30
			Slow growth	10
1967 (10)	WT	Glucose-1-O^{18}, ratio of isotope recovered CO_2	Exponential growth in salts medium	25
			Growth period in salts medium	16
			Stationary phase in salts medium	10
			During or after nitrogen deprivation	13-19
			Minimal media with yeast extract or nutrient broth	13-14
			Anaerobiosis	7
			Anaerobiosis plus nitrate	13
1967 (11)	K-10	Glucose-1-^{14}C, gluconate-1-^{14}C, radio-labeled alanine measurements	Growing cells	Both PPP and EMP pathway active, ED pathway inactive
	K-10 Δ*pgi*			PPP major, ED pathway minor extent
1968 (12)	B	Glucose-1-O^{18}, O^{18} in ribose and deoxyribose moieties measured by liquid chromatography – MS	Growing cells during early logarithmic phase	30

[a]PPP: Pentose Phosphate Pathway

Table 1-1. Continued.

Year (Ref.)	*E. coli* strain	Methods and Tools	Physiological conditions	PPP(%)
1969 (13)	B	[1-^{18}O], [2-^{18}O] and [6-^{18}O] glucose and [2-^{18}O] fructose O^{18} in ribose and deoxyribose moieties measured by liquid chromatography - MS	Growing cells in minimal media contained a limited amount of glucose	28-30
1972 (14)	K-12	Enzymatic and end products determination	Transition from aerobiosis to anaerobiosis	20-30
1974 (15)	DF100 (K-12 derivative), DF102 (zwf 10-fold-higher level mutant)	C^{14}-lebeled glucose at 1 or 6 position, rediorespirometric measurements, intracellular intermediates concentration measurements, in vivo and in vitro rates of glucose oxidation via PPP	Growing cells during early logarithmic phase	0.4-fold higher rate of glucose oxidation via PPP in the mutant strain
1977 (16)	K10	[1-^{3}H, *U*-^{14}C]glucose, [3-^{3}H, *U*-^{14}C]glucose, [4-^{3}H, *U*-^{14}C]glucose, [6-^{3}H, *U*-^{14}C]glucose, amino acids from hydrolysates of the cellular protein were separated with an amino acid analyzer and their ^{3}H/^{14}C ratios calculated	Cells growing in glucose minimal medium aerobically	5-10
	K10		Anaerobically	< 5-10
	K10 Δ*zwf*		Aerobically or anearobically	0
1979 (17)	DF567 (K-12 derivative)	C^{14}-lebeled glucose at 1 position, radiolebeled alanine measurements	Cells growing aerobically in minimal medium	16

Radiorespirometric Measurements

As the word implies, radiorespirometric methods measure the respiratory function of an organism by a combination of CO_2 production and radioactive tracer techniques.[8] In early attempts, the evolution of $^{14}CO_2$ from *E. coli* cells growing under different conditions in presence of [1-^{14}C]glucose was calculated[18] based on the fact that the PP pathway will convert the C-1 carbon of glucose (colored in red in Figure 1-3) into CO_2 much faster than the combination of EMP pathway and TCA cycle. However, the $^{14}CO_2$ produced from the latter pathways (after 3 turns of TCA cycle, Figure 1-4) complicates

the calculations, but a correction for the TCA cycle-associated contribution to the recovered $^{14}CO_2$ was made by performing a parallel experiment[8] in presence of [6-^{14}C]glucose ($^{14}CO_2$ cannot be produced from the PP pathway starting from labeled glucose at position 6, colored in blue in Figure 1-3).

To circumvent the two major problems inherent with ^{14}C, namely: i) the possibility of conversion of glucose-6-^{14}C to glucose-1-^{14}C via the isomerization of the triose phosphate and ii) the fact that the final results depend on the relative degree of utilization of the 6 carbon atoms of glucose not only for CO_2 but also for the synthesis of various cell components, Rittenberg and Ponticorvo[9] developed a procedure based on $C^{18}O_2$ measurements. This approach is independent of the function of TCA cycle. When either glucose-1-^{18}O or glucose-6-^{18}O passes through the EMP pathway, the ^{18}O is lost from the molecule at the formation of the PEP and oxidation of PYR yields nonlabeled CO_2. On the other hand, when glucose-1-^{18}O is oxidized to pentose via the PP pathway, the CO_2 produced should contain ^{18}O (colored in red in Figure 1-3). Consequently, the concentration of ^{18}O in the CO_2 will be proportional to the fraction of glucose-1-^{18}O that enters the PP pathway. Regardless, of the specific labeled glucose used, the results led to estimations of between 10 and 40 % for the relative participation of the PP pathway into glucose utilization from the *E.coli* cells, with high dependence on the physiological conditions under which the experiments were carried out.[10]

The validity of the radiorespirometric measurements came under severe criticism by Katz and Wood,[19, 20] who pointed out that theoretically, the PP pathway should be considered as a cycle and recycling of the resynthesized F6P is possible if the latter is isomerized back to G6P (hashed line in Figure 1-3). In such a case, the degree of recycling plays a vital role on fate of the labeled CO_2, which is diluted by unlabeled CO_2, and the PP pathway partition is underestimated. Nevertheless Katz and Rognstad,[21] with the aid of a 7090 IBM computer and a mathematical model that they wrote in

FOTRAN 2 language to fit the experimental data, showed that especially in *E. coli* cells, the impact of the carbon randomization during the concurrent operation of the PP and EMP pathway on radiorespirometric measurements is negligible.

Destructive Techniques

The attractiveness of the radiorespirometric method is based on its simplicity, since it is non-destructive and the only prerequisite is an apparatus to trap the released CO_2, though only a single measurement can be made on each sample. On the other hand, due to many assumptions made in the calculations of the results, many investigators tried to verify those values by performing measurements on end-products other than CO_2. Unfortunately, all these methods required the rupture of the cell membrane with unpredictable consequences on the measurements associated with it.

Measurements based on labeled nucleic acids

Caprioli and Rittenberg [12, 13, 22] examined the levels of radioactivity in the nucleic acids of the *E. coli* cells that had been grown on labeled glucose. The logic of these experiments lies on the fact that glucose metabolized exclusively by the PP pathway would produce a nucleoside labeled in the pentose moiety only if it is labeled as [6-^{18}O] ([1-^{18}O]glucose will give rise to unlabeled R5P and $C^{18}O_2$ while [2-^{18}O]glucose would produce labeled in the C-1 oxygen R5P, but the ^{18}O would be lost in the formation of the glycosidic linkage with base). The concentration of ^{18}O in the C-5 atom of the pentose would be equal to that of C-6 oxygen atom of the original glucose. On the other hand, if glucose was metabolized exclusively via the EMP pathway, both [1-^{18}O]glucose and [6-^{18}O]glucose would give rise to [3-^{18}O] 3PG and [2-^{18}O]glucose would form [2-^{18}O] 3PG. Through the reverse action of transketolase (tklAB in Figure 1-3), [5-^{18}O] R5P would be produced from both [1-^{18}O]glucose and [6-^{18}O]glucose and [4-^{18}O] R5P from the [2-^{18}O]glucose. Hence, the growth of bacteria using [1-^{18}O], [2-^{18}O] and [6-^{18}O]glucose as the sole carbon sources was terminated in early logarithmic phase, RNA and DNA were

isolated, enzymatically degraded to the nucleoside level, purified further by liquid chromatography and the content of the O^{18} label in the pentose of nucleosides was determined directly by mass spectroscopy (MS). Two major conclusions emerged from this study: i) in line with the radiorespirometric measurements, 28-30 % of the pentose arose via the PP pathway, ii) the resynthesis of hexose phosphate is limited to about 3 %.

Measurements based on labeled amino acids

In an effort to investigate the function of the Entner-Doudoroff pathway in *E. coli* cells, Zablotny and Fraenkel[11] isolated a Δ*pgi* strain and fed both wild type and mutant with two different carbon sources, glucose-1-^{14}C and gluconate-1-^{14}C. Labeled glucose used by the EMP pathway would give rise to methyl-labeled PYR. Labeled gluconate used by the ED pathway could give rise to carboxyl-labeled PYR and should give unlabeled PYR when used by the PP pathway. Assuming that the alanine comes from the transamination of PYR, the authors isolated alanine from lysed cells and measured the radioactivity. Their results ruled out the function of the ED pathway as a third possible route in glucose utilization by *E. coli* cells. Later, Silva and Fraenkel[17] estimated the PP partition at 16 % using the same method.

In all previous studies, the amount of NADPH formed relative to the amount of consumed glucose can be calculated indirectly from the percentage of PP pathway since 1 mole of glucose yields 2 moles of NADPH when the pentose phosphate shunt is used exclusively from the cells. In 1977, however, Csonka and Fraenkel[16]raised a very interesting question: if a Δ*zwf E. coli* strain, which cannot utilize glucose through the shunt, can grow easily on glucose[23] how is it producing the 17 mmols of NADPH required from biosynthetic reactions to form 1 g of cells? In other words, if the PP pathway is not essential, how could NADPH be made in *E. coli* cells? To address this issue the investigators worked with *E. coli* strains that had mutations affected either

directly or indirectly, putative NADPH-forming reactions. Specifically one of the following enzymes was deleted:

- phosphoglucose isomerase (Δ*pgi*),
- glucose 6-phosphate dehydrogenase (Δ*zwf*),
- isocitrate dehydrogenase (Δ*icd*),
- gluconate 6-phosphate dehydrase (Δ*edd*),
- malate dehydrogenase (Δ*mdh*),
- a factor coupling electron transport to ATP formation (Δ*uncB*) or a combination of them such as Δ*pgi*Δ*edd,* Δ*icd*Δ*zwf* and Δ*pgi*Δ*uncB* mutants.

They grew the different strains aerobically or anaerobically in presence of glucose labeled uniformly with ^{14}C and specifically with ^{3}H in positions 1, 3, 4 or 6 and they isolated two pairs of amino acids: threonine and aspartate, or proline and glutamate from protein hydrolysates. This technique ensured that: i) the number of radioactive hydrogens derived from a particular position of glucose (1, 3, 4 or 6) can be normalized per carbon atom (according to ^{14}C) in the compound isolated and ii) since the pairs of the amino acids selected differ by two NADPH-dependant reductions, the different $^{3}H/^{14}C$ ratios between them reflect labeling of the NADPH pool, even if there were also present radioactive hydrogens remaining carbon-bound from glucose.[24] The most important observations from this thorough study are:

- Hydrogens from the 3 and 4 positions of glucose should only appear in end-products from the NADPH-dependent action of the gnd and the NADH-dependent action of the 3GP dehydrogenase respectively.

- In the Δ*pgi* mutant, under anaerobic conditions, the hydrogen at position 3 made no contribution to the reduction of the end-product isolated where the hydrogen at position 1 or 6 made a similar contribution aerobically or anaerobically. Therefore, the PP pathway is not an obligatory source, at least anaerobically, and the hydrogens at position 1 or 6 of glucose must serve as reductive hydrides via other pathways.

- The Icd, a possible source for hydrides from the 6 position of glucose, is not essential even in cells also lacking the Zwf and the radioactivity from the hydrogens at position 1 and 6 is not decreased in a strain lacking the enzyme. Thus, a third source should be account for the labeled NADPH found.

- The NADH contribution to biosynthesis cannot be explained with a futile cycle proposed by Lowenstein[25] which involves the ATP-dependent conversion of PYR

to OAA, its NADH-dependant reduction to MAL (catalyzed by mdh) and the NADPH-dependant oxidative decarboxylation of MAL to PYR (catalyzed by meaB), since a Δ*mdh* stain gave the same contribution of tritium from the C-4 of glucose as the wild type.

- The fact that the 4 hydrogen of glucose (NADH via the 3PG dehydrogenase) made a minor but measurable contribution to the biosynthetic reactions could be explained by the action of an energy-linked transhydrogenase since this contribution was abolished in the Δ*uncB* mutant strain.

Most of the drawbacks of the aforementioned study were pointed out from the authors. Namely: i) the possible isotope discrimination against the tritium atom[26] should result in underestimation of the PP pathway; a factor of two is suggested as a correction (i.e., the PP pathway contributes to 20-40% of the total NADPH pool), ii) unfortunately strains missing a transhydrogenase (i.e., Δ*pntAB*) or the NAPDH-dependant malic enzyme were not available, at that moment, for the construction of all possible mutants, iii) the indirect measurements based on a Δ*uncB* mutant were of limited value due to marginal growth characteristics of this particular strain. Nonetheless, the message from this work is clear: the PP pathway should not account for more than 50 % of the NADPH pool and it is not an obligatory route for NADPH formation in *E. coli* cells especially under anaerobic conditions or in Δ*zwf* mutant.

Regulation of Pentose Phosphate Pathway

The results of isotopic experiments under various physiological conditions suggested that the PP pathway is regulated.[10, 27] Stronger evidence for the regulation of the first step of the shunt came from Orthner and Pizer's study.[15] They calculated, using a mutant strain with 10-fold higher amount of Zwf compared to wild type, that the shunt was not used much faster in the mutant and that both Zwf and Gnd are not operating at their maximal velocity in the cell. Additionally, according to their data, glucose utilization by the shunt is not limited by the $NADP^+$ or the $NADP^+$/NADPH ratio since the concentration of NADPH in the mutant is not sufficient for the 90% inhibition required to justify the only 40% higher flux. A survey by Silva and Fraenkel[17] for effectors that might

control *in vivo* the Gnd reaction in *E. coli* was unsuccessful. In an elegant study,[28] Wolf et al. showed the growth-rate-dependant alteration of zwf and gnd levels in *E. coli*. They varied the specific growth rate, while using the same carbon source, by feeding the cells with different ratios of glucose/ α-methylglucose (a competing with glucose for transport, but non-metabolizable, analog) and observed that the levels of the pertinent enzymes are proportional to growth rate. Interestingly, the regulatory site for the translational control of gnd lies within the protein-coding region of the regulated gene, as proved later by Baker and Wolf.[29-31]

The Present: The Interplay of NADPH with the Metabolic Network

We may describe the first three decades of the NADPH-regeneration research as the 'reductionist' era. At this point, there are well-documented speculations for all the possible sources of NADPH in *E. coli* metabolism. However, crucial questions for the physiology of the *E. coli* cell are still unanswered. Namely, are all the NADPH sources active under any physiological conditions? If so, to which extent does each one contribute to the overall NADPH pool and from which factors, if any, is the contribution regulated and how is it adjusted? The reconstruction of all the pertinent biochemical pathways with the help of new tools and methods (Figure 1-5) may give an answer to this problem.[68] The results from these efforts are summarized in Table 1-2 with an emphasis on PP pathway flux, and they will be discussed in detail below.

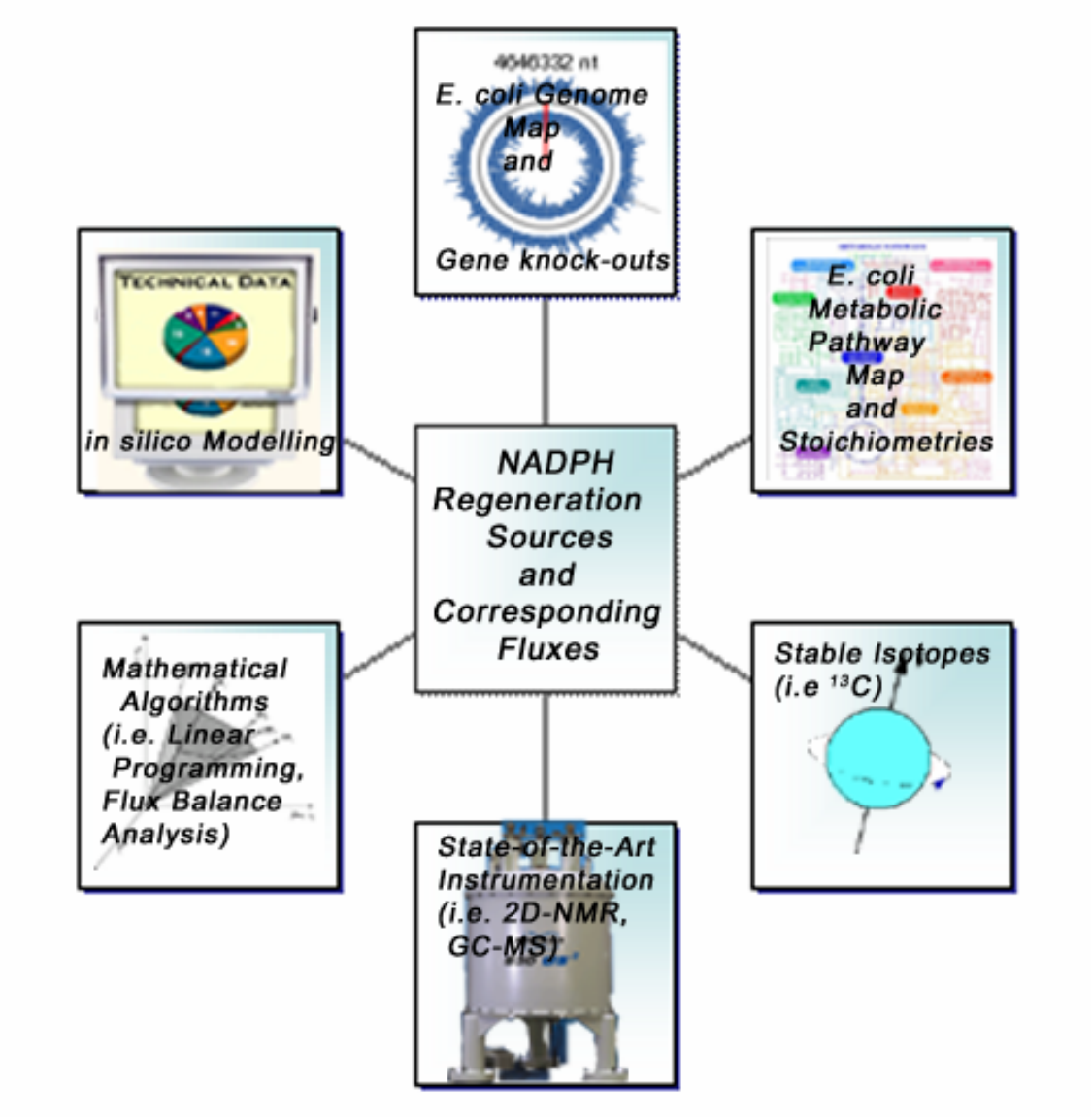

Figure 1-5. Tools and methods used in the last 25 years for elucidation of metabolic pathways.[32, 33]

Theoretical Methods

There is no 'pure' theoretical method for the calculation of a biochemical pathway flux (i.e., the rate at which input metabolites are processed to form output metabolites).[68] In this context theoretical methods are considered all the approaches that are not using isotope tracers. Theoretical methods are coming in different 'flavors'[68, 69-70] but the keystone in all of them is the principle of mass conservation.

Table 1-2. Estimated fluxes though the PP pathway.

Year (Ref.)	*E. coli* Strain	Methods and Tools	Physiological Conditions	PPP[a] (%)
1980 (34)	K12	Glucose-1-^{13}C, ^{1}H correlation NMR	Resting cells	22
			Cells grown anaerobically in M9 medium	
1992 (35, 36)	K12	FBA[b]	Aerobic growing cells without ATP maintenance requirements	90
			Aerobic growing cells with ATP maintenance requirements	20-40
1995 (37)	W 3110	90% unlabeled glucose plus 10% [*U*-^{13}C]glucose, 2D [^{13}C,^{1}H]-COSY NMR of the purified and hydrolyzed P22 c2 repressor peptide	Aerated culture (in a fermenter) overexpressing P22 c2 repressor protein	20-30
			Air contact (in a conical flask)	
			Anaerobic (in a conical flask after purged the medium with argon)	
1996 (38, 39)	MG1655	Enzymatic analysis of end-products, FBA	Fed-batch cultivation of exponential grown VHb-expressing cells	Higher PP partition compared to wild type
1996 (40)	W 3110	90% unlabeled glucose plus 10%[*U*-^{13}C]glucose, 2D [^{13}C,^{1}H]-COSY NMR of the purified and hydrolyzed P22 c2 repressor	Aerobic growing cells in minimal medium overexpressing P22 c2 repressor protein	15
1997 (41)	JM101	[1-^{14}C]glucose, radiorespirometric method	Exponential-phase growing cells in M9 medium	20-30%
	JM101 Δ*pykA*Δ*pykF*			Mainly through the PP pathway
1998 (42)	not reported	[2-^{14}C]glucose	Slow growth	2
			Log-growth phase	9
			Stationary phase	16

[a] PPP: Pentose Phosphate Pathway. [b]FBA: Flux Balance Analysis.

Table 1-2. Continued.

Year (Ref.)	*E. coli* Strain	Methods and Tools	Physiological Conditions	PPP(%)
1999 (43)	W 3110	90% and 92% unlabeled glucose plus 8 and 12% [*U*-^{13}C]glucose, 2D [^{13}C,^{1}H]-COSY NMR and GC/MS analysis of biomass samples	Aerobic growth without recycling	46
			Anaerobic growth without recycling	74
			With recycling	20-30
1999 (44)	MG1655	90% unlabeled glucose plus 10% [*U*-^{13}C]glucose, 2D [^{13}C,^{1}H]-COSY NMR of hydrolyzed cell proteins, enzymatically analysis of excreted metabolites	Fed-batch cultivation of cells carrying a high copy number plasmid under microaerobic conditions	32
1999 (45)	B (ATCC 11303)	85-90% unlabeled glucose plus 15-10%[*U*-13C] glucose, 2D [^{13}C,^{1}H]-COSY NMR of hydrolyzed cell proteins, metabolic flux ratio (METAFoR) analysis	Mid-exponential	29
			Late exponential	25
			Stationary	24
2000 (46)	MG1655	FBA was used with objective of maximizing growth and examination the change in the metabolic capabilities caused by gene deletions	Simulated aerobic environment with glucose as carbon source	33
2000 (47, 48)	K-12	FBA with objective to calculate the sensitivity of optimal cellular growth to altered flux levels of PP pathway genes	Growing cells in glucose minimal medium	2-25%
2000 (49)	MC 4100	Glycerol, acetate, glucose, DNA microarray technology for detection of differential transcription profiles of a total of 111 genes involved in central carbon metabolism	Exponential growth phase in a minimal medium	the PP genes were not regulated significantly with exception of *gnd* down-regulated in glycerol and acetate
2001 (50)	MG1655	0.45% (w/v) unlabeled glucose and 0.05% [*U*-^{13}C]glucose2D [^{13}C,^{1}H]-COSY NMR of hydrolyzed cell proteins, metabolic flux ratio (METAFoR) analysis	Mid-exponential growth phase in M9 medium	5-10
	W 3110 Δ*pgi*			100

Table 1-2. Continued.

Year (Ref.)	*E. coli* Strain	Methods and Tools	Physiological Conditions	PPP (%)
2002 (51)	JM101	10% [U-^{13}C]glucose, 2D-NMR, METAFoR analysis	Glucose-limited chemostat or ammonia-limited chemostat	21-44 C-limited), 1 (N-limited)
	JM101 (Δ*pykAF)*			1-28 (C-limited) 31 (N-limited)
2002 (52, 53)	MG1655	Glucose used as a carbon source, FBA and phenotype phase planes (PhPPs) analysis	Growing cells under different oxygen uptake rates	Flux decreases as oxygen uptake rate decreases
2002 (54)	JM101	[1-^{14}C]glucose, [1-^{13}C]glucose and [U-^{13}C]glucose , a combination of of genetic, biochemical and NMR techniques	Growing cells during logarithmic phase in M9 medium	23
	JM101 PTS$^-$ Glc$^-$			59
2003 (55)	MG1655, W3110, JM101	20% or 100% [U-^{13}C]glucose, GC-MS	Mid-exponential growth-phase, batch cultures	4 (anaerobic)-14-20 (fully aerobic)
2003 (56)	K12	Glucose, enzyme activity assays and proteome analysis by 2-dimensional electrophoresis (2DE)	Aerobic versus microanaerobic growth	Zwf and gnd down-regulated in micro-anaerobic growth
2003 (57, 58)	JM109 Δ*pgi*	Semi-quantitative RT-PCR, intracellular NADPH measurements, extracellular metabolites analysis	Batch cultivation in rich LB medium	overproduction of NADPH, high flux through the PP
2003 (59)	AB1159	Nicotinamide nucleotide enzyme levels, and cellular ratios of NADPH/ NADH measured after exposure of cells to H_2O_2	Growing cells in presence of H2O2	The activity of zwf was induced by 2.9 fold upon H_2O_2 challenge
2003 (60)	W3110	90% unlabeled glucose plus 10% [*U*-^{13}C]glucose, extracellular metabolites analysis, enzyme activity assays, [^{13}C, ^{1}H]-COSY NMR analysis of amino acids, glycerol, glucose in the hydrolysates	Aerobic chemostat cultivation in glucose or ammonia-limited minimal medium	9 ± 2 (C limited) 4 ± 2 (N limited)
	W3110 Δ*pgi*			47 ± 9 (C limited) 37 ± 9 (N limited)
	W3110 Δ*zwf*			0 ± 2 (C limited) 0 ± 2 (N limited)

Table 1-2. Continued.

Year (Ref.)	*E. coli* Strain	Methods and Tools	Physiological Conditions	PPP(%)
2003 (61)	K12	7.5 % [*U*-^{13}C]glucose and 7.5 % [1-^{13}C]glucose in presence of naturally labeled glucose, extracellular metabolites analysis, GC-MS analysis of biomass hydrolysates	Aerobic chemostat cultivation in glucose minimal medium at dilution rate (D) 0.11 h^{-1}	43
			At dilution rate (D) 0.22 h^{-1}	28
2003 (62, 63)	BW25113	10 % [*U*-^{13}C]glucose and 10 % [1-^{13}C]glucose in presence of unlabeled glucose, enzyme activity assays, GC-MS and NMR analysis of biomass hydrolysates	Aerobic chemostat cultivation in glucose minimal medium at dilution rate (D) 0.2 h^{-1}	20
	BW25113 Δ*gnd*			10
2004 (64)	K12	10 % [*U*-^{13}C]glucose and 10 % [1-^{13}C]glucose in presence of unlabeled glucose, enzyme activity assays, GC-MS and NMR analysis of biomass hydrolysates	Aerobic chemostat cultivation in glucose minimal medium at dilution rate (D) 0.2 h^{-1}	34
	K12 Δ*pykF*			79
2004 (65)	BW25113	10 % [*U*-^{13}C]glucose and 10 % [1-^{13}C]glucose in presence of unlabeled glucose, enzyme activity assays, GC-MS and NMR analysis of biomass hydrolysates	Aerobic chemostat cultivation in glucose minimal medium at dilution rate (D)	20
	BW25113 Δ*zwf*			0
2004 (66)	MG1655	20% or 100% [U-^{13}C]glucose, GC-MS	Aerobic batch cultures in M9 medium	17-23
2005 (67)	TG1 (a K-12 strain)	FBA , extracellular metabolites analysis, determination of ATP, ADP, AMP	Cells growing aerobically in glucose limited continuous culture at D= 0.044 h^{-1}	39 % mol mol^{-}
			Cells growing anaerobically in glucose limited continuous culture at D= 0.44 h^{-1}	73 % mol mol^{-}

Similar to Kirchhoff's current law, (Figure 1-6) the fundamental equation for the flux balance analysis (FBA) states that a metabolite cannot be accumulated inside the metabolic network, therefore, over long period of time, the formation fluxes of a metabolite must be balanced by the degradation fluxes.[72] For the FBA to be applicable:[78]

- All possible biochemical pathways for the particular organism must be known.
- The stoichiometry of the biochemical reactions constituting the metabolic network should be well defined.
- The elemental composition of the biomass should be estimated.
- Physiological data such as nutrients uptake rates, metabolites secretion rates and biomass production rates should be calculated.
- The assumption of steady-state operation of the bioreaction network should be applied.

For a network composed of n metabolites and m fluxes, this yields a system of *n* differential equations with *m* unknown fluxes which are time-independent when the network operates under steady-state conditions. Although, a number of constraints are applied to the specific system, based on experimental data, the number of unknown fluxes usually exceeds the number of metabolites and the solution is underdetermined. Thus, a multidimensional solution space satisfies the constraints. To reach a single flux distribution further biochemical experiments (e.g. identification of active pathways under certain physiological conditions) must be performed and certain objectives need to be set (e.g. maximal cell growth or maximal production of a cofactor or metabolite). Then, an appropriate optimization algorithm may produce a unique solution.

In silico* estimations for NADPH-related fluxes in *E. coli

In one of the earliest applications of the FBA approach in *E. coli*, Palsson and coworkers[35, 36] calculated that the maximum yield of NADPH produced, per mole of glucose consumed, is 11 moles. When the optimal growth for *E. coli*, in the presence of glucose, was set as objective, the PP pathway was found to be used almost exclusively from the bacterium.

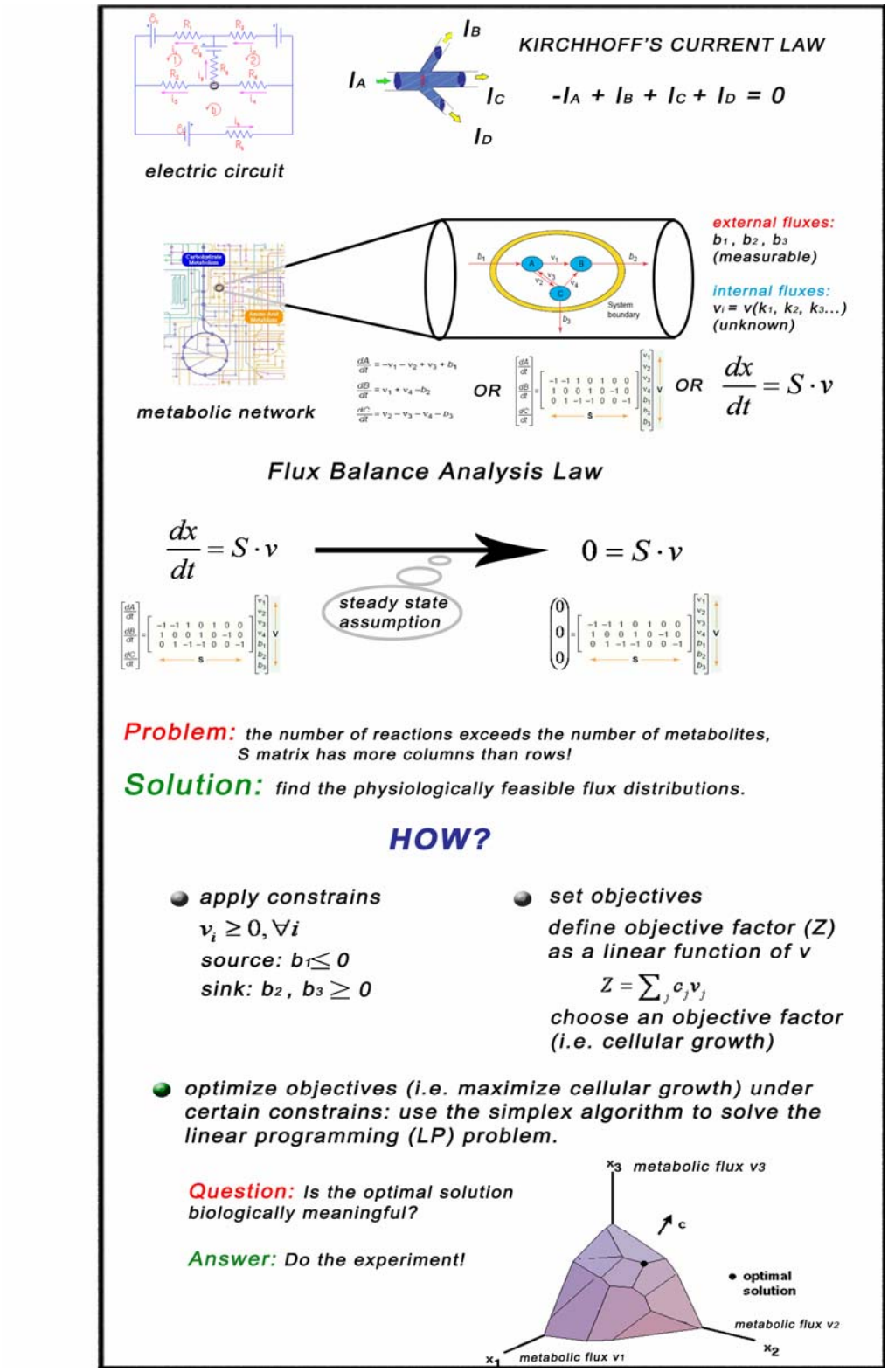

Figure 1-6. Basics of Flux Balance Analysis (FBA) approach (Adapted from references 72, 73, and 74)

Realizing based on experimental data that this value is an overestimation they applied energy constraints to their model and showed that the PP pathway flux is very sensitive to the ATP maintenance requirements (e.g. maintenance of cellular osmolarity, transmembrane gradient, etc.).

In an effort to evaluate the effects of gene knockouts in the *E. coli* metabolic network, Edwards and Palsson[46] applied *in silico* gene deletions and calculated the resultant effects on growth flux. In line with the experimental data, they reported that the *in silico zwf* mutant had a growth rate of 99% of the 'wild type' value with a concomitant increase of the TCA flux. In addition, the *in silico pgi* deletion strain had a decreased normalized growth yield under oxygen-limited conditions.

The robustness (i.e. the ability of an organism to operate under a wide range of conditions)[75] of *E. coli* was also examined. When the optimal flux for an essential for the PP pathway gene, *tkt*, was decreased to 15% of that of the *in silico* wild type, the optimal growth flux did not change, but a utilization of a transhydrogenase that converted NADH to NADPH was observed in addition to an increased TCA cycle flux. Also, under oxygen-limited conditions, the oxidative part of PP pathway was not functional, the transhydrogenase reaction was again activated and the TCA cycle did not operate cyclically.[52, 53] In a similar manner, but also measuring experimentally the energetic state of the cells, Weber et al. demonstrated that the flux towards the PP pathway is increased at the cost of TCA cycle activity when growth rate increases in glucose-limited chemostat cultures.[67]

Computational methods: limitations

Basically, the power of the computational approaches is based on the experimenters' failure to estimate the *in vivo* kinetic parameters in a metabolic network. Under steady-state conditions the time-factor is cancelled out and the differential equation system is transformed to a set of linear equations that can be solved by matrix

theory. In principle, this assumption holds true due to high turnover of the pools of metabolites, especially in continuous cultures and in exponential phase of a batch culture.[76] However, several drawbacks are evident:[77, 78]

- Metabolic flux analysis (MFA) fails to predict intracellular in parallel or cyclic metabolic pathways fluxes which are not coupled to measurable fluxes.
- MFA measures net fluxes. Therefore, it fails in bidirectional reaction steps such as the transaldolase and transketolase reactions in PP pathway.[79]
- Assumptions made on the global currency metabolites ATP, NADH and NADPH are controversial. For example, in microorganisms bearing a transhydrogenase which can equilibrate both NADH and NADPH pools, the typical use of separate balances is an oversimplification. In addition, ATP-futile cycles cannot be estimated precisely.[80]
- The accuracy of MFA on calculated fluxes is directly related to the experimental error of the measured extracellular rates.
- The postulation that a metabolism of a particular organism is designed by nature to follow a certain objective may or may not be true. Even thought the *in silico* predictions have been consistent with experimental data in an *E. coli* wild type strain[81] they are questionable in a perturbed system, like the knock-out strains.[82]

Experimental Methods

Nuclear Magnetic Resonance (NMR) spectroscopy and mass spectroscopy (MS) are the dominant tools used during the last two decades for the elucidation of metabolic networks. Stable isotopes such as ^{18}O, ^{2}H, ^{13}C had been used as tracers in some early studies in combination with MS, but radioactive tracers and the liquid scintillation counting technique was more approachable in the post Word War II era, for metabolic physiologists due to the high sensitivity of this method.[83] The last two decades, the advent of high field NMR instruments and the coupling of MS with liquid (LC-MS) or gas chromatography (GC-MS) tipped the balance in favor of stable isotope tracers since problems due to detection limits are eliminated. Considering the fact that carbon is the central atom in biomass it is not a surprise that ^{13}C is the predominant stable isotope for the labeling measurements in the latest studies especially when the ^{12}C and ^{13}C differ not only in mass but also in nuclear spin. Hence, their different physical properties can be detected by either of the abovementioned analytical instruments.

Also, complementary information could be drawn by these two methods since both have the same starting point: Cells are growing in minimal medium containing a carbon labeling source, uniformly and/or 1-^{13}C glucose is used almost exclusively (see Table 1-2). As the labeled substrate is traveling through the metabolic network, stable isotope labeled carbons are exchanged, diluted, recycled and finally accumulated into different metabolites in a very specific manner, which is dictated from the pathway that they followed.[84] When a steady-state condition is established, biomass hydrolysates such as proteinogenic amino acids are subjected to NMR and/or GC analysis and the isotopic enrichment is measured. The isotopomer patterns (i.e. isomers differing only in isotope distribution) of the amino acids reflect the patterns of their related precursors which are usually key intermediate metabolites of the central carbon metabolism. It is not easy to detect these intermediates due to their low abundance in the cell, amino acids detection is relatively easy since approximately 55 % of biomass is proteins.[85]

Finally, what holds true for the theoretical methods is also true for the experimental studies: The complexity of the metabolic networks makes the mathematical and computational models absolutely necessary tools for the experimentalists who want to fully exploit the meaning of their experimental data. Thus, in the last step of quantitative analysis, an isotopomer model of metabolism is integrated with an iterative fitting procedure of the measured data and the intracellular metabolic fluxes are derived (Figure 1-7).

NMR analysis for ^{13}C labeled amino acids

Two types of information are usually derived from NMR ^{13}C isotopomer analysis data.[86] The first involves fractional enrichment measurements in which glucose labeled at a specific position (e.g. [1-^{13}C] glucose) is used and the degree of ^{13}C enrichment (i.e., the ratio of molecules bearing a ^{13}C spin at a given position over the total number of molecules) is calculated.[87] In the second and the most commonly employed method,

uniformly labeled glucose, 'diluted' with unlabeled glucose, is administrated into the cells and the conserved ^{13}C-^{13}C connectivities in the metabolic network are traced (Figure 1-8). This technique makes use of the fact that upon 90 % ^{12}C dilution of ^{13}C with random distribution of carbon atoms, the probability that any two adjacent carbon atoms are labeled in an individual molecule is approximately equal to the natural abundance of ^{13}C (1.1 %). However, if the two adjacent carbon atoms in the final product derive from the same source molecule, the probability that both positions are labeled is about 10%. The extent to which a certain carbon atom has neighboring carbons that originate from the same source molecule of glucose is calculated from the quantitative analysis of the ^{13}C fine structures. [88]

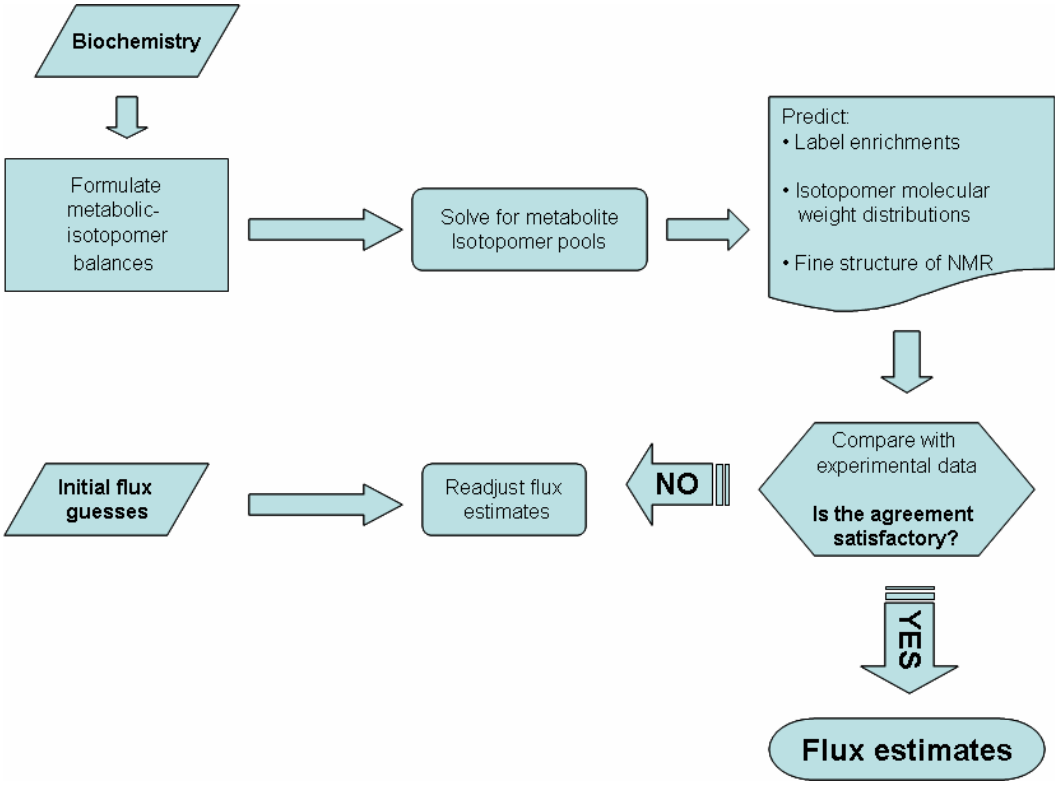

Figure 1-7. Synergy of experimental and computational methods towards the calculation of metabolic fluxes (Adapted from reference 68).

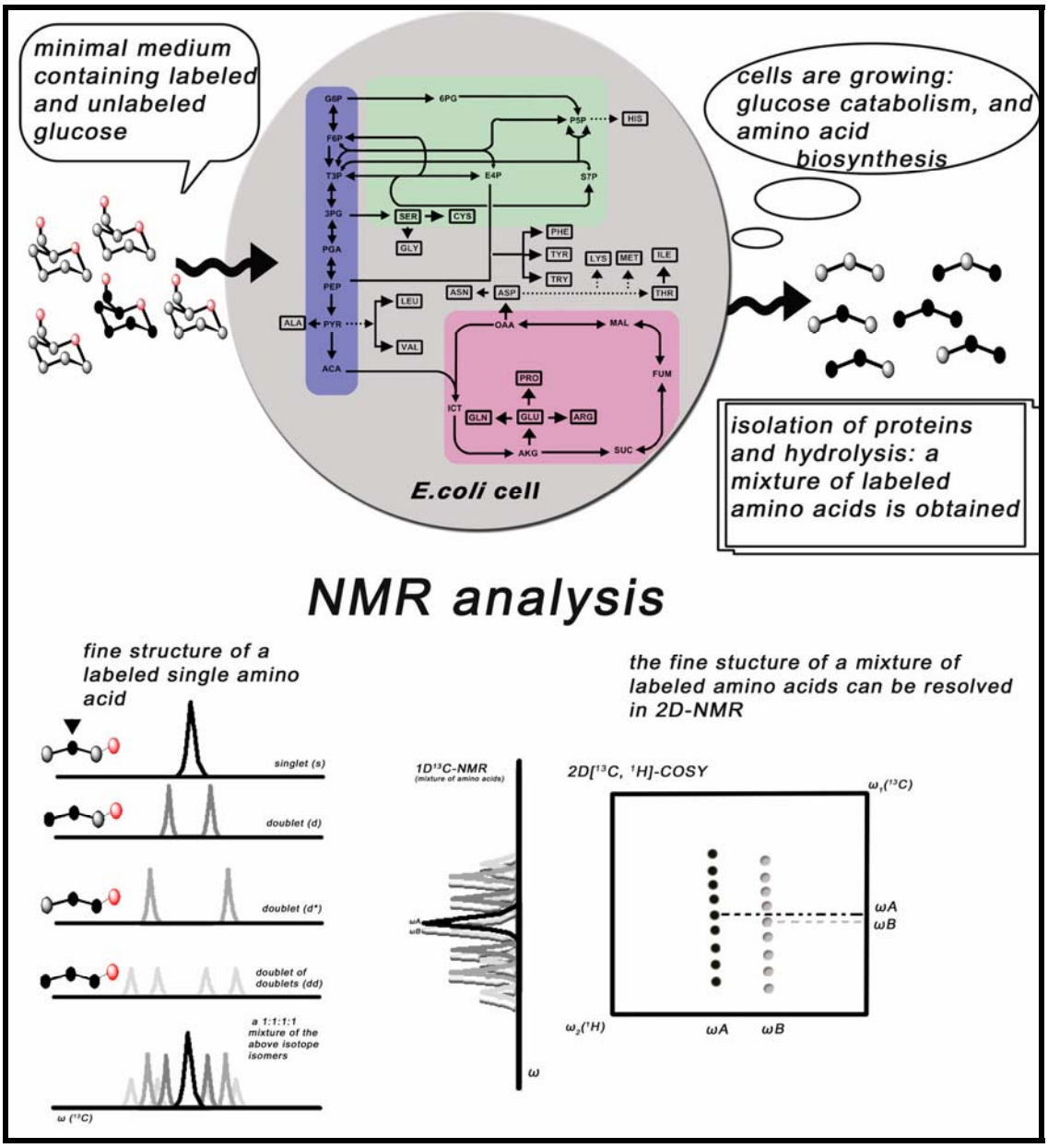

Figure 1-8. Basics of NMR analysis of biosynthetically directed fractional ^{13}C labeling amino acids. (Adapted from references 87, 88)

2D heteronuclear single-quantum coherence [^{13}C, ^{1}H]-correlation NMR spectroscopy (2D [^{13}C, ^{1}H]-COSY) offers the highest sensitivity in deciphering the ^{13}C-^{13}C spin-spin scalar coupling fine structures. In addition, the two dimensional dispersion of ^{13}C resonances enables the analysis of a mixture of amino acids without further purification. Subsequently, the relative intensities of the superimposed multiplets are

determined and the metabolic flux ratios are estimated using a number of probabilistic equations and keeping in mind the biosynthetic reaction network of *E. coli*. [89]

MS analysis for ^{13}C-labeled amino acids

Compared to NMR instrumentation, MS offers higher sensitivity in a shorter time frame. Hence, a greater number of smaller volume samples can be analyzed, minimizing the otherwise high cost of labeled glucose and improving the accuracy of the calculated fluxes. The coupling of MS with gas chromatography (GC) enables the analysis of mixture of labeled amino acids eliminating laborious purification steps. However, in contrast to NMR, a derivatization step of the protic sites of the amino acids by silylation is required to increase the volatility of these polar compounds for GC separation before the MS analysis.[91] Also, the MS data are difficult to interpret intuitively: for a molecule with three carbons, 2^3 positional isotopomers are expected, but a MS peak at M+2, for example, represents all isotopomers with two ^{13}C nuclei, irrespective of their location in the carbon backbone (Figure 1-9). Consequently, in addition to analysis of mass isotopomer distribution (MID) for the molecular ion, corresponding fragments should be available for further interpretation. Taking into account that the production rate of each isotopomer depends on the probability of its formation, which is equal to the probability of formation of its precursor metabolite which, in turn, depends on real metabolic fluxes, correlation between isotopomer and MIDs is accomplished by using matrix calculus.[90]

Estimated fluxes from ^{13}C labeling experiments

In one of the earliest attempts to elucidate metabolic fluxes by NMR, Ogino et al. used ^{1}H correlation NMR to follow glucose catabolism in anaerobic *E. coli* cells under various conditions.[34] First the cells were growing in M9 minimal medium in the presence of glucose. Cells harvested at exponential or early stationary phase, were resuspended in the same buffer in a 5-mm NMR tube and incubated in a NMR spectrometer at 30 °C,

using glucose -1-^{13}C as the sole carbon source. Spectral assignments for succinate, pyruvate, acetate, lactate and ethanol were made based on chemical shifts, spin coupling patterns and ^{13}C-^{1}H coupling constants. The ^{13}C label is lost as CO_2 via the PP pathway, whereas it is incorporated into the methyl carbon of pyruvate via the EMP pathway. Hence, it was estimated that in the case of resting cells or growing cells in M9 medium 22% of the glucose utilized by *E. coli* follows the PP pathway.

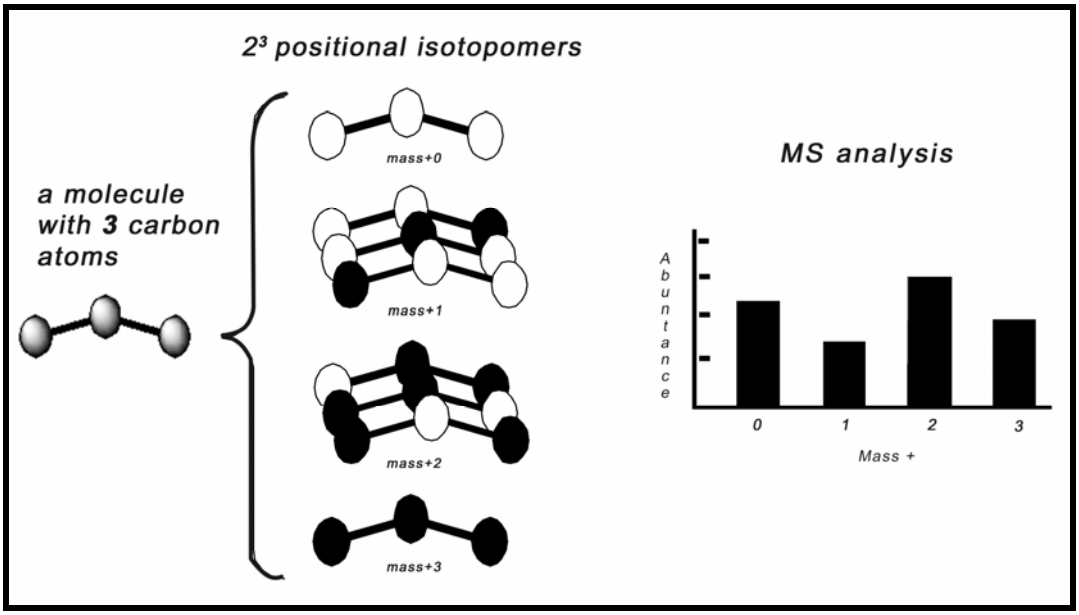

Figure 1-9. MS analysis: mass isotopomer distribution (MID) for the molecular ion. (Adapted from reference 90)

In 1995 Thomas Szyperski demonstrated the power of biosynthetically directed fractional ^{13}C-labeling of proteinogenic amino acids in estimation of intracellular fluxes in *E. coli.*[37] A K-12 derivative *E. coli* strain producing the P22 c2 repressor in high levels was used in this study. The overexpressed peptide was purified and subjected to hydrolysis. The labeled amino acids were analyzed as described before. Despite the examined physiological conditions from fully aerobic to strictly anaerobic, the flux through the PP pathway was set at 20-30 %. Interestingly, Schmidt et al. using the same set of experimental data, but applying a different mathematical model for the quantification of metabolic fluxes, arrived at twice higher numbers: 46 % under aerobic

and 74 % under anaerobic conditions.[43] The authors explained the deviation of their calculations by mentioning that the reversibility of reactions involved in PP pathway (e.g. pgi, tkt, tal) was not considered from the outset. Also, in their estimations the flux from ICT to AKG (the third source of NADPH) in TCA cycle was found to be 25 % under aerobic conditions and 2.2 % under anaerobic conditions.

Trying to stimulate a situation met frequently in the biotechnological industry, Fiaux et al. performed a ^{13}C NMR flux ratio analysis on a wild type *E. coli* MG1655 strain carrying a high copy number plasmid under microanaerobic conditions ($[O_2] < 0.02$ mmol/L).[39] The PP phosphate flux was 32%, whereas the flux from AKG to OAA was zero, showing that the TCA cycle is interrupted under anaerobiosis. In 1999 the term METAFoR (metabolic flux ratio) was introduced by Sauer et al. to describe the technique of imprinting the central carbon network history into cell proteins.[45] In this study the interstrain differences among four strains (JM101, a K-12 strain, PB25, a pyruvate kinase-deficient JM101 strain, ATCC 11303, a wild type B strain, and KO20, an ethanol producing ATCC 11303 strain) were examined under different growth conditions. The major observations were: i) the impact of enzyme overexpression and gene disruption on central metabolism of *E. coli* was negligible, ii) of all central carbon fluxes, those in the TCA cycle were the most sensitive to environmental conditions and iii) surprisingly, the METAFoR patterns among *E. coli* strains with different genetic backgrounds were very similar in exponentially growing cells under aerobic conditions.

In 2000, Dauner and Sauer introduced the GC-MS analysis of proteinogenic amino acids as a rapid method for the calculation of the isotopomer distributions.[91] Three years later, Zhao and Shimizu combined the above technique with the theoretical approach of metabolic flux analysis, in order to estimate the net flux distribution in glucose metabolism in *E.coli* K-12 strain.[61] The flux via the PP pathway was dependant on growth rate with higher values at higher dilution rates. This observation suggested that

under increased growth rate, the flux through icd could not fulfill the NADPH demand for growth and as a consequence higher flux through the PP pathway is required.

The old and popular method of creating mutants and reexamining the differences in fluxes in the genetically perturbed strains compared to the parent strain provide a new insight into metabolism of *E. coli* cell in recent years. Precise gene deletion in *E.coli* is a routine technique nowadays that the whole *E. coli* genome is annotated. Using METAFoR analysis by NMR, Canonaco et al. reinvestigated the impact of *pgi* deletion on glucose catabolism and confirmed the flux rerouting via the PP pathway.[50] The observation of reduced specific growth and glucose-uptake rates due to Pgi-knockout was explored further by overexpressing the soluble transhydrogenase SthA in the mutant and the parent strain. While no difference was found in the wild type strain, the specific growth of the Pgi mutant increased by about 25%, but it could not be restored to 100% even when a 10-fold higher overexpression of SthA was attempted. This suggested that the kinetic limitation of glucose catabolism in the Δ*pgi* strain is due to both the inability of the PP pathway to support higher fluxes and the limited capability of *E.coli* to reoxidize excess amounts of NADPH. Also, Fischer and Sauer observed a 30 % contribution of ED pathway for the pgi mutant when they applied a GC-MS analysis to labeled proteinogenic amino acids from *E. coli*.[55] The phenomenon could be explained by recalling that the ED pathway produces twice fewer moles of NADPH per mole of glucose compared to the PP pathway and thus it may serve as an alternative route for the reduction of the excess amounts of NADPH in pgi-knockout.

Shimizu's group combined the ^{13}C-labeling data from NMR analysis with biomass composition and extracellular flux data in order to quantify intracellular fluxes in pgi and zwf knockouts.[60] Interestingly, in an effort to minimize the overproduction of NADPH, the Pgi mutant bypassed the isocitrate dehydrogenase reaction by rerouting carbon flow through the glyoxylate shunt which is otherwise inactive in the wild type. Disruption of

G6P dehydrogenase leads to activation of transhydrogenase activity towards the production of NADPH, especially in a nitrogen limited chemostat. Elevated maeB activity was also apparent in this mutant. The overall picture of regeneration rates of NADPH as they were estimated in this study is depicted in Figure 1-10. It is worth noting that the rates attributed to MaeB are based on the assumption that both NAD^+ and $NADP^+$ dependant malic enzymes (MaeA and MaeB) are equally active.

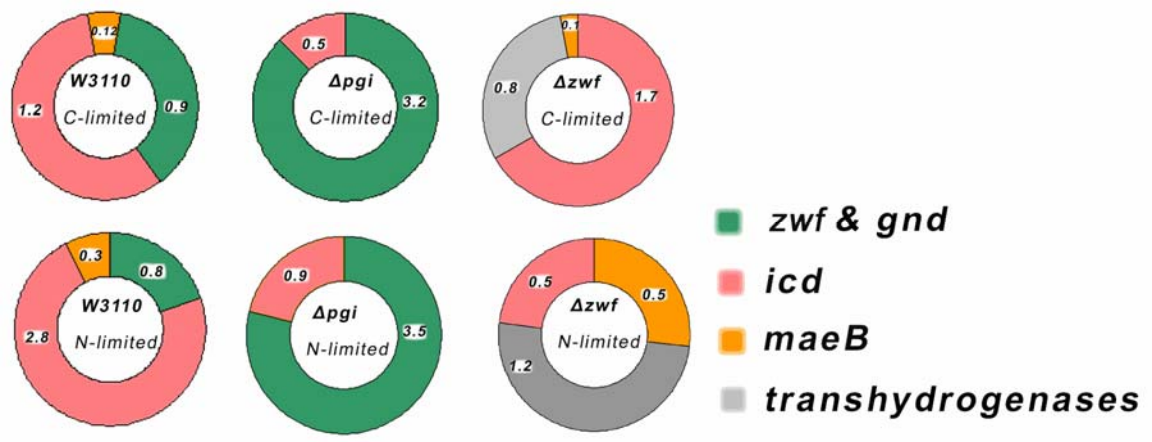

Figure 1-10. Specific rates of NADPH production in glucose (C)- and ammonia (N)-limited chemostat cultures of *E. coli* W3110. The numbers in doughnuts are in mmol g^{-1} h^{-1} units. (Adapted from reference 60)

A similar pattern with the one observed for the zwf mutant[65] was also found when the 6-phosphogluconate dehydrogenase (gnd) deletion was studied by Jiao et al.[62] Activation of the ED pathway, induction of malic enzyme and decreased flux through the PP pathway were the major features of this strain.

The abovementioned work by Hua et al.[60] introduced experimentally, for the first time since 1977,[16] the transhydrogenases as players in NADPH production, at least in Δ*zwf* mutant strain. With Enterobacteriaceae being the only known microbes containing both the soluble, SthA and the membrane bound, PntAB transhydrogenase[92] the question of which contributes to NADPH pool remained open. Speculations for the physiological role of PntAB as NAPDH producer had existed since 1980 when Hanson and Rose carried out phenotypical studies on a *zwf pnt* double mutant and showed that

it grew slower than the *zwf* mutant, as it would be expected when pntAB produces NADPH in absence of the PP pathway.[93] The experimental answer for the physiological role of PntAB in the wild type *E. coli* strain came from Sauer's group in 2004.[66] First, in addition to the Δ*pgi* strain, a new set of mutant strains such as Δ*pntAB*, Δ*udhA*, Δ(*udhA pntAB*) and Δ(*zwf edd eda*) were constructed. Second, the consumption rate of NADPH was estimated based on the growth rate of each mutant strain. Third, the specific rate of NADPH formation from PP phosphate pathway, from the icd and from the maeB was calculated based on METAFoR analysis of ^{13}C-labeled amino acids by GC-MS and metabolic flux analysis. In the Δ*pgi* strain, the specific rate of NADPH formation was two-fold higher than the rate of NADPH consumption. In Δ*pntAB*, Δ(*udhA pntAB*) and Δ(*zwf edd eda*) strains, the two rates were almost equal, but in Δ*udhA* as well as in the wild-type strain, the rate of NADPH depletion surpassed by 20-40% the total rate of NADPH production from the three aforementioned source. These measurements led the authors to conclude that about 40% of the NADPH required to compensate for the imbalance between NADPH depletion and formation in the wild type strain must come from a transhydrogenase activity, especially from the PntAB transhydrogenase (Figure 1-11). Another interesting outcome from this study was the observation that the Δ(*pgi udhA*) strain had lethal phenotype on glucose. Growth was recovered only upon plasmid expression of *udhA*. This result showed that the physiological role of SthA is to reoxidize the excess amounts of NADPH, restoring the imbalance of NADPH metabolism in the Δ*pgi* strain.

Besides the enzymes within the glucose-6-phosphate (G6P) node, enzymes related to phosphoenolpyruvate (PEP) node have also been examined for their ability to control the NADPH metabolism. One modification was the disruption of the *pykA* and *pykF* (Figure 1-12), which encode the two pyruvate kinases (PKs) in *E. coli*. Radiorespirometric assays by Ponce et al.[41] with resting cells of the mutant strain,

lacking both PKs, metabolized glucose mainly through the PP pathway. A reexamination of the same mutant by Emmerling et al. with METAFoR analysis by NMR confirmed the observation only in ammonia-limited chemostat cultures.[51] In glucose-limited cultures, similar or lower fluxes compared to parent strain were calculated for the PP pathway with concomitant higher fluxes for the TCA cycle, especially in the chemostat with the lower dilution rate. A single mutant Δ*pykF* strain examined by Al Zaid Siddiquee et al.[64] showed the same trend as the double mutant under non-growing conditions, i.e. elevated fluxes thought the PP pathway. In addition, activation of the malic enzyme with a flux about 10% towards the formation of PYR from MAL was calculated.

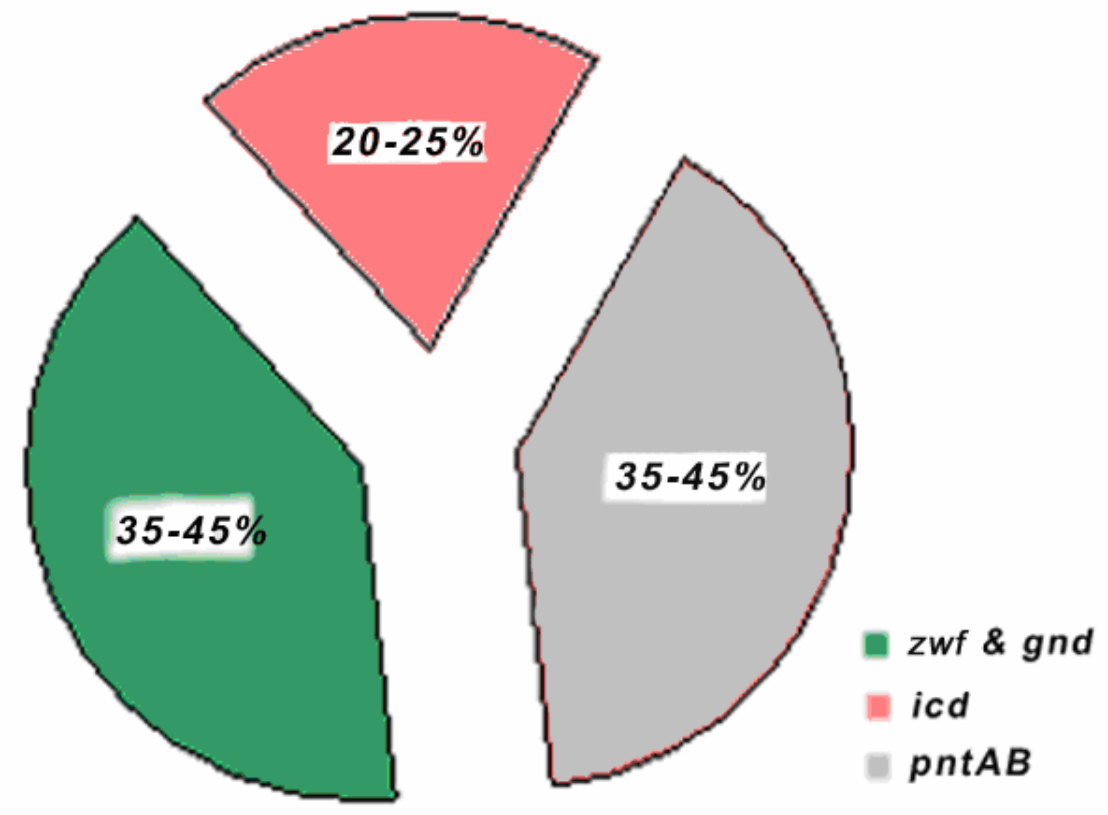

Figure 1-11. The percent of NADPH produced by PP pathway, TCA cycle and PntAB transhydrogenase activity in *E. coli* during standard aerobic batch growth on glucose. (Adapted from reference 66).

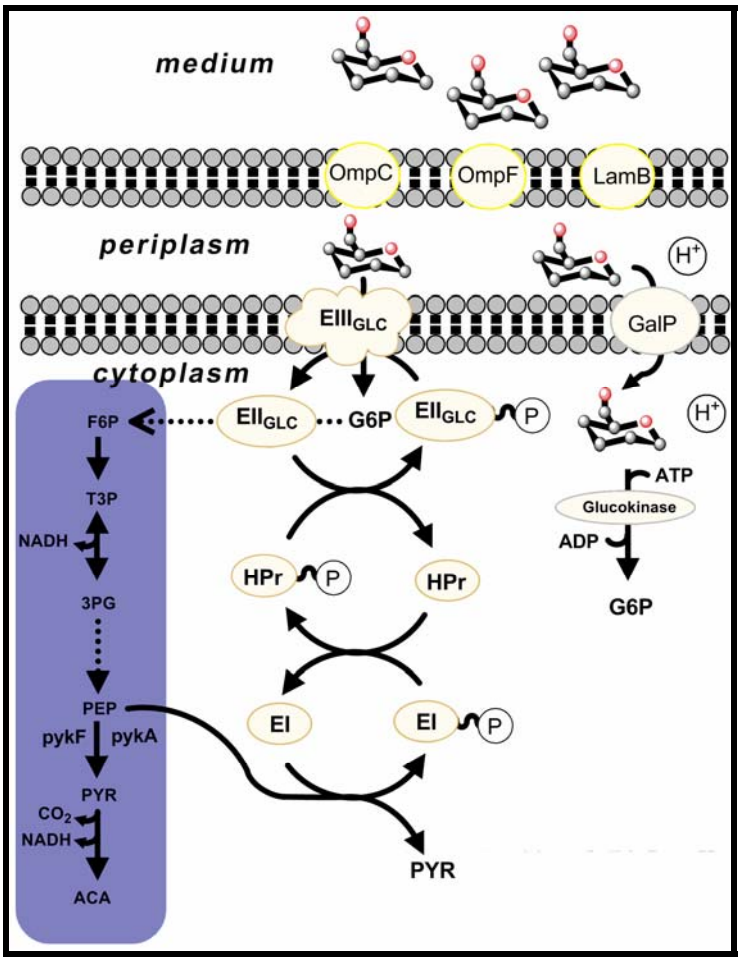

Figure 1-12. Glucose transport systems in *E. coli*. The phosphoenolpyruvate: carbohydrate phosphotranferase system (PTS) and the galactose permaese (GalP) system. (Adapted from reference 94)

Another modification around the PEP node was the disruption the of phosphotranferase transport system (PTS) which consumes at least 50% of PEP.[94] Starting from a strain lacking PTS (PTS^-), which has a limited ability to grow on glucose, a method based on continuous culture was applied to select for mutants (PTS^-GLC^+) with growth rates similar to wild type strain JM101 (a functional *galP* gene is required for this phenotype, Figure 1-12). METAFoR analysis of ^{13}C-labeled amino acids by NMR revealed reduced carbon flux through the PP pathway and a 4-10% flux through the malic enzymes for the PTS^-GLC^+ mutant strain.[54] Interestingly, in the PST^-GLC^- mutant,

in which glucose transport capacity is 10 times lower than the wild type JM101 strain, twice higher flux via the PP pathway was observed compared to parent strain.

Other experimental methods: metabolic regulation analysis of NADPH related metabolic pathways at gene and protein expression level.

Two dimensional electrophoresis (2DE) is a powerful technique for separation of complex protein mixtures and based on their different MWs and pIs. Ultimately, regulation of metabolic fluxes depends on enzyme activity which depends, to some extent, on protein expression levels. Thus, the different protein expression levels under different physiological conditions can be estimated and correlated to regulation of metabolic pathways[95] by separating a protein mixture in the cell lysate by 2DE and quantifying each protein spot after electrophoresis. Utilizing this approach in combination with *in vitro* measurements of enzymes activities in *E. coli*, Peng and Shimizu found that the two proteins involved in the PP pathway and related to NADPH production, zwf and gnd, are down-regulated during microanaerobic growth in glucose medium.[56] This result was not a surprise because both enzymes were known to be subject of growth rate regulation, in fact the cells growth was quite slow under microanaerobic conditions. For isocitrate dehydrogenase, a source of NADPH in TCA cycle, the correlation of expression by activity was not linear since it is known that ICDH activity is regulated by reversible inactivation via phosphorylation. [96]

Another technique for monitoring metabolic regulation at gene expression level is the reverse transcription polymerase reaction (RT-PCR) analysis. It is currently the preferred method for quantifying mRNA due to its higher sensitivity compared to other RNA analysis techniques such as Northern blot. In addition, it is relatively easy to run: isolated RNA is used as a template in order for a retroviral reverse transcriptase to create a complementary DNA (a cDNA) transcript. This product is subjected to a common PCR, where in the exponential phase, the signal is proportional to the amount

of input RNA template or number of cycles. The measurements of relative changes in mRNA levels are reproducible as long as the PCR volumes are the same from tube to tube and the data are collected before the reaction reached a plateau. Finally, a standard curve is required to correlate the signal with the specific amount of mRNA. Kabir and Shimizu applied this approach, also known as semi-quantitative RT-PCR, to investigate patterns in a *pgi* knock-out *E. coli* strain expressing genes for poly(3-hydoxybutyrate) (PHB) production (Figure 1-13).[57, 58]

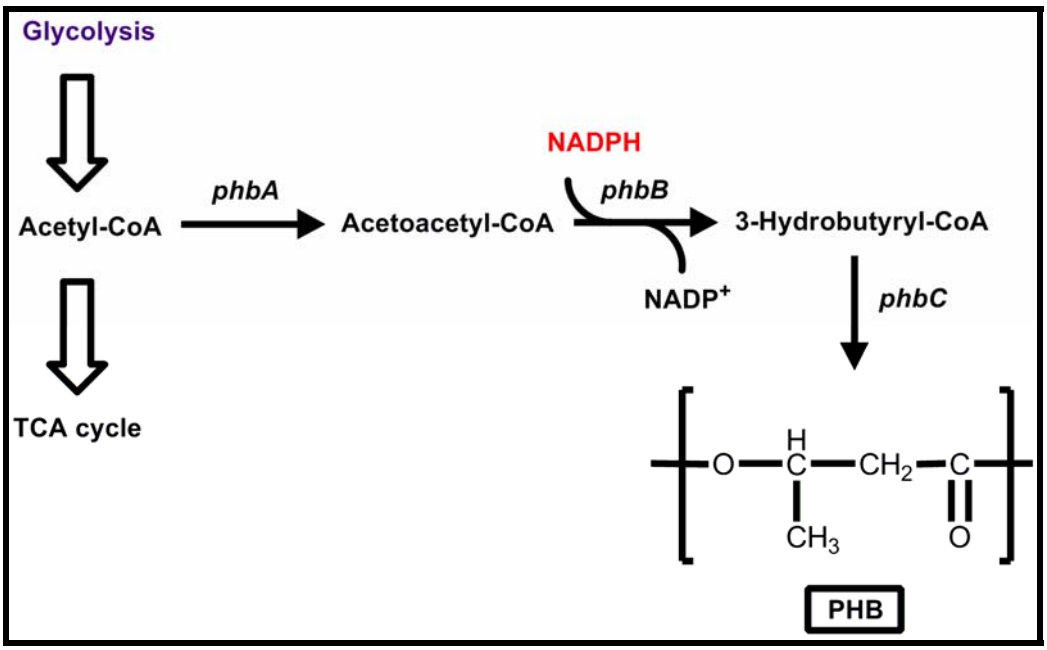

Figure 1-13. Poly(3-hydroxybutyrate) PHB synthesis: the acetoacetyl-CoA synthase requires NADPH.

Sauer's group had shown that the deleterious effect on cell growth caused by the NADPH imbalance in *the pgi E. coli* mutant can be partially compensated by expressing an enzyme consuming NADPH such as SthA. A similar consequence may have the expression of the acetoacetyl-CoA synthase in Shimizu's studies, which also requires NADPH. Indeed, expression of *phbB* in *E. coli* (*Δpgi*) increased the true cell mass by about 19%. Further measurements of NADPH concentrations confirmed the higher levels of NADPH in the mutant strain without *phbB* compared to the PHB producer

strain. The transcript level analysis of 87 central metabolic pathway genes revealed upregulation of most of the genes in PP pathway except *gnd*. The most interesting observation from this proteome analysis study was the absence of *ptsG*, which encodes for a protein that is a component of PTS system, in 2DE gel for both *pgi* mutants even though the RT-PCR revealed the presence of *ptsG* transcript in both cases. This result led the authors to propose that the mutation of pgi affects *ptsG* expression after transcription initiation and an RNAaseE-mediated degradation of *ptsG* transcript[97] might be another reason for lower glucose consumption rates in this mutant.

Experimental methods: limitations

Undoubtedly, the experimental techniques discussed in the second part of this chapter offer a more holistic picture of the NADPH regeneration sources in *E. coli*; however, possible limitations and pitfalls of them must be encountered. Specifically for the ^{13}C metabolic flux analysis:

- METAFoR analysis fails in the case that two alternative pathways operate according to the same carbon-carbon bond rearrangements.
- METAFoR analysis of ^{13}C NMR and/or GC-MS data provides direct evidence for a particular flux or reaction in a metabolic network, but only ratios between fluxes around a metabolic node can be calculated. In order for the absolute intracellular fluxes to be estimated, ^{13}C isotopic measurements must be applied, in parallel, with the theoretical approach of FBA, in which the ^{13}C data are acting as additional constraints.[51] As a consequence, prerequisites stated above for the FBA to be valid must be followed here as well.
- The merging of METAFoR analysis and FBA requires 'heavy' mathematical and computational analysis[98] which is usually performed by specially designed software with little interaction between the program and the experimentalist.[99]
- Isotope abundances calculated from ^{13}C data should be independent of possible limitations of the technique used for their derivatization such as ^{13}C spin relaxation, strong spin-spin coupling effects, ^{13}C isotope effects on carbon chemical shifts, isotope fractionation of the amino acids during the GC separation and nonlinearity of the MS detector response at different mass isotopomer ratios or different sample concentrations.[78]
- In addition to a known metabolic network, ^{13}C isotope effects on metabolic reactions must be negligible and metabolite channeling (i.e., when an intermediate

metabolite is transferred from one enzyme to the other without previous equilibration with the rest of the molecules in the medium) should be absent.[100]

- The accuracy of ^{13}C data depends on the $^{13}C/^{12}C$ glucose with higher accuracy at a ratio of 50:50. The relative high cost of labeled sugars usually prohibits this type of experiments.

- The METAFoR analysis based on NMR data is quite laborious, time-consuming and expensive due to low sensitivity of the technique: about 300-400 ml of sample and 4-5 days are required before the calculation of the first set of data.[101] In recent years, the problem was partially bypassed with the use of the GC-MS, but interpretation of the MS data is more complicated.

- The ^{13}C metabolic flux analysis is currently restricted to two physiological conditions: continuous cultures and exponentially growing cells, because isotopic equilibrium must be established before the first measurement.

- Last but not least this approach is not applicable in biological systems like resting cells performing biotransformations, due to insufficient *de novo* synthesis of biomass.[87]

2DE and RT-PCR, are still in their infancy. A common problem associated with 2DE is the identification of each spot. Amino acid sequencing and enzyme activities must be employed in parallel for the 2DE data to be justified. The RT-PCR is, in principle, a quick and extremely sensitive technique, but many parameters concerning the amount of PCR ingredients and the duration of PCR cycles must be verified and controlled carefully in advance. The design and quality of primers is also of paramount importance since genomic DNA contamination in a RNA preparation may be amplified too and produced false positives. Both techniques fail to detect post-translational regulation of enzymes and become extremely costly if we consider all the additional control experiments that are required for their justification.

Conclusion

The aim of this chapter was to demonstrate the different tools and methods that researchers used the last six decades in order to answer two key questions regarding the NADPH metabolism in *E. coli*: Which are all the possible sources of NADPH in *E. coli*? Most probably those five depicted in Figure 1-2. To which extent each source

does contribute to the total NADPH pool? Unfortunately, as our discussion and a quick look at the last column of Table 1-1 and Table 1-2 revealed a global answer does not exist. In fact, the answer is another question: under which physiological conditions and based on which genetic background we are seeking for an answer? Different *E. coli* strains, in different environments, are using some or all of the abovementioned NADPH sources to a different degree in order to accommodate their needs. This statement may satisfy a physiologist who is trying to understand how a biological system works. Definitely, it does not fulfill the ambitions of a metabolic engineer:

> Metabolic engineering is the improvement of cellular activities by manipulation of enzymatic, transport and regulatory functions of the cell with the use of recombinant DNA technology.
> [Toward a Science of Metabolic Engineering, James E. Bailey][102]

In the next chapter, a couple of examples related to metabolic engineering of NADPH redox metabolism in *E. coli* will be introduced. A particular interesting case in redox biocatalysis, in which the NAPDH regeneration machinery of resting *E. coli* cells was used to produce a chiral compound in a gram-scale level will be discussed in detail.

CHAPTER 2
INVESTIGATION OF NAPDH REGENERATION SOURCES IN RESTING *ESCHERICHIA COLI* CELLS ENGINEERED TO OVERPRODUCE A NAPDH-DEPENDENT KETOREDUCTASE

> So far, the more valuable products, chiral building blocks for the synthesis of pharmaceuticals, flavors and agrochemicals, are potentially obtained with NADPH-dependant enzymes.
>
> -Andreas Liese, Head of Institute of Technical Biocatalysis at TUHH[103]

Introduction

NAPDH is an extremely 'high-priced' hydride donor for an *E. coli* cell as well as for an organic chemist when stoichiometric amounts of it are required (Table 2-1 and Figure 2-1). Therefore, a reductive reaction would be economically feasible only upon regeneration of the core molecule at the expense of another cheaper reductive source. For example, the biosynthesis of one gram CDW (cell dry weight) of *E.coli* cells requires more than 15 mmols of NADPH; however, this amount of biomass barely contains 0.0014 mmols of the reduced cofactor.[104] In other words, the same nicotinamide molecule has been recycled more than 10,000 times during this process, usually at the expense of a carbon source such as glucose.

Accordingly, a plethora of ingenious NAD(P)H regeneration strategies have been employed by researchers who are exploring the possibility to use a NAD(P)H-dependent reductase in their asymmetric synthesis. Modifying slightly the original classification by Chenault and Whitesides,[105] we should recognize that among the four general regeneration strategies (Figure 2-1): chemical, photochemical, electrochemical and biological, only the latter has unlimited compatibility with biological systems. In between the enzymatic and microbiological methods, the former has found a great deal of applications in laboratory as well as in industrial scale, especially when the regeneration

of NADH is utilized.[106] In contrast, the NADPH regeneration techniques are lagging behind.

Table 2-1. Cost of nicotinamide cofactors and their content in *E. coli.*

Cofactor	MW	Cost[a] ($/g)	Specific cost ($/mmol of delivered [H])	Number of molecules per *E. coli* cell[b]	Intracellular molarity (mM)[b]	Cofactor content in *E. coli* (μmol/g CDW)[c]
NADPH · Na_4 (~95%)	833.35	837	697	250,000	0.22	1.370
NADP+ · Na (≥95%)	765.39	211	161	190,000	0.17	1.041
NADH · Na_2 (~95%)	709.4	70	50	440,000	0.90	2.411
NAD+ · Na (~95%)	685.45	30	20	1,000,000	0.40	5.479

[a]Based on Sigma-Aldrich catalog (2006)[107] [b]Adapted from reference 104 [c]Assuming that the mass of one cell is 3.0×10^{-13} g (DW).[108]

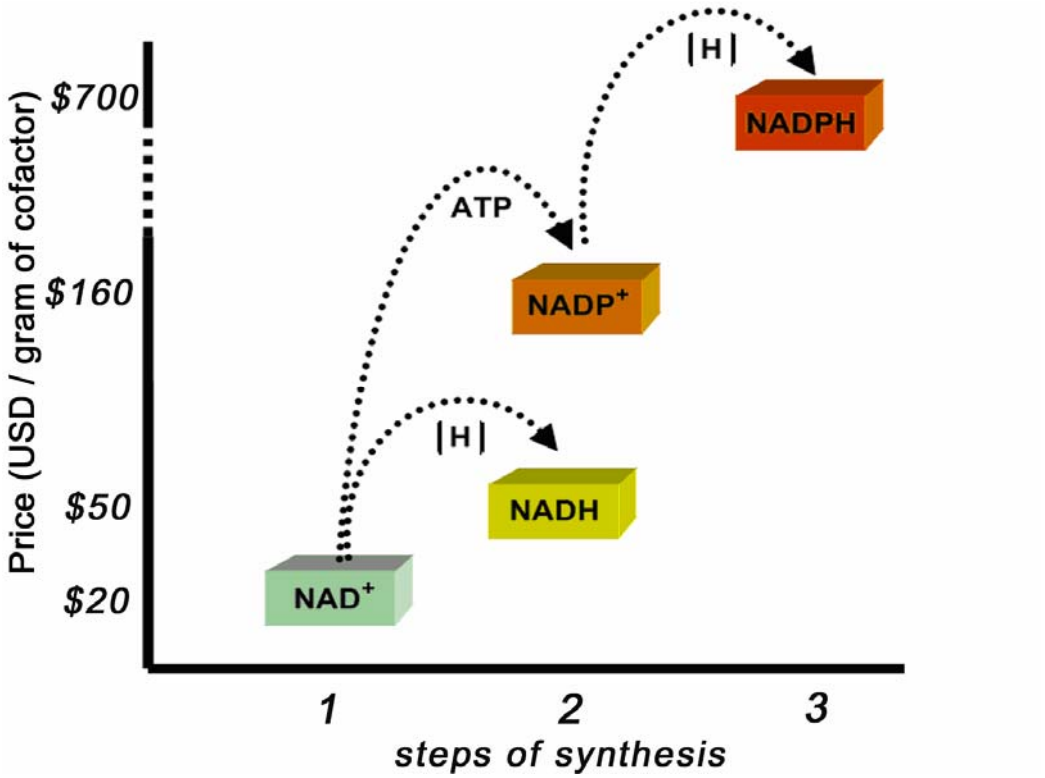

Figure 2-1. Explanation of the relative prices among nicotinamide cofactors.[109] Step 1: Isolation of NAD^+ from bakers' yeast (1mmol/0.55kg CDW). Step 2: Reduction or phosphorylation of NAD^+ leads to NADH or $NADP^+$ respectively. Step 3: Reduction of $NADP^+$ produces NADPH. Depending on the pH, NAPDH is 3 to 10 times less stable than NADH.

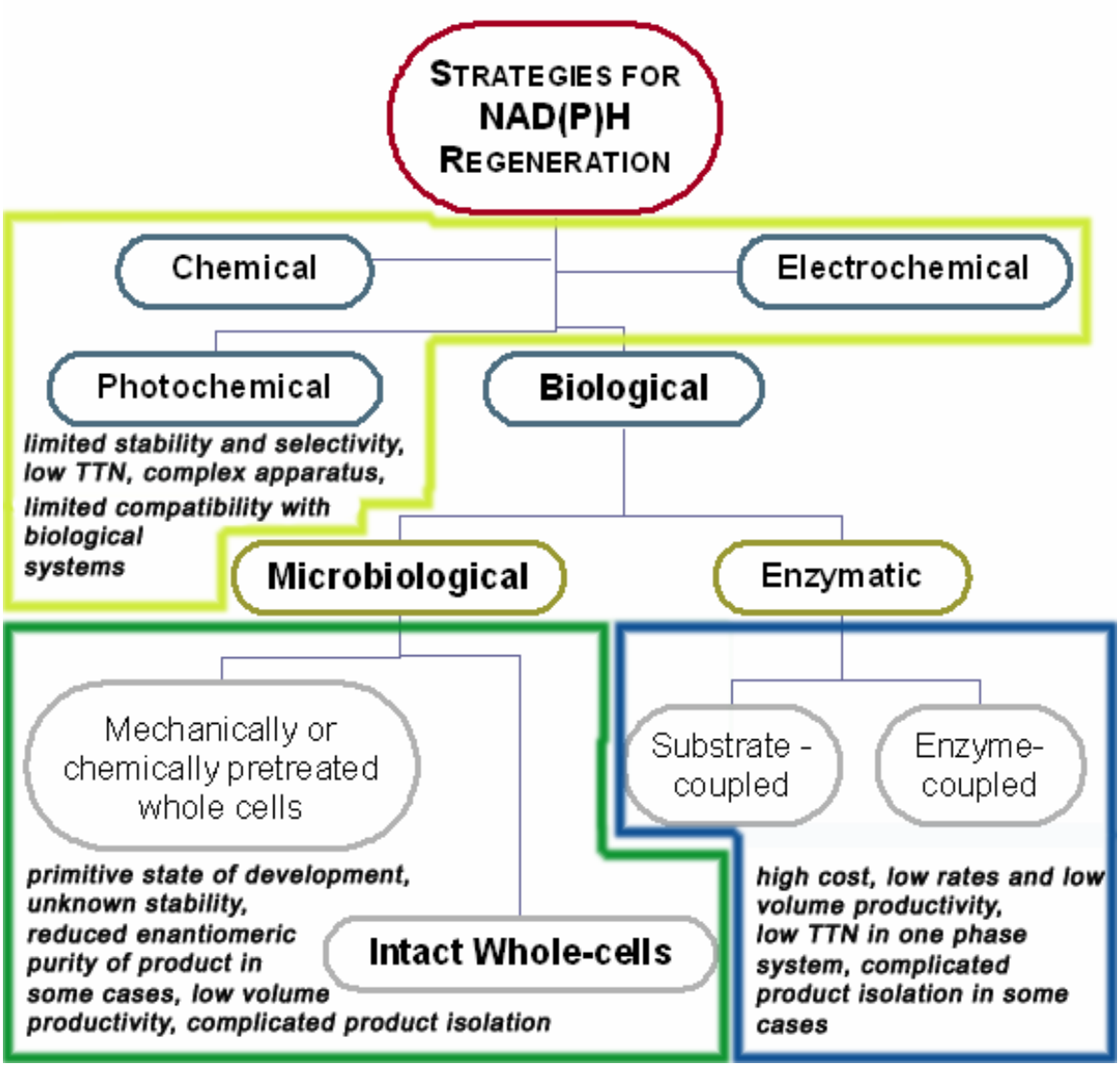

Figure 2-2. NAD(P)H regeneration strategies and major disadvantages for each method. (Adapted from reference 106)

The aim of this introduction is not to extensively review all the NAP(D)H regenerations methods, since this has been done recently.[106, 110] In contrast, by selectively analyzing a few examples from the current literature, we will acknowledge the limitations of the enzymatic strategies in NAPDH regeneration, and we will point out the importance of the experimental work that follows.

Examples of Enzymatic NADPH Regeneration Methods

A substrate-coupled NADPH regeneration scheme, like the one depicted in Figure 2-3, is probably the most self-sufficient method in this category. In the presence of excess isopropanol, a recombinant alcohol dehydrogenase from *Lactobacillus brevis* (LBADH) reduced catalytic amounts of $NAPD^+$ and simultaneously acted as an excellent regio- and enantio-selective reductive catalyst on a number of 3,5-dioxocarboxylates.[111] Unfortunately, the method is limited by the enzyme's substrate specificity. Thus, when the opposite enantiomer was the desired product, the same researchers switched to one of the most well-established,[112] enzyme-coupled, regeneration systems using glucose-6-phoshate as a sacrificial cosubstrate (Figure 2-4).[113] The subsequent hydrolysis of the corresponding lactone renders the reaction irreversible in this approach.

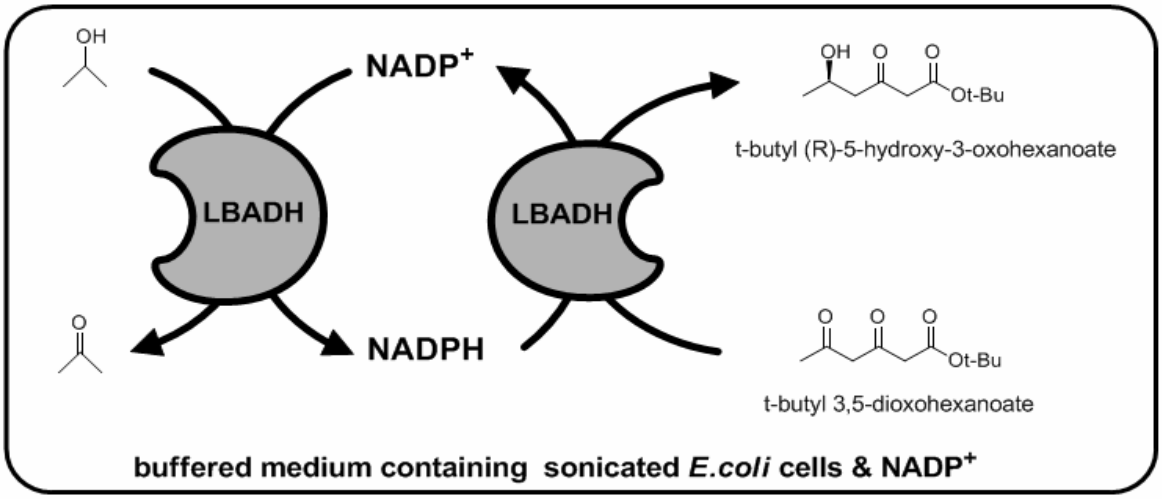

Figure 2-3. A substrate-coupled enzymatic regeneration method for NADPH.

Due to the relatively high cost of phosphorylated glucose, G6PDH has been replaced the recent years by glucose dehydrogenase (GDH), which accepts glucose as reductant (Figure 2-5).[114] Unfortunately, the net benefit from this replacement, in terms of cost, is negligible due to a much higher price of GDH compared to that of G6PDH.

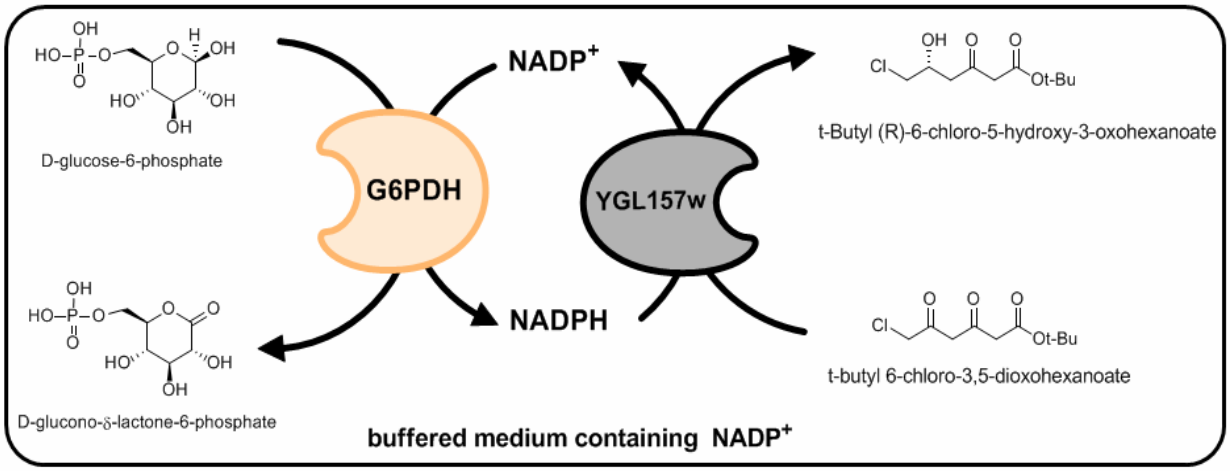

Figure 2-4. Glucose-6-phosphate dehydrogenase (G6PDH) as an auxiliary enzyme.

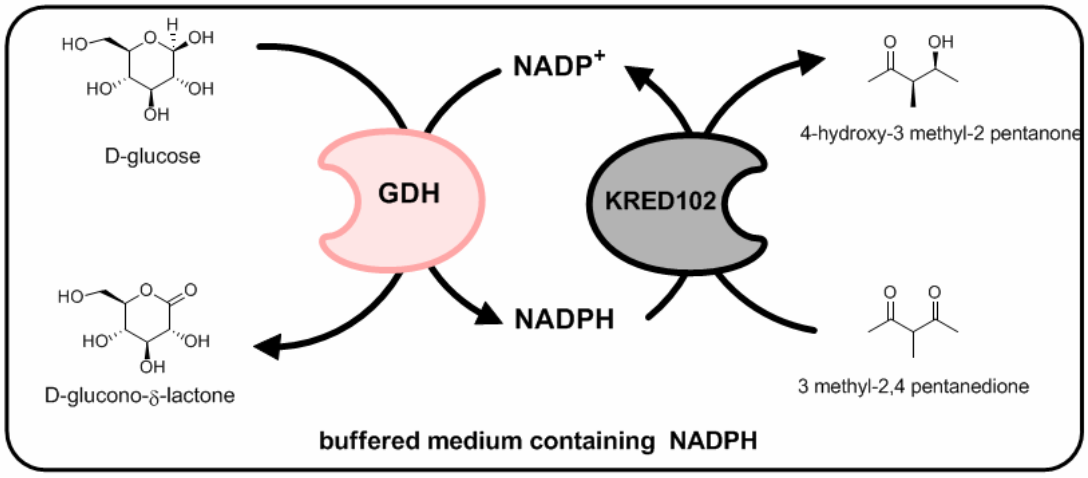

Figure 2-5. Glucose-6-phosphate dehygrogenase as an NAPDH regeneration catalyst.

Another concern about G(6P)DH regeneration systems is that both produce stoichiometric amounts of gluconic acid, which may impede the downstream purification process. To circumvent this issue, two routes have been explored so far: i) the use of a hydrogenase, which regenerates NADPH at the expense of the cheapest reducing agent, dihydrogen[103] (Figure 2-6) and ii) the change of an enzyme's cofactor 'diet' from NAD^+ to $NADP^+$. The latter approach was first attempted for formate dehydrogenase (FDH), which releases CO_2 as the only by-product.[115] The first $NADP^+$-dependant FDH from *Pseudomonas sp.* (mut-Pse FDH) is commercially available from Jülich Chiral Solution GmbH at a cost similar to GDH.[116] In addition, a phosphite dehydrogenase

(PTDH) has been converted to an $NADP^+$ dependent enzyme with promising characteristics since phosphite is a very low cost reductant and the only by-product in this case is a phosphate ion.[117] However, to the best of our knowledge, none of the three abovementioned systems have been applied to a larger, at least 1 mmol, reaction scale and thus we will not consider them further.

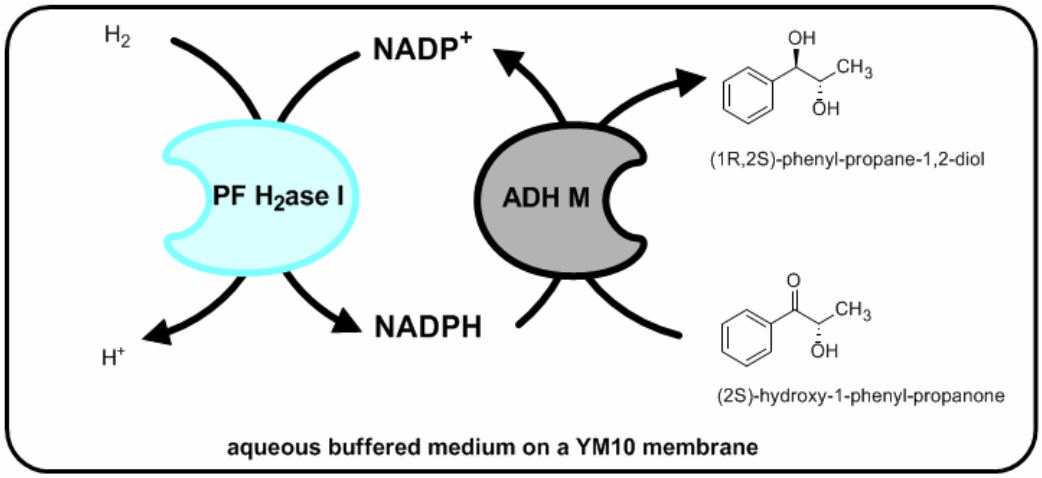

Figure 2-6. Hydrogenase I from *Pyrococcus furiosus* for NADPH regeneration.

Examples of Microbiological NADPH Regeneration Methods

Under the umbrella of microbiological regeneration techniques, we may recognize two slightly different approaches, one in which the permeabilization of the cell membrane is intended and the other in which the *E. coli* cells are considered as absolutely self-contained bioreactors. This feature implies that the cells are metabolically active and thus the integrity of their membrane is a prerequisite for a successful biotransformation.

Permeabilized *E.coli* cells

In one of the first examples of permeabilized *E. coli* cells, Kataoka et al.[118] grew separately two JM109 *E. coli* strains, one overexpressing a GDH from *Bacillus megaterium* and another overproducing an aldehyde reductase from *Sporobolomyces salmonicolon* (Figure 2-7). The harvested cells were mixed together in different ratios and resuspended in potassium phosphate buffer containing catalytic amounts of $NADP^+$.

The presence of an organic layer of n-butyl-acetate rendered the cell membrane susceptible to the free transport of nicotinamides in between the two different strains.

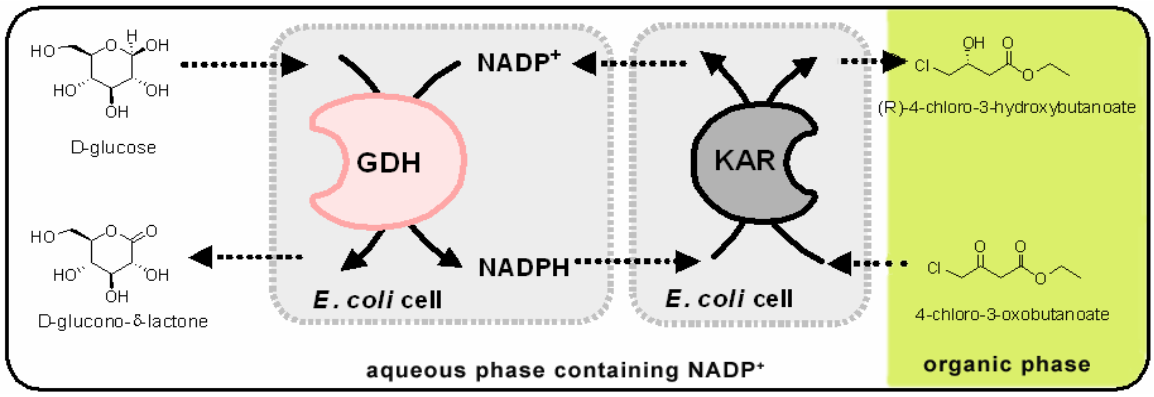

Figure 2-7. An example of two coupled *E. coli* strains in a two-phase system.

A slightly modified approach will be the overproduction of both the auxiliary enzyme and a reductase in the same *E. coli* cell (Figure 2-8). Ema et al.[119] applied this concept coupling the regeneration of NADPH by GDH with the reduction of 2, 4 octanedione by the Gre2 from *Saccharomyces cerevisiae*. Even though a disruption of cell membrane or a pretreatment of the cells with organic solvent was not employed in this case, the authors reported that they froze the cells at -20°C before their utilization. Hence, a semi-permeabilization of the cell membrane could be assumed due to this treatment. Interestingly, a 10% conversion was observed even with cells that overexpressed only Gre2.

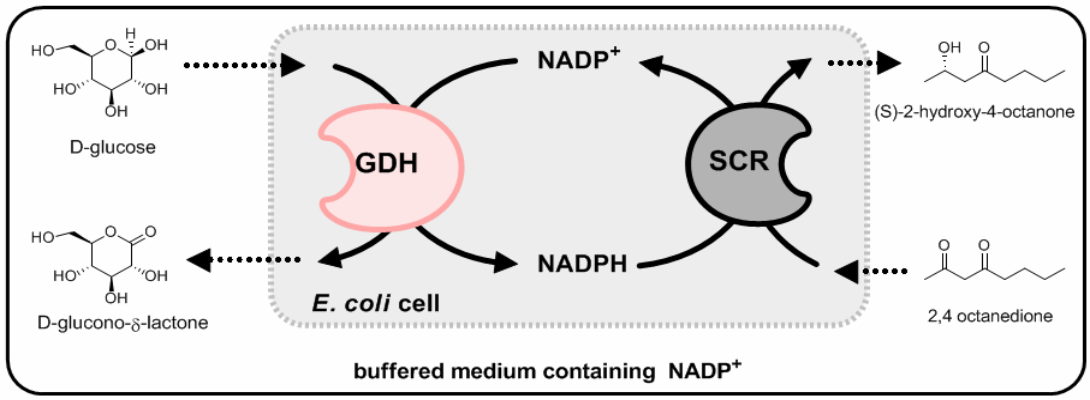

Figure 2-8. An example of an *E. coli* cell overexpressing both GDH and a reductase.

A more complex scenario is depicted in Figure 2-9. In this case the authors tried to couple the most popular auxiliary enzyme for the regeneration of NADH (i.e. formate dehydrogenase (FDH) from *Candida boidinii*) with the recombinant membrane-bound transhydrogenase from *E. coli* (PNTAB) which in turn shuttled the hydride from NADH to $NADP^+$.[120] The NADPH produced was used by an alcohol dehydrogenase (ADH from *Lactobacillus kefir*) for the reduction of acetophenone. The whole process was carried out in the same *E. coli* cell, permeabilized with 1% toluene. Unfortunately, no application on a larger scale (i.e. > 1mmol) is reported for this system.

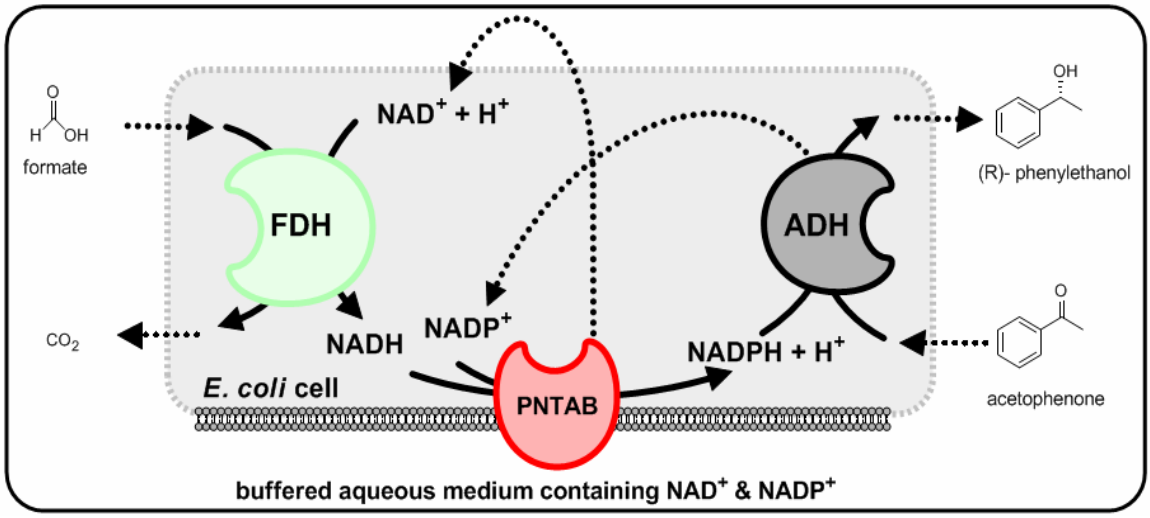

Figure 2-9. An example of an *E. coli* cell overexpressing two auxiliary enzymes and a reductase.

Surprisingly, Xu et al.[121] reported recently that under optimal conditions, a two strain system similar to the one developed by Kataoka et al., is able to perform the same bioconversion without the addition of an organic solvent and/or extra $NADP^+$. In this example, the overproduction of GDH in the first *E. coli* strain with the aid of high concentrations of 4-chloro-3-oxobutanoate caused an efflux of NADPH into the medium in the presence of glucose. Subsequently, the reduced nicotinamide was transferred into the second *E. coli* strain which is responsible for the transformation of the keto-ester to the corresponding chiral alcohol (Figure 2-10). A transmembrane transportation of

NADPH was hypothesized and the percentage conversion found dependent on the initial concentration of the ketone with higher conversions at higher concentrations. It is worth noting that external addition of $NADP^+$ did not improve the bioconversion in the two strain system but was found necessary when a one strain system, overexpressing both auxiliary and alcohol dehydrogenase, was utilized.

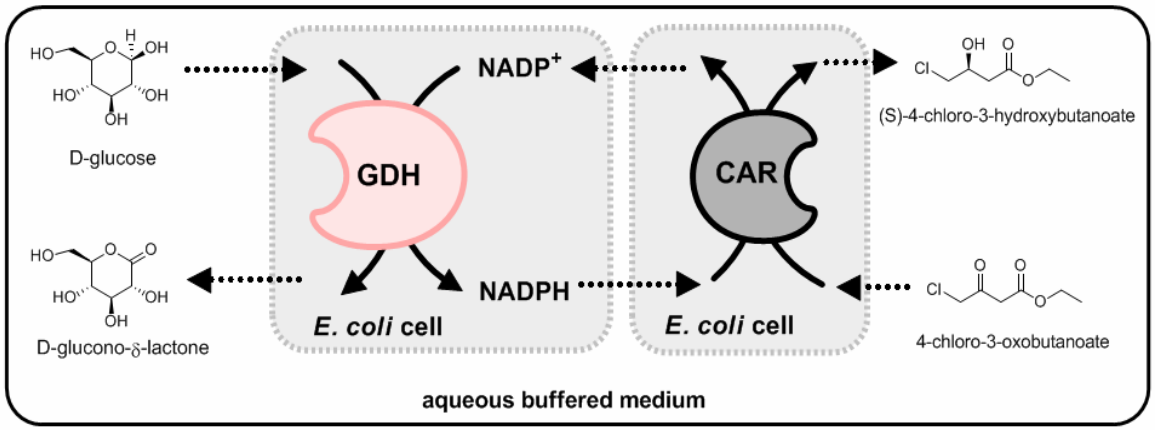

Figure 2-10. An example of two *E. coli* strains coupled for regeneration of NADPH in one phase system.

Intact *E.coli* whole cells

In 2004, Walton and Stewart reported one of the most self-sufficient systems in this category.[122] In this approach, the workers relied absolutely on the *E. coli* metabolism for the NADPH regeneration without the need to overexpress any auxiliary enzyme and/or add extra amounts of $NADP(^+/H)$ in the aqueous medium (Figure 2-11). Additionally, this example is one of the rare cases where the amount of sacrificial substrate (i.e. glucose) added is not in excess, as compared to the amount of product made. The overproduced reductase was Gre2 from bakers' yeast.

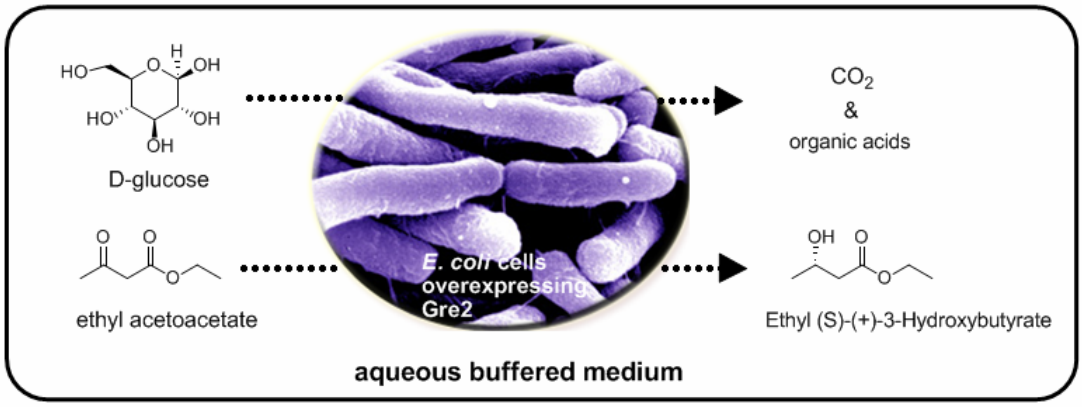

Figure 2-11. An example of intact *E. coli* cells capable to regenerate NADPH for ethyl acetoacetate reduction by a ketoreductase.

A more sophisticated *E. coli* strain (SC16529) was developed by Hanson and coworkers[123] to meet the needs for the production of a chiral chloro-alcohol (Figure 2-12) on a large scale. In this case, G6PDH from *Saccharomyces cerevisiae* was overexpressed with a ketoreductase from *Hansenula polymorpha* in the same *E. coli* cell. The authors relied on the *E. coli*'s PTS activity for the phosphorylation of glucose. However, the addition of catalytic amounts of $NADP^+$ was found necessary for the completion of this biotransformation.

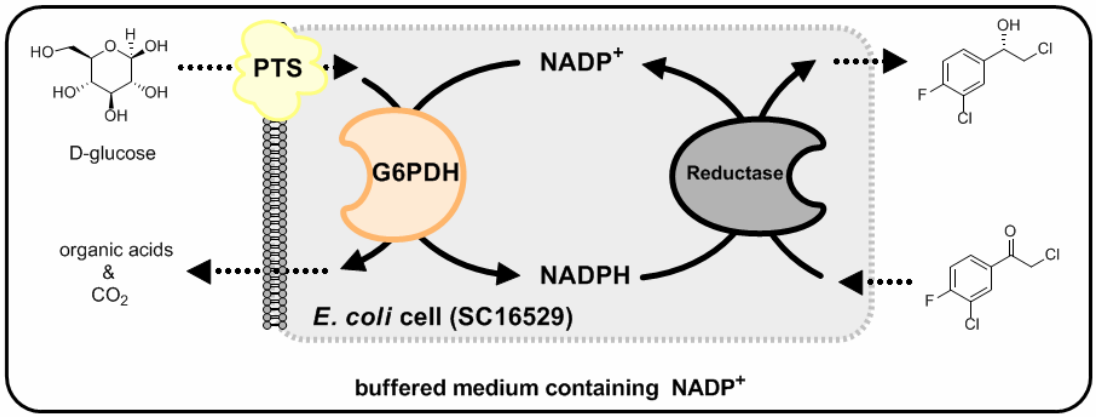

Figure 2-12. An example of intact *E. coli* cells overexpressing a G6PDH and a reductase.

Economical Analysis

How the different NADPH regeneration approaches could be evaluated from an economical perspective? A very informative parameter regarding this issue is the total turnover number (TTN), which is defined as the molar amount of product made by the end of the reaction per molar amount of cofactor used.[124] This number embraces several factors such as the relative stability of the cofactor under the reaction conditions, the reaction time-frame and the catalysts turnover number.[125] It is apparent from the Figure 2-13 that the higher the TTN, the more cost-efficient the bioprocess is. As proof, we present a cost analysis of the aforementioned examples and a tabulation of the corresponding TTN for each of them in Table 2-2. An estimation of intracellular NADP($^+$/H) content has to be made for those cases that whole cells were used. For this calculation we assumed 440,000 molecules of NADP($^+$/H) per *E. coli* cell.

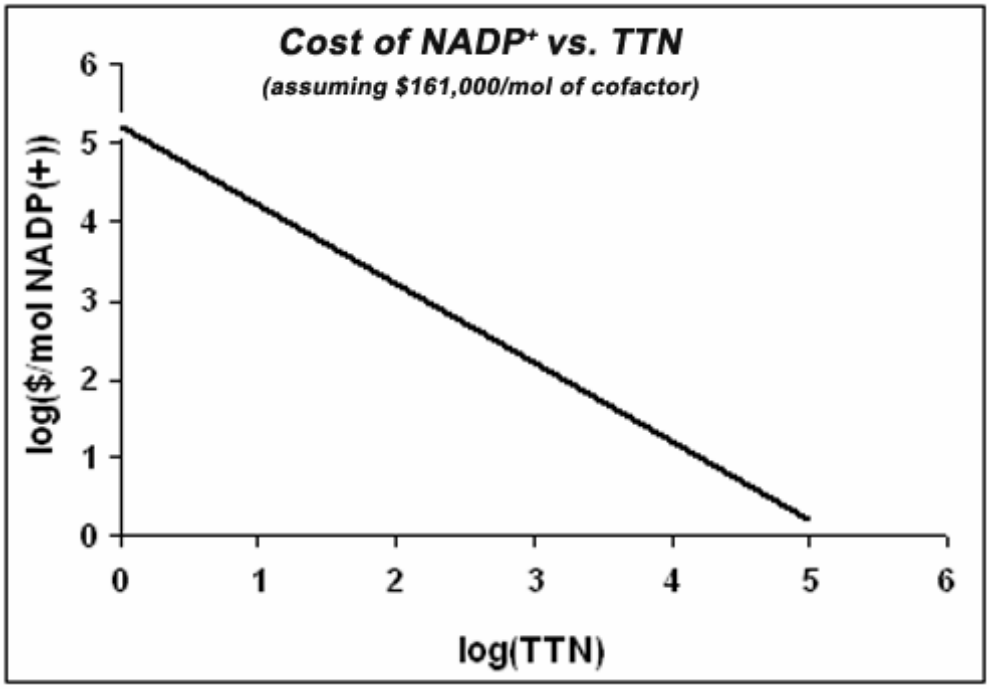

Figure 2-13. Cost of NADP$^+$ as a function of TTN.

Table 2-2. Cost analysis of different NADPH regeneration methods and tabulation of TTNs.

Year (ref.)	Cofactor used (amount, cost)	Sacrificial substrate (amount, cost)	Auxiliary enzyme (amount, cost)	Biomass in grams (cost)[a]	Theoretical Yield in mmols (Total cost)	Productivity (mmol h^{-1} g^{-1} CDW)	Specific Cost ($/mol)	TTN
1998 (118)	$NADP^+$ (0.019 mmol, $3.1)	glucose (166 mmol, ngl)	GDH[b] (261U, ngl)	3 ($4.5)	83.6[c] ($7.6)	4.2	100	3,980[d,o]
2000 (111)	$NADP^+$ (0.033 mmol, $5.3)	acetone (66 mmol, ngl)	recLBADH (600U, $39)[m]	---	9.9[e] ($44.3)	---	4,400	300[f]
2004 (113)	$NADP^+$ (0.17 mmol, ($27.3)	G6P[g] (4.4 mmol, $140)	G6PDH[g] (2mg, $100)	---	2.8[e] ($267)	---	95,000	16.5[f]
2004 (122)	---	glucose (216 mmol, ngl)	---	17.5 ($26)	348[j] ($26)	7.0	70	27,840[f,n]
2005 (114)	NADPH (0.05 mmol, $35)	glucose (10 mmol, ngl)	GDH[h] (50mg, $395)	---	4[i] ($410)	---	103,000	80[f]
2005 (123)	$NADP^+$ (0.15 mmol, $24)	glucose (167 mmol, ngl)	G6PDH (na, ngl)	75 ($112.5)	72.4[l] ($136.5)	0.13	1,890	337[d,o]
2006 (119)	$NADP^+$ (0.012 mmol, $ 1.9)	glucose (8mmol, ngl)	GDH (na, ngl)	2 ($3)	4.0[k]($ 4.9)	0.7	1,200	296[d,o]
2006 (121)	---	glucose (10mmol, ngl)	GDH (27U, ngl)	0.22 ($0.2)	5.7[c]($ 0.2)	7.8	30	35,625[d,n]

[a] Assuming $1.5/g (wet weight). [b] In-house prepared. [c] Product recovery was not attempted. [d] Optimized conditions. [e] 77% recovered product. [f] not optimized conditions. [g] Based on Sigma-Aldrich catalog (2006).[107] [h] Based on Biocatalytics Inc. catalog (2006).[106] [l] 90% recovered product. [j] 76% purified product. [k] 71% recovered product. [l] 89% recovered product.[m] Based on Jülich Chiral Solution GmbH catalog (2006).[116] [n] For this calculation, the sum of $NADP^+$ and NADPH pool is considered based on the values given in Table 1 and assuming that the mass of one cell is $1.0x10^{-12}$ g (wet weight).[108] [o] Based on the $NADP^+$ added and $NADP(^+/H)$ content of biomass used. Abbreviations: ngl, negligible; na, not applicable.

The major conclusions from this analysis are:

- Regeneration methods based on pure auxiliary enzymes are too expensive even on a gram-scale reaction. Only in-house prepared crude extracts of overexpressed proteins might accommodate the problem.[127]
- A substrate-coupled regeneration method may be affordable if a TTN of 300 or higher is achieved and a high-value product is produced.
- The utilization of whole cells, intact or permeabilized, is the only foreseeable avenue for the large-scale production of fine chemicals, in which NADPH is mediated. This is particularly true for low-value chemicals.
- The misconception that an *E. coli* cell does not contain an efficient NADPH-regeneration system is a myth,[128] at least for NADPH regeneration rates in the order of 120 U/g (CDW).

At the moment, several different methods that utilize *E. coli* whole cells overproducing oxidoreductases are under development. Therefore, caution must be paid when we are evaluating data such as the one presented in the first and the last row of Table 2-2 since isolated yields were not reported and the reaction scale in the last case was quite low (< 10 mmol). We should also be aware of a possible failure to repeat successful stories as the one presented in the forth row of Table 2-2 with substrates that may interfere with the intracellular metabolism of *E. coli* or they could not access the cell's membrane.

We also should not mislead the reader by making her or him believe that the TTN is the only effector on the final cost of a large-scale bioprocess. Useful reviews[129-131] and discussions[132, 133] exist in the literature about other factors that should be evaluated before a biocatalytic process could be considered successful, but they are beyond the scope of this introduction.

Manipulations of NADP(H/$^+$) Levels in *E. coli* towards the Improvement of Biotechnological Processes

A number of researchers have studied the manipulation of the redox-metabolism in various microorganisms hoping to improve the biosynthesis of metabolites of industrial importance.[134-137] However, similar efforts in *E. coli* are rare[138, 139] In one of them, Flores et al.[140] tried to determine if the overexpression of *zwf* in an *E. coli* JM101 strain could

overcome the metabolic burden imposed on it by the presence of a high copy plasmid. Often, plasmid-DNA replication and synthesis of plasmid-encoded proteins reduce the growth rate of the producing culture. By increasing the expression of zwf and hence increasing the carbon flux through the PP pathway, the authors were able to partially recover the growth capabilities of an *E. coli* strain harboring a multicopy plasmid responsible for the production of a recombinant TrpLE-proinsulin peptide. The growth-rate values were three times higher upon overexpression of zwf, but still twice lower than the rates for the wild type. When the degree of *zwf* gene induction was altered from 3 to 100 times in terms of higher levels of zwf expression, it was found that an overexpression as little as three fold was adequate for the growth-rate of the strain overproducing the TrpLE-proinsulin to reach a plateau. Unfortunately, it is not clear from this study if NADPH or another metabolite from the oxidative part of PP pathway, which might be produced in excess, was responsible for the observed results.

The second example is related to biosynthesis of the biodegradable polymer PHB from acetyl-CoA (Figure 1-13). The process requires one equivalent of NAPDH from each unit attached to the polymer. Lim et al.[141] constructed plasmids containing *zwf* or *gnd* co-integrated with the *phb* operon and introduced them into *E. coli*. The amount of PHB increased after expressing the genes, especially *zwf*. However, this increment may be due to altered NADPH/$NADP^+$ (i.e. six times higher compared to wild type), or redirection of the flux through the AcCoA, or the increased activity (i.e. 1.16-1.30 fold) of all the enzymes involved in PHB synthesis upon zwf overexpression. Again, which one was the crucial parameter was not clear from this study.

In a very recent study Sánchez et al.[142] followed a different approach to tackle the same problem. They overexpressed the soluble pyridine transhydrogenase, UdhA, in order to increase the yield and productivity of PHB in *E. coli*. The outcome from this manipulation is crystal clear: almost double yield of PHB obtained in the strain

overproducing UdhA (Table 2-3). However, their discussion about the reason behind this outcome is controversial. The authors stated that by inducing a high level of UdhA, they increased the NADPH availability and thus the yield and productivity of PHB. They also commented that the drop of NADPH/$NADP^+$ with the concomitant increment of NADH/NAD^+ in the UdhA overexpressing strain suggests a depletion of NADPH pool and a higher NADH conversion rate matched with the PHB formation demands. Recalling, though, our discussion in the first chapter about the physiological role of UdhA (i.e., transfer of hydrides from NADPH to NAD^+) we can also arrive at the same observations about the nicotinamide ratios in this example (Table 2-3). Nevertheless, this is the first example in the literature in which a NADPH manipulation in *E. coli* caused increased productivity of a NADPH-dependent compound. Also, it is worth noting the high TTN that this system reached. Analogous studies overexpressing the membrane-bound transhydrogenase, PNTAB, for the overproduction of xylitol in *E. coli* have not yet been fruitful.[143]

Table 2-3. Cofactor levels of PHB producing strains and tabulation of TTN.

Strain	Total yield (mmol g^{-1} DCW)	Productivity (mmol h^{-1} g^{-1} DCW)	NADPH (NADH) (µmol/gDWC)	$NAPD^+$ (NAD^+) (µmol/gDWC)	NADPH /$NADP^+$ (NADH/NAD^+)	TTN[C]
Control[a]	11.4	0.44	0.375 (0.6)	0.165 (2.6)	2.27 (0.23)	21,111
GJT001	22.8	0.88	0.250 (0.9)	0.185 (2.0)	1.35 (0.45)	52,413

[a] Expressing only *phb* operon. [b] Expressing both *phb* and *udhA*. [c] Based on the calculated $NADP(^+/H)$ content.

Description of the System under Study

In all three aforementioned examples, the merits of the NADPH perturbations to the obtained results are not clear due to the fact that the provided carbon source contributes to bioprocess not only by providing reducing equivalents but also by supplying carbon atoms to the final product with bits of carbon atoms. In contrast, a single-step biotransformation by a NADPH-dependant reductase like the one presented in Figure 2-11 has as a net gain only a pair of electrons and a proton, in the form of

hydride. Thus, it exclusively depends on a metabolically active NADPH regeneration system, without causing a drain to other intracellular metabolites.

In a preliminary attempt to shed light on the NADPH regeneration system within a resting *E. coli* cell during the course of a redox enzymatic reaction Walton and Stewart made the following observations:

- The profile of glucose consumption by the resting *E. coli* cells was the same in the presence and in the absence of the biotransformed starting material, in otherwise identical conditions.
- Both [NADH]/[NAD^+] and [NADPH]/[$NADP^+$] ratios remained constant at about 0.4 each, with an intracellular concentration for NADPH about 180 μM.
- The molar ratio between product formation and glucose consumption was about 2.3.

Consequently, they concluded that the relatively low level of [NADPH]/[NADP+] ratio, which is normally in the range of 0.7-1.3, may be due to additional needs of the overexpressed NADPH-dependent enzyme. In addition, they made an effort to identify the NADPH sources in this system by correlating the stoichiometry linking the product formation with glucose consumption in their system (i.e. 2.3 molar ratio) with the stoichiometry linking the product formation with glycerol consumption in a similar system developed by Woodley and coworkers (i.e. 0.96 molar ratio).[144] Recognizing the PP pathway and the TCA cycle as the only NADPH sources in *E. coli* and setting the efficiency of the latter at 96% (each mole of glycerol can produce maximum 1 mole of NADPH), they suggested that the icd was responsible for around 83% [0.96 x 2.0)/2.3] of the NAPDH consumed by the ketone reduction. Therefore, less than 10% of glucose might be metabolized through the PP pathway in that system.

The ‘weak’ points of the abovementioned discussion are the following:

- The [NADPH]/[$NADP^+$] ratio was 0.4 even at time, t=0 h, which is the point just before the beginning of the bioconversion. Therefore, this ratio simply may reflect the ratio of the nicotinamide levels at the end of the growing phase of cells and after their overnight storage at 4°C.

- Even though there is a significant scattering in the data related to phosphorylated nicotinamide levels, it is obvious the trend of faster depletion of NADPH compared to $NADP^+$ but this was not recognized by the authors. The observed drop in all nicotinamides levels could be easily explained in a system such as non-growing cells, in which *de novo* synthesis of those metabolites is excluded due to lack of a nitrogen source. Also, the integrity of the cell membrane is under question especially during the last 12 h of the bioprocess when high concentrations of organic material have been accumulated. Nevertheless, the estimated TTN for this system, based on the $NADP(H/^+)$ content provided by authors for it, is as high as 31,650 (assuming the volume of an *E. coli* cell = 1×10^{-15}L).[108]

- The data provided by Woodley et al. by no means could be correlated with the data obtained from Stewart's study because: i) the two *E. coli* strains were not isogenic (i.e. Woodley's host strain is isogenic to *E. coli* K-12 strain, Stewart's host strain is isogenic to *E. coli* B strain); ii) the calculated efficiency for the Krebs cycle is based on completely different carbon sources. Glycerol transport in *E. coli* is a facilitated diffusion process (i.e. requires no energy expenditure)[68] whereas glucose transport process requires a high energy phosphate group from PEP; iii) when Woodley and coworkers examined their system further found that the amount of product formed within one hour, when glucose was used as a carbon source was half compared to what they obtained when glycerol was added to the medium.[145] Unfortunately, the amount of consumed glucose was not reported. In addition, specific activity measurements with crude extracts revealed that the rate limiting step in Woodley's bioprocess is the transport of starting ketone through the cell membrane.

To this end, the specific aims of the current work were threefold:

- To develop a method that will allow us to identify the NADPH regeneration sources in resting *E. coli* whole cells overexpressing a ketoreductase, a model system for bioreductions in lab-scale.

- To perturb the $NADP(H/^+)$ levels of the host cell by environmental and genetic manipulation means in order to test the capabilities of the methodology invented in the first step (Figure 2-14).

- To evaluate the effects of those perturbations on the productivity of the system under study.

Experimental Strategy

In lab-scale biotransformations, resting cells are usually the preferred method compared to batch and continuous culture methods. Non-growing cells are live cells that retain most of the enzymes activities of growing cells and are obtained from the culture medium at the time in which the activity of the overexpressed enzyme is at satisfied levels. Thus, the bioconversion is divided into two parts. In the first phase, cells are

grown in rich medium (e.g. LB medium) while overproducing the desired biocatalyst. In the second phase, the concentrated cells are resuspended in a modified culture medium lacking nutrients for growth (e.g. M9 medium without NH_4Cl) and the bioconversion takes place. This approach ensures 'cleaner' reactions and easier isolation of products. In addition, cells from the first phase could be stored and used on demand at the desired amounts and under controlled conditions in the second phase. However, in such a system, the popular method of METAFoR analysis of ^{13}C-labeled amino acids by NMR or GC-MS cannot be applied for the calculation of NADPH-related fluxes. An alternative choice would be a radiorespirometric method with all the disadvantages that we discussed in the first chapter.

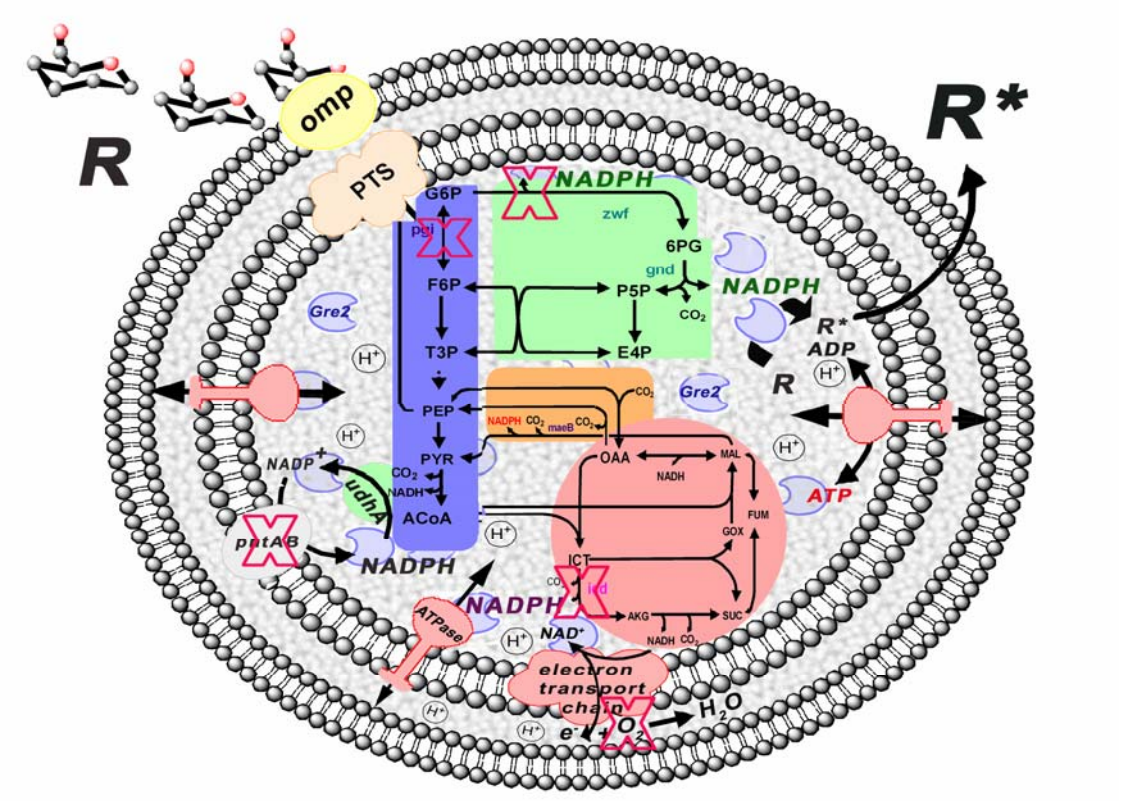

Figure 2-14. Cartoon represents the system under study. The perturbed points represented with X.

Instead, we thought that a modified approach similar to one employed by Csonka and Fraenkel, which was described in detail in the first chapter, would be more

informative. The major difference between the two systems is that in their system the labeled at a specific position of glucose atom (i.e. tritium) was transferred to $NADP^+$ and then to certain amino acids, whereas in our case the labeled atom is transferred to ethyl-acetoacetate by the overexpressed NADPH-dependant keto-reductase, Gre2. An overview of the experimental strategy is depicted in Figure 2-15. The tritium was replaced with the stable isotope deuterium and thus GC-MS can be used to directly measure the deuterium content in the ethyl-3-hydroxybutyrate. The major advantage of this method is that is sensitive and not destructive. Thus, a small volume of sample is required and numerous of samples can be analyzed during the course of the same biotransformation.

The labeled sugars that could possibly give useful information about the NADPH sources in this system are listed in Table 2-4. In this study only the glucose-1-d, -3-d, and -6,6 d_2 were used. A detailed description about the fate of each of these isotopomers in the central carbon catabolism is given in Chapter 1 (see Figure 1-1,1-2,1-3 and1-4). In summary, glucose-1d and -3d could 'trace' the NADPH sources in PP pathway and they could prove or eliminate the existence of the ED pathway. The glucose -6,6 d_2 could trace the activity of icd in the TCA cycle and perhaps the activity of meaB. The glucose-4d should give labeled NADH, which in turn should label $NADP^+$ if a transhydrogenase activity is hypothesized. In principle, if glucose labeled in each position was used, almost all the produced NADPH should be labeled.

Table 2-4. Labeled sugars. Cost and possible application.

D-Glucose	Cost ($/g)[a]	Application
-1-D	180	Zwf activity
-3-D	570	Gnd activity
-4-D	1,700	transhydrogenases activity
-6,6 D_2	75	icd activity
-(1,2,3,4,5,6-D_7)	570	Total activity (Control)

[a] Based on Medical Isotopes Inc. catalog.[146]

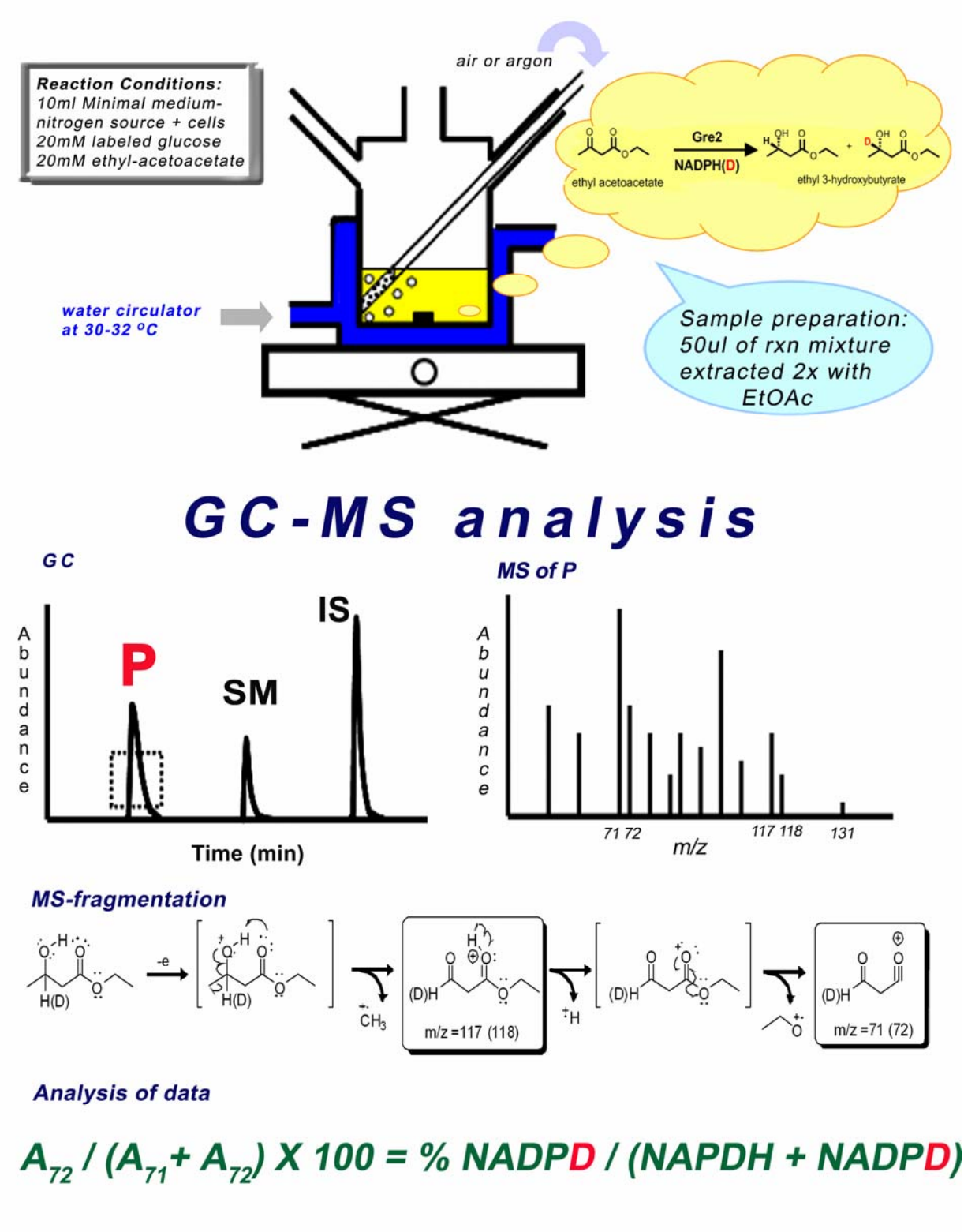

Figure 2-15. Illustration of the experimental procedure. Abbreviations: P, product. SM, starting material; IS, internal standard.

The original bioreduction described by Walton and Stewart was carried out in a 3 L-scale containing 4 g/L glucose. Considering the high cost of the labeled sugars (Table 2-4), all biotransformations in this study were carried out in a 10 ml or 100 ml-scale under two distinct physiological conditions: i) under argon atmosphere (i.e. anaerobically) and ii) under air atmosphere (i.e. aerobically). In this context, the conditions under air atmosphere are named 'aerobic', but they may also be called 'microanaerobic' due to relatively high density of cell cultures ($O.D._{600}$~8.0) used.[147, 148]

In addition to environmental perturbations, we also genetically perturbed the system at four positions. The first two were around the G6P node, disrupting either the *pgi* or the *zwf* gene. We expected that in the former mutant, the flux through the PP pathway would be maximized whereas in the latter case it would be diminished. The third one, an icd mutant, was at the isocitrate node, hence excluding the possibility of NADPH production from TCA cycle. The last disruption was the *pntAB* gene, which encodes the membrane-bound transhydrogenase responsible in the wild type strain for the production of NADPH from NADH. All mutant strains are isogenic to original strain BL21(DE3) used by Walton and Stewart for the ethyl-acetoacetate reduction. This host is necessary for the overproduction of Gre2, for which the expression is under the control of T7 promoter.

We should make clear at this point that the measurements with labeled sugars and the different BL21(DE3) strains performed in this study allowed us to calculate the contribution of each NADPH source to the total NADPH pool present in the cell, in each strain. By no means is this method capable to measure net fluxes in the metabolic network.

Finally, we examined the capabilities of the mutant strains toward the production of ethyl-3-hydroxybutyrate compared to that for the wild type in a shake flask.

Experimental Procedures

Materials

D-Glucose-1-d (97% enrichment), D-Glucose-6,6-d_2 (98% enrichment) 2-propanol-d_8 and sodium deuteride (98% enrichment) obtained from Aldrich. D-Glucose-3-d (98% enrichment) was obtained from Medical Isotopes Inc. Glucose-6-phosphate dehydrogenase (from Bakers yeast Type XI) and alcohol dehydrogenase (from *Thermoanaerobium brockii*) were purchased from Sigma. The purified GST-Gre2 fusion reductase from *S. cerevisiae* was prepared by Dr I. Kaluzna in our lab.[149]

Oligonucleotides were purchased from IDT (Coralville, IA) as deprotected and desalted. Long primers were IE-HPLC purified. *Taq* and Vent polymerases were obtained from New England Biolabs. In-house prepared *Pfu* was used instead of *Vent* in some cases.

Trinder reagent, for glucose assay was purchased from Chemical Diagnostics.

Bacterial Strains and Plasmids

Bacterial strains and plasmids were obtained from the Coli Genetic Stock Center (CGSC) (Appendix B). The *icd* knockout strain (BL21(DE3)Δ*icd*) designated as MA1935 was kindly provided from Dr M. Aoshima.[150] The pntAB knockout strain, (BL21(DE3)Δ*pntAB*) was made by Sylvie Boualavong in our lab. Plasmids were purified by density ultracentrifugation with CsCl in the presence of ethidium bromide. Genomic DNA from *E. coli* BL21(DE3) strain was purified as describe elsewhere.[151] *E. coli* strain overexpressing *S. cerevisiae* Gre2p [BL21(DE3)(pAA3)] has been described elsewhere.[152] All mutant strains were transformed with pAA3 via electroporation.

Cell Cultivations

LB medium used for cell growth contained Bacto-Tryptone (10 g/L), Bacto-Yeast Extract (5 g/L) and sodium chloride (10 g/L). Agar (15 g/L) was used to solidify media for plates. M9 nitrogen-free medium used for bioconversions under non-growing

conditions contained disodium phosphate (12.8 g/L), monopotassium phosphate (3 g/L), sodium chloride (0.5 g/L), magnesium sulfate (2 mM) calcium chloride (0.10 mM) and glucose (0.4%). The last three ingredients were added as sterile aqueous solutions (1 M, 0.10 M and 20%, respectively) after other materials had been autoclaved. M9 minimal medium used for phenotypic characterization of mutants was supplemented with ammonium choride (1 g/L) and glutamate (0.5 mM) in case of MA1935 strain. SOB and SOC media was prepared as described by Sambrook et al.[153]

Analytical Methods

GC-MS analyses were conducted with a Hewlett-Packard Model 5890 GC/MS fitted with a 30 m DB-17 column using helium as carrier gas and a temperature gradient from 60°C to 180°C at 10°C/min with initial and final times 2 and 5 min, respectively. The MS was operating at electron impact ionization mode. Biotransformation reaction mixtures were sampled for GC/MS analysis by mixing 50 µl of the aqueous reaction mixture with 100 µl of ethyl acetate containing 1.0 mM methyl benzoate (internal standard). After vortex mixing, the organic layer was separated and the aqueous layer was extracted a second time in the same manner. A sample of the combined organic layers was analyzed by GC/MS. A standard curve for ethyl-(*S*)-3-hydroxybutyrate linear up to 70 mM was constructed by preparing aqueous solutions containing varying concentrations of single analyte which was extracted and analyzed by GC/MS as described above.

Glucose concentrations were determined using the Trinder reagent kit. Five µl aliquots of water (blank), 5 mM glucose (standard) and the unknown sample, after centrifugation, were added to three separate 1 ml aliquots of reconstituted Trinder reagent. After gentle inversion, the tubes containing each were incubated at 37°C for five minutes. Immediately following incubation the absorbance (A) at 505 nm was

measured. Unknown concentrations were determined based on the equation: [glucose] = 5 mmol/L x ($A_{sample}/A_{standard}$)

In vitro Construction of a Linear Targeting Fragment by PCR: Synthesis of Targeting Marker with Long Flanking Homologous Regions (LFH)

The synthesis of the FRT-kan-FRT cassette with long flanking homologous (LFH) regions of *E. coli* BL21 (DE3) DNA was carried out as described by Derbise et al.[154] The procedure is based on the overlap extension PCR method and illustrated in Appendix A. In the first step two sets of primers were used to amplify the ~500-bp regions flanking the target gene of the *E.coli* BL21(DE3) chromosomal DNA. The chimeric primers used in each pair contained a 5' end homologous to one of the ends of the FRT-kan-FRT marker and a 3'end that primed to the upstream or downstream region of the desired knockout fragment (step A). The sequence of primers was based on the known genomic DNA sequence of the *E. coli* K-12 MG1655 strain.[155] The plasmid pKD13 was used as a template to amplify the kanamycin cassette with the primers set pKD13 F/R (step B). In the second step ~200 ng of upstream and downstream PCR megaprimers were mixed with ~1000 ng of the FRT-kan-FRT fragment, and with a second set of short primers annealing at the two ends of the targeting cassette. PCR cycling conditions were: 25-30 cycles of 94°C for 1 min, 54°C for 2 min and 72°C for 3 min followed by 1 cycle of 72°C for 10 min. In the first and second step Taq and Vent polymerases were mixed in ratio 3 to 1.

The obtained products were concentrated by ethanol precipitation and purified by low melt agarose gel electrophoresis. The *DpnI* treatment of the PCR product from Step A before the gel-purification facilitates the degradation of the methylated plasmid template, which otherwise generates the selective genotype after the transformation with the targeting marker. The purified products were suspended in TE buffer (10 mM Tris-HCl, pH 8.0, 1 mM EDTA, pH 8.0) and quantified by agarose gel electrophoresis.

Gene Replacement

E. coli BL21(DE3) cells were transformed, by electroporation, with the temperature sensitive replicon plasmid pKD46 containing the λ red recombinase genes under the control of the inducible arabinose promoter. BL21 (DE3) [pKD46] cells were grown at 30°C overnight to saturation in LB medium with ampicillin (100 µg/ml), diluted 100-fold in 50ml SOB (plus 100ug/ml ampicillin) and grown to OD_{600} of 0.1. L-Arabinose was added to 1 mM final concentration to induce the expression of the recombinase genes, and cells were grown to an OD_{600} ~ 0.5, before chilling into an ice slurry for 20 min. Cells were then centrifuged at 7000 rpm for 10min at 4°C. The pellet was resuspended in ice-cold deionized water and centrifuged. Then the pellet was resuspended in ice-cold 10% glycerol and centrifuged again. The washing step with glycerol 10% was repeated twice, and the cell pellet was suspended in a final volume of 300-500 µl ice-cold 10% glycerol.

Electroporation was performed using ice-cold cuvettes and a Bio-Rad Gene Pulser set at 2.5kV, 25 uF with pulse controller of 200 Ohms. Transformations were usually performed: 40 µl of induced cells, 40 µl and 50 µl of induced cells mixed with 1µl (30~70ng) or 2µl (60~140 ng) of linear marker, respectively. SOC medium (0.6 ml) was added after electroporation. The cells were transferred to 15 ml test tubes and incubated at 37°C for 1-2h with shaking. The transformants were spread on LB plates containing 20-40 µg/ml kanamycin. The plates were incubated at 37°C to select for recombinants.

Detection and Analysis of Recombinants

Bacterial colony PCR was used to detect *E. coli* transformants having an altered structure caused by replacement of a gene. Each colony was touched with a sterile yellow tip and the cells were resuspended in 4-8 µl of sterile water. The PCR reaction mixture for 2 µl of the above suspension in 100 µl of total volume was 1 µl of Taq, 10 µl 10x Pfu buffer (200 mM Tris-HCl pH 9.0, 0.2 mM $MgSO_4$, 10 mg/ml BSA, 1 mM KCl, 1

mM $(NH_4)_2SO_4$, 1% Triton X-100) 0.2 mM dNTPs and 200 ng of each primer. Thermocycler parameters were the same as described before. Primers used for screening are listed in Appendix C. Products were analyzed on an agarose gel.

Deletion of the Inserted Marker

The *E. coli* BL21(DE3) clones resistant to both kanamycin, kan^R, and ampicillin, amp^R, were cured of the pKD46 plasmid by growth at 37°C, a temperature not permissive for this replicon, and spread on LB, on LB plus amp (100 µg/mL) and on LB plus kan (40 µg/mL) in different dilutions to select for amp^S colonies. Kan^R mutants were transformed with pCP20 that has a temperature-sensitive replication and thermal induction of FLP recombinase synthesis. Since the kan gene is flanked by the short direct repeats called Flp Recombinase Targets (FRT sites) the Flpase promotes recombination at those specific sites excising the kan cassette and leaving behind a short nucleotide sequence with one FRT site. Ampicillin-resistant transformants were selected after 1-day incubation at 30°C, and were screened for *kan* deletion with colony-PCR as described above. Colonies having the deletion were grown non-selectively at 37°C and then tested for loss of all antibiotic resistances.

Preparation of [4S-^{2}H] NADPH

The preparation of (*S*)NADPD was based on a method described by Viola et al.[156] 31mg $NADP^+$ and 1.5 fold excess of D-glucose-1-d were dissolved in 4.3 ml phosphate buffer, 83mM, pH 8, containing DMSO at 40% (v/v) final concentration. 50 U of glucose-6-phosphate dehydrogenase were added and the reaction mixture was stirred gently at RT. The progress of the reaction was followed by taking aliquots every hour and measuring the increment of the absorbance at 340nm. Maximum absorbance was achieved after 5h, conversion 95%. The reduction of $NADP^+$ was almost complete because of the hydrolysis of gluconolactone to gluconate.

The reduced nicotinamide was purified by a method described by Orr et al.[157] with minor modifications. The G6PDH was separated from the solution by ultrafiltration (10.000 molecular weight cutoff filter). The $NADPD_B$ sample (5 x 1ml) was loaded on a FPLC Mono Q HR5/5 anion exchange column and was eluted by a 0-1 M ammonium bicarbonate gradient.[158] Fractions showing a A_{260}/A_{340} ratio between 2.3-2.7 were pooled (total volume: 15 ml) and lyophilized overnight affording 20 mg of white powdery solid containing 12.5 mg NADPD (based on A_{340}). Final yield: 43%.

Preparation of [4R-^{2}H] NADPH

The preparation of (*R*)NADPD was based on a method described by Gready et al.[159] 33 mg $NADP^+$,1.2 ml isopropanol-d8 and 4U of TBADH were added in 15ml of 25mM Tris buffer, pH 9 and the reaction mixture was stirred gently at 43 ˚C. The thermostability of TBADH allowed the reaction to be carried out at this temperature, which also prevented the reverse reaction by evaporating the volatile product, acetone. The progress of the reaction was followed as before and the maximum conversion, 75%, was achieved after 3h. The reduced nicotinamide was purified as described above. Final yield: 39%.

Preparation of D-glucose-1d

A 5 ml aqueous solution of sodium borodeuteride (222 mg or 5.3 mmol) was added dropwise to a 10 ml aqueous solution of δ-gluconolactone (1.3 g or 7.3 mmol) at -4°C-0 °C at such a rate that all the reducing agent was added in 20 min.[160] The pH of the reaction mixture was kept at 3-4 (for every ~10 drops of $NABD_4$ solution, 4-5 drops of 1 M of H_2SO_4 solution were added). 10 min after the last addition of the reducing agent the reaction was quenched with 0.5 ml of 1 M H_2SO_4 and the solution was neutralized with 2 M NaOH. 50 ml of methanol was added and solvent was evaporated off under reduced pressure as methyl borate.[161] The procedure was repeated four times until no boron was present in the solution based on the carmine reagent.[162] The obtained syrup

was lyophilized overnight, redissolved in 2 ml D_2O and lyophilized again for 20 h affording 1.9 g of white powdery solid containing 1.3 g of glucose based on Trinder reagent assay. The labeled glucose was used without further purification.

Reduction of Ethyl-acetoacetate by Gre2p GST-fusion Reductase Using $NADPD_B$ or $NADPD_A$

The stereospecificity of hydrogen transfer of NADPH catalyzed by Gre2p was determined by reacting 7mg (~1.6 µmol) of $NADPD_B$, with 3.2 µmol ethyl-acetoacetate and ~450 µg enzyme in total volume of 2.5 ml 100mM KPi pH 7. The reaction was monitored by following the decrement in A_{340}. The oxidized co-factor was purified by FPLC as described before, lyophilized, resuspended in D_2O and analyzed by ^{1}H-NMR. The procedure was repeated for the $NADPD_A$. The obtained ethyl-3-hydroxybutyrate was also analyzed by GC-MS.

Reduction of Ethyl-acetoacetate by Gre2p GST -fusion Reductase Using a mixture of NADPH and $NADPD_B$

In a solution of 704 µl 100mM KPi pH 7.0 were added 83 µl of a stock solution of $NADPD_B$ (24.8 mM), 83 µl of a stock solution of NADPH (21 mM) and 80 µl of a stock solution of ethyl-acetoacetate (80 mM). The reaction was initiated by adding 50 µl of a stock solution of Gre2 (~2.4 µg/ml) and was monitored by following the absorbance at 340 nm and by extracting 50 µl aliquots for GC-MS analysis.

Standard Procedure for Ethyl-acetoacetate Biotransformations with Resting cells

A single colony of the appropriate stain harboring the pAA3 was used to inoculate 10 ml of LB media supplemented with 40 µg kanamycin and the culture was shaken overnight at 37°C. Five ml of this solution was added to a 2 L baffled flask containing 500 ml of LB media, 4 g/L glucose, 40 µg/ml kanamycin. The culture was incubated at 37°C with shaking. Upon reaching an OD_{600}~0.7, IPTG was added to a final concentration of 0.1 mM and the incubation was continued at 30 °C for 6 to 8h. The

harvested cells were resuspended in 5 ml nitrogen free medium and kept overnight or until used (maximum 2 days later) at 4 °C.

Bioconversions of ethyl-acetoacetate were carried out either in a 1 L flask or in 300 ml vessel or in 25 ml vessel containing 100 or 10 ml M9 medium without NH_4Cl and cells prepared as described above at different optical densities. At the beginning, glucose and the organic compound were added to a concentration of 20mM and then appropriate amounts of both were added whenever was necessary based on glucose consumption and product formation measurements The reaction was incubated at 32°C with shaking, when in flask, or by stirring, when in vessel. The vessels were equipped with a magnetic bar and an ace gas dispersion tube connected to an air or argon line. Most experiments regarding the Δ*icd* and Δ*pntAB* strains were performed by Sylvie Boualavong.

Results

Characterization of Mutated Strains

All knockout mutants (Table 2-5) but Δ*icd* were constructed by a marker-free deletion method[163] of genes from start to stop codon as described in experimental section.

Table 2-5. *E. coli* strains used in this study.

Strain	Pertinent genetic markers
WT [BL21(DE3) (pAA3)]	wild-type strain overexpressing Gre2 reductase
Δ*pgi* (DJB254)	BL21(DE3) Δ*pgi* (pAA3) (phosphoglucose isomerase deficient)
Δ*zwf* (DJB370)	BL21(DE3) Δ*zwf* (pAA3) (glucose-6-phosphate dehydrogenase deficient)
Δ*icd* (MA1935)	BL21(DE3) Δ*icd* (pAA3) (isocitrate dehydrogenase deficient)
Δ*pntAB* (SB2)	BL21(DE3) Δ*pntAB* (pAA3) (membrane-bound transhydrogenase deficient)

Generally any number from one to 50 kanamycin resistant colonies was obtained after the transformation of parent strain with the FRT-kan-FRT cassette. The recombination efficiency was from zero to 100 % based on about 13 colonies screened.

In the former case the transformation was repeated with same or fresh-prepared linear DNA.

Correct marker integration and excision was verified in all mutant stains by colony PCR. The PCR primers used were annealing either at the 5' and 3' of the target gene or 500 and 550 bp outside of target's gene coding region. Wild-type starting strain BL21(DE3) was used as a comparison. Results are summarized in Table 2-6, Table 2-7 and Table 2-8 and are depicted in Figure 2-16, Figure 2-17 and Figure 2-18.

Table 2-6. Colony PCR for pgi knock-out.

E. coli strain	Primers Set	Expected Size (kbp)	Observed Size (kbp)
BL21(DE3) Δ*pgi* :: FRT-*kan*-FRT	pgiF, pgiR	no band	~1.65, ~0.9, ~ 0.8 (major)
BL21(DE3) Δ*pgi* :: FRT-*kan*-FRT	Up500pgi, Down500pgi,	2.33	~2.3
BL21(DE3) Δ*pgi* :: FRT-*kan*-FRT	Up500pgi, k2	1.21	~1.2
BL21(DE3) (pKD46)	Up500pgi, k2	no band	no band
BL21(DE3) Δ*pgi* :: FRT-*kan*-FRT	Down500pgi, k1	1.0	~1.0
BL21(DE3) (pKD46)	Down500pgi, k1	no band	no band
BL21(DE3) (pKD46)	pgiF, pgiR	1.65	1.65 (major), 0.8
BL21(DE3) (pKD46)	Up500pgi, Down500pgi	2.65	~2.6
BL21(DE3) Δ*pgi* :: FRT-*kan*-FRT	Up550pgi, Down550pgi,	2.43	~2.4
BL21(DE3) (pKD46)	Up550pgi, Down550pgi	2.75	~2.7
BL21(DE3) Δ*pgi* :: FRT	pgiF, pgiR	no band	~1.65, ~0.9, ~ 0.8 (major)
BL21(DE3) Δ*pgi* :: FRT	Up500pgi, Down500pgi	1.1	~1.0

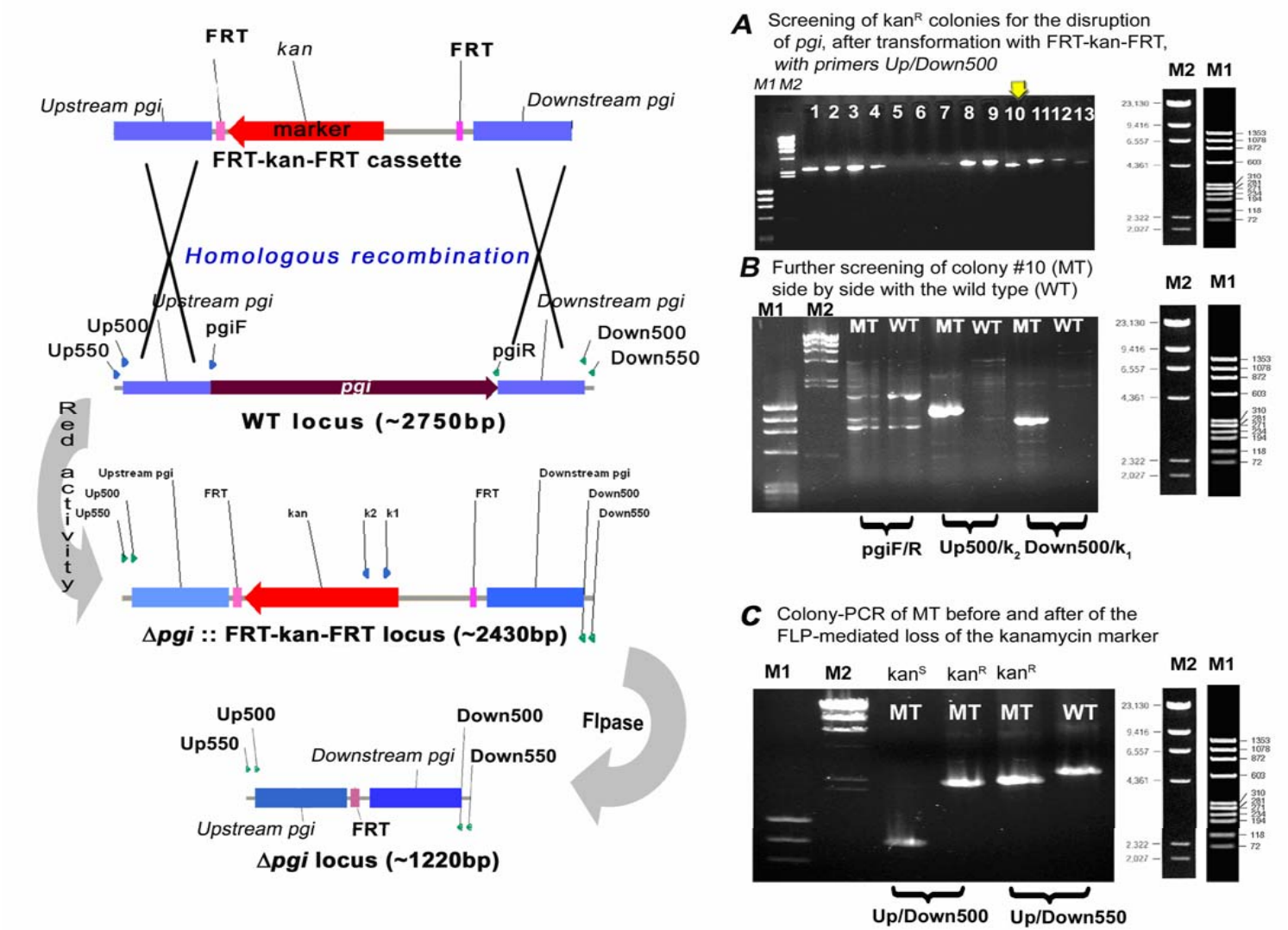

Figure 2-16. Results from colony PCR reactions probing the pgi locus before and after the disruption. Abbreviations: WT (wild type), MT (mutant strain); kan^R, kanamycin resistant; kan^S, kanamycin sensitive; M1and M2, DNA markers.

In case of *pgi* deletion, a weak band with size similar for the structural gene was detected in kanamycin resistant colony along with multiple other weak bands when the pair of pgiF/R primers was used. However, we suspected that these low levels PCR products are due to aerosol contamination or mis-priming since colony PCR with outside primers confirmed the right construct.

Table 2-7. Colony PCR for zwf knock-out

E. coli strain	Primers Set	Expected Size (kbp)	Observed Size (kbp)
BL21(DE3) Δ*zwf*:: FRT-kan-FRT	zwfF, zwfR	no band	~1.3, ~1.2, ~0.9
BL21(DE3) Δ*zwf*:: FRT-kan-FRT	Up550zwf, Down550 zwf	2.43	~2.4
BL21(DE3) Δ*zwf*:: FRT-kan-FRT	Up570zwf, Down550zwf	2.45	~2.4
BL21(DE3) (pKD46)	Up570zwf, Down550zwf	2.62	~2.5
BL21(DE3) Δ*zwf*:: FRT-kan-FRT	Down570zwf, Up550zwf	2.45	~2.5
BL21(DE3) (pKD46)	Down570zwf, Up550zwf	2.62	2.55
BL21(DE3) (pKD46)	Up550zwf, k2	no band	~0.8
BL21(DE3) Δ*zwf*:: FRT-kan-FRT	Up550zwf, k2	1.23	~1.2 (major), ~0.8
BL21(DE3) (pKD46)	zwfF, zwfR	1.5	~1.5 (major), ~0.9
BL21(DE3) (pKD46)	Up550zwf, Down550zwf	2.6	~2.5
BL21(DE3) Δ*zwf*:: FRT-kan-FRT	Down550zwf, k1	1.1	~1.1
BL21(DE3) Δ*zwf*:: FRT-kan-FRT	zwf F, Down550zwf	no band	no band
BL21(DE3) (pKD46)	zwfF, Down550zwf	2.0	~2.0
BL21(DE3) (pKD46)	Down550zwf, k1	no band	~0.4
BL21(DE3) Δ*zwf*:: FRT	Up550zwf, Down550zwf	1.2	~1.2

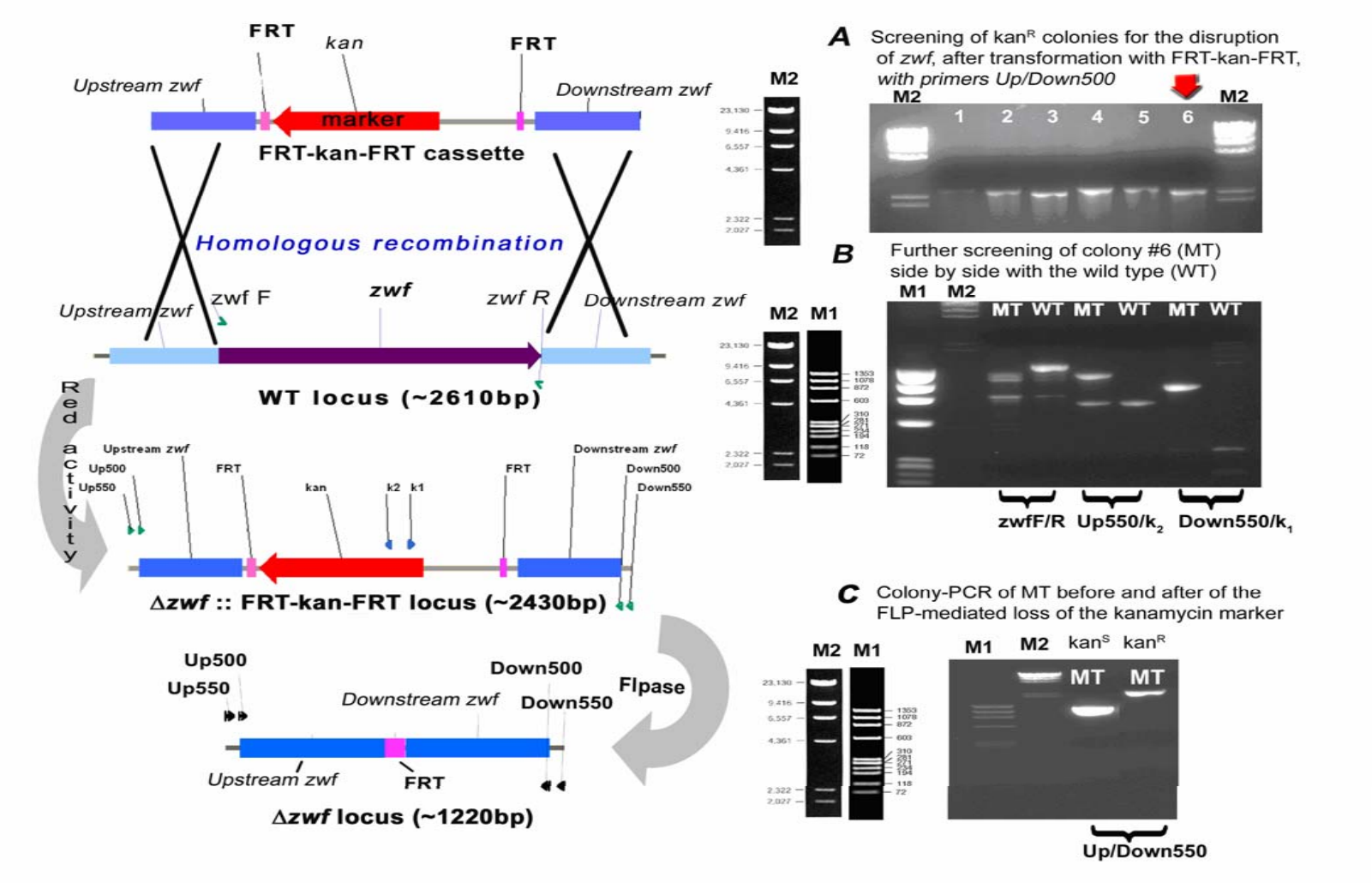

Figure 2-17. Results from colony PCR reactions probing the zwf locus before and after the disruption. Abbreviations: WT (wild type), MT (mutant strain); kan^R, kanamycin resistant; kan^S, kanamycin sensitive. M1and M2, DNA markers.

Table 2-8. Colony PCR for *pntAB* knock-out.

E. coli strain	Primers Set	Expected Size (kbp)	Observed Size (kbp)
BL21(DE3) Δ*pntAB* :: FRT-*kan*-FRT	Up510PntAF, Down510PntBR	2.35	~2.3
BL21(DE3) Δ*pntAB* :: FRT-*kan*-FRT	PntAF, PntBR	no band	no band
BL21(DE3) Δ*pntAB* :: FRT-*kan*-FRT	Up510 PntA, k2	1.23	~1.2
BL21(DE3) (pKD46)	Up510 PntA, k2	no band	no band
BL21(DE3) Δ*pntAB* :: FRT-*kan*-FRT	Down510 PntBR, k1	1.03	~1.1
BL21(DE3) (pKD46)	Down510 PntBR, k1	no band	no band
BL21(DE3) (pKD46)	Up510PntAF, Down510PntBR	4.13	~4.1
BL21(DE3) (pKD46)	PntAF, PntAR	1.53	~1.5
BL21(DE3) Δ*pntAB* :: FRT-*kan*-FRT	PntAF, PntAR	no band	no band
BL21(DE3) (pKD46)	PntBF, PntBR	1.39	~1.4
BL21(DE3) Δ*pntAB* :: FRT-*kan*-FRT	PntBF, PntBR	no band	no band
BL21(DE3) Δ*pntAB* :: FRT	Up510PntAF, Down510PntBR	1.11	~1.0

The growth rate of mutant strains was compared with that of wild type in M9 minimal media. Δ*zwf* strain grew almost as fast as the WT, at least for the first 8h, as it was reported before (Figure 2-19A).[164] The Δ*pgi* mutant showed limited growth and consumption of glucose (Figure 2-19A), as expected.[165] In contrast to what has been observed for a K-derivatived *E. coli* strain[166] lacking *pntAB*, our Δ*pntAB* mutant grew without any difference from the WT (Figure 2-19B). Finally, the *icd* mutant strain showed the reported elsewhere[150] glutamate auxotrophy (Figure 2-19C). In this case, an additional portion of glutamate was added after 20h.

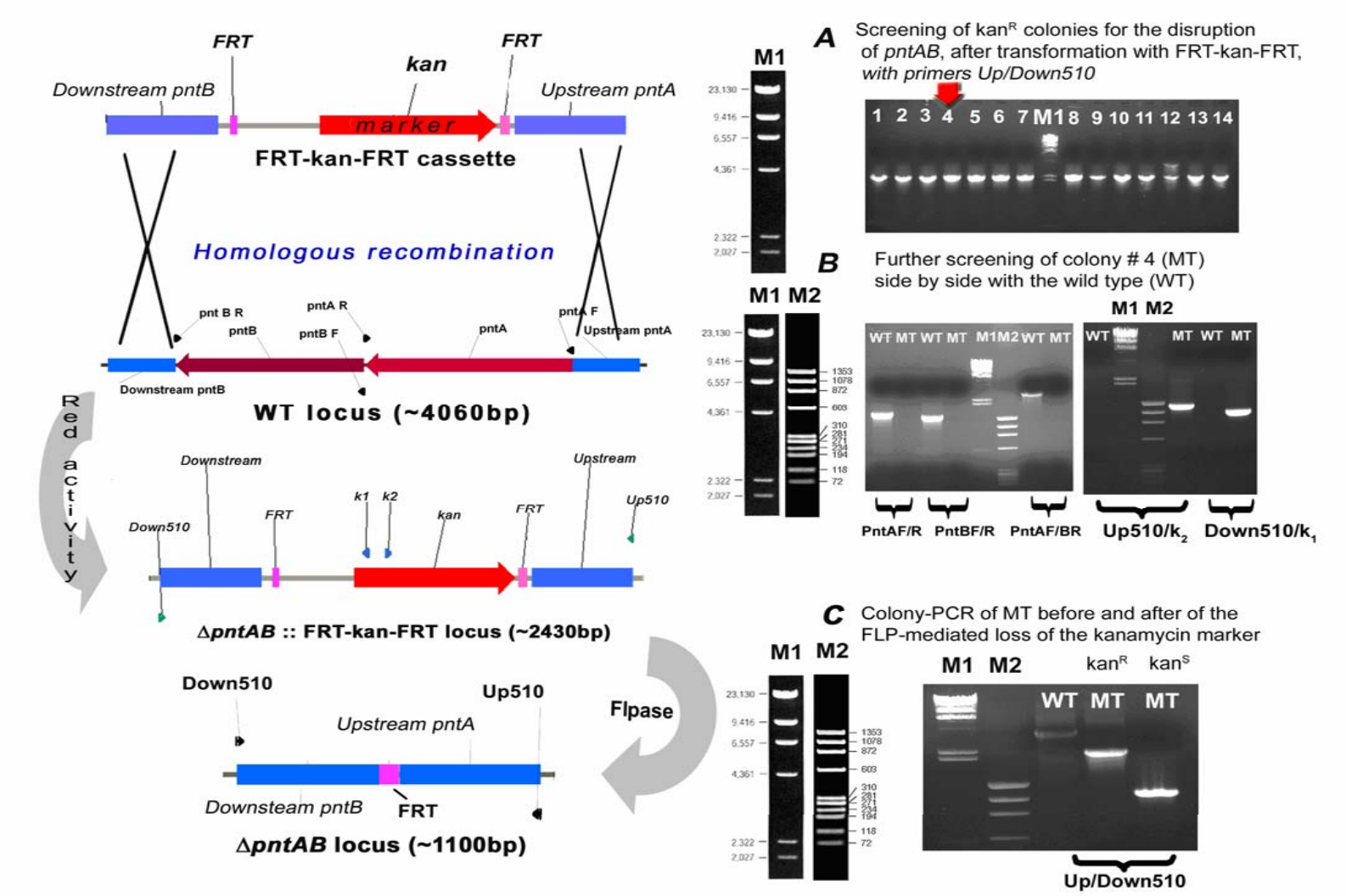

Figure 2-18. Results from colony PCR reactions probing the pntAB locus before and after the disruption. Abbreviations: WT (wild type), MT (mutant strain); kan^R, kanamycin resistant; kan^S, kanamycin sensitive. M1 and M2, DNA markers.

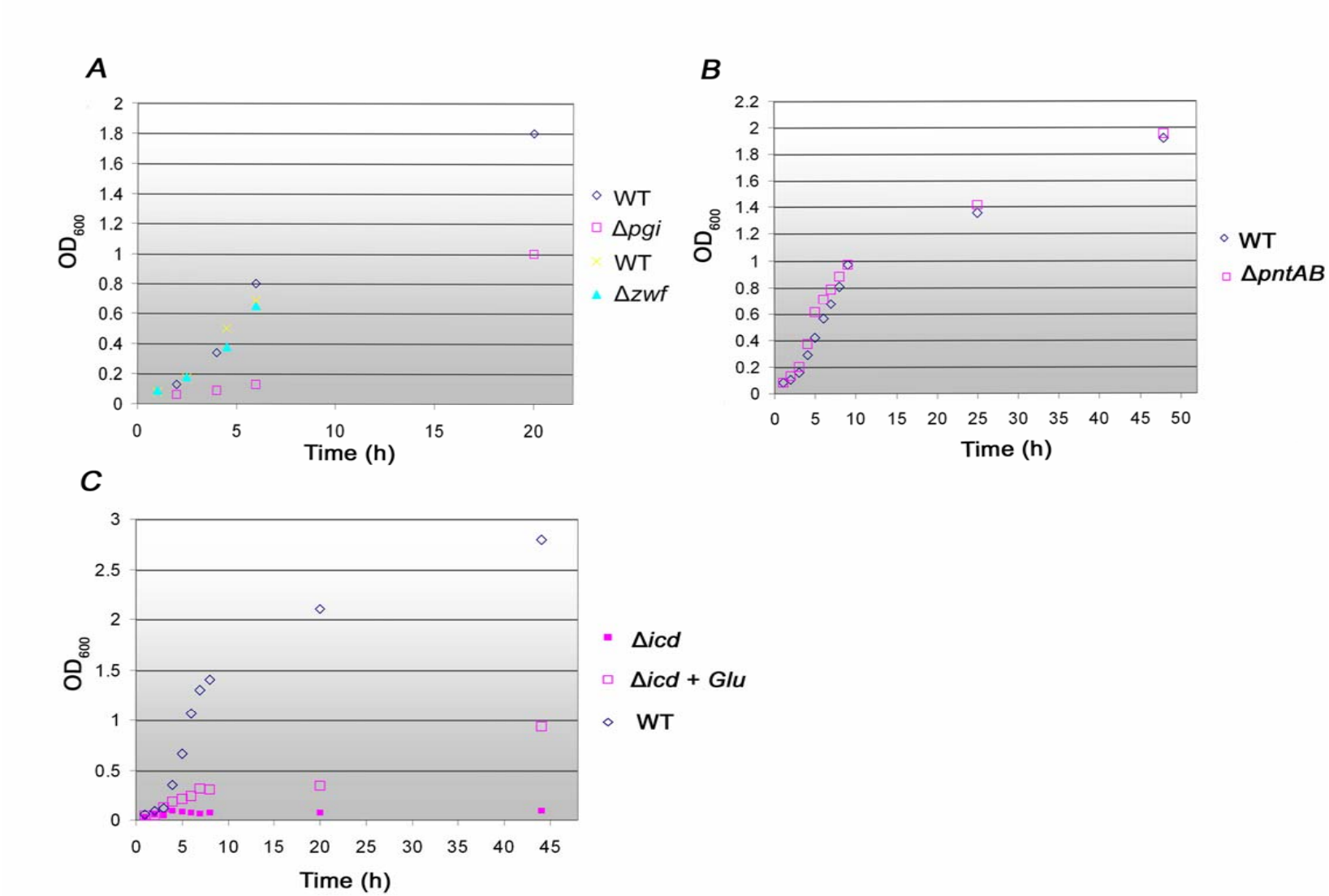

Figure 2-19. Phenotype analysis of constructed mutants in M9 medium. A. Growth curves for Δ*pgi* and Δ*zwf* strains. B. Growth curve for Δ*pntAB* strain. C. Growth curves for Δ*icd* strain with (opened squares) or without (closed squares) glutamate.

MS Data Analysis

In this section, the raw MS data will be presented in a form of % fractional abundance of 72 (m/z) fragment (A_{72}) of ethyl-hydroxybutyrate (EHB) obtained under different physiological conditions using different glucose isotopomers for all the aforementioned strains.

In the first experiment, the WT strain was fed with Glc-1D under aerobic conditions. A 20±2% incorporation of deuterium into product was observed. This experiment was repeated at least eight times (Figure 2-20) using different amount of cells, at two different scales and it was reproducible. In all cases, a plateau for the A_{72} (%) was observed after the first 2.5 h. We expected that pgi activity should give rise to labeled product whereas any other NADPH source should not contribute significantly to it. The second NADPD source in this case is the icd, albeit minor (i.e. pyruvate produced from Glc-1D is labeled at maximum 17%, Figure 1-3, Chapter 1).

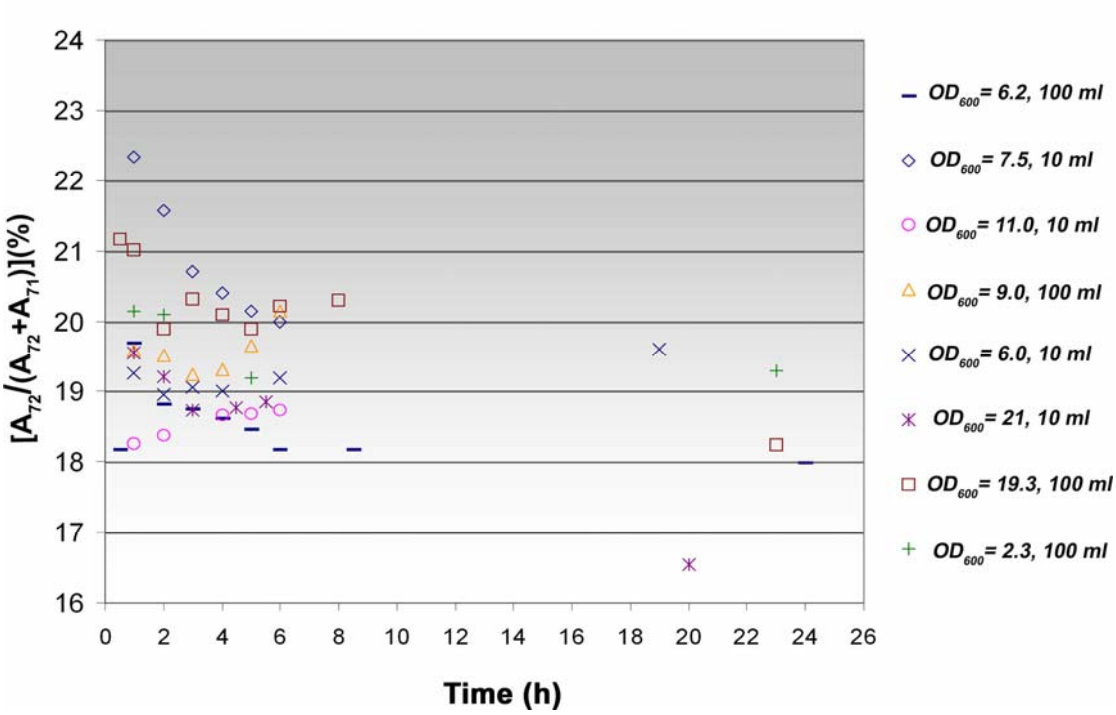

Figure 2-20. Fractional abundance (%) of 72 m/z fragment (A_{72}) of EHB produced by the wild-type strain (WT) using Glc-1D, under aerobic condition.

When the experiment with Glc-1D was repeated under anaerobic conditions for the WT, EHB was found labeled at a higher extent, up to 35% (Figure 2-21). However, a plateau value, if any, was not obtained at the first 6 h. Keeping in mind the equation presented in Figure 2-15 for the analysis of the data, a higher A_{72} (%) could be observed if a higher flux through the PP pathway occurred (i.e higher [NADPD]) or if a major NADPH source was ceased (i.e. lower [NADPH]) under anaerobic conditions.

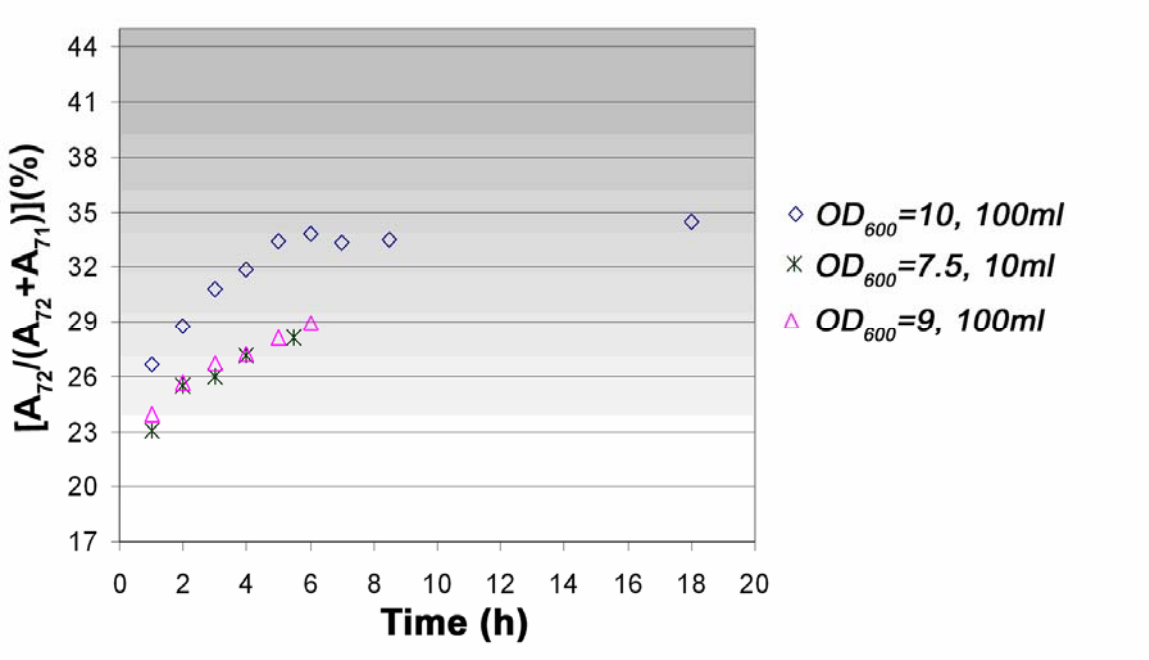

Figure 2-21. Fractional abundance (%) of 72 m/z fragment (A_{72}) of EHB produced by the wild-type strain (WT) using Glc-1D, under anaerobic condition.

The distinct labeled pattern of EHB under aerobic or anaerobic conditions was confirmed with a third independent experiment in which the cells were fed with Glc-1D under aerobic conditions for the first 8h and then the air supply was halted (Figure 2-22).

The possibility of a branch-point (i.e ED pathway) in between the pgi and the gnd was excluded by feeding the WT strain with Glc-3D (Figure 2-23). Almost the same degree of incorporated deuterium into the EHB (i.e., (18±2)%) was observed as when Glc-1D was used.

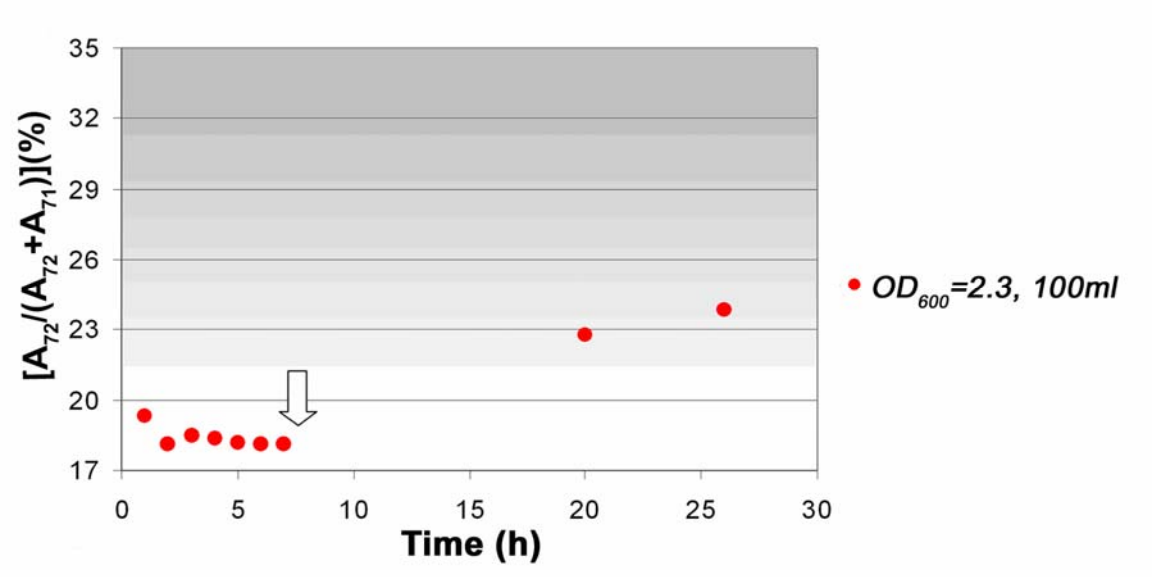

Figure 2-22. Fractional abundance (%) of 72 m/z fragment (A_{72}) of EHB produced by the wild-type strain (WT) using Glc-1D, under aerobic and anaerobic conditions. (Arrow indicates the time at which the air supply was turned off).

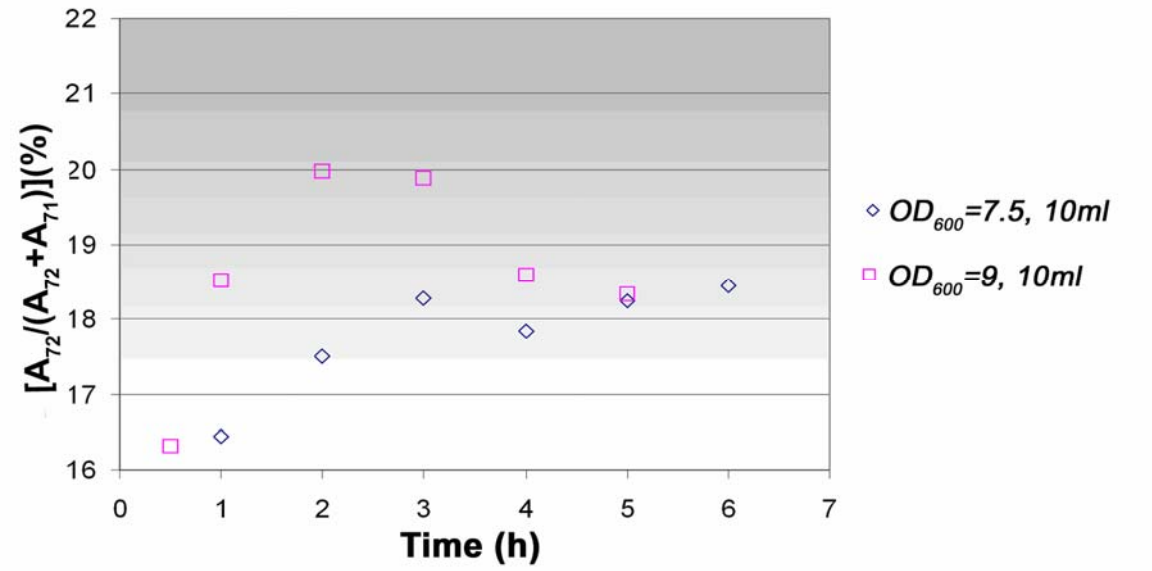

Figure 2-23. Fractional abundance (%) of 72 m/z fragment (A_{72}) of EHB produced by the wild-type strain (WT) using Glc-3D, under aerobic conditions.

Glc-6,6D_2 could 'trace' a possible icd activity. Indeed, when the WT strain was fed with it, 11-13% of EHB was labeled under aerobic conditions. This is not a minute number, especially if we consider that less than a half of the pyruvate (i.e. maximum 33%) entering the TCA will be labeled (Figure 2-24).

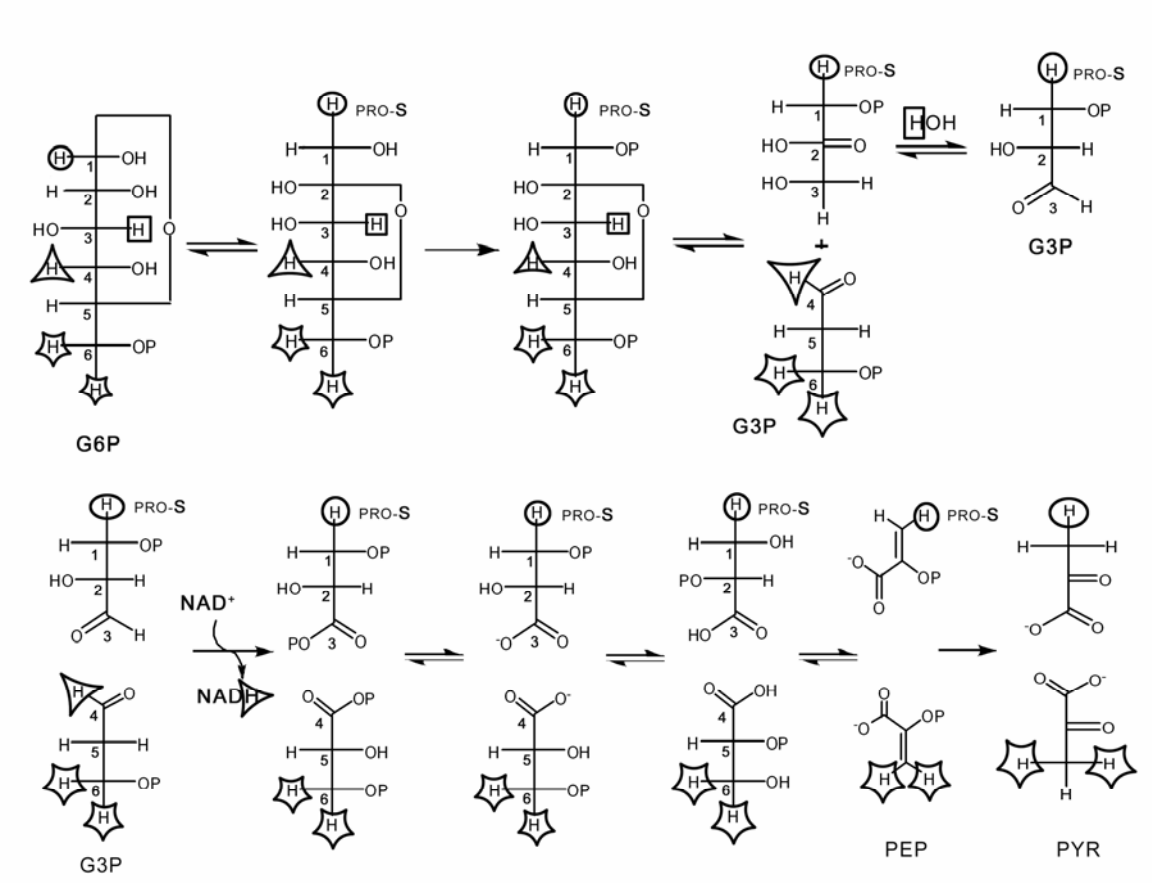

Figure 2-24. Fate of deuterium atoms of glucose at position 1, 3, 4 and 6 through glycolysis. Deuterium at position 1 should end up in PEP (25%), however only the position trans to carboxylic acid should be labeled, and PYR (only 16% labeled). Deuterium at position 3 should be found in water. Deuterium at position 4 should label NAD^+. Deuterium atoms at position 6 should have the same fate as the atom at position 1, however PEP and PYR should bear twice more labeled atoms (50% and 33% respectively) (Adapted from references 176, 177)

In contrast, under anaerobic condition the % A_{72} was diminished to 4%, a negligible number if we consider that even a reduction of EAA with $NaBH_4$ is showing a 3.8% A_{72} due to the natural abundance of isotopes, as we will discuss in the next section.

A very similar trend for the produced labeled EHB was detected when the WT strain was replaced by the Δ*pgi* strain and fed with Glc-6,6D_2 under either aerobic (i.e., 10-12%, Figure 2-26) or anaerobic conditions. The major difference compared to WT

was observed when Glc-1D or Glc-3D was administrated to Δ*pgi* strain under aerobic conditions. A higher amount of EHB (i.e., about 27±3% for Glc-1D and about 25% for Glc-3D) was found labeled (Figure 2-27 and Figure 2-28). These results could be easily explained since in this strain all labeled sugar should be catabolized through the PP pathway (i.e., higher [NADPD]).

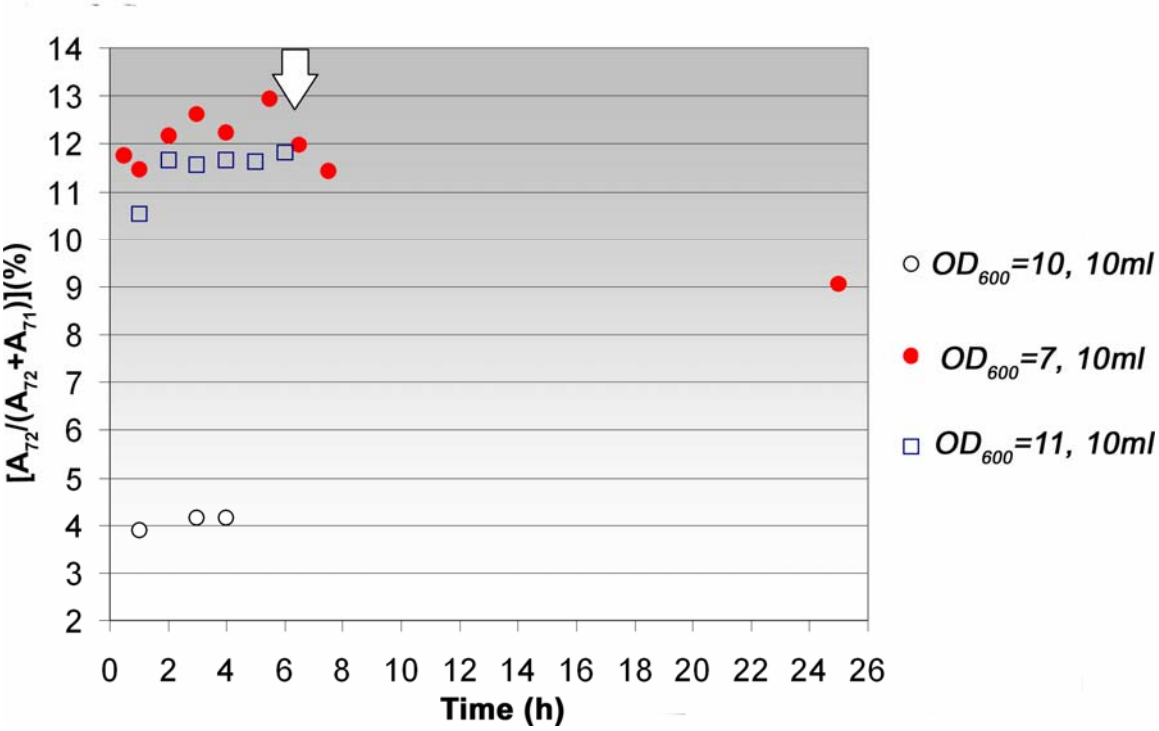

Figure 2-25. Fractional abundance (%) of 72 m/z fragment (A_{72}) of EHB produced by the wild-type strain (WT) using Glc-6,6 D_2, under aerobic (open squares and closed circles) and anaerobic conditions (open circles). (Arrow indicates the time at which the air supply was turned off)

In contrast to what was observed for the Δ*pgi* strain, the contribution of labeled Glc-1D or Glc-3D in EHB for Δ*zwf* strain was negligible since the route through the PP pathway was disrupted (Figure 2-29). However, the contribution was maximized in this strain when Glc-6,6D_2 was used under aerobic conditions. (Figure 2-30).

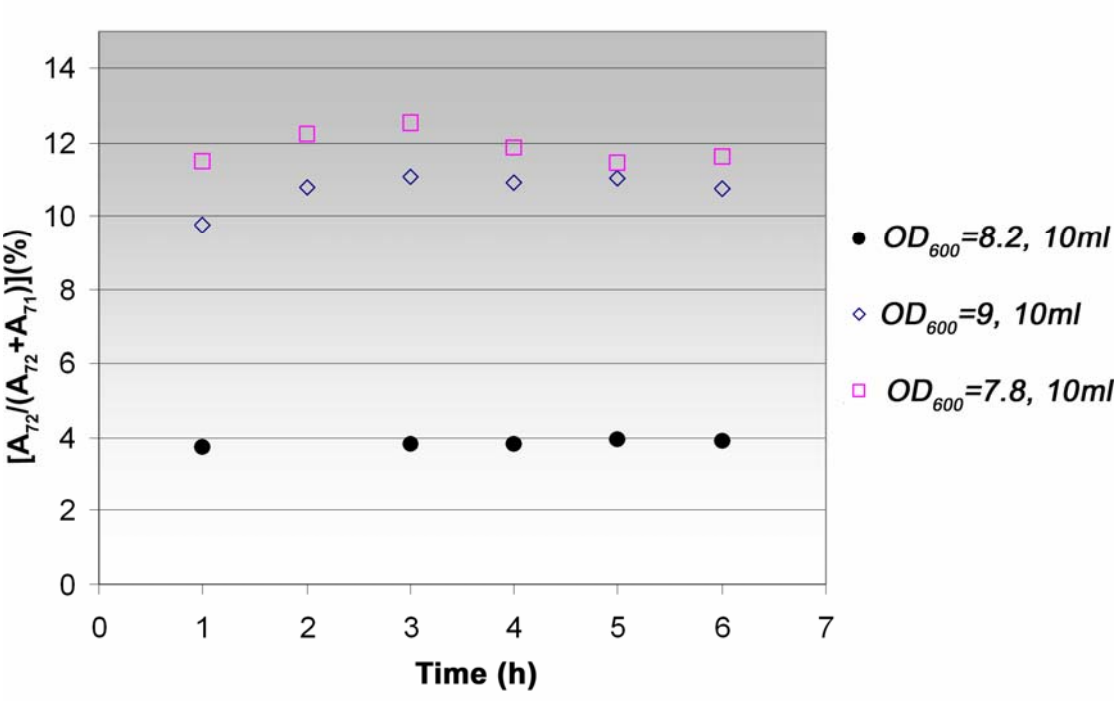

Figure 2-26. Fractional abundance (%) of 72 m/z fragment (A_{72}) of EHB produced by Δ*pgi* strain using Glc-6,6 D_2, under aerobic (opened symbols) and anaerobic conditions (closed circles).

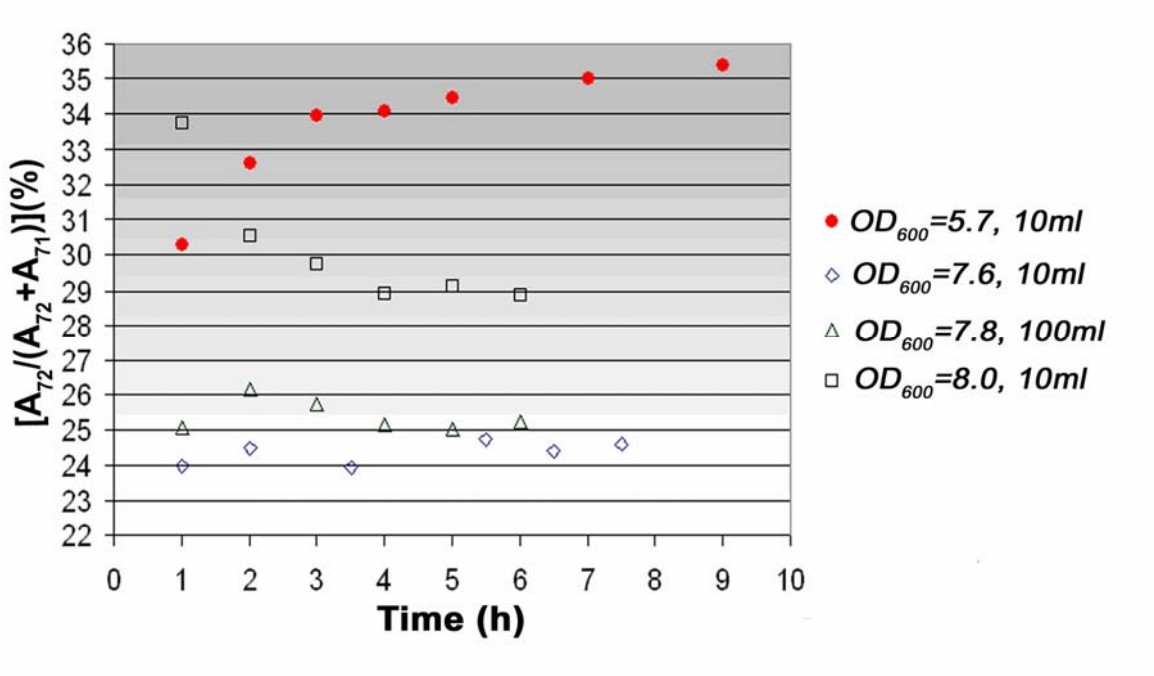

Figure 2-27. Fractional abundance (%) of 72 m/z fragment (A_{72}) of EHB produced by the Δ*pgi* using Glc-1D, under aerobic (opened symbols) and anaerobic conditions (closed circles).

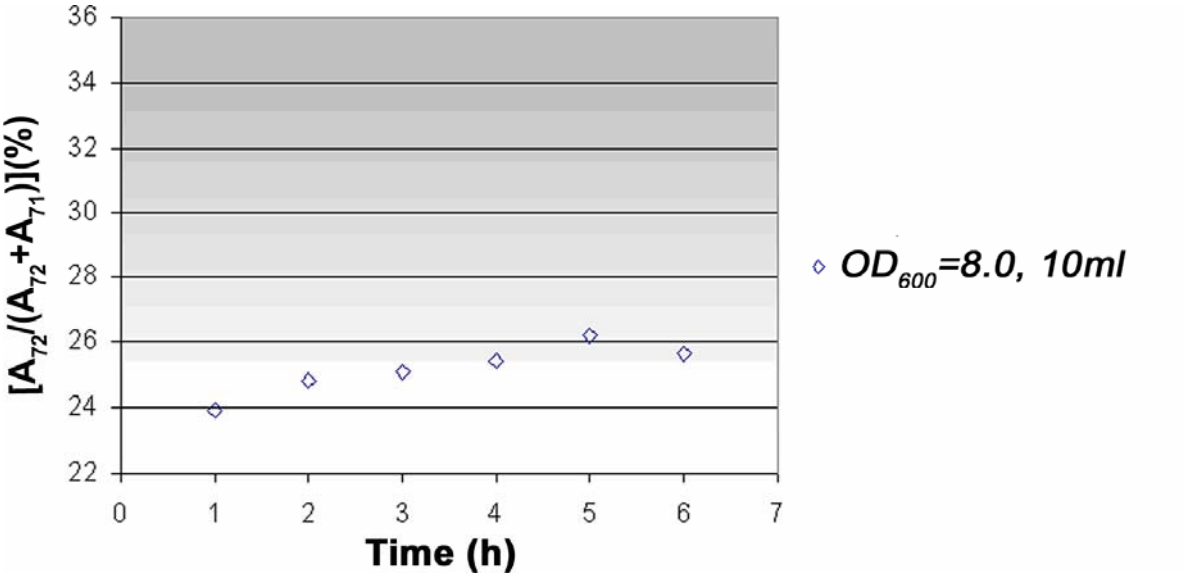

Figure 2-28. Fractional abundance (%) of 72 m/z fragment (A_{72}) of EHB produced by Δ*pgi* strain using Glc-3D.

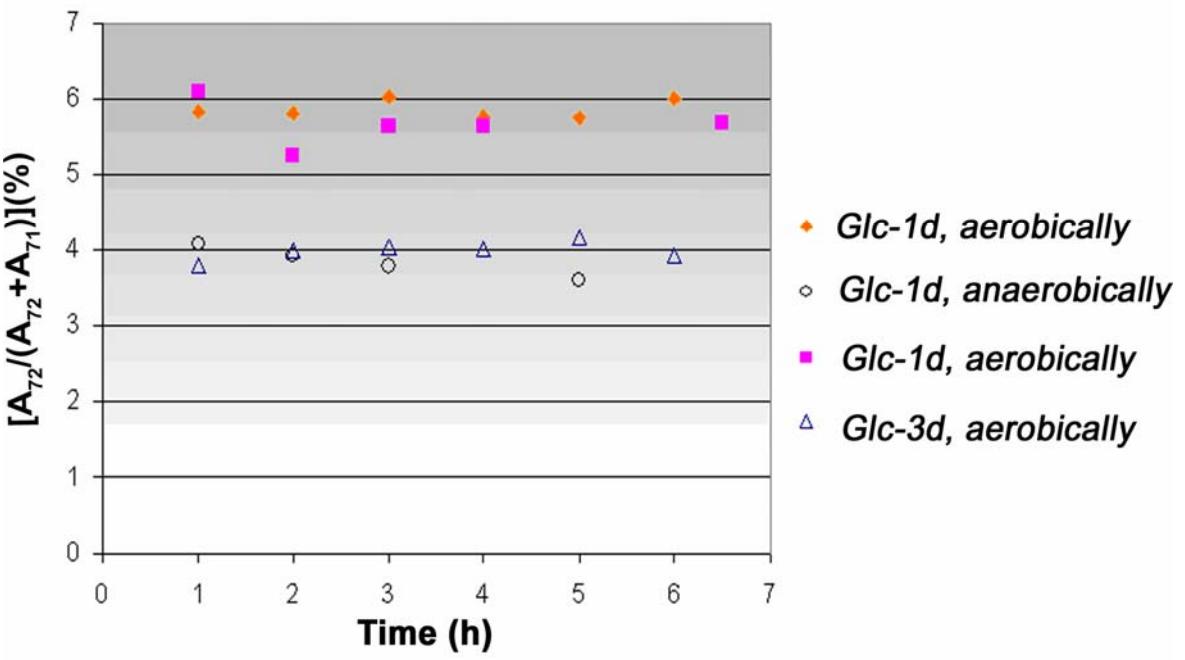

Figure 2-29. Fractional abundance (%) of 72 m/z fragment (A_{72}) of EHB produced by Δ*zwf* strain using Glc-3D, or Glc-1D under anaerobic (opened circles) and aerobic conditions in 10 ml scale, OD_{600}=7.0-9.0.

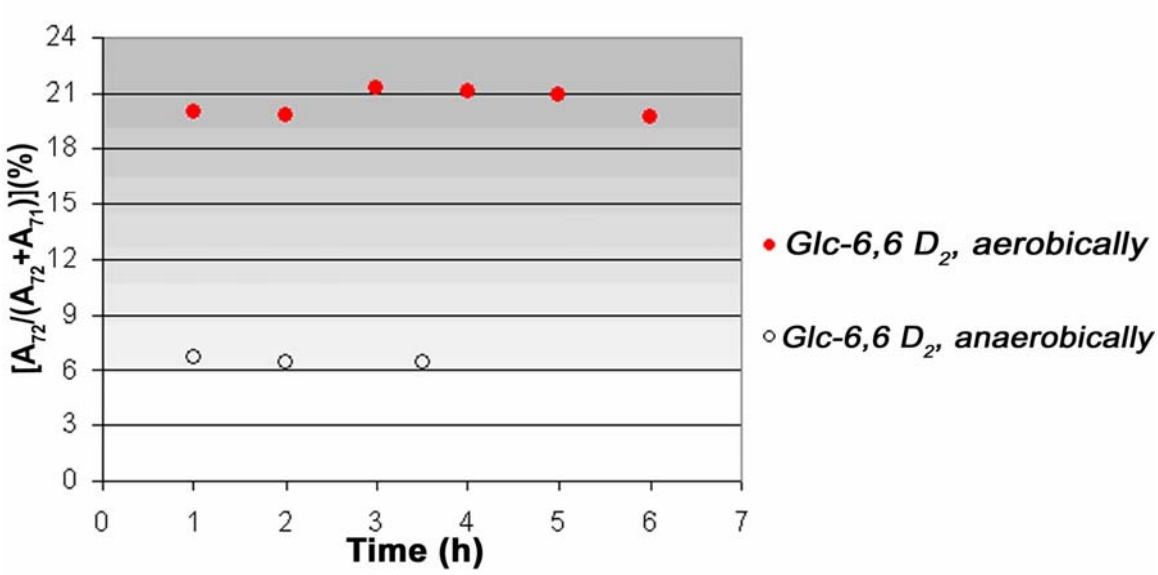

Figure 2-30. Fractional abundance (%) of 72 m/z fragment (A_{72}) of EHB produced by Δ*zwf* strain using Glc-6,6 D_2, under aerobic (closed circles) and anaerobic conditions (opened circles) in 10 ml scale, OD_{600}=8.0.

The results for the obtained labeled EHB were reversed when an Δ*icd* strain was used instead for a Δ*zwf* strain. Maximum deuterium content in EHB was detected when Glc-1-D was used (Figure 2-31) and minimum when Glc-6,6-D_2 was administrated (Figure 2-32).

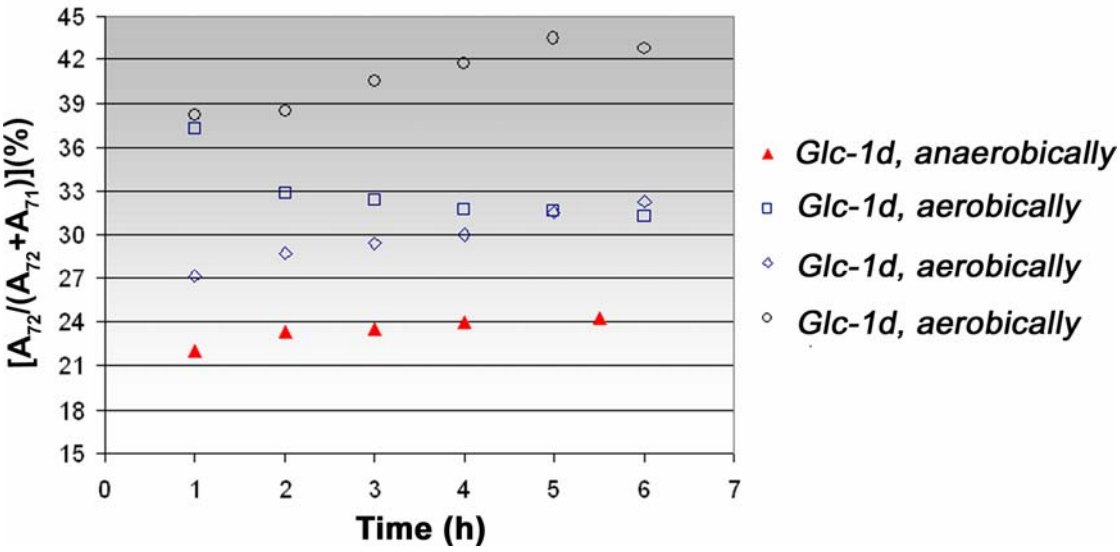

Figure 2-31. Fractional abundance (%) of 72 m/z fragment (A_{72}) of EHB produced by Δ*icd* strain using Glc-1D, under aerobic (opened circles) and anaerobic conditions (closed triangles) in 10 ml scale, OD_{600}=7.0-8.0.

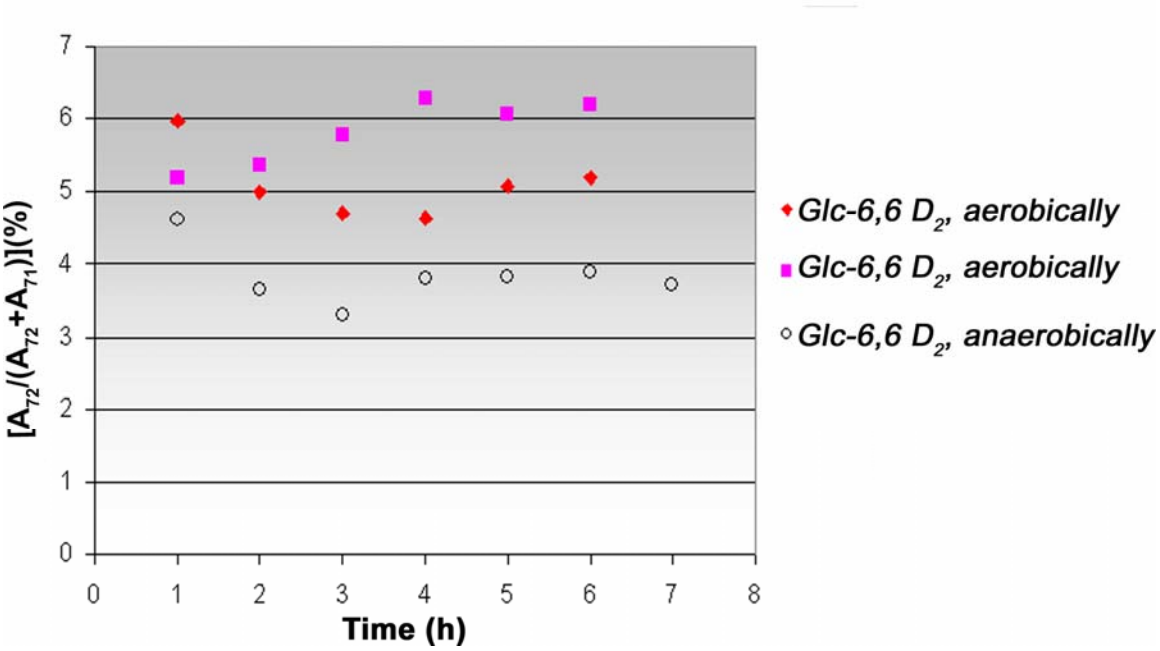

Figure 2-32. Fractional abundance (%) of 72 m/z fragment (A_{72}) of EHB produced by Δ*icd* strain using Glc-6,6 D_2 and anaerobic conditions in 10 ml scale, OD_{600}=7.0-9.0.

Finally, a very similar to Δ*pgi* pattern was observed for the Δ*pntAB* strain. (Figure 2-33).

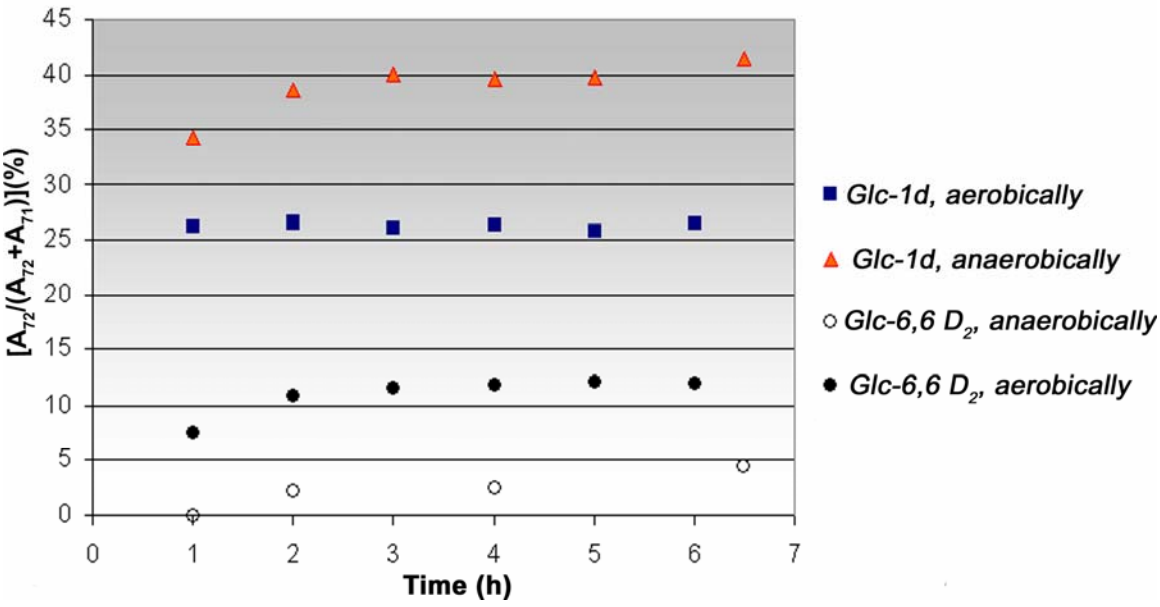

Figure 2-33. Fractional abundance (%) of 72 m/z fragment (A_{72}) of EHB produced by Δ*pntAB* strain using Glc-1D, or Glc-6,6 D_2 and anaerobic conditions in 10 ml scale, OD_{600}=7.0-9.0.

Evaluation of the MS Data

The quality of the MS data and the physiological conditions under which they were collected were verified by number of control experiments.

Physiological conditions

E. coli K strain is unable to grow on glycerol under anaerobic conditions.[168] In our experiments the conditions described as 'anaerobic' were justified by the inability of the WT strain to produce EHB in presence of glycerol when the sparger fitted to the reaction vessel was connected to an argon line (Figure 2-34). In contrast, the same strain reduced the ethyl-acetoacetate when a stream of air passed through the reaction mixture in otherwise identical conditions. In presence of glucose, formation of product was observed when the biotransformation was carried out either anaerobically or aerobically (Figure 2-35).

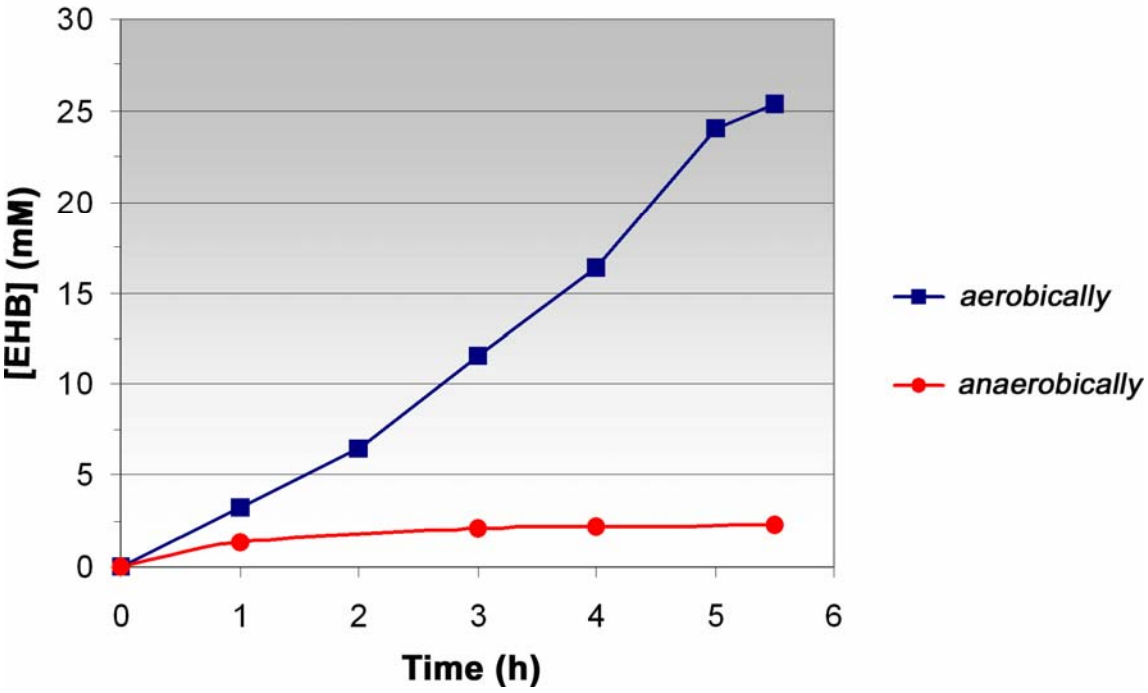

Figure 2-34. Production of EHB by WT strain fed with glycerol under aerobic and anaerobic conditions. OD_{600}=8.5

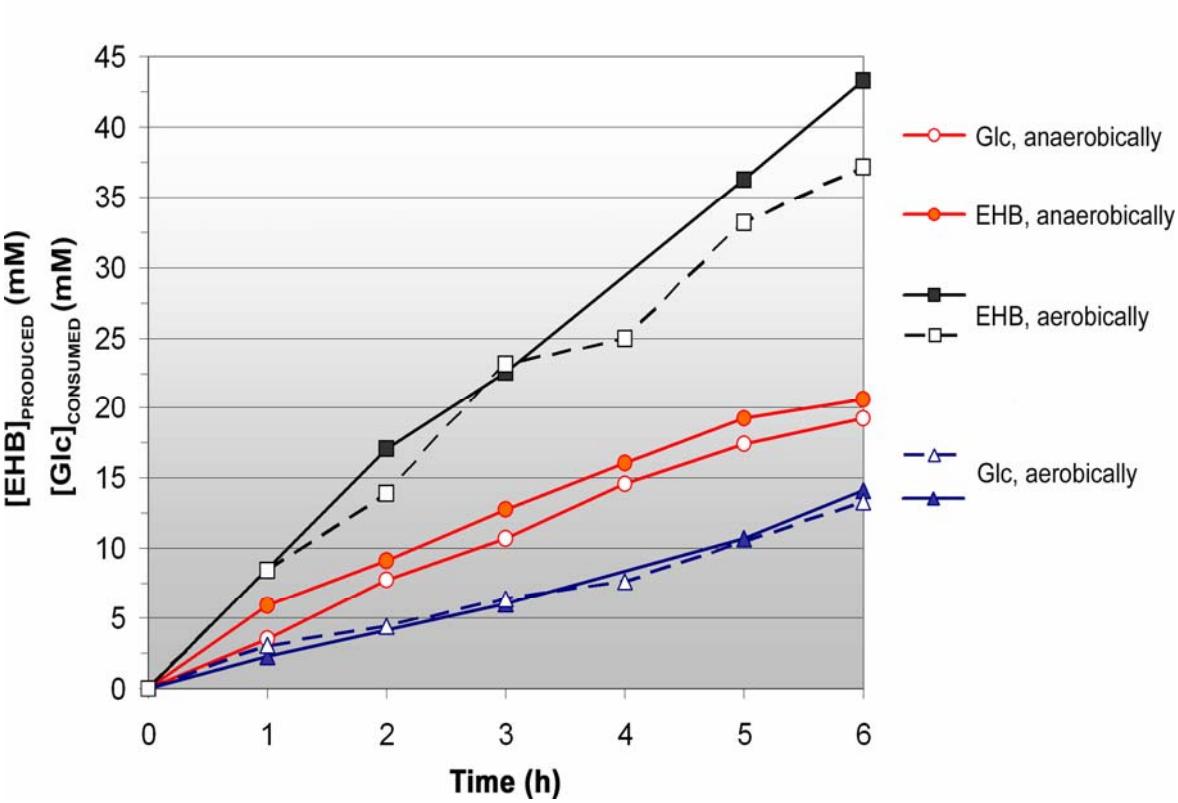

Figure 2-35. Production of EHB by WT strain fed with glucose under aerobic and anaerobic conditions. OD600=8.5-9.5.

Calculation of the intracellular ratio NADPH/NADPD from mass data

A typical fragmentation pattern of EHB is shown in Figure 2-15. Based on it, the ratio of unlabeled product ($\mathbf{P}_H$)/ labeled product ($\mathbf{P}_D$) could be calculated either from the pair of peaks A_{71}, A_{72} or from A_{117}, A_{118} if the naturally occurring elemental isotopes are also considered (i.e. the natural abundance of ^{13}C is 1.1%). Even though both pairs gave similar results, we based our data analysis on the former pair due to its higher abundance. For the correction regarding the 72 peak, a sample of unlabeled EHB prepared from the reduction of ethyl-acetoacetate (EAA) with sodium borohydride was injected multiple times in the GS-MS and the % fractional abundance of A_{72} was found 3.8%. A similar correction was applied to peak 71. Apparently, when the EAA was reduced by sodium borodeuteride the % fractional abundance of A_{71} was 4.6%.

Therefore the corrected ratio $(A_{71}/A_{72})_{COR}$ could be derived from the observed ratio $(A_{71}/A_{72})^{OBS}$ if the estimated error for each peak $(A)^{ER}$ is subtracted (Figure 2-36).

$$\left(\frac{A_{71}}{A_{72}}\right)_{COR} = \frac{A_{71}^{OBS} - A_{71}^{ER}}{A_{72}^{OBS} - A_{72}^{ER}}$$

$$\text{where } A_{71}^{ER} = \frac{A_{71}^{100\%LAB} \times (A_{71}^{OBS} + A_{72}^{OBS})}{(A_{71}^{100\%LAB} + A_{72}^{100\%LAB})} \text{ or } A_{71}^{ER} = 0.046 \times (A_{71}^{OBS} + A_{72}^{OBS})$$

$$\text{and } A_{72}^{ER} = \frac{A_{72}^{0\%LAB} \times (A_{71}^{OBS} + A_{72}^{OBS})}{(A_{71}^{0\%LAB} + A_{72}^{0\%LAB})} \text{ or } A_{72}^{ER} = 0.038 \times (A_{71}^{OBS} + A_{72}^{OBS})$$

Figure 2-36. Equation for derivatization of the corrected A_{71}/A_{72} from the observed ration.

A second concern was the possibility of an undesired isotope fractionation of the EHBs, labeled and unlabelled, during the GC separation. It is known that molecules bearing heavier atoms but otherwise identical are eluted first from the capillaly columns.[169] To avoid bias due to this fractionation the full peak range of the EHB signal was integrated.

The statement that the ratio $\mathbf{P}_H/\mathbf{P}_D$, derived from the corrected ratio A_{71}/A_{72}, is at any time equal to intracellular NADPH/NADPD ratio is true only if the two reduced nicotinamide cofactors substituted with different isotopes (i.e NADPH and NADPD) reduce, via Gre2, the EAA, with the same rate. This may or may not be true for an enzyme-catalyzed reaction depending on whether or not the component step related with the cleavage of the bond containing the isotope is rate-determining for the overall reaction.[170] In the latter scenario, the $\mathbf{P}_H/\mathbf{P}_D$ is proportional but not equal to NADPH/NADPD ratio and a correction including the kinetic isotope effect factor ($\mathbf{f_{KIE}}$) must be employed (Figure 2-37).

$$\frac{P_H}{P_D}=\frac{k_H}{k_D}\times\frac{[NADPH]}{[NADPD]}=f_{KIE}\times\frac{[NADPH]}{[NADPD]}\quad\text{or}\quad\frac{[NADPH]}{[NADPD]}=\frac{P_H}{P_D\times f_{KIE}}\quad\text{or}$$

$$1+\frac{[NADPH]}{[NADPD]}=\frac{P_H}{P_D\times f_{KIE}}+1\ \text{or}\quad\frac{[NADPD]}{[NADPD]}+\frac{[NADPH]}{[NADPD]}=\frac{P_H}{P_D\times f_{KIE}}+\frac{P_D\times f_{KIE}}{P_D\times f_{KIE}}\quad\text{or}$$

$$\frac{[NADPD]}{[NADPH]+[NADPD]}=\frac{P_D\times f_{KIE}}{P_H+P_D\times f_{KIE}}=\frac{1}{\left(\frac{P_H}{P_D}\right)\times\frac{1}{f_{KIE}}+1}\quad\text{or}$$

$$\frac{[NADPD]\%}{[NADPH]+[NADPD]}=\frac{100}{\left(\frac{A_{71}}{A_{72}}\right)_{COR}\times\frac{1}{f_{KIE}}+1}$$

Figure 2-37. Proposed correction for the NADPD fraction based on the corrected A_{71}/A_{72} ratio and a kinetic isotope effect factor $\mathbf{f_{KIE}}$.

Unfortunately, the experimental determination of $\mathbf{f}_{KIE}$ is not a facile task, especially if we consider that the intracellular concentration of substrate, coenzyme, enzyme, product and potential inhibitors are not well defined and the absolute value of $\mathbf{f_{KIE}}$ may depend on any of these effectors. Nevertheless we attempted to verify if an *in vitro* isotopic discrimination is plausibly for Gre2. To do so, we first determined the strereospecificity of Gre2.

Numerous of methods have been developed, in the past, for labeling each of the diastereomeric protons of NADPH at the 4-position.[171] We prepared both $NADPD_B$ and $NADPD_A$ using a known B-specific enzyme (Figure 2-28A) and an A-specific enzyme (Figure 2-38B) correspondingly, as described in experimental section. Both nucleotides reacted separately with Gre2 and EAA ((Figure 2-38C). When $NADPD_B$ was the reduced cofactor, deuterium found incorporated into product, as confirmed by GC-MS, and the oxidized cofactor was unlabeled, as confirmed by H-NMR (Figure 2-38D1).[172] The opposite pattern was observed when $NADPD_A$ replaced $NADPD_B$ (Figure 2-38D2).

Therefore, the Gre2 is a B-specific enzyme as predicted by its sequence similarity to 3-β-hydroxysteroid dehydrogenases and to plant cinnamoyl- CoA reductases (all of which are B-specific enzymes).[173]

Finally, for an estimation of the apparent kinetic isotope effect (f_{KIE}) by a competitive method, a mixture of NAPDH and $NADPD_B$ was allowed to react with the same substrate (i.e. EAA) in the presence of Gre2 simultaneously. The rationale behind this experiment is that at 100% conversion, the fractional abundance of peak 72 should reflect the initial fraction of labeled and unlabeled cofactors and should be constant during the time course of the reaction, in absence of an isotopic discrimination. Clearly, this was not the case at least under the conditions that this experiment was carried out (Figure 2-39). At a conversion lower that 50 % a 'lag-phase' for the deuterated species was detected and we may assume $f_{KIE} = \left(A_{71}/A_{72}\right)_{initiail} \Big/ \left(A_{71}/A_{72}\right)_{final}$ or f_{KIE}~1.3.

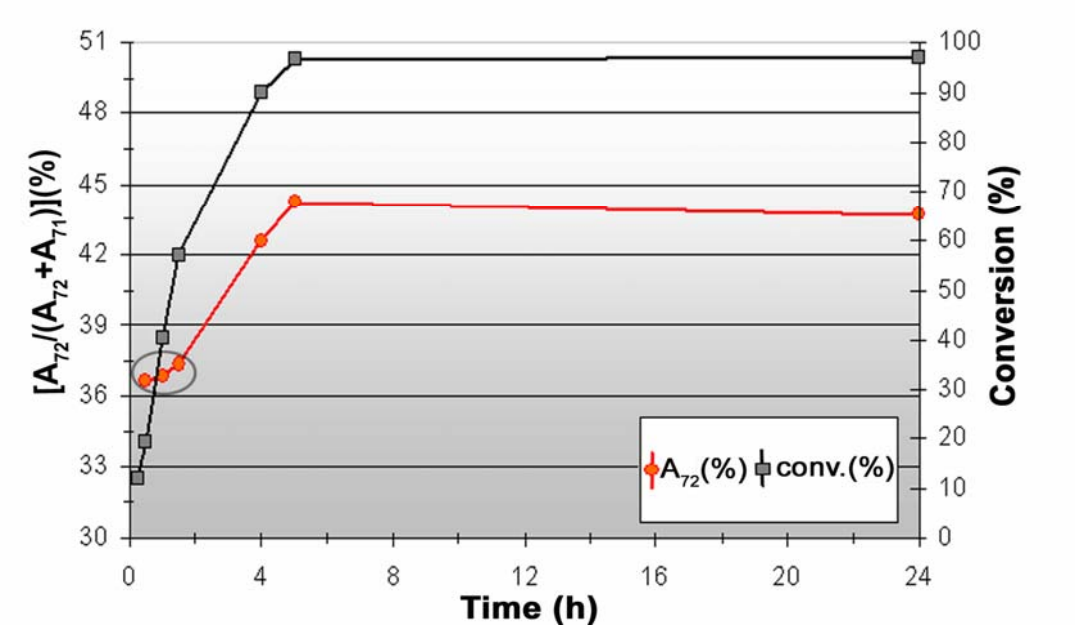

Figure 2-39. Fractional abundance (%) of 72 m/z fragment (A_{72}) of EHB produced by Gre2 in presence of NADPH and NADPD.

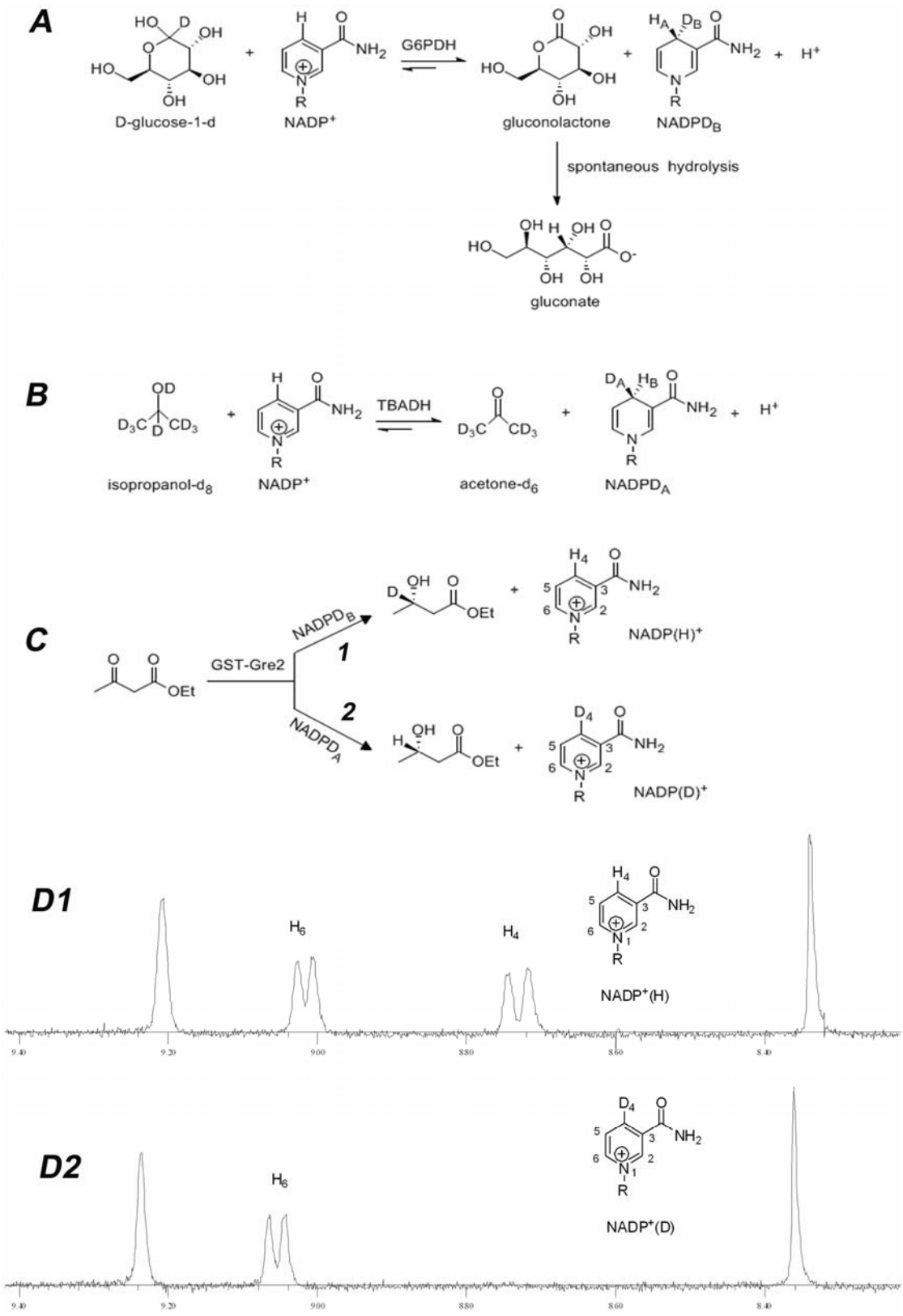

Figure 2-38. Preparation of stereospecific labeled NADPH and elucidation of Gre2 facial selectivity by H-NMR.

Another question related to isotopic discrimination is if the extent by which its each particular pathway is utilized, is changing when the unlabeled sugar is replaced by the deuterated one. In such a case an underestimation of the partition from the step related to reduction of $NADP^+$ is possible but a correction is not straightforward. Also, we should mention that the results presented above are the average incorporation during the time-frame reported for each biotransformation. Even though under aerobic conditions a plateau was achieved relatively early, this was not the case under anaerobic conditions. The lower rate of product formation as well as changes on relative fluxes, KIEs and physiological conditions (i.e., pH changes) may account for this phenomenon. Lastly, when labeled EHB was incubated only with cells and glucose, a 1.1 % loss of deuterium per hour was observed: however, this may not happen in presence of EAA and in any case since most data were collected during the first 5-6 hours the overall loss should not exceed the 5-6%.

The best way to evaluate the consistency of the suggested corrections is by applying them to the initial MS data. The overall results are summarized in Table 2-9.

Table 2-9. Fractional abundance of NADPD.

E. coli strains	Fractional abundance of NADPD (%), aerobically			Fractional abundance of NADPD (%), anaerobically		
	Glc-1-D	Glc-3-D	Glc-6,6-D_2	Glc-1-D	Glc-3-D	Glc-6,6-D_2
WT	21-23	20-22	10-12	30-40	---[a]	0.1-0.5
Δ*pgi*	28-34	27-30	9-12	37-41	---	0.1-0.5
Δ*zwf*	2-3	0.0-0.3	22-23	0.0-0.4	---	3.0-4.0
Δ*icd*	35-49	---	1-2	25-27	---	0.0-0.1
Δ*pntAB*	29-30	---	10-11	44-48	---	0.0-0.8

[a]Not determined.

Experiments under anaerobic conditions in presence of Glc-1D could serve as a guide for this evaluation. Under these conditions and especially in absence of a possible PntAB transhydrogenase activity, the theoretical maximum value for the fractional abundance of NADPD should be 50%, since there is no icd activity (< 1% deuterium content from Glc-6,6-D_2) and the protium at position 3 of glucose should contribute the

rest 50 % of the unlabeled product via Gnd. The experimental value, with corrections included, is 44-48%. Slightly lower numbers were estimated for the WT and Δ*pgi* strains. The null incorporation for Δ*zwf* strain is also expected in the absence of G6PDH activity in this mutant. The only inconsistency is the somewhat lower value calculated for Δ*icd* strain, even though this number is based only on one experiment. However, the same sugar under aerobic conditions labeled the product at 35-49% as if, in absence of icd, zwf and gnd are almost the exclusively contributors on $NADP^+$ reduction. In contrast, in the WT strain under the same conditions, the two NADPH sources in PP pathway contribute at levels of ~21% each. The strong participation of icd in regeneration of NADPH is apparent for the WT. The ~11% labeled EHB when cells were fed with Glc-6,6-D_2 suggests this trend. This number must be multiplied by an additional factor of 2 to 3 (Figure 2-24) in order for it to reflect the real contribution of TCA cycle in NADPH production in WT strain, under aerobic conditions. This participation is almost absent under anaerobic conditions in all strains but Δ*zwf*. It is unclear is this small, but measurable amount of deuterated product is due to maeB activation in this particular strain or due to experimental error. Also, one may ask if the small (2-3%) but measurable difference of deuterium content in EHB in between cells fed with Glc-1D and cells fed with Glc-3D is due to a small participation of ED pathway. This is unlikely at least for the WT strain. The most probable explanation is that the amount of labeled product in presence of Glc-1D reflects the sum of PP pathway activity and TCA cycle activity, whereas in presence of Glc-3D only the PP pathway activity is detected since deuterium at position 3 of glucose should be lost in water through glycolysis (Figure 2-24). Nevertheless, the contribution of deuterium from position 1 of glucose to the NADPD pool, due to icd activity only, is more than twice lower than the one from Glc-6,6-D_2. In principle, we should expect exactly twice less contribution (i.e.

two over one atoms labeled). For example, in Δ*zwf*, if Glc-6,6-D_2 contributed to 22% the Glc-1-D should have participated at 11%, but only 2-3% was the experimental obtained labeled product. The hydrogen atom at position 1 may be prone to exchange with water more easily than the hydrogen atoms at position 6.[167] Issues related with the stereospecifiity of TCA cycle's enzymes may be another explanation.[174]

Productivity of Mutant Strains versus the Wild Type in a Shake Flask

The Δ*zwf* and Δ*icd* strains produced EHB to lesser extents as compared to wild type (Figure 2-40). This was an expected outcome if we consider that the reaction is absolutely NADPH-dependant and both strains are missing two and one NADPH-regeneration enzymes, respectively. Less problematic was the productivity of Δ*pntAB* strain (Figure 2-40) indicating a minor contribution, if any, of this source to NADPH regeneration machinery.

What about the Δ*pgi* strain? All literature data suggested that the NADPH produced in this strain is in excess compared to its NADPH biosynthetic needs. Our experiments in a shake flask showed no significant difference from the WT strain, within the experimental error, in product rate formation at least for the first four hours. The observed retardation of product formation for the WT strain after the first six hours was due to faster pH drop in the flask containing this strain compared to the one containing cells of Δ*pgi* strain. When the pH was adjusted manually in both flasks every three hours, the previously observed difference was diminished (data not shown). The same trend was observed when the rate of product formation of the two strains was tested in a 2-L fermenter under supervised conditions.[175] The lower rate of glucose consumption observed for Δ*pgi* may contribute to slower production of organic acids by this strain.

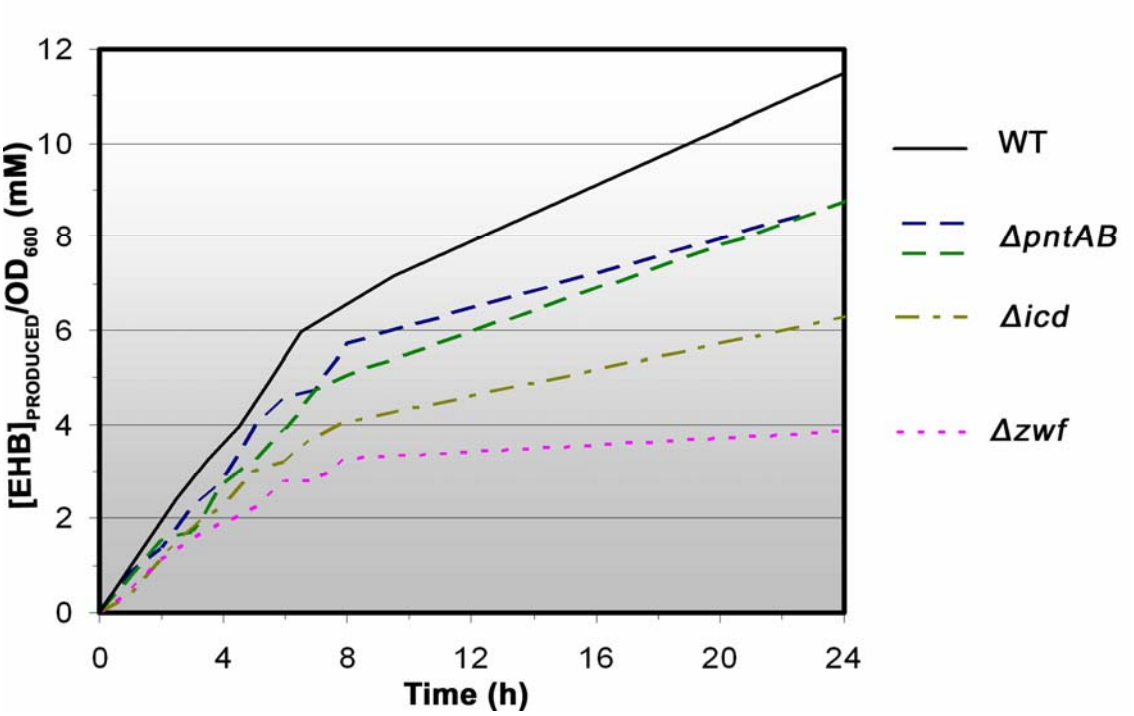

Figure 2-40. Product formation of Gre2 overexpressed either in Δ*zwf* or Δ*icd* or Δ*pntAB* strain. Data are normalized per biomass concentration expressed as optical density of culture medium at 600 nm.

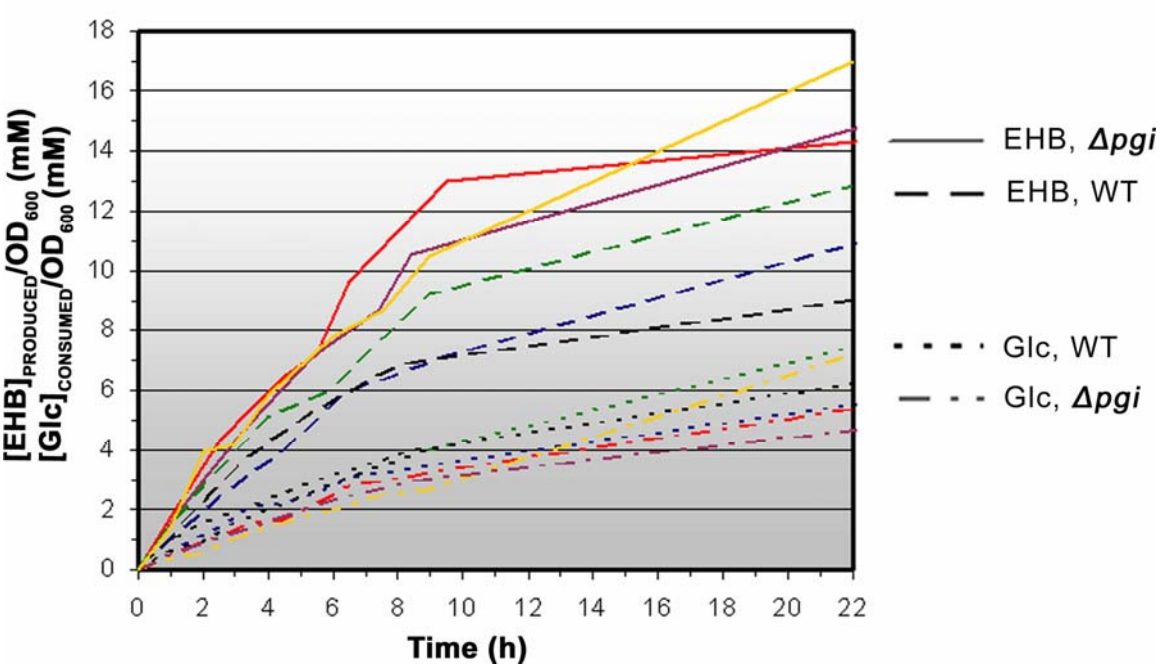

Figure 2-41. Product formation of Gre2 overexpressed either in Δ*pgi or* WT strain. Data are collected from three independent experiments and normalized per biomass concentration expressed as optical density of culture medium at 600 nm.

Discussion

By combing isotopic tracer experiments with the overexpression of a NADPH-dependant reductase in a *E. coli* BL21(DE3) strain and using a very simple experimental setup, we successfully revealed at least three NADPH regeneration sources within this biocatalyst when glucose was used as a carbon source. The validity of our results in the wild-type strain was justified further by repeating the labeled studies in isogenic to WT strains overexpressing Gre2. Even though the presented methodology belongs to low resolution techniques for elucidation of metabolic fluxes, it still allows us to draw some conclusions about the relative participation of each NADPH source to ethyl-acetoacetate reduction in WT strain. Unfortunately, due to the additional, albeit not well defined, adjustments required for the derivatization of the icd contribution to NADPD pool from the experimental data (i.e. not one to one ratio of deuterium atoms between the donor and acceptor molecules and possible dilution of deuterium through glycolysis) this estimation is prone to higher error. Nonetheless, in order to ease our discussion in this section, we multiplied our numbers for the Glc-6,6D_2 experiments by a factor of 3 assuming that trioses from the EMP pathway are accessing the TCA cycle only via pyruvate and that no scrambling from protium atoms occurred during this process.

Clearly, both the PP pathway and the TCA cycle are competing equally in producing reductive equivalents for bioreduction (Figure 2-42) in this bioprocess. It would be beyond the resolution of this method to state which source dominates. Unfortunately, labeled experiments with Glc-4D, which may uncover a transhydrogenase role, were not performed in this study because of the high cost of this isotopomer sugar. However, we may be able to predict if a transhydrogenase activity is possible if we compare the results obtained from the WT strain with those from the ΔpntAB strain.

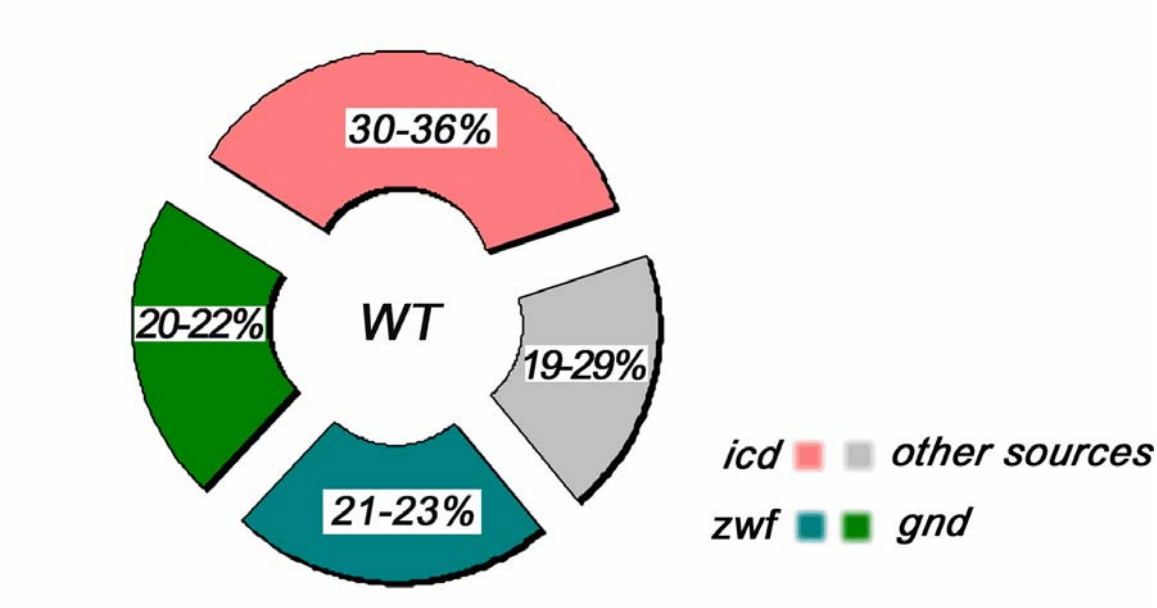

Figure 2-42. Proposed participation of NADPH regeneration sources in *E. coli* BL21(DE3)(pAA3) resting cells.

In both Figure 2-42 and Figure 2-43, a transhydrogenase activity may fit under the label 'other sources'. But, at least for the latter strain, a transhydrogenase activity towards the production of NADPH (i.e. pntAB) must be excluded since the structural gene is deleted. Hence, in WT strain, only half of the percentage denoted as 'other sources' should be ascribed to possible pntAB action (i.e.10-20%). This hypothesis reveals that in Δ*pgi* strain such an activity is also unlikely. A participation of pntAB similar to one observed for the wild type could be assumed in case of Δ*zwf* mutant whereas more uncertain are the results for the Δ*icd* strain.

Ultimately, the question that is coming next is how our results could be correlated to the data obtained from similar studies for other systems. Before we attempted such a comparison, it is worth noting that the prediction made by Walton and Stewart about the importance of TCA cycle's contribution in NADPH production, in our system, was on the right track. One reason for the possible overestimation of this contribution by a factor of

2 compared to the data obtained in this study is that the authors almost ignored that oxidative catabolism does not necessarily imply complete oxidation of glucose.[147]

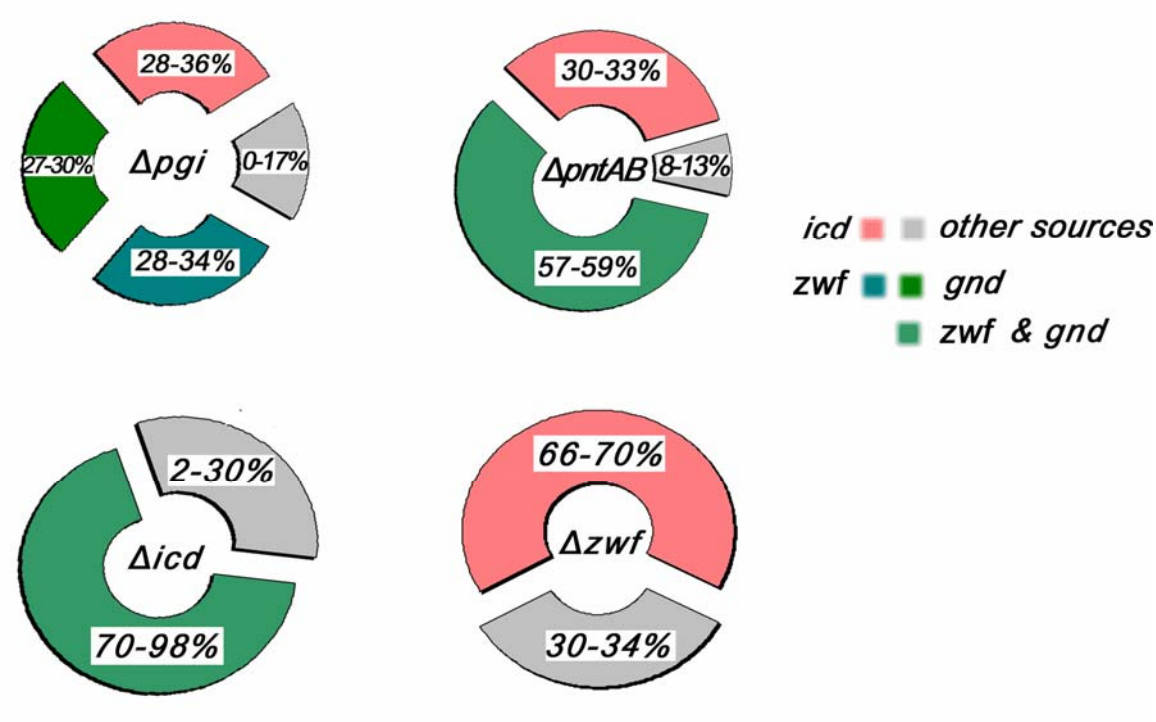

Figure 2-43. Proposed participation of NADPH regeneration sources in *E. coli* BL21(DE3)(pAA3) mutant stains under non-growing conditions.

To compare our results with the already published data we will use two studies as references: i) the work reported by Csonka and Fraenkel[176] because the methodology used in that work is more similar to our study (i.e. both are low resolution methods based on labeled hydrogen atoms attached to glucose molecule) and ii) the work done by Sauer et. al.[177] because it is offering the most complete picture of the glucose catabolism in *E. coli* since is based on net flux measurements. In sharp contrast to what the data from the former study showed, our experimental results implied a strong participation of Icd in the intracellular NADPH pool. Despite the controversial issue about the exact percent of contribution from this NADPH source, the facts that i) we observed higher deuterium content in product from the Glc-6,6D_2 than from the Glc-1D, which the

previous authors did not, ii) they observed incorporation of deuterium into amino acids from position 6 of the glucose even under anaerobic condition or even when they used a Δ*icd* mutant and we did not, suggested, at least in our system, participation of icd to NADPH regeneration sources. Their suggestion for about 40% participation of PP pathway in NAPDH pool is inline with our results. Open is the possibility for a fourth regeneration source, most likely a transhydrogenase activity, in both studies. The most solid experimental evidences for the pntAB participation are provided by Sauer's laboratory. We should mention, though, that even with their high resolution technique, the 35-45% estimation for the PntAB partition was based on an indirect calculation. They calculated the specific rate of NADPH production from the PP pathway and TCA cycle (i.e., 3.9 mmol h^{-1} g^{-1}(DCW) and 2.3 mmol $^{-1}$ g^{-1}(DCW) respectively) from the metabolic flux analysis data. They then estimated the specific rate of NADPH consumption (i.e. 11 mmol h^{-1} g^{-1}(DCW)) for biosynthetic needs of *E. coli* cell, using literature data and the calculated growth rate and since they found that the latter is higher than the former they proposed that the gap should be covered by the pntAB activity. Despite that, they also arrived to the same conclusion about the approximately 40% contribution from the PP pathway to NADPH pool as we did, whereas they estimated the merits for icd to 25% maximum.

The last question, and most difficult to answer, is why our Δ*pgi* strain did not show an improved productivity. We should not conceal the fact that the ultimate goal of this study was to improve the productivity of this NADPH-dependant bioprocess. But, in order to improve any process, we should be aware of the theoretical maximum that we are seeking to reach. Unfortunately, this is not a straightforward estimation due to the inherent complexity of our system. For example, what if the productivity of our system is limited by the rate of EAA transfer through the cell membrane? Or what if it is limited by

the amount of the overproduced enzyme? Someone may suggest *in vitro* measurements for calculating the specific activity of Gre2, but again this kind of measurements may serve as a guide but they could exclude a higher or lower *in vivo* activity for the same biocatalyst. Therefore, if the productivity of our system is limited by a factor other than the NADPH availability within the cell, any manipulation regarding this issue will fail to improve the rate of product formation. To modify our original question we will ask if the apparent failure of the Δ*pgi* strain towards the improvement of product rate formation is evidence that our system's maximum limit does not depend on NADPH regeneration rate. The answer is, absolutely not. Our study does not exclude the possibility of a back-flux from the NADPH to NAD^+ via the soluble transhydrogenase UdhA as well as the co-existence in Δ*pgi* mutant of a novel PEP-glyoxylate cycle, which does not produce NADPH and is redundant to UdhA activity.[178] For example, from Sauer's study we know that the production rate of NADPH in Δ*pgi* stain is the same as the one in the WT, the difference is, the much lower specific rate consumption which in turn activates the back-flux activity via UdhA. A more clear solution to our problem it would be to use a double Δ*pgi*Δ*udhA* knockout strain. Unfortunately, the Pgi-UdhA phenotype is lethal on glucose and it is unknown how this mutant grows on complex media.

Future Work

The ultimate goal of any bioprocess optimization is to increase the rate of product formation per liter of medium (volumetric productivity) and to improve the final product yield per liter (product titre) by using the minimum amount of biomass and carbon source. For a two step process, as the one that we described in this chapter, the expression levels of the NADPH regeneration sources are governed by the biosynthetic needs of the *E. coli* cell in the first phase (i.e. growth in complex media). Those levels

may not be sufficient to meet the needs of an overproduced, NADPH-dependent biocatalyst in the second phase. Based on Walton and Stewart data, the productivity of this bioprocess was ~120 U/g (DCW) for resting cells, whereas the NADPH regeneration rate of aerobic growing *E. coli* cells in M9 medium is 180U/g (DCW).[177] Therefore, we cannot exclude the possibility that in rich media, the cells are not adjusting their metabolism for the optimum NADPH regeneration rates observed in minimal, glucose-limited media. Controlled induction of *zwf* with concomitant deletion of competing for NADPH utilization enzymes may shed light on this problem. In addition, replacement of the NAD^+ -dependant D-glyceraldehyde-3-phosphate dehydrogenase (GAPDH) with a novel $NADP^+$-GAPDH from *Kluyveromyces lactis* [179, 180] and or overexpression of a transhydrogenase may add a NADPH regeneration source in the EMP pathway level and thus bypass the product formation dependence on TCA cycle which in turn depends on oxygen availability. In cases where glucose must be replaced by glycerol, expression of the *dha* operon (i.e., glycerol dehydratase (*dhaB*), 1,3-propanediol oxidoreductase (*dhaT*), glycerol dehydrogenase (*dhaD*) and dihydroxyacetone kinase (*dhaK*)) from *Klebsiella pneumoniae* for dissimilation of glycerol under anaerobic conditions[181, 182] could enhance the productivity of biocatalyst under oxygen-limited conditions.

The above suggestions may be proved useful for ‘easy’ substrates in other words for substrates that the cell membrane does not impose a barrier and the glucose catabolism is not poisoned by them. Unfortunately, those substrates are rather the exception than the rule in whole-cells biocatalysis. For those ‘difficult’ substrates any combination of overexpressed reductase with an overexpressed NADPH-regeneration enzyme in the same or in separate, intact or permeabilized cells must be first employed in a small, exploratory scale before the progression to the final scale-up process.

CHAPTER 3
E. COLI BL21 (DE3) Δ*yqhE* STRAIN: A 'CLEANER' HOST FOR OVERPRODUCTION OF NADPH-DEPENDENT KETOREDUCTASES

> Of the chemical aids in the living organism the ferments - mostly referred to nowadays as enzymes - are so pre-eminent that they may justifiably be claimed to be involved in most of the chemical transformations in the living cell. The examination of the synthetic glucosides has shown that the action of the enzymes depends to a large extent on the geometrical structure of the molecule to be attacked, that the two must match like lock and key. Consequently, with their aid, the organism is capable of performing highly specific chemical transformations which can never be accomplished with the customary agents. To equal Nature here, the same means have to be applied, and I therefore foresee the day when physiological chemistry will not only make extensive use of the natural enzymes as agents, but when it will also prepare synthetic ferments for its purposes.
>
> -Syntheses in the purin and sugar group, Emil Fischer[183]

Introduction

In 2000, seventy-six percent of the new drugs introduced in the market were single enantiomers, compared with 21% in 1991.[184] The reasons for this include the established, by pharmacological research, differential, enantiomer-specific, relationship between the drug and the target biological macromolecule and the desire to minimize the cost and the wastage resulting from the production of unwanted enantiomers.[185] The benefits derived from the asymmetric and catalytic operation of enzymes have been recognized today by both the academic and the industrial community.[186-189]

The most popular biocatalytic approach to asymmetric ketone reduction is the use of commercial bakers' yeast.[190] Whole cells of this microorganism provide a simple and inexpensive way to produce chiral alcohols since they possess a vast number of keto-reductases and they are able to regenerate simultaneously the required cofactors through the dissimilation of a cheap carbon source. Unfortunately, the reductive power of yeast, due to plurality of reductases in it, can also become a disadvantage in

situations where two or more reductases with conflicting stereoselectivities are acting on the same pro-chiral ketone.[191] The net result for this operation, which is not rare for this biocatalyst, is a product with a low enantiomeric purity. A number of empirical methods were developed in the past in an effort to improve the stereoselectivies of this microorganism.[190, 191] Additionally, strain engineering strategies, including gene disruption and overexpression of the desired reductase in the same host, showed promising results but they did not completely overcome the problem.[192, 193]

An alternative strategy, initiated and completed by former students in our laboratory, gave an almost 'checkmate solution' to the aforementioned problem.[194, 195] Briefly, a list of potential keto-reductases (ca. 50) was compiled by analyzing the complete genome sequence of *S. cerevisiae*[196] and the genes encoding half of them were cloned, as GST-tagged, and overexpressed in the *E. coli*, one by one. This methodology leads to:

- higher amounts of the desired biocatalyst,
- higher flexibility in choosing expression vectors,
- a simple and relatively fast enzyme-purification protocol,
- flexibility in using, at any time, the biocatalyst either as a single purified protein or as an overproduced enzyme in intact *E. coli* cells.

The last point is of paramount importance for verifying the inherit stereospecificity of each biocatalyst since the *ee* values obtained when the purified enzyme is employed should match with the ones obtained when the same biocatalyst is used in whole-cells, in absence of competing *E. coli* reductases. Unfortunately, even this microorganism is not totally devoid of endogenous carbonyl-reductase activities.

Carbonyl Reductases in the *E. coli*

In 1996, two reports described the presence of carbonyl reductases in *E. coli*. Miya et al.[197] showed that whole cells of a number of Gram-negative bacteria, including *E. coli*, reduced one specific β-keto ester (ethyl 2-methylacetoacetate) to *syn*-(2*R*,3*S*) alcohol, whereas Misra et al.[198] reported the purification of two enzymes, one NADH-

dependent and another NADPH-dependent, from the *E. coli* capable to reduce methylglyoxal to acetol. Even though the molecular weight of both reductases was estimated by gel filtration on Sephacryl column (i.e. ~ 100.000 Da), the amino acid sequences were not determined and therefore the genes encoding them remained unknown. Yum et al.[199] were the first who identified the *yqhE* and *yafB* genes as potentially encoding 2,5-diketo-D-gluconate reductases because of their high sequence similarity to other bacterial homologues with known function. They verified further their prediction by cloning and overexpressing the gene products in the same host. Although they showed that both enzymes catalyzed the reduction of 2,5KDG to 2-keto-L-gulonate, no other substrate was tested in that study.

In our laboratory, the activity of keto-reductases in unmodified *E.coli* cells was recorded, for the first time, when two members of the aldo-keto reductase (AKR) superfamily (Gre3p and Gcy1p) were overexpessed in *E. coli* and the whole cells were used to reduce a panel of β-keto esters.[194] Subsequently, reductase activity against ethyl 2-methylacetoacetate was used to purify the enzyme responsible for this bioreduction from 100 g of *E. coli* BL21(DE3) cells.[200] The N-terminal amino acid sequence analysis of the purified reductase matched with the protein encoded by the *yqhE* gene.

A BLAST search of YqhE sequence against the EcoGene[201] database revealed the presence of nine putative AKRs in *E. coli* (Table 3-1). Recently, an independent study by Ko et al.[202] indicated that four of them (*yafB, yqhE*, *yeaE* and *yghZ*), out of the five tested, are involved in the conversion of methylglyoxal (MG) to acetol in presence of NADPH. The authors suggested that MG may serve as endogenous substrate for these AKRs based on the fact that: i) 2,5-DKG does not appear to be an endogenous substrate of the *E. coli* cell ii) MG could be accumulated into the cells under physiological conditions with an uncontrolled carbohydrate metabolism and iii) the k_{cat}/K_M

of YqhE for 2,5-DKG is lower than the one obtained for MG. However, strain lacking the *yqhE* did not exhibit the increased *in vivo* MG susceptibility that was observed for the other three knockout strains.

With the dkgA reductase being the best characterized enzyme, with broad substrate specificity (Figure 3-1), among the AKRs in *E. coli*, the question for their physiological role remains unanswered.[203] However, multiple sequence alignment of all nine open reading frames (Figure 3-2) revealed the presence of the conserved among AKRs superfamily catalytic tetrad of amino acids (Tyr, His, Asp and Lys) in all but ydbC (i.e., His is replaced by Arg, not shown in Figure 3-2) which facilitate the transfer of a hydride ion from NADPH to the substrate with a concomitant protonation of the nascent alcohol. In addition to conserved catalytic mechanism, the recently obtained crystal structure of DkgA[204] showed the characteristic $(\alpha/\beta)_8$ TIM barrel motif (Figure 3-3), common for all AKRs.[205]

Table 3-1. Putative AKRs in *E. coli*.

Primary gene name (alternative name)[201]	Function	Identity (%)	Crystal structure (PDB)[206]	Ref.
dkgA (*yqhE*)	2,5-diketo-D-gluconate reductase A, beta-keto ester reductase; methylglyoxal reductase; NADPH-dependent	100	1MZR	199, 200, 202
dkgB (*yafB*)	2,5-diketo-D-gluconate reductase B, methylglyoxal reductase	38	---	199
yeaE	Methylglyoxal to acetol; NADPH-dependent	28	---	202
ydjG	function unknown; NADH-dependent; use methylglyoxal as substrate	25	---	201
yajO	2-carboxybenzaldehyde reductase, function unknown	22	---	201
ydhF	Unknown	25	1OG6	201
tas (*ygdS*)	Suppresses tyrosine requirement of tyrA14 O6 strain	31	1LQA	207
ydbC	Unknown	23	---	201
yghZ	Methylglyoxal reductase	34	---	208

Because our laboratory had accumulated strong evidences for the participation of YqhE in the reduction of β-keto esters, the aims of this work were:

- To knock out the *yqhE* gene in *E. coli* BL21(DE3) strain using a methodology which enables marker-free deletions.
- To assess the impact of the mutated strain on β-keto esters reductions.

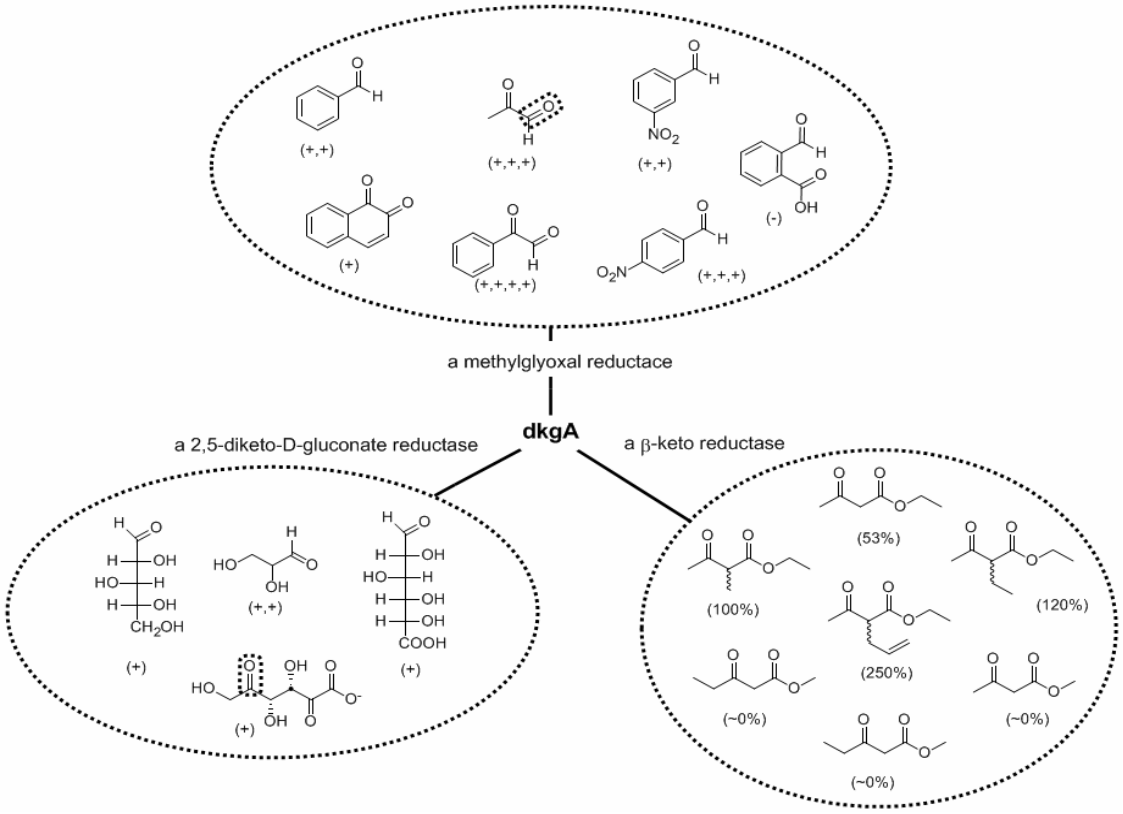

Figure 3-1. Substrate specificity of dkgA. Relative activity among different substrates is indicated in parentheses (e.g. (++++), highest, (-) lowest).

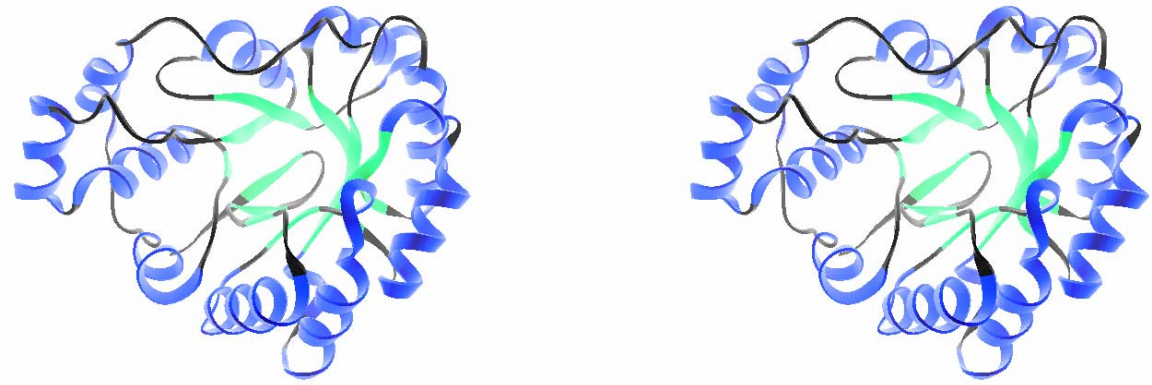

Figure 3-2. Stereoview of the ribbon structure of DkgA (chain A). This picture was rendered in 3D-Mol Viewer.

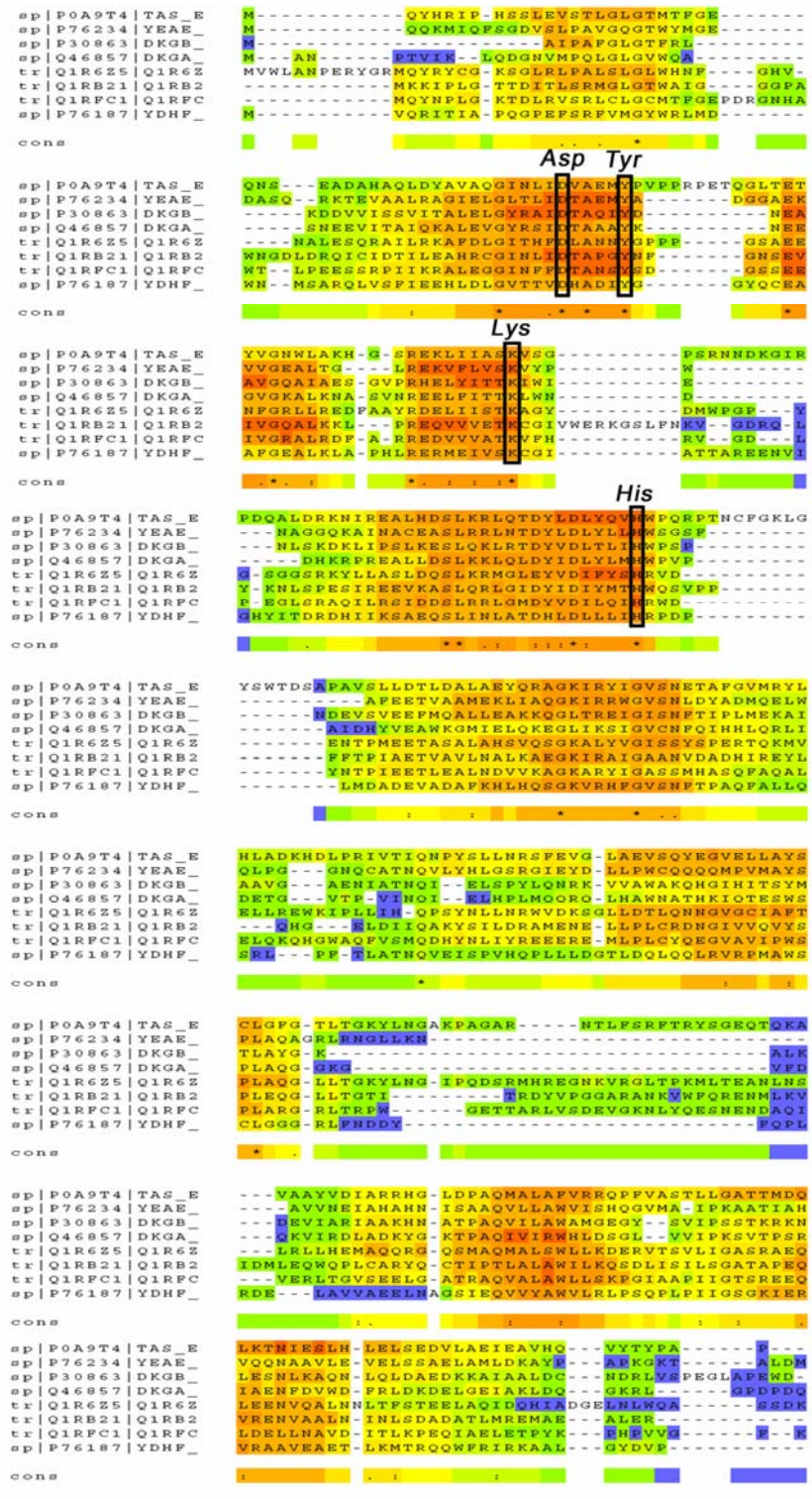

Figure 3-3. Multiple alignment of eight AKRs from *E .coli*. The alignment was generated using the TCoffee web server software.[209]

Experimental Procedures

Most of the experimental procedures were described in Chapter 2.

Superbroth (SB) medium used for cell growth contained Bacto-Tryptone (32 g/L), Bacto-Yeast Extract (20 g/L), sodium chloride (5 g/L) and 5 ml 1M NaOH.

The analytical separation of the diasteroisomers obtained from the bioreduction of ethyl 2-fluoroacetoacetate was conducted with a Hewlett-Packard Model 5890 GC fitted with a 30 m DB-17 column and a temperature gradient from 55°C to 180°C at 5°C/min with initial and final times 2 and 5 min, respectively.

The synthesis of the FRT-kan-FRT cassette with short flanking homologous regions of *E. coli* BL21 (DE3) DNA was carried out in one-step PCR using long chimeric primers in which the 3' end primed to beginning or the end of the FRT-kan-FRT cassette and the 5' end (46nt) was homologous to upstream or downstream region of the yqhE (Appendix C).

Results and Discussion

Characterization of Δ*yqhE* Strain

Initially, we attempted to disrupt the *yqhE* in the *E. coli* BW25113 strain using the FRT-kan-FRT cassette flanking with short homologous regions (ca. 50 bp), as described by Datsenko and Wanner.[210] In total, 50 kan^R colonies from six independent transformations were screened. Unfortunately, none of them contained the desired replacement. Taken into account both the lower transformation efficiency of the *E. coli* BL21(DE3) strain, which was the desired host for the overexpression of the keto-reductases and the higher recombination efficiency observed by Court et al.[211] when markers with longer homologous arms were used, we shifted to a marker cassette with longer (ca. 500 bp) homologous regions. One kan^R colony was obtained after the

transformation with the longer piece. Colony PCR confirmed the desired disruption (Figure 3-4 and Table 3-2).

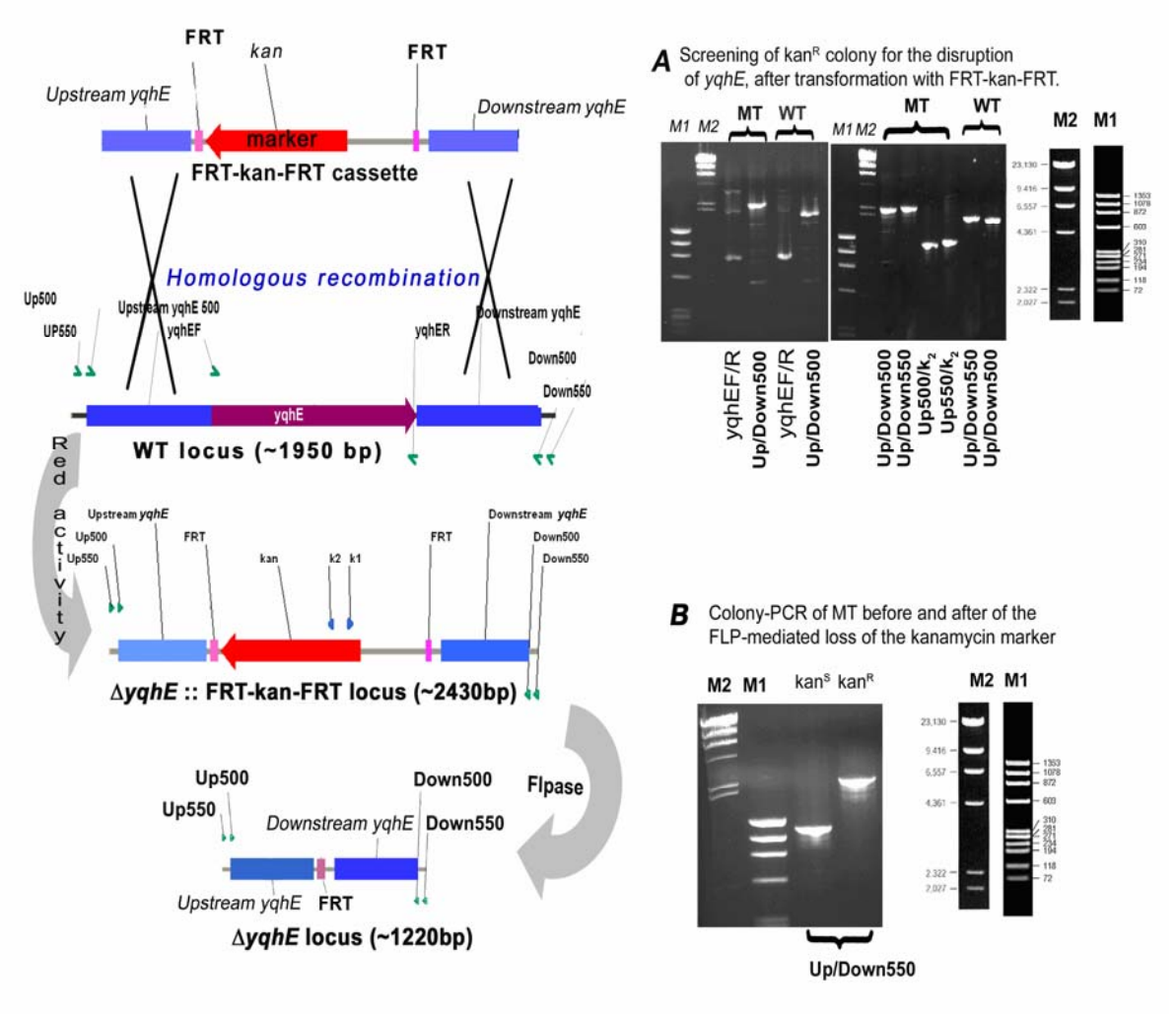

Figure 3-4. Results from colony PCR reactions probing the *yqhE* locus before and after the disruption. Abbreviations: WT (wild type), MT (mutant strain); kan^R, kanamycin resistant; kan^S, kanamycin sensitive; M1and M2, DNA markers.

Table 3-2. Colony PCR for *yqhE* knock-out.

E. coli strain	Primers Set	Expected Size (kbp)	Observed Size (kbp)
BL21(DE3) Δ*yqhE*:: FRT-kan-FRT	yqhEF, yqhER	no band	~2.6, ~1.9, ~0.8, (all minor)
BL21(DE3) Δ*yqhE*:: FRT-kan-FRT	Up500yqhE500, Down500yqhE500,	2.3	~2.3
BL21(DE3) Δ*yqhE*:: FRT-kan-FRT	Up550yqhE, yqhER	no band	no band
BL21(DE3) (pKD46)	Up550yqhE, yqhER	1.38	~1.4

Table 3-2. Continued.

E. coli strain	Primers Set	Expected Size (kbp)	Observed Size (kbp)
BL21(DE3) Δ*yqhE*:: FRT-kan-FRT	Up500yqhE500, k2	1.18	~1.2
BL21(DE3) (pKD46)	yqhEF, yqhER	0.8	0.8
BL21(DE3) (pKD46)	Up500yqhE, Down500yqhE	1.8	~1.8
BL21(DE3) Δ*yqhE*:: FRT-kan-FRT	Up550yqhE, Down550yqhE,	2.4	~2.4
BL21(DE3) Δ*yqhE*:: FRT-kan-FRT	Up550yqhE, k2	1.24	~1.25
BL21(DE3) (pKD46)	Up550yqhE, Down550yqhE	1.9	~1.9
BL21(DE3) Δ*yqhE*:: FRT	Up550yqhE, Down550yqhE	1.2	~1.2

Biotransformations

To assess the impact of the single knockout *E. coli* strain on β-keto ester reductions, we carried out three sets of bioconversions using known substrates for the DkgA reductase. Cultures of both strains were grown in 100 ml SB medium at 37°C under aerobic conditions in 1 L Erlenmeyer flasks. There was essentially no difference in growth rates between the parent and the yqhE knockout strain (Figure 3-5). After 3.5 h of growth, substrate was added to a final concentration of 5 mM. Both ethyl-2-methylacetoacetate and ethyl 2-allylacetoacetate were reduced completely by intact *E. coli* BL21(DE3) cells (WT) under growing conditions. By contrast, even extended reaction times (48 h) failed to result in formation of the corresponding, substituted at alpha position, β-hydroxy esters when the mutated strain (MT) was employed instead. However, the reduction of the unsubstituted ethyl acetoacetate was only slightly affected by the presence or absence of the dkgA reductase (Table 3-3). Also, it is worth noting that when the bioconversion of ethyl-2-methyl acetoacetate was attempted with resting cells (OD_{600}= 9.0) no conversion was observed, by either strain, even after 2 days incubation.

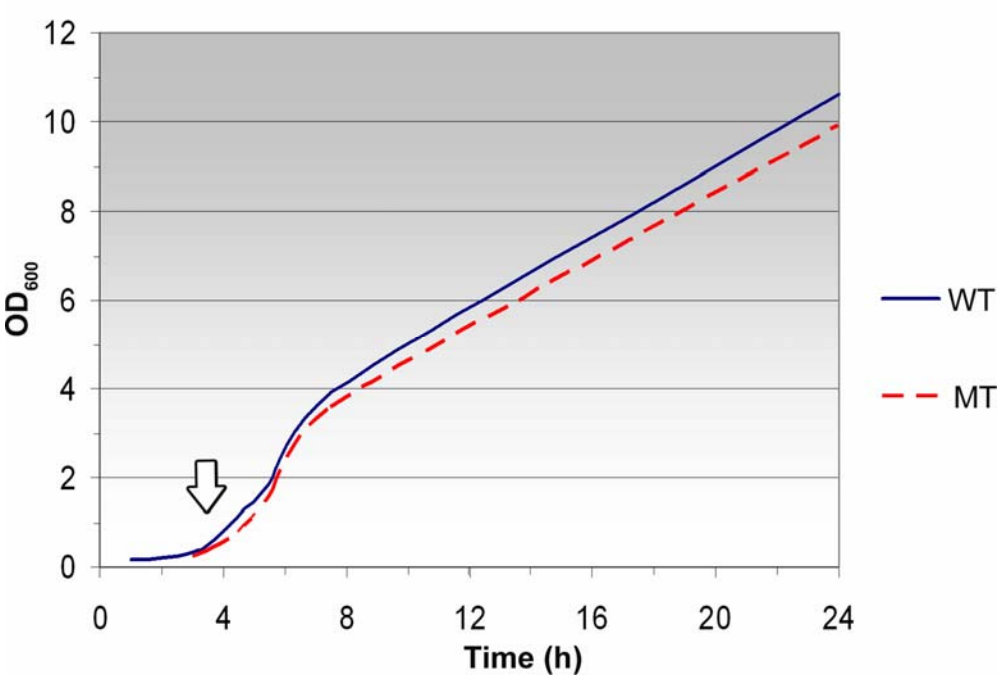

Figure 3-5. Growth curves for *E. coli* BL21(DE3) and Δ*yqhE* strains. Arrow indicates the time point at which β-keto ester was added.

Table 3-3. β-keto ester reductions by the starting and *yqhE* knockout strains.

Strain	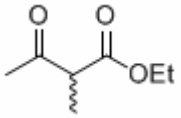	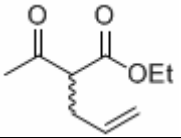	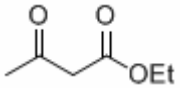
BL21(DE3)	100% reduction, 24h	100% reduction, 40h	96% reduction, 36h
BL21(DE3) Δ*yqhE*:: FRT-kan-FRT	no reduction product detectable, 48h	no reduction product detectable, 48h	72% reduction, 36h

Another interesting group of chiral synthons[212] was prepared recently in our laboratory by reducing stereoselectively mono-substituted, at alpha position, fluoro keto-esters by a set of purified keto-reductases from bakers' yeast.[213] Reduction of the simplest fluoro compound, ethyl 2-fluoroacetoacetate, could lead to four possible stereoisomers (Figure 3-6).

Both *E. coli* stains, wild type and Δ*yqhE,* reduce the abovementioned compound under non-growing conditions, albeit with different rates (Figure 3-7). The bioconversion by the parent stain was completed in 7 hours, whereas only about 50 % of the 10 mM

starting material (SM) was converted to diastereisomeric procucts (P_A, erythro) and (P_B, threo) by the mutated strain at the same time.

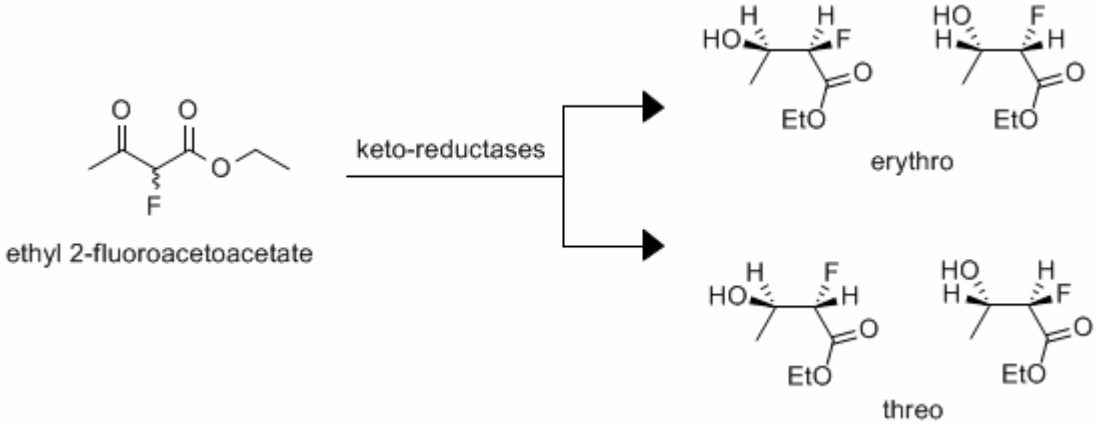

Figure 3-6. The four possible stereoisomers of ethyl 2-fluoroacetoacetate reduction.

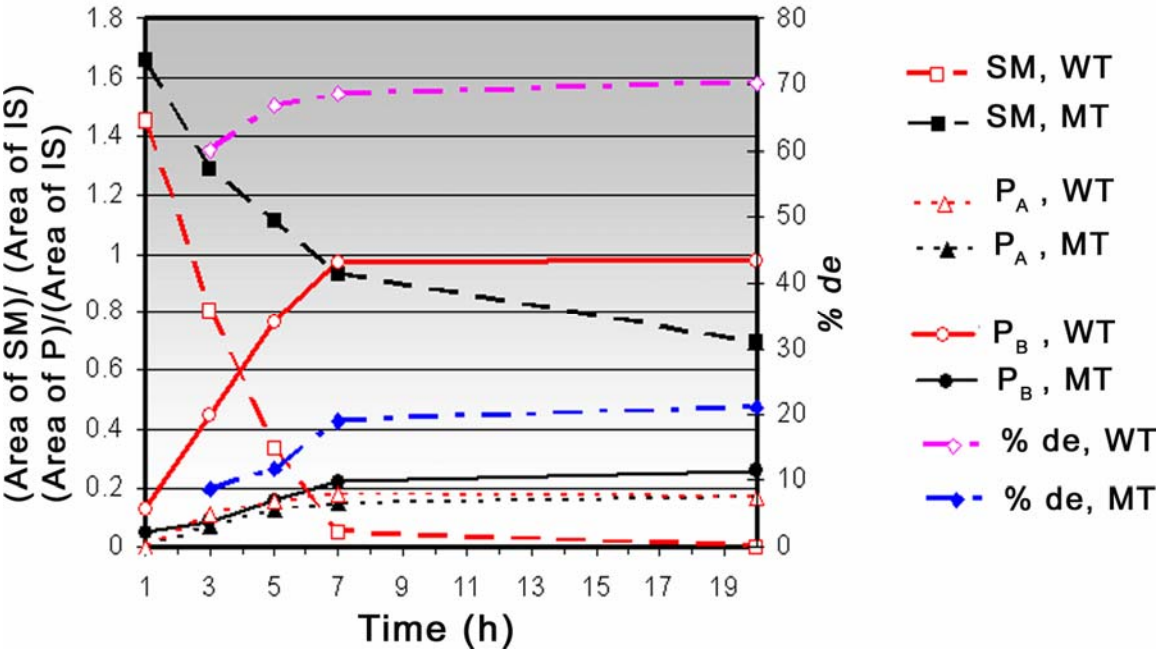

Figure 3-7. Profile of ethyl 2-fluoroacetoacetate reduction from *E. coli* BL21(DE3) (WT) and Δ*yqhE* (MT)strains. The peak area of each eluted compound from the GC column was intergraded and normalized based on the peak area of the methyl-benzoate which was used as internal standard (IS).

Interestingly, the rate formation of the one diastereisomer (P_A) was unaffected by the absence of dkgA reductase, whereas the formation of the second one (P_B) was drastically diminished in case of Δ*yqhE* strain. The results clearly suggest the presence

of at least one more active keto-reductase in *E. coli* with different stereospecificity from the dkgA.

Conclusion

The single knockout *E. coli* BL21(DE3) Δ*yqhE* strain constructed in this work succeeded in eliminating the reduction background observed initially for a number alpha substituted β-keto-esters. However, as new substrates are screened (i.e., fluoro-substituted keto-esters) and other type of reductases are overexpressed in this host (i.e., en-one(al) reductases) in our laboratory, we cannot exclude the possibility for a requirement of double or triple *E. coli* mutant in the future. Fortunately, the experimental method elected for the disruption of the *YqhE* gene is compatible with the deletion of additional genes using the Δ*yqhE* as parent strain, in a time frame of one to three weeks.

CHAPTER 4
BIOCATALYTIC REDUCTION OF FUNCTIONALIZED ALKENES: A SURVEY FOR EN-REDUCTASES

> When in 1933 I went on a Rockefeller fellowship to Otto Warburg's institute in Berlin, Warburg and Christian had in the previous year produced a yellow-coloured preparation of an oxidation enzyme from yeast. It was here for the first time possible to localize the enzymatic effect to a definite atomic constellation: hydrogen freed from the substrate (hexose monophosphate) is, with the aid of a special enzyme system (TPN-Zwischenferment) whose nature was elucidated somewhat later, placed on the nitrogen atoms of the flavin (1) and (10), giving rise to the colourless leucoflavin. This is reoxidized by oxygen, hydrogen peroxide being formed, and may afterwards be reduced again, and so forth. This cyclic process then continues until the entire amount of substrate has been deprived of two hydrogen atoms and been transformed into phosphogluconic acid; and a corresponding amount of hydrogen peroxide has been formed. At the end of the process the yellow enzyme is still there in unchanged form, and has thus apparently, as Berzelius expressed himself, aroused a chemical affinity through its mere presence.
>
> -The nature and mode of action of oxidation enzymes, Hugo Theorell[214]

Introduction

Asymmetric hydrogenation of prochiral functionalized alkenes by chiral rhodium or ruthenium phosphines has resulted in an impressive number of enantioselective transformations during the last twenty years.[215] A more critical evaluation reveals that the presence of certain functional groups (amide, carboxylate, alcohol) in proximity to the carbon-carbon double bond is a prerequisite for a high enantiomeric excess. However, aprotic oxygen functionalities such as ketones or esters have rarely been employed with success.[216-217] Moreover, the harsh reaction conditions that are often required, the complex preparation of the chiral reducing agents, as well as the demand for environmentally friendly chemical processes are placing the organometallic methodology far behind from an ideal approach. Biohydrogenation on the other hand appears as an attractive alternative route.

In the field of biotransformations, intact cells mediate the majority of the biocatalytic reductions of unsaturated compounds reported in the literature.[220] There are two major reasons: i) the absolute requirement of reducing equivalents in the form of NAD(P)H, which can be easily and inexpensively regenerated in a cell, and ii) the lack of awareness, in many cases, with regards to particular enzyme catalyzes the saturation of the carbon-carbon double bond.

The dominant term for describing the abovementioned enzymes, especially among organic chemists involved in biohydrogenations, is 'enoate-reductases'.[221, 222] We will not adopt this term here, but we will rather assign them the more generic term, 'en-reductases'. We will not also follow the common pattern observed in most reviews related to this subject[220, 222-224] in which unsaturated compounds were grouped based on a common function group (e.g. enoates, enones, enals, nitro-alkenes etc.) or based on a common carbon skeleton (e.g. aliphatic, alicyclic etc.) and then biocatalysts, capable of reducing certain class were listed. Most often, these reductions utilized whole cells. While this type of classification beautifully demonstrates the enormous reductive capabilities of these 'bugs' and the diversity of functional groups that they could accept,[225, 226] it does not contribute to our understanding in terms of which specific enzyme is responsible for each particular bioreduction. This is the major scope of the present chapter. We will briefly introduce the biohydrogenations with whole cells in the first part whereas in the second part we will assign substrates to different en-reductase families. Structure-function implications will be also discussed.

Biohydrogenation with Whole Cells

Bakers' yeast is more frequently used for the reduction of aliphatic α,β unsaturated aldehydes and ketones leading to chiral synthons (Figure 4-1) that can be used to synthezise natural phytol,[227] α-tocopherol[228, 229] and insect pheromones.[230, 231]

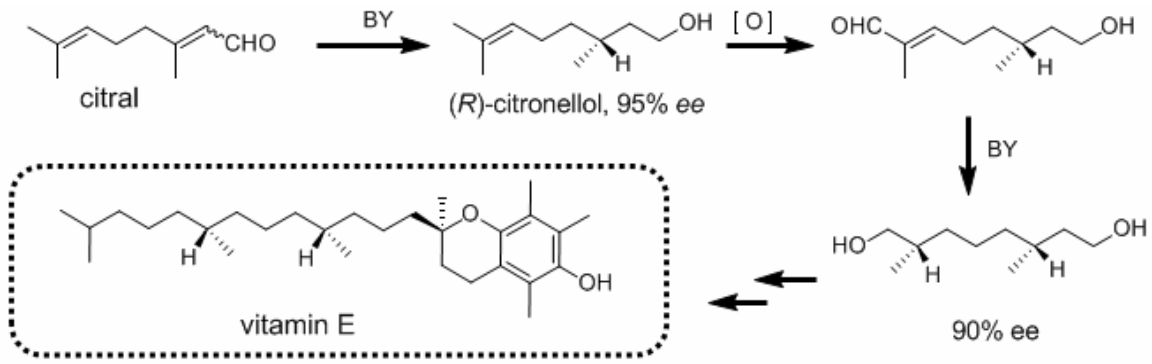

Figure 4-1. Preparation of a building block with two chiral centers from citral using bakers' yeast (BY) as biocatalyst.

The reduction of unsaturated aldehydes is usually accompanied by the reduction of carbonyl group to the corresponding alcohols.[232] By contrast, allylic alcohols must be first oxidized to corresponding aldehydes[233-235] in order for the saturation of the C-C double bond to occur (Figure 4-2). However, the reduction of the double bond (db) is chemo-selective in the sense that only the db that is conjugated to the carbonyl group is reduced (Figure 4-3).**Error! Bookmark not defined.**

Figure 4-2. Proposed hydrogenation of allylic alcohols by bakers' yeast.

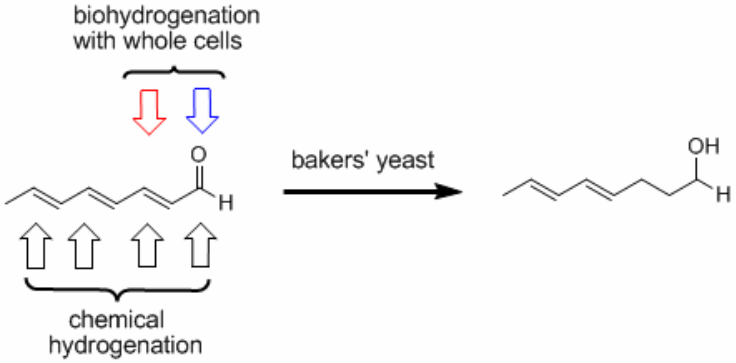

Figure 4-3. Chemo-selective reduction of a trienal by bakers' yeast.

Bakers' yeast cannot reduce unsaturated carboxylic acids unless a halogen is attached to α carbon.[236] The stereochemical outcome in this case depends on the initial

diasteroisomer used (i.e. *E* or *Z*).[237] Unsaturated esters also cannot be reduced by BY with the exception of the unsaturated lactones (Figure 4-4)[238]

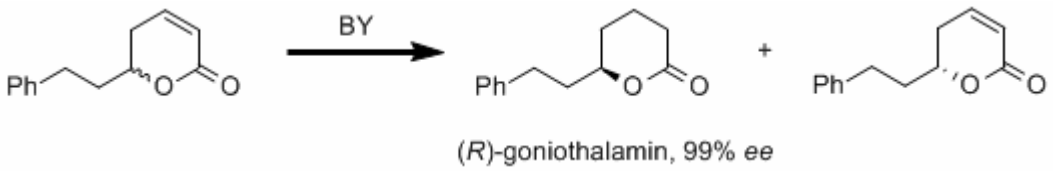

(*R*)-goniothalamin, 99% *ee*

Figure 4-4. Preparation of goniothalamin, a putative anticancer compound.

Hydrogenation of nitro-alkenes by bakers' yeast afforded optically active nitro compounds[239, 240] which are important intermediates in asymmetric synthesis. However, when a substituent other than hydrogen is present at α position the obtained nitro-alkanes are racemic.[241]

The unsaturated ketone in Figure 4-5 was used by Servi and coworkers in the production of raspberry ketone, a key component of the flavor of raspberry fruit,[242] by natural means.[243] This conversion also shed light on bakers' yeast mediated reductions.[244, 245] When the reaction was carried out in deuterated water, deuterium was found only at the α-carbon whereas when specifically labeled cofactors $NADPD_A$ or $NADD_B$ were used the deuterium was attached to β carbon. Deuterium was not incorporated into the product when $NADPD_B$ was used instead. Therefore hydride attack at the β-carbon occurs by an A-type mechanism, for NADPH, with concomitant proton uptake from the solvent at the α-position.

Servi has also formulated some 'rules' regarding the stereochemical outcomes of bakers' yeast bioreductions with acyclic unsaturated compounds (Figure 4-6).[222, 226] He proposed that the stereochemistry of double bond reduction occurs with *trans*-hydrogen delivery when α-substituted alkenes are employed (type A reaction) and the chirality of the obtained product is as depicted in Figure 4-6A. The opposite stereochemistry was proposed for β-substituted alkenes (type B reaction). The question raised by Crout and coworkers[246] is how we can explain those observations while taking into account the

catalytic site of the enzyme responsible for the reaction? If we assume that the type A reaction was catalyzed by one enzyme, should we assume that the same enzyme also catalyzed B type reactions and that the compound adopted a different conformation (Figure 4-6B1)? Or we should assume that a second enzyme acted in *syn* mode (Figure 4-6B2) or even in *trans* mode but with opposite orientation from the one depicted in Figure 4-6A?

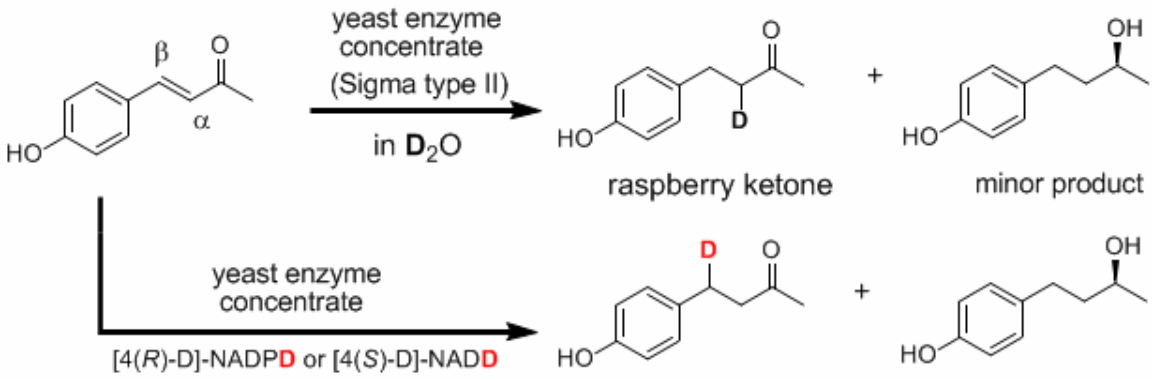

Figure 4-5. Preparation of raspberry ketone by bakers' yeast reduction.

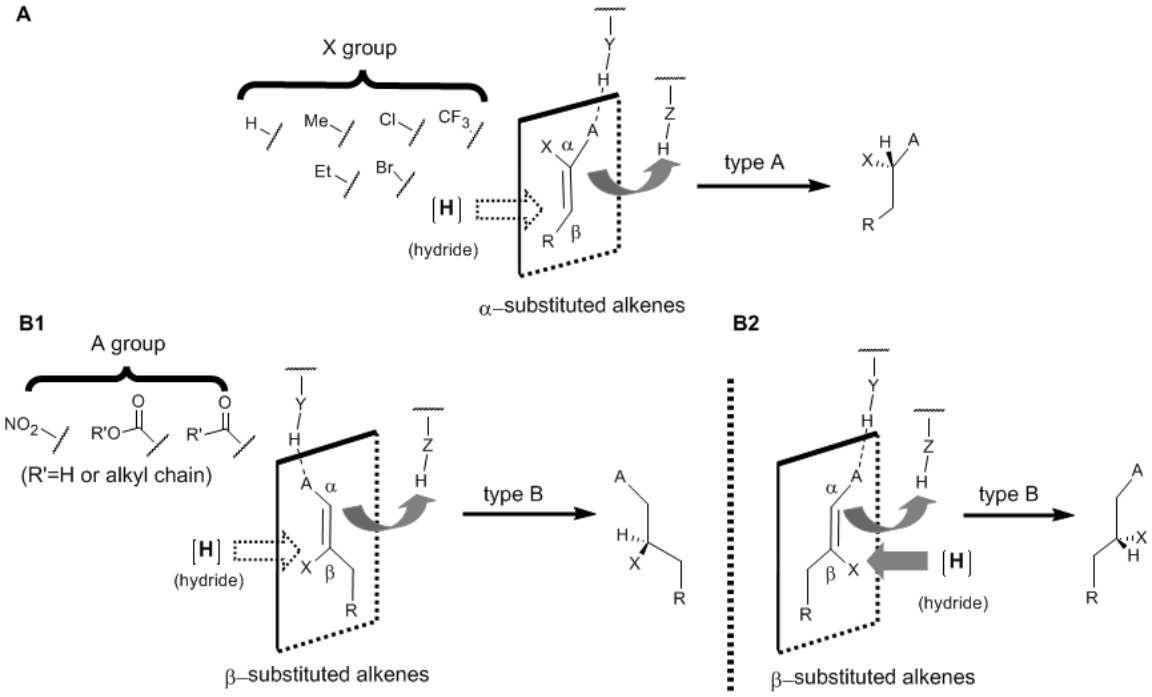

Figure 4-6. Servi's rules for A and B type reduction in bakers' yeast.

The biohydrogenation of cyclopentenone and cyclohexenone derivatives has been reported to afford chiral building blocks useful for the syntheses of prostaglandins,[247] carotenoids[228] and other terpenoid compounds.[248] In fact, the reduction of 3-methyl-2-cyclohexenone, in the impressive scale of 30 g, by *Saccharomyces cerevisiae* was the first reported reduction of enone by Fischer and Weidemann, in 1935 (Figure 4-7).[249]

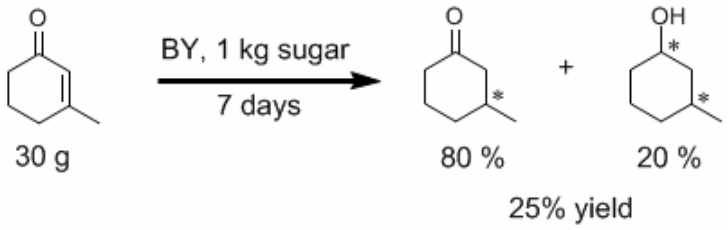

Figure 4-7. The first reported enone reductase activity in bakers' yeast.

Bakers' yeast has also been used extensively for the production of levodione, a key intermediate in synthesis of carotenoids[228] and flavor compounds.[250] In contrast to routes using chemical means for this transformation to control the chemo-selectivity of this reaction by utilizing different metals and varying solvents and reaction conditions[251-253] bakers' yeast affords pure, crystalline levodione in 85% yield and excellent enantioselectivity (Figure 4-8).[254]

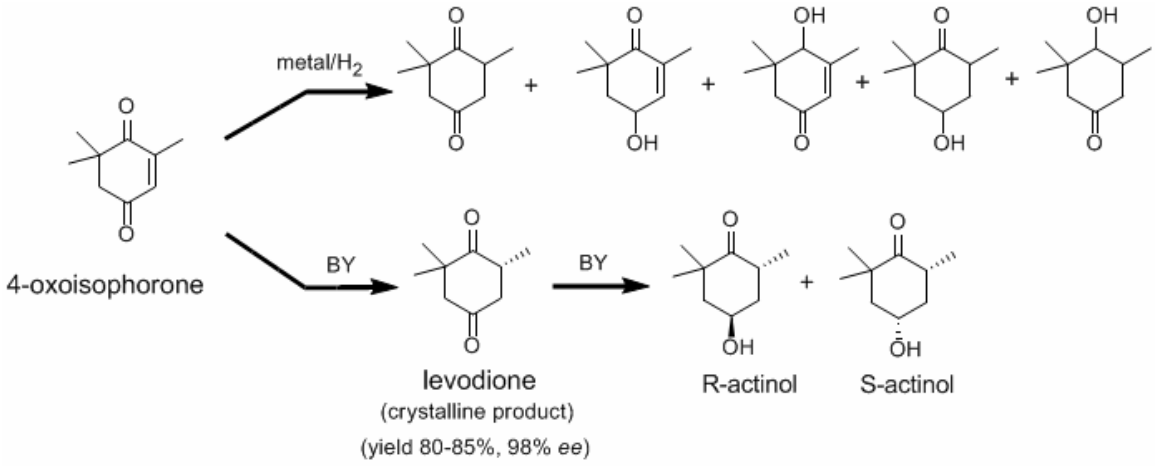

Figure 4-8. Bakers' yeast versus chemical mediated reduction of 4-oxo-isophorone.

Unfortunately, moderate chemo-selectivity is a common problem when whole cells are utilized. One of the most impressive example is provided by zearalenone also known as RAL and F2 toxin. This mycotoxin is produced by some *Fuasarium* species when they grow on corn and other small grains in storage. It is a heat stable compound and causes infertility and other breeding problems, especially in swine. In an effort to understand better the metabolism of this compound in mammalian species, about 170 microorganisms were screened for their ability to produce different zearalenone analogues.[255] Only *Saccharomyces cerevisiae* NRRL Y2034 was found to selectively reduce the carbon-carbon double bond without simultaneously acting on other functional groups of this molecule, as the rest of microorganisms did (Figure 4-9).

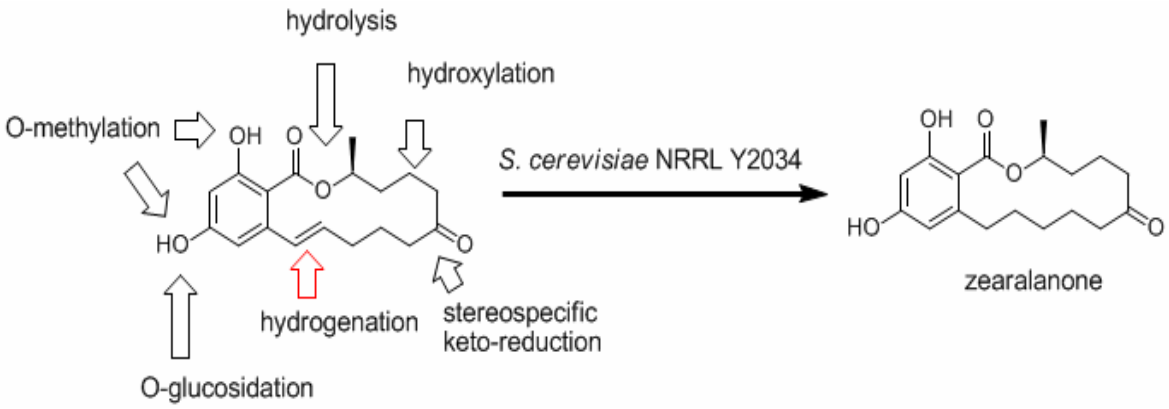

Figure 4-9. The six possible microbial transformations of zearalenone.

Other fungi have been also employed for the reduction of simple cyclic unsaturated compounds[256-258] as well as for more 'exotic' derivatives[259, 260] (Figures 4-10 and 4-11). In addition, cyanobacteria and plant cells lines have shown notable, and in certain cases, complementary stereoselectivities as compared to bakers' yeast[261-264] but their applicability among organic chemists is narrow simply because complex and time-consuming cultivation techniques are required.

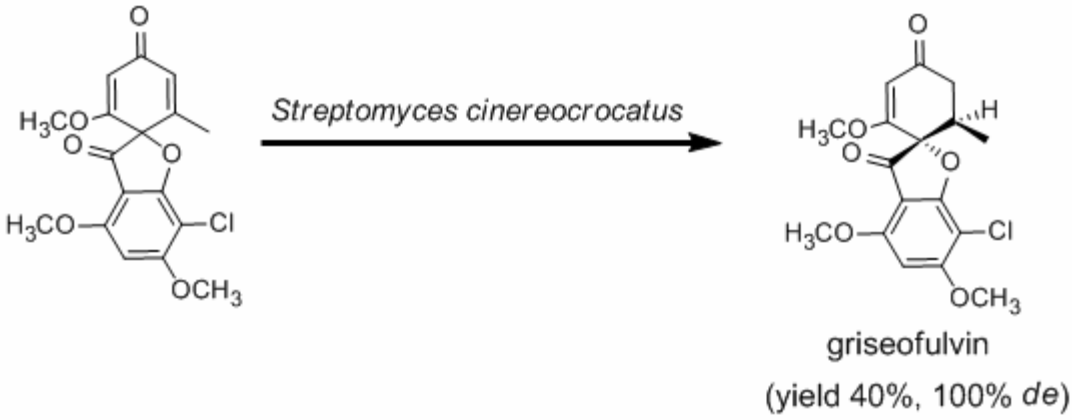

Figure 4-10. Preparation of griseofulvin, an antifungal agent.

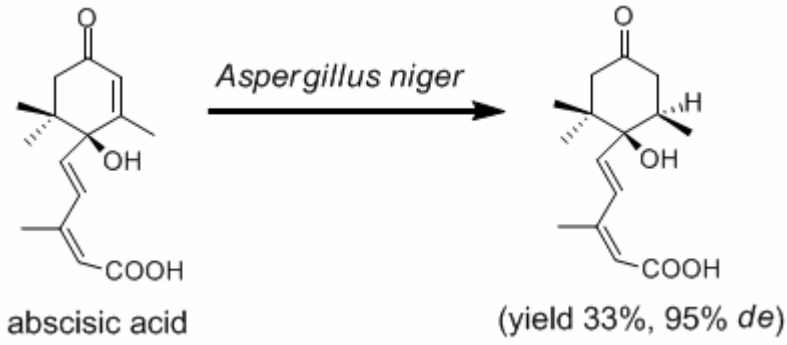

Figure 4-11. Biohydrogenation of abscisic acid, a plant stress hormone.

We should recognize that bakers' yeast may be the most frequently used microorganism for biohydrogenations but it is certainly not the most powerful one. The reductive capabilities of several *Clostridia* species are remarkable.[265, 266] Their ability to reduce unsaturated carboxylic acids, in a stereospecific and NAD(P)H-free manner, renders them a very attractive system (Figure 4-12). It is not an overstatement to say that Helmut Simon's laboratory has examined virtually every possible trisubstituted enoate as a substrate for these microorganisms.[267, 268] In addition, numerous and sometimes innovative techniques for supplying cheap and by-product-free reductive equivalents have been combined with this system.[269, 270] The simplest scheme comprises a cathode electrode, an electron 'mediator' such as methyl-viologen, the unsaturated acid and the biocatalyst in a form of intact-cells, cell-extract or even purified

enoate reductase. Unfortunately, most organic chemists do not enjoy working with electrochemical cells under strictly anaerobic conditions. The lack of oxygen is a prerequisite for these strict anaerobes to grow and retain their reductive ability. Therefore, none outside Simon's laboratory have attempted to take advantage of their hidden reductive power, until now.

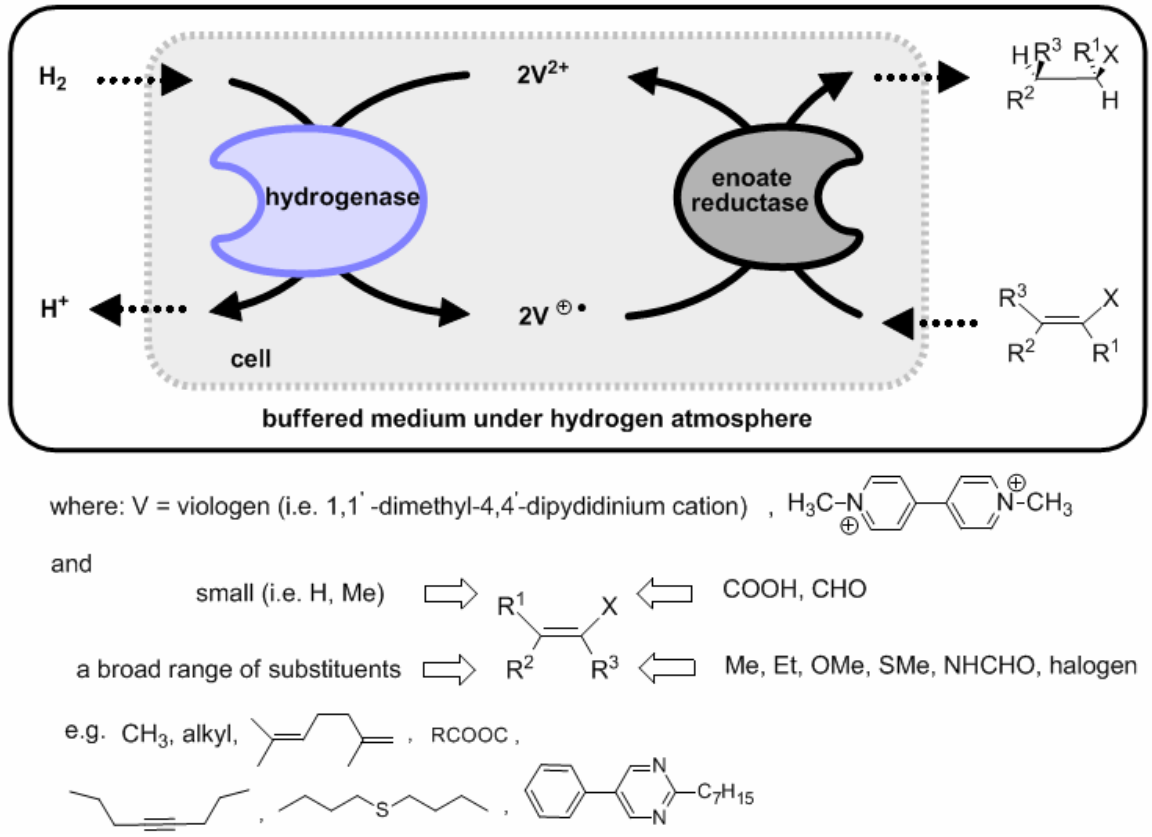

Figure 4-12. General scheme of biohydrogenation with *Clostridia* species.

If we compare the bakers' yeast substrate specificity with that of *Clostridia* species it is clear that *Clostridia*, in addition to reducing unsaturated carboxylic acids, also accepts as substrates most of the enones and enals known to react with bakers' yeast. However, both microorganisms share a common disadvantage: they cannot tolerate double bulky substituents at β position.

En-Reductases: Substrate Specificity

What is the color of an en-reductase? An answer to this seemingly trivial question could in fact facilitate many efforts to classify and therefore understand known and putative en-reductases. Based on our proposed categorization (Figure 4-13), an en-reductase preparation may be yellow if it contains flavin and thus belongs either to the old yellow enzyme (OYE) family or to the enoate-reductase family (a distant relative to OYE family) or it may not possess any color if it belongs to medium or short chain dehydrogenase/reductase family.

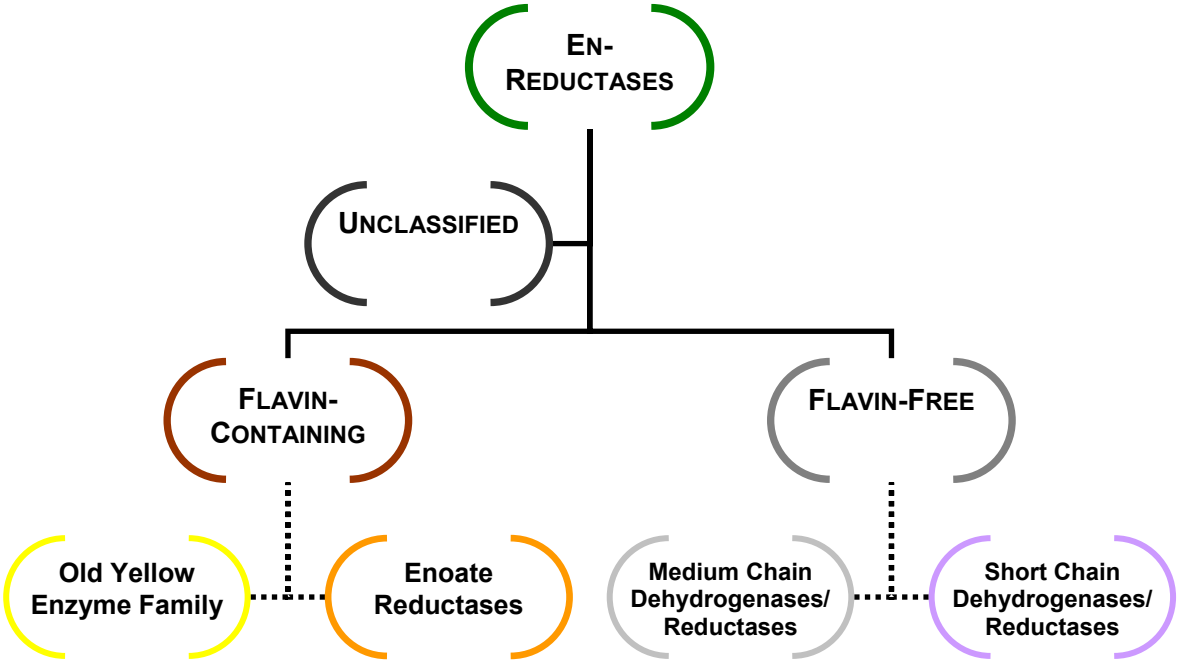

Figure 4-13. A proposed classification of en-reductases.

Especially in the early days, most of these enzymes have been purified from their native hosts on the basis of their en-reductase activity. Only the last decade, and with the aid of bioinformatics has it become apparent that these enzymes may share common structural features and catalytic activities. We will build on these different families in order to describe the substrate specificity of en-reductases. We will also present cases in which a protein was purified because of its en-reductase activity but no

additional effort was made for the determination of its amino-acid sequence. These 'orphan' en-reductases may or may not belong to one of the abovementioned families and thus they will be discussed separately.

Old Yellow Enzyme Family

The isolation of the first biocatalyst capable of reducing 'activated' carbon-carbon double bonds preceded[271] even Fischer's observation for bakers' yeast reductive capabilities on the same functional group.[249] Paradoxically, this particular molecular function of the so-called 'old yellow enzyme' (OYE1) remained obscured to scientific community for about six decades since its first purification from brewers' bottom yeast. Today, the old yellow enzyme family embraces relatives found in numerous fungi, bacteria and plants.[272] All members contain flavin mononucleotide (FMN) as a non-covalent prosthetic group, require NAD(P)H as cofactor and all are able, at least to some extent, of reducing functionalized alkenes. However, the cellular role of most of them is still unclear. Recent experimental evidences support defense against acrolein[273] stress and protection of actin cytoskeleton in case of yeast OYEs.[274]

In the following discussion, we will present the substrate specificity of the OYE1 separately, whereas the rest of the purified OYEs are grouped based on their source of isolation.

Old yellow enzyme from *Saccharomyces carlsbergensis*

The detailed characterization of OYE1[275] could be described as one man's accomplishment. We owe most of our knowledge today about the extraordinary and extremely divergent catalytic activity of the OYEs from yeasts to Professor Vincent Massey's laboratory.[276]

β-NADPH is considered to be the physiological reductant (2 electrons per flavin) for the OYE even thought the uncommon α-anomer is actually slightly better reductant (Figure 4-14).[277] Sodium dithionite can also be used, but in this case, the reduction

proceeds via a formation of semiquinone intermediate (one electron reduced flavin), which disproportionates slowly into fully reduced and oxidized OYE. An electron mediator such as methyl viologen may accelerate the process. Only a few other reductants could be used, however, flavin reoxidation can be achieved by a number of oxidants (Figure 4-14) with the molecular oxygen being an opportunistic one and yielding hydrogen peroxide and superoxide as products.[278]

The ability of the oxidized form of OYE1 to bind aromatic compounds, and especially phenols, gives rise to new, long wavelength, absorbance bands (green form of OYE) due to transfer of charge from the phenolate to flavin.[279-281] This property was exploited for the purification of OYE1 by affinity chromatography on N-(4-hydroxybenzoyl) aminohexyl agarose.[282] Upon reduction with sodium dithionite, OYE1 has greatly diminished affinity for the phenol and hence is eluted from the column in an almost pure form. A second class of binding ligands is small molecules such as the monovalent anions: acetate, chloride and azide with the later binding tighter. (Figure 4-14).[277, 278] The last class of OYE1 inhibitors are pyridine nucleotide derivatives such as the acid hydrolysis products of NADPH. All three types of inhibitors compete with one other for OYE1 implicating a common binding site on the enzyme.

In 1993, Stott et al.[283] reported for the first time that 2-cyclohexenone could act as alternative electron acceptor for the reduced OYE1. Two observations stimulated Massey to test an enone as a substrate for OYE: i) the sequence similarity of OYE1 with a bile-acid-inducible protein in *Eubacterium sp.* and ii) the fact that all the reductive steps in the 7a-dehydroxylation of the bile acids in this microorganism involve the reduction of cyclohex-2-enone-like functional group. Indeed, in that work, Massey's spectrophotometric assays clearly showed that 2-cyclohexenone, similar to quinones, stopped the utilization of oxygen as electron acceptor during the reoxidation of OYE1.

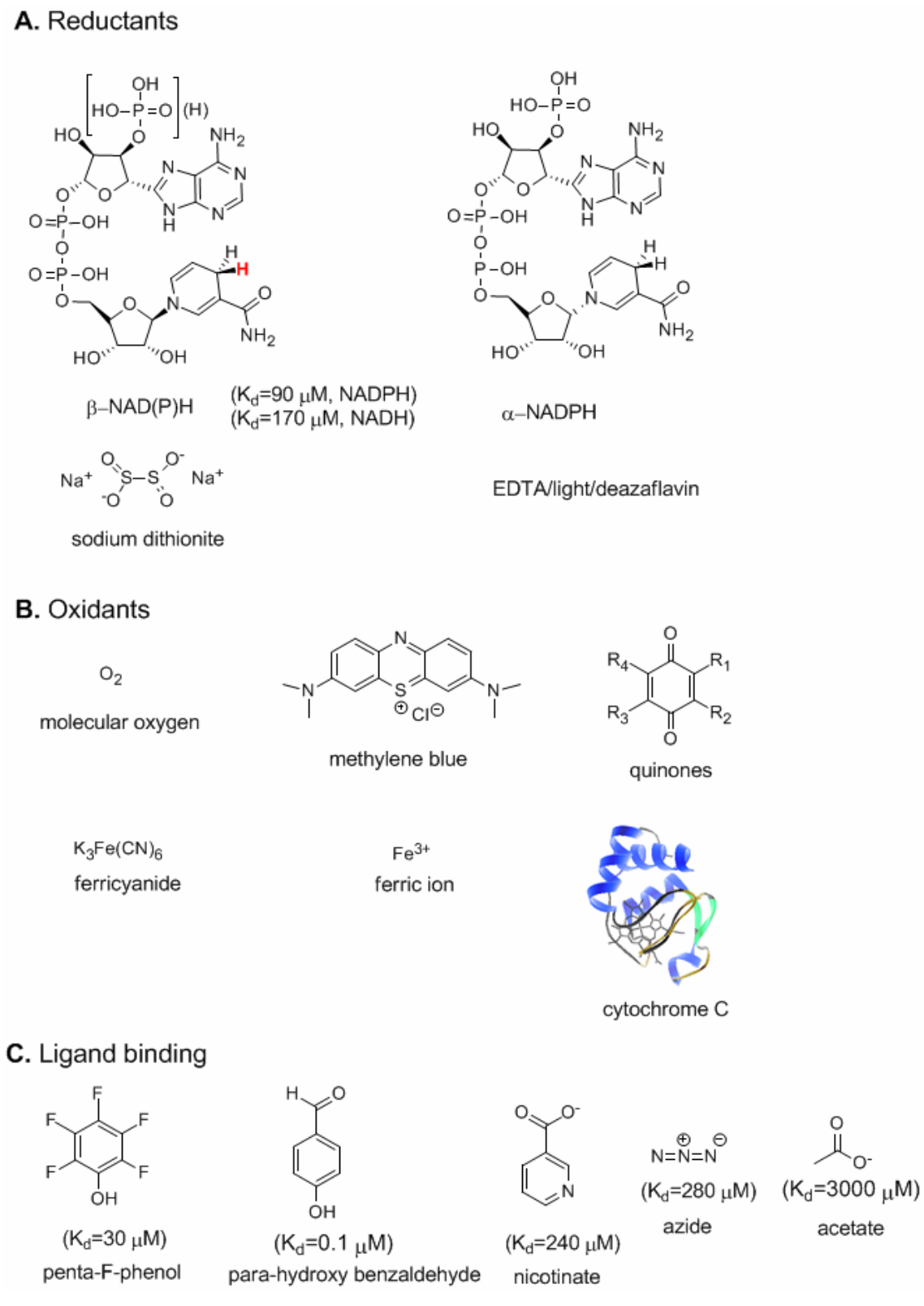

Figure 4-14. First generation of substrates and inhibitors for OYE1.

The reduction, as it would be proved later, is stereospecific and involves a *trans*-addition across the double bond with transfer of the pro-*R*-hydrogen of NADPH as a hydride [via the flavin N(5)] to the *β*-carbon with a concomitant uptake of a solvent-derived proton at the *α*-position (Figure 4-15).[284-286] The overall process is showed to be concerted.

Two years later, the same laboratory published an extensive study regarding the en-reductase potential of OYE1.[287] Almost 50 compounds were tested spectrophotometrically for their ability to reoxidize OYE1 under anaerobic conditions (Figure 4-15). Several enones and enals were found to be good substrates for NADPH-mediated reduction by OYE1, whereas unsaturated acids, esters, nitriles and amines did not react. The effect of substituents (i.e., substitution at *α* or *β* position and mono- or di-substitution at *β* position) on the rate of reduction was also explored and the general trend is depicted in Figure 4-17. Di-substitution at *β* position, especially with substituents bigger than methyl, significantly reduced the rate of reaction of aliphatic compounds. According to the authors, the problem is not the binding of these compounds in the catalytic active site *per se*, since comparable perturbation of the flavin spectrum was observed in each case, but in the oxidation rate of NADPH.

In an independent study, Swiderska and Stewart used whole *E. coli* cells in which OYE1 was overexpressed and these authors showed a similar trend for 2-substituted cyclohexenones.[288] Only the 2-methyl substituted compound was reduced completely, whereas bulkier alkyl groups (e.g. propyl, *n*-butyl) impeded the bioreduction. Even worse was the case when the methyl group at position 1 was replaced by an ethyl chain. Only 16% of the starting olefin (20 mg) was reduced even after prolonged incubation (i.e., 2 days). On the other hand, the recorded *ee* was higher than 90% in all cases. The stereochemical outcome of these biotransformations (Figure 4-19) is predictable

and it could be derived from the crystal structure of the OYE1 with the para-hydroxy benzaldehyde (Figure 4-18).[289, 290]

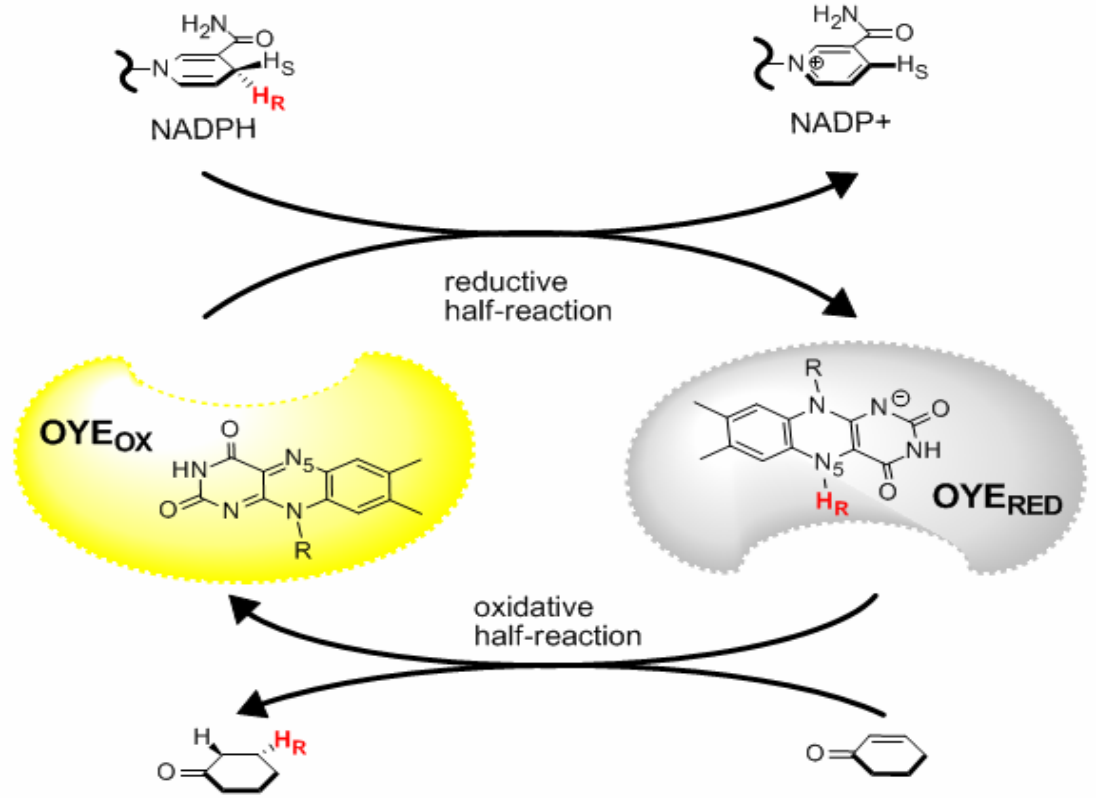

Figure 4-15. Representation of catalytic cycle of Old Yellow Enzyme.

The Stott et al. study also reported a new NADPH-independent dismutation reaction catalyzed by OYE1. In absence of any nicotinamide cofactor, 2-cyclohexenone was oxidized to phenol by reducing the OYE1 (Figure 4-20A, step 1) while in the second step, a second molecule of 2-cyclohexenone acted as an electron acceptor to reoxidize the OYE. The net result of the dismutation reaction is a 1:1 ratio phenol and cyclohexanone. Not all the substrates could undergo a dismutation reaction, however. For example 4,4 dimethyl-2-cyclohexenone is reduced in a NADPH-dependant manner by OYE1, but it could not reduce OYE1 in absence of cofactor. One explanation could be the unfavorable redox potential for such enones (i.e. a disubstituted at the same position cyclohexenone is not aromatizable after oxidation).

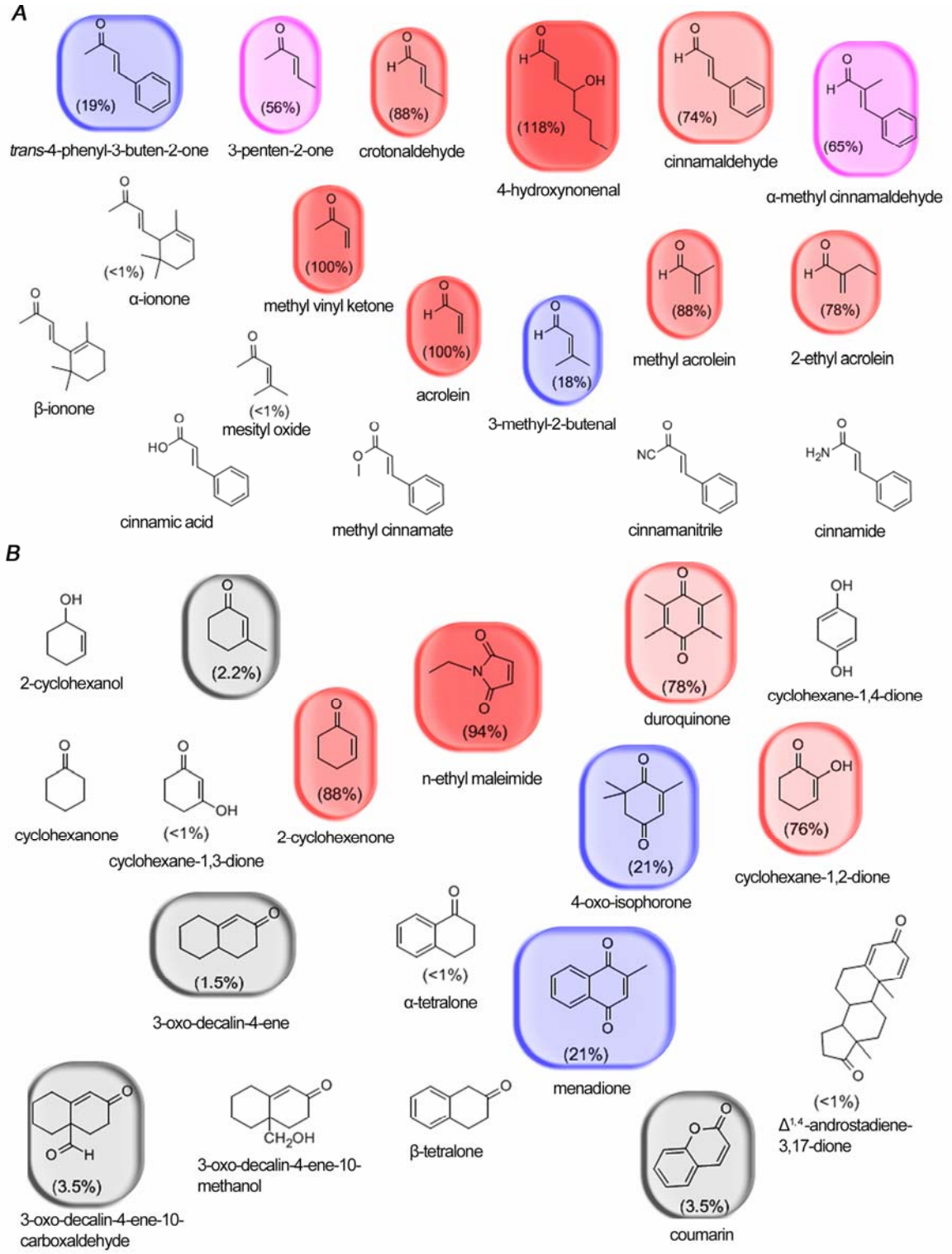

Figure 4-16. Second generation of substrates for OYE1 (Numbers in parentheses indicates relative activity based on the measured turnover number for acrolein 170 min^{-1}). Most reactive compounds are highlighted by red and less reactive by grey color. Compounds that did not react are not highlighted.

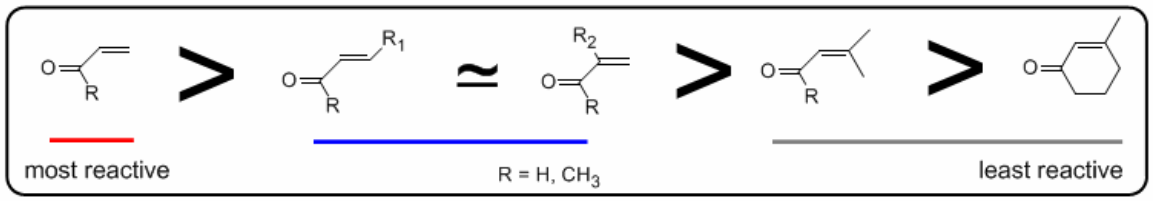

Figure 4-17. Relative reactivity of substituted en-ones (als) based on Massey's studies.

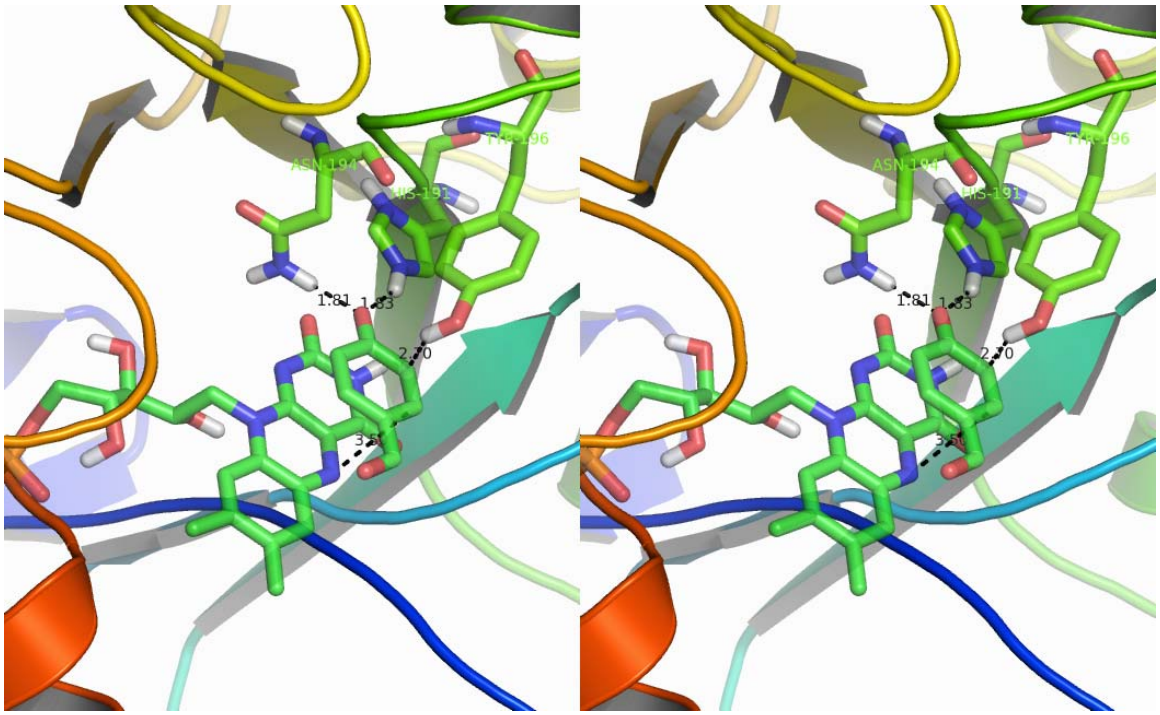

Figure 4-18. Stereoview of active site architecture of OYE1 with para-hydroxy-benzaldehyde (1OYB). Picture was rendered in Pymol.[291]

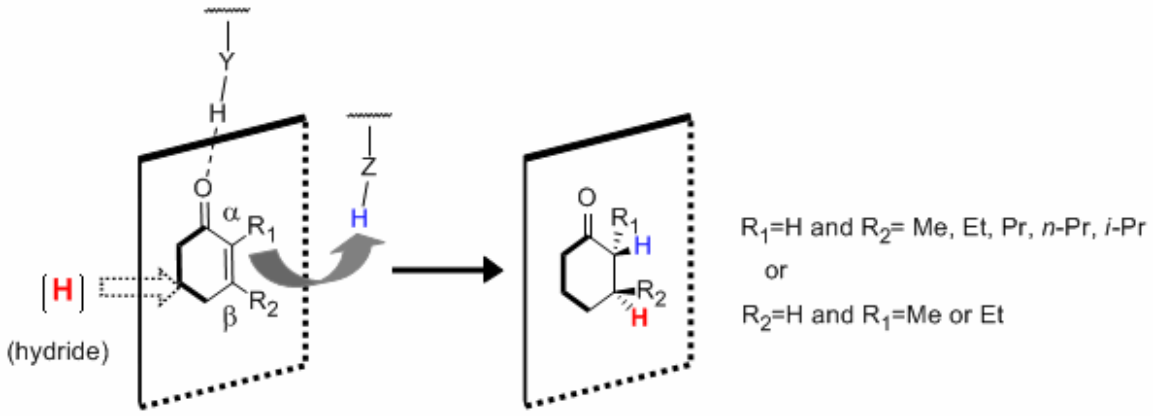

Figure 4-19. Stereochemical outcome of reduction of substituted cyclic enones by OYE1.

Using a stereospecifically labeled substrate, it was demonstrated that the second step of the dismutation reaction proceeds with a way similar to the one observed for the normal NADPH reduction whereas *trans* elimination was observed for the first step (Figure 4-20C) In order for the same substrate (e.g. ODE) to be able to reduce and then oxidize the flavin, a different accommodation above the *si* face must be assumed for the reductive (Figure 4-21A) and the oxidative steps (Figure 4-21B), respectively.[292] Also, under aerobic conditions and for bulkier than 2-cyclohexenone substrates (e.g. ODE and ODEC), molecular oxygen may compete for reoxidation of OYE1 (Figure 4-20B and C).

Most of steroids tested in that work, even though are bound strongly to OYE, did not undergo either an oxidation or an NADPH-dependent reduction by OYE1. The only exceptions were 1,4 adrostadiene,3,17-dione (Figure 4-22) and 19-nor-testosterone (Figure 4-22).

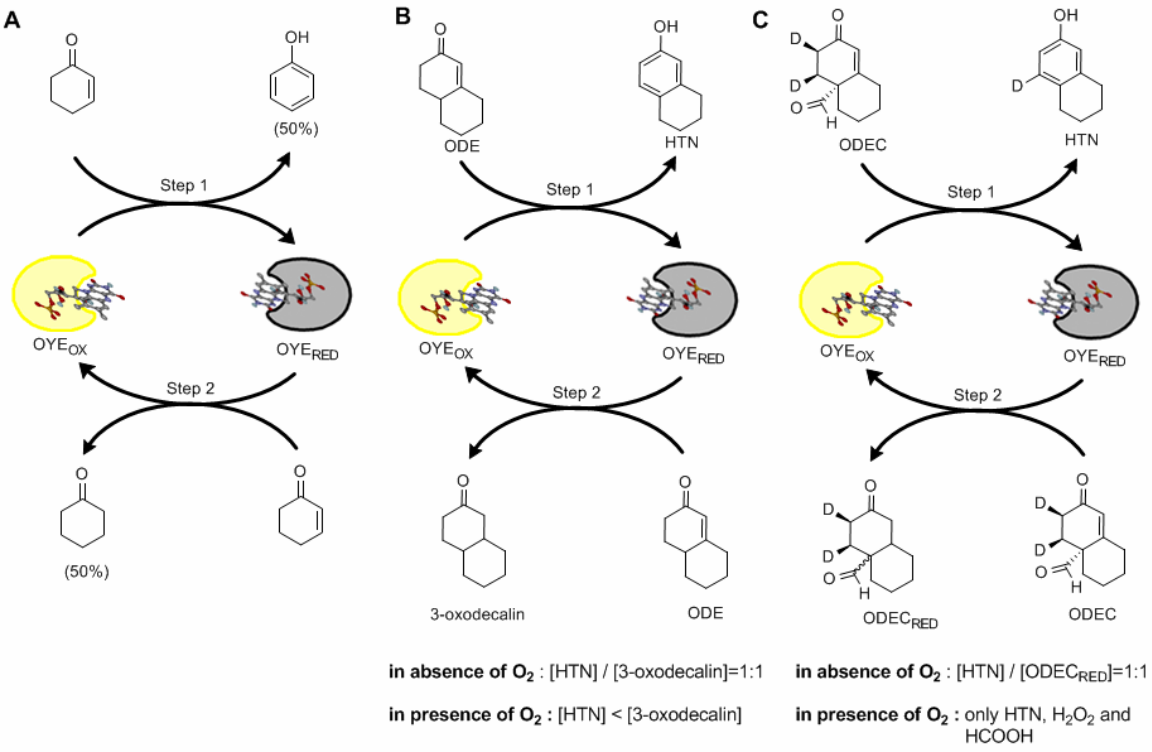

Figure 4-20. First generation of desaturation reactions by OYE1 in absence of NADPH. (ODE, 3-oxodecalin-4-ene; ODEC 3-oxodecalin-4-ene-10-carboxaldehyde; HTN, 3-hydroxy-6,7,8,9-tetrahydronaphthalene)

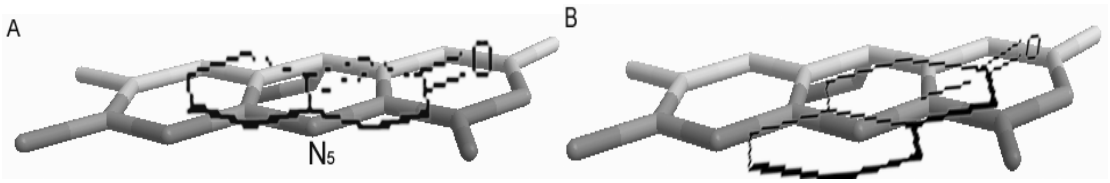

Figure 4-21. Proposed orientation of ODE above the *si* face of flavin during: the reductive (A) and the oxidative half (B) of the dismutation reaction.

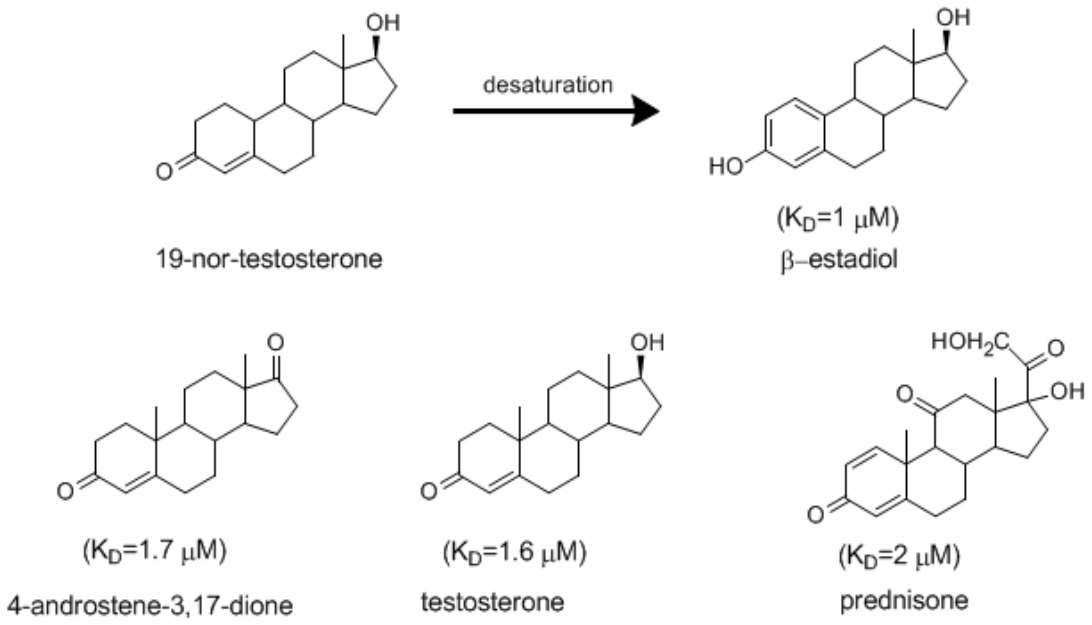

Figure 4-22. Second generation of binding ligands for OYE.

Murthy et al. took advantage of the desaturase activity of the OYE1 to kinetically resolve recemic ketones and aldehydes (Figure 4-23).[293] While this a nice example as a proof of principle, it is unlikely to find broader applications for three main reasons: i) the redox potential of flavin in OYE1 must become significantly less negative[294-295] (this was accomplished by replacing the native FMN by a synthetic flavin-analog)[296] ii) the yield of the reaction could not exceed the 50% and iii) the subsequent separation of the saturated chiral product from the corresponding enone may be difficult due to high similarity of both compounds.

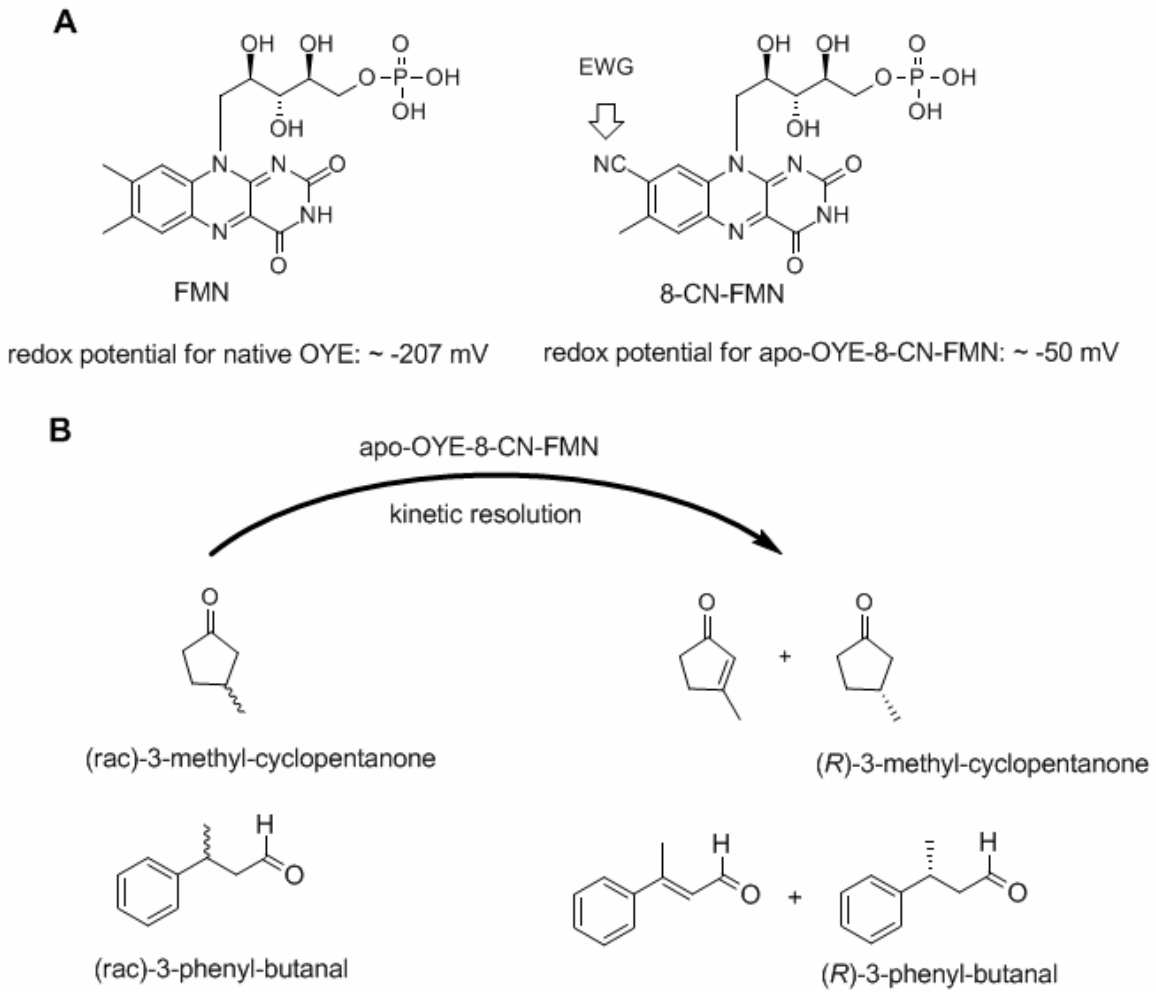

Figure 4-23. Second generation of desaturation reactions by modified-OYE in absence of NADPH.

Nitro-alkenes could also be reduced easily by OYE1 (Figure 4-24A). Similar to a carbonyl group, a nitro moiety strongly polarizes a carbon carbon double bond, facilitating thus the hydride attack at the β-carbon and enhancing the acidity of the proton at α position.[297]

Lastly, OYE1 also shares a catalytic activity that has been mostly explored in OYEs from bacteria: reducing highly explosive organic nitrates such as GNT (Figure 4-24B). Massey and coworkers observed that the reductive cleavage of nitro-esters is also mediated by reduced free-flavin, but the ratio of the obtained products is different

compared to that produced by the enzymatic reduction. OYE1 showed strong preference for the primary nitrates.[298]

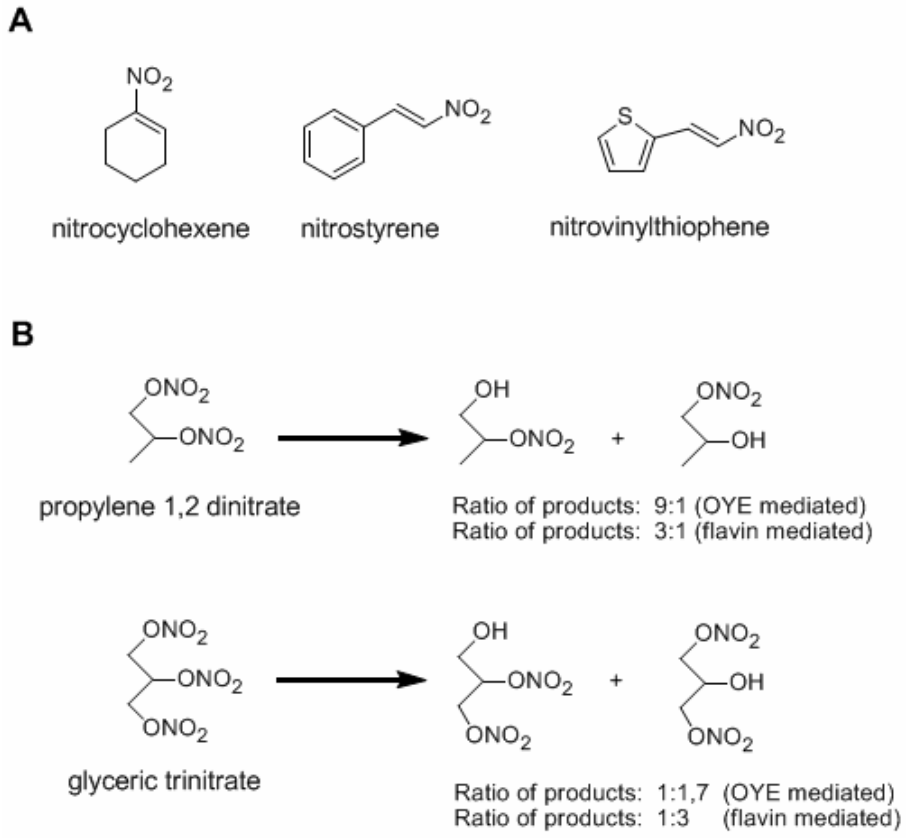

Figure 4-24. Third and fourth generation of substrates for OYE1.

Old yellow enzymes from yeasts

Other OYEs from different yeast strains are listed in Table 4-1. *OYE2* was detected in the bakers' yeast genome after screening an *S. cerevisiae* DNA library using the OYE1 gene as a probe.[283] OYE3 was discovered unexpectedly when a ΔOYE2 yeast strain was found to retain OYE activity.[299] Oye, initially named keto-isophorone (KIP) reductase, was first purified from its native host after a preliminary screening of different fungal species for the ability to reduce 4-oxoisophorone stereoselectively.[300]

Estrogen binding protein was initially purified from 200 g of *C. albicans* cells, the most common fungal pathogen for humans.[391] Interestingly, the amino acid sequence showed no similarity to human estrogen receptor, as was initially suspected. Instead,

the 46% amino acid identity with OYE2 forced the researchers to investigate a possible 'OYE' activity. EBT1 not only reduces common OYE1 substrates and possesses desaturase activity but can also reduce 19-nor-testosterone in an NADPH-dependent manner whereas OYE1 can only aromatize the same compound.[302]

The methylotrpophic yeast *Hansenula polymorpha*, overexpression of the *HYE* gene cluster confers resistance towards high concentrations of allyl alcohol in presence of alcohol oxidase (AO).[303] The observation suggested that the AO's product (i.e. acrolein) is subsequently reduced by HYEs, thereby diminishing thus its otherwise high toxicity.

The purification of N-Ethylmaleimide Reductase (NEM) from *Yarrowia lipolytica* was the result of researchers' failure to purify a similar protein from *E. coli.*[304] In 1979, Mizugaki and co-workers reported the isolation of an enzymatic fraction able to reduce *cis*-2-alkenoyl-Coenzyme A to the corresponding saturated acyl-CoA derivatives in the presence of NADPH.[305] During the course of inhibition studies on the same protein preparation, they found that including N-ethylmaleimide (a common binding reagent for thiol groups of cysteines) in the NADPH assay did not inhibit the reaction but instead accelerated NADPH reduction. The NEM reductase co-eluted in the same fraction with *cis*-2-enoyl-CoA reductase on Sephacryl S-200 Superfine gel-filtration column. These unsuccessful efforts to separate the two proteins led to a revised strategy of isolating a protein with similar catalytic activity from another host.[306] Even though neither the amino acid sequence nor the UV-VIs spectrum of the protein was reported, this protein most likely belongs to OYE family. A BLAST search using OYE1 as a probe reveals six putative OYEs in *Yarrowia lipolytica*.

Table 4-1. List of OYEs from yeasts and corresponding substrate specificity.

Year (Ref.)	**Organism**	**Protein (Swiss-Prot accession no.)**	**Gene**
Substrates			Binding Ligands, inhibitors
1994 (301)	***Candida albicans***	**Estrogen binding protein (P43084)**	***EBP1***
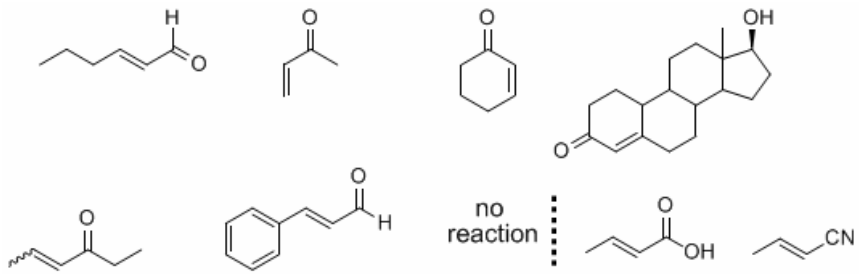			
1993 (283) 1995 (299)	***Saccharomyces serevisiae***	**Old yellow enzyme 2 Old yellow enzyme 3 (Q03558, P41816)**	***OYE2* (YHR179W) *OYE3* (YPL171C)**
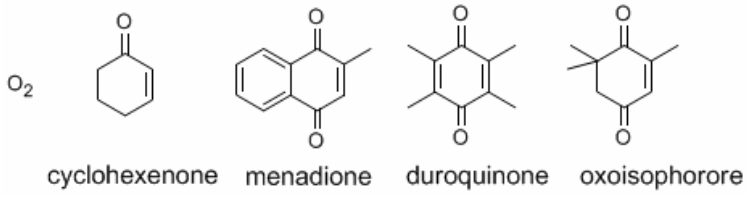			
2002 (303)	***Hansenula polymorpha***	**Hansenula yellow enzyme 1, 2, 3 (Q8J293, Q8J292, Q8J291)**	***HYE1*, *HYE2*, *HYE3***
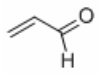			
2004 (309)	***Kluyveromyces lactis***	**Kluveromyces yellow enzyme (P40952)**	***KYE1***
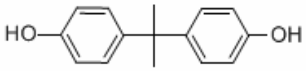			
1997[a] (306)	***Yarrowia (Candida) lipolytica***	**N-Ethylmaleimide Reductase of *Y. lipolytica***	**Unknown**
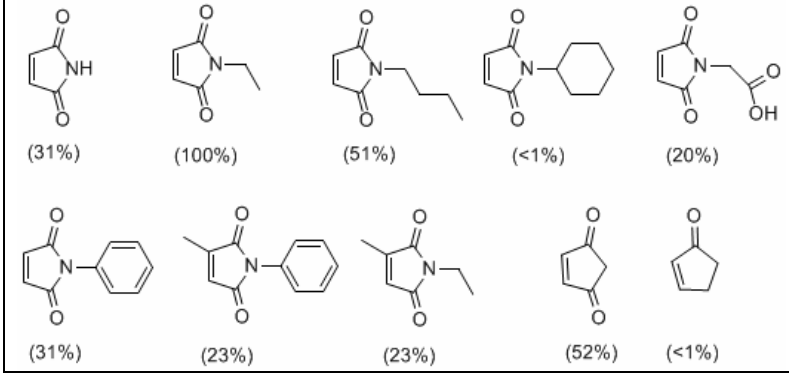			

Table 4-1. Continued.

Year (ref.)	**Organism**	**Protein (Swiss-Prot accession no.)**	**Gene**
Substrates			
2002[b] (300)	***Candida macedoniensis* (*Kluyveromyces marxianus*)**	**Old yellow enzyme (Q6I7B7)**	***oye***
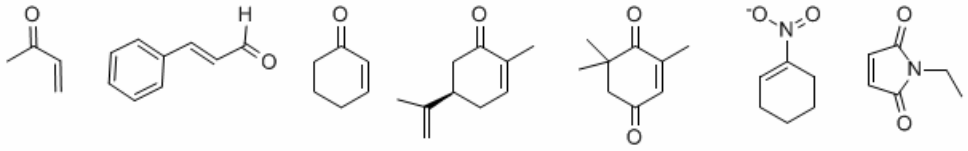 (100%) (54%) (61%) (14%) (25%, 99% *ee*) (93%)			

[a] Numbers in parentheses indicate relative activity based on the measured Vmax number for N-ethylmaleimide 216 nmol min^{-1} mg^{-1}. [b] Numbers in parentheses indicate relative activity based on spectrophotometric assays.

In terms of biotechnological applications, the examples are limited. Oye, OYE2 and OYE3, have been cloned and overexpressed in *E. coli* and their activity towards the reduction of ketoisophore was evaluated. All of them produce (6*R*)-levodione in excellent enantiomeric purity.[307] Moreover, when both oye and glucose dehydrogenase were co-expressed in *E. coli*, 100 times higher productivity was achieved, compared to the one reported with bakers' yeast cells.[308] In addition, when a second enzyme (a keto-reductase) was added to the reaction mixture after the completion of the first reduction step, the doubly chiral compound *R*-actinol was obtained in 94% *ee*.

Mergler et al. demonstrated a technique with which OYEs could be used as biological filters.[309] KYE was displayed on the surface of an engineered *Pichia pastoris* cell. The novel strain was able to bind bisphenol A, a monomer used in industry for the production of polystyrene and polycarbonates and a known endocrine disruptor (i.e., it competes with estradiol for binding with estrogen receptors).

Old yellow enzymes from bacteria

In 1979, old yellow enzyme activity was detected in bacterium *Gluconobacter suboxydans*. At that time the enone reductase activity of OYEs had not yet been recognized.[310]

In 1994, Bruce's laboratories painstaking efforts to elucidate the degradation pathway of morphine alkaloids in *Pseudomonas* species lead to the isolation of morphinone reductase from *Pseudomonas putida* M10.[311, 312] The purified enzyme reduced the olefin bonds of both morphinone and codeinone. The products obtained, hydromorphone and hydrocodone, not easy to synthesize by chemical means and are important pharmaceutical drugs with useful analgesic and antitussive properties.[313] Massey's 1993 report did not pass unnoticed in the Bruce lab, who demonstrated the ability of a bacterial old yellow enzyme (morB) to reduce 2-cycloxehenone in an NADH-dependent manner for the fist time. Progesterone and cortisone bind to morphinone reductase but do not react.

OYEs have been also isolated from other *Pseudomonas* species (Table 4-2) and other bacteria such as *Agrobacterium radiobacter and Enterobacter cloacae* species, albeit not for their action on alkaloids. Instead, it is their reductive power on organic nitrate esters that has been explored more while their enone reductase activity has been examined only superficially. It is beyond the scope of this introduction to discuss in detail the denitration activity of OYEs. Of particular importance is their ability to degrade the aromatic explosive 2,4,6-trinitrotoluene (TNT), persistent pollutant in military sites.[314, 315] Since the first old yellow enzyme (pentaerythritol tetranitrate reductase) was expressed in transgenic tobacco plants and its bioremediation capabilities was demonstrated,[316] the exact mechanism of this reaction is under vigorous investigation.[317-323]

The NAD(P)H dependent 2-cyclohexen-1-one reductase from phytopathogenic bacterium *Pseudomonas syrigae* pv. Glycinea was found to be preferentially present in soluble cellular protein fraction of this microorganism when the latter was cultivated at low temperatures (i.e 18 °C). The protein spot was isolated from a two-dimensional electrophoresis gel and the N-terminal amino acid sequence showed similarity to

morphinone reductase. Interestingly, the 3-methyl-2-cyclohexe-1-one significantly inhibit the activity of the purified as Ncr-His_6 reductase while norsteroid compounds such progesterone and cortisone were not bound.

Table 4-2. List of OYEs from bacteria and corresponding substrate specificity.

Year (Ref.)	**Organism**	**Protein (Swiss-Prot accession no.)**	**Gene**
Substrates		Inhibitors (Binding Ligands)	
1979 (310)	***Gluconobacter suboxydans***	**old yellow enzyme**	**unknown**
O_2			
1994 (311)	***Pseudomonas putida* M10**	**morphinone reductase (Q51990)**	***morB***
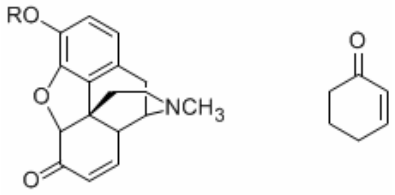 R=H, morphinone R=Me, codeinone		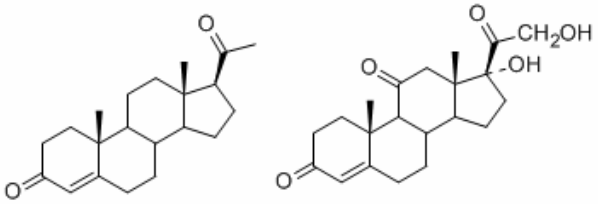 progesterone cortisone	
1999[a] (324)	***Pseudomonas putida* II-B**	**nitroester reductase (Q9R9V9)**	***XenA***
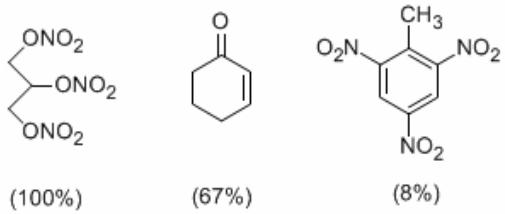 (100%) (67%) (8%)			
1999[b] (324)	***Pseudomonas fluorescens* I-C**	**nitroester reductase (Q9RPM1)**	***XenB***
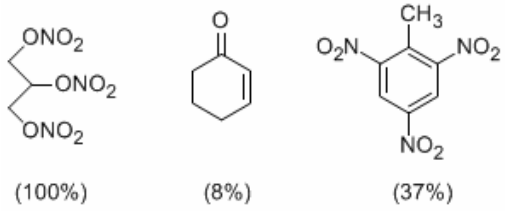 (100%) (8%) (37%)			

Table 4-2. Continued.

Year (Ref.)	**Organism**	**Protein (Swiss-Prot accession no.)**	**Gene**
Substrates		Inhibitors	
2004 (325)	***Agrobacterium radiobacter***	**glycerol trinitrate reductase (O31246)**	***Ner***
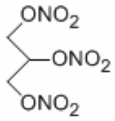			
1996 (326)	***Enterobacter cloacae* Pb2**	**Pentaerythritol tetranitrate reductase (P71278)**	***Orn***
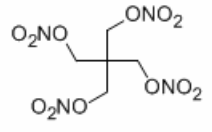 (PETN) 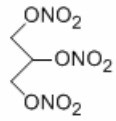 (GTN) 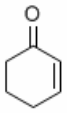 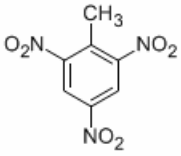 (TNT) 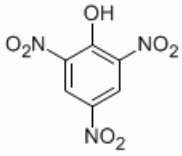 (picric acid) 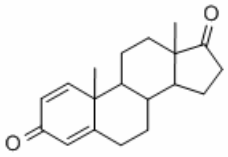 (1,4-androstadiene-3,17-dione) 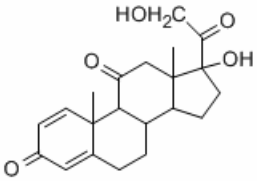 (prednisone)		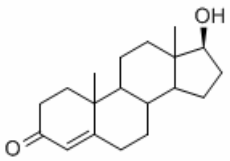 (testosterone) 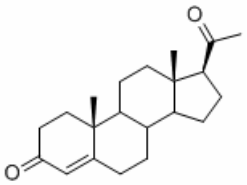 (progesterone) 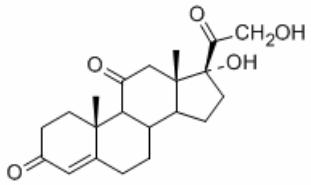 (cortisone)	
2003[c] (327)	***Bacillus subtilis Escherichia coli* JM109**	**YqjM (Q2B6D5**	**B14911_08447**
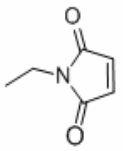 (100%) 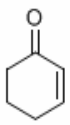 (0.19%) 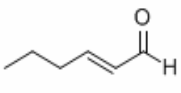 (0.02%) 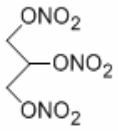 (0.06%) 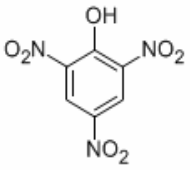 (0.4%) no reaction 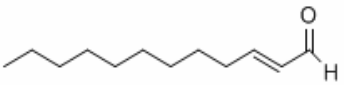 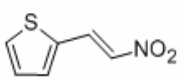 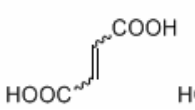 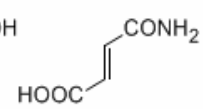			

Table 4-2. Continued.

	Organism	Protein (Swiss-Prot accession no.)	Gene
Substrates		Inhibitor	
1999 (329)	***Escherichia coli* JM109**	**N-ethylmaleimide reductase (P77258)**	**nemA**
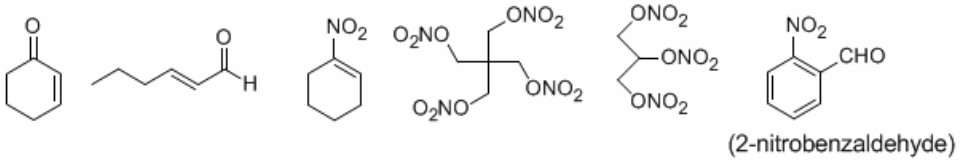 (2-nitrobenzaldehyde)			
2005[d] (328)	***Shewanella oneidensis***	**SYE1,SYE3, SYE4**	**AAN55488.1, AAN57126.1, AAN56390.1**
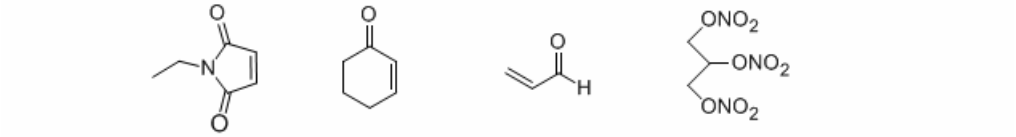 SYE1 (11.7%) (0.4%) (0.6%) (0%) SYE3 (22.3%) (0.3%) (0.4%) (0%) SYE4 (100%) (14.6%) (1.8%) (0.4%)			
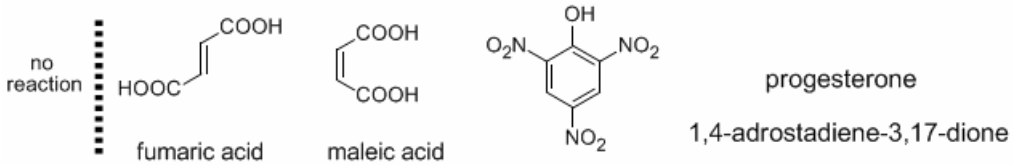 no reaction; fumaric acid; maleic acid; progesterone; 1,4-adrostadiene-3,17-dione			

[a, b] Numbers in parentheses indicate relative activity based on the measured specific activity (U/mg) for the enzyme with nitroglycerin (NG) as substrate (6.1 U/mg for XenA and 6.8 U/mg for XenB). [c] Numbers in parentheses indicate relative activity based on the measured k_{cat}/K_M number for the reaction N-ethylmaleimide with YqjM ($8.07 \mu M^{-1}$ sec^{-1}). [d] Numbers in parentheses indicate relative activity based on the measured k_{cat}/K_M number for the reaction N-ethylmaleimide with SYE4 ($5.96 \mu M^{-1}$ sec^{-1})

In 2003, the first gene encoding an OYE from a gram-positive bacterium (*Bacillus subtilis*) was cloned and the protein was overexpressed and isolated from *E. coli* in a particularly high yield (161 mg/L culture).[327] In addition to some limited spectrophotometric studies regarding its substrate specificity, it was found that the presence of xenobiotics such as TNT or agents contributing to oxidative stress such as hydrogen peroxide led to rapid induction of YqjM in *B. subtilis*. The observation further supports the notion that the physiological role of OYEs is for detoxification.

The first comparative study among OYEs in the same bacterium was reported for *Shewanella oneidensis*.[328] Out of the four putative OYEs in this species, three were successfully overexpressed in *E. coli* and purified in a GST-tagged and untagged form. Their relative activity towards four different substrates is summarized in the last entry of Table 4-2 for the untagged form. The corresponding GST-SYEs showed similar pattern but the k_{cat}/K_M values were lower in most of the cases.

A more comprehensive comparative study among OYEs from five different species had been earlier published by Bruce and coworkers.[329] The results from this study are summarized in Table 4-3. The numbers are normalized based on the specific activity observed for N-ethylmaleimide reductase (NemA) from *E. coli* with glycerol trinitrate (GNT) as substrate (i.e. 37.9 U mg^{-1}). Since the spectrophotometric assays were carried out under aerobic condition the background oxidase activity was determined and subtracted. The substrate preference for each enzyme is highlighted.

Table 4-3. A comparative study among different OYEs from yeast and bacteria.

OYE from	GNT	PETN	TNT	2-cyclo hexenone	trans-2-hexenal	1-nirtro cyclohexene	2-nitro benzaldehyde	Codeinone
E. coli	100%	84%	0%	12%	7%	22%	14%	0%
E. cloacae (type strain)	94%	59%	1%	7.1%	5.8%	20%	14%	0.3%
E. cloacae Pb2	52%	56%	4%	2%	4%	4%	5%	0.3%
P. putida M10	-1%	-1%	2.6%	-1%	-1%	1%	1%	36%
S. carlsbergensis	1%	-1%	8%	13%	11%	13%	8%	-0.3%

Old yellow enzymes from plants

In the early 80s, the elucidation of octadecanoid biosynthesis in several plant tissues by Vick and Zimmerman led to the purification of the so-called 12-oxophytodienoic acid reductase (OPR) from corn.[330] OPR catalyzes the forth step in the jasmonic acid biosynthetic pathway starting from linolenic acid (Figure 4-25), reducing

the endocyclic double bond of 12-oxo-10,15(Z)-phytodienoic acid (OPDA) to produce 3-oxo-2-(2'(Z)-pentenyl)-cyclopentane-1-octanoic acid (OPC-8:0).[331]

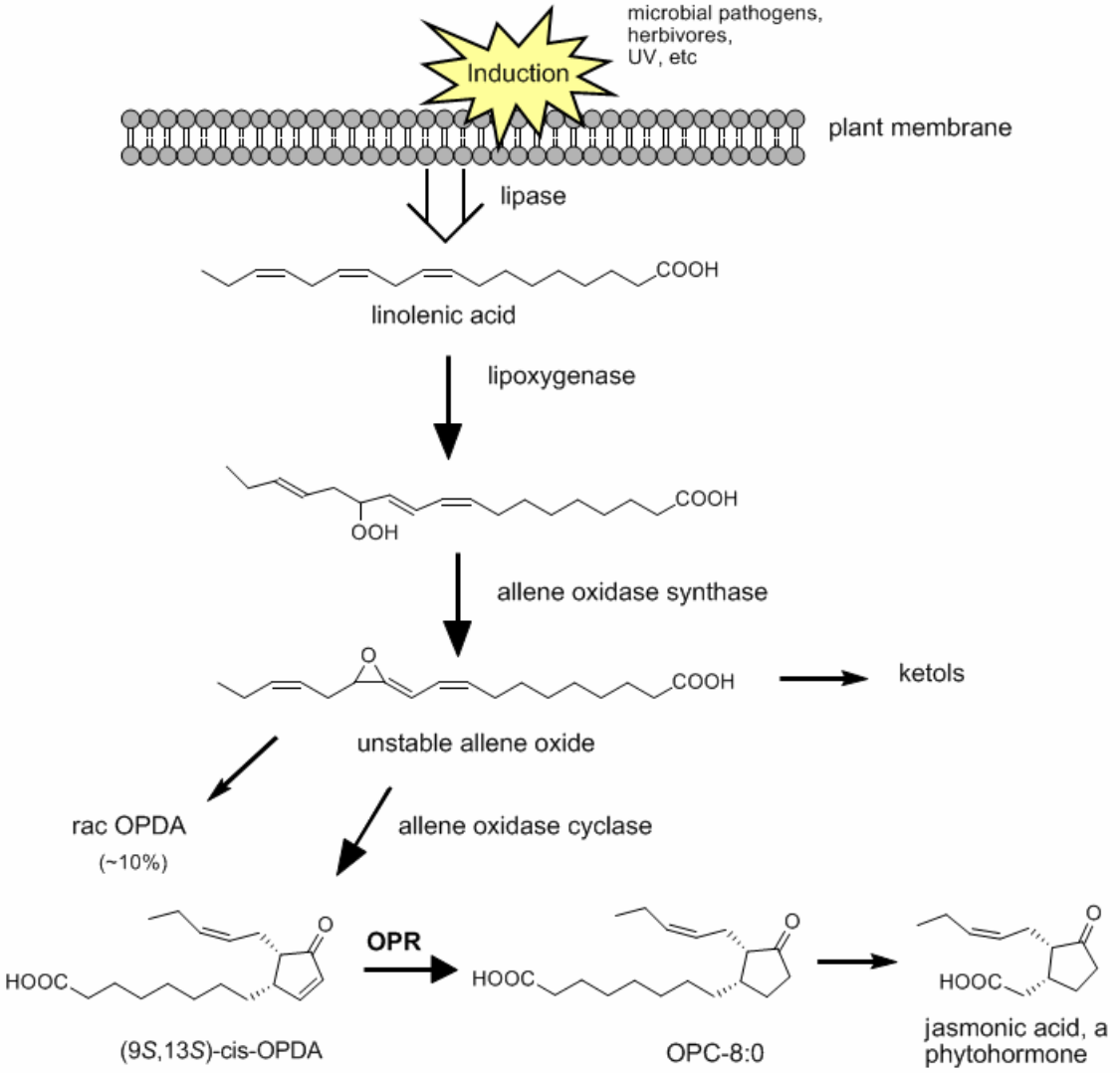

Figure 4-25. Jasmonic acid biosynthesis.

Ten years later, Schaller and Weiler purified a second homologue from *Corydalis sempervirens* after examination of the OPR activity in five different plants.[332] They wisely recognized that if the physiological role of OPR is the reduction of OPDA then their enzymatic preparation should preferably reduce the *cis* and not the *trans* diastereoisomer since the former and not the latter is found naturally from the allene oxidase/cyclase. Their GC/MS results were encouraging (6:1 preference for the *cis*

isomer), but not conclusive. Unexpectedly, their additional experiments showed that this enzymatic preparation, known today as OPRI, as well as another homologue from *Arabidopsis thaliana* (OPR1) reduced the (9*R*,13*R*)-*cis* diastereoisomer and not (9*S*,13*S*)-*cis* diastereoisomer, which is however the natural product.[333, 334] The validity of their initial hypothesis was reestablished in the subsequent publication in which a second isoenzyme (OPRII) was purified and showed a slight preference for the naturally occurred (9*S*,13*S*)-*cis*-OPDA diastereoisomer.[335, 336] Interestingly the OYE from *S. cerevisiae* also showed preference for the same diastereoisomer.

Today, the dominant trend regarding the substrate specificity of the OPRs is that they should be divided into two subgroups.[337] Subgroup I consists of AtOPR1, AtOPR2, LeOPR1 (from tomato) and OsOPR1 (from rice) with uncertain biological function and subgroup II consists of AtOPR3 and LeOPR3 whose physiological activity is the reduction of the (9*S*,13*S*)-*cis* OPDA (Table 4-4).

Table 4-4. List of OYEs from plants and corresponding substrate specificity.

Year (Ref.)	**Organism**	**Protein (Swiss-Prot accession no.)**	**Gene**
Substrates			Inhibitors
1986 (330)	***Zea mays* (corn)**	**2-oxo-phytodienoic acid reductase**	**not determined**
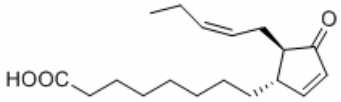 (9*S*,13*R*)-trans-OPDA			
1997 (332)	***Corydalis sempervirens***	**OPRI**	**not determined**
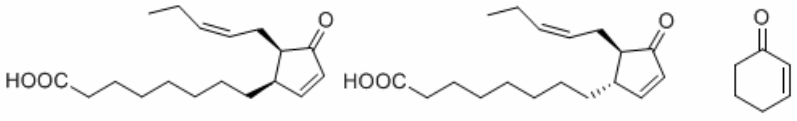 (9*R*,13*R*)-cis-OPDA (9*S*,13*R*)-trans-OPDA			
1997 (333)	***Arabidopsis thaliana***	**12-oxophytodienoate reductase 1, (Q8LAH7)**	***OPR1***
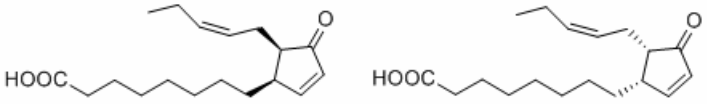 (9*R*,13*R*)-cis-OPDA (9*S*,13*S*)-cis-OPDA			

Table 4-4. Continued.

Year (Ref.)	Organism	Protein (Swiss-Prot accession no.)	Gene
Substrate			Inhibitors
2000 (336)	***Arabidopsis thaliana***	**12-oxophytodienoate reductase 2, (Q8GYB8)**	***OPR2***
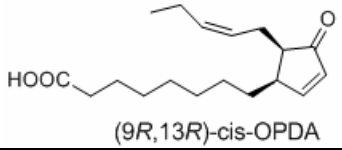			
2000 (336)	***Arabidopsis thaliana***	**12-oxophytodienoate reductase 3, (Q9FUP0)**	***OPR3***
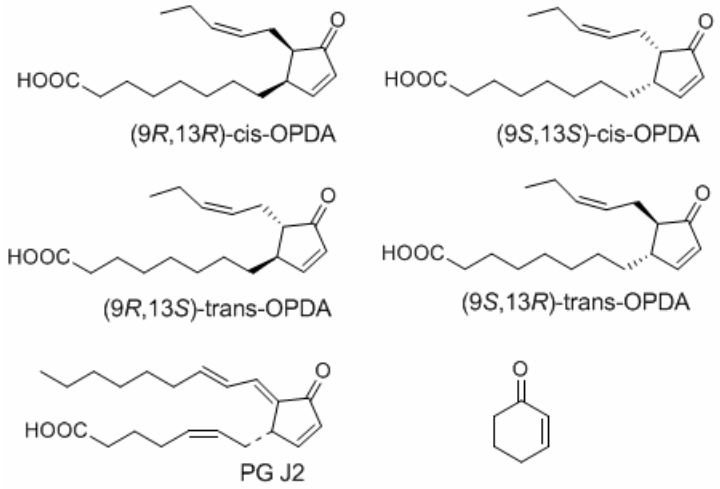			
2003 (337)	***Oryza sativa* L. (rice)**	**12-oxophytodienoic acid reductase, (Q84QK0)**	***opda***
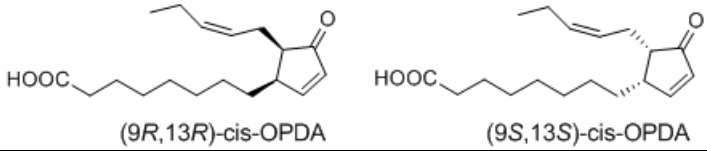			
1999 (339)	***Lecopersicon esculentum* cv. Castlemart II (tomato)**	**12-oxophytodienoate reductase 1, LeOPR1 (Q9XG54)**	***OPR1***
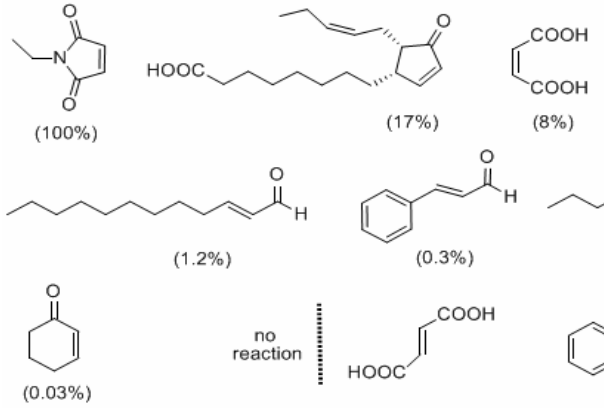			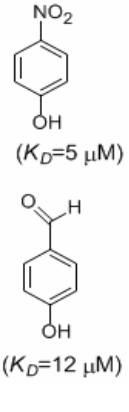

Table 4-4. Continued.

Year (Ref.)	**Organism**	**Protein (Swiss-Prot accession no.)**	**Gene**
Substrate			
2003 (338)	***Pisum sativum* (garden pea)**	**PsOPR1-6 (Q76FS1, Q9AVK9, Q76FS0, Q76FR8, Q76FR9, Q76FR7)**	***PsOPR1, OPDRA, PsOPR3-6***
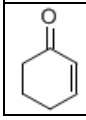			

LeOPR1 is the only OYE in this category which is known to accept compounds other than 2-cyclohexenone and OPDA.[339] In fact, the highest catalytic activity was observed for N-ethylmaleimide. It is interesting that activity was also recorded for maleic acid but not for fumaric acid.

Matsui et al. classified the six OPR-like enzymes from pea into four groups based on their ability in reduction of 2-cyclohexenone.[338] They observed no catalytic activity for PsOPR5, little for PsOPR3, moderate activity for PsOPR1, 4 and 6 and highest activity for PsOPR2.

To conclude, we should mention that almost all the experiments regarding the substrate specificity of OYEs have been performed only spectrophotometrically. In addition, despite the large number of isolated OYEs from bacteria and plants and the numerous biophysical studies of their structure and function, little is known about their substrate specificity.

Enoate Reductases

Enoate reductases (ERs) belong to a rare class of flavoenzymes containing both FMN and flavin adenine dinucleotide (FAD).[340] In addition, four iron and four labile sulfur atoms are present per enzyme subunit. The mechanism of this class of enzymes is not as well studied as for the OYEs but EPR studies[341] have shown that electrons from NADH flow via FAD and [4Fe-4S] cluster to FMN cofactor. The FMN domain is very

similar to OYE structure and in that respect enoate reductases are considered distant relatives to OYEs.

These multi-domain, gigantic (i.e.~ 940 kDa), enzymes have the unique ability to catalyze the reduction of non-activated 2-enoates, in contrast to what is observed for the enoyl-CoA and 2, 4-dienoyl-CoA reductases.[342, 343] For the latter, conversion of the carboxyl group to the corresponding CoA ester is a prerequisite for the saturation of the carbon-carbon double bond to take place (Figure 4-26). [342, 344, 345]

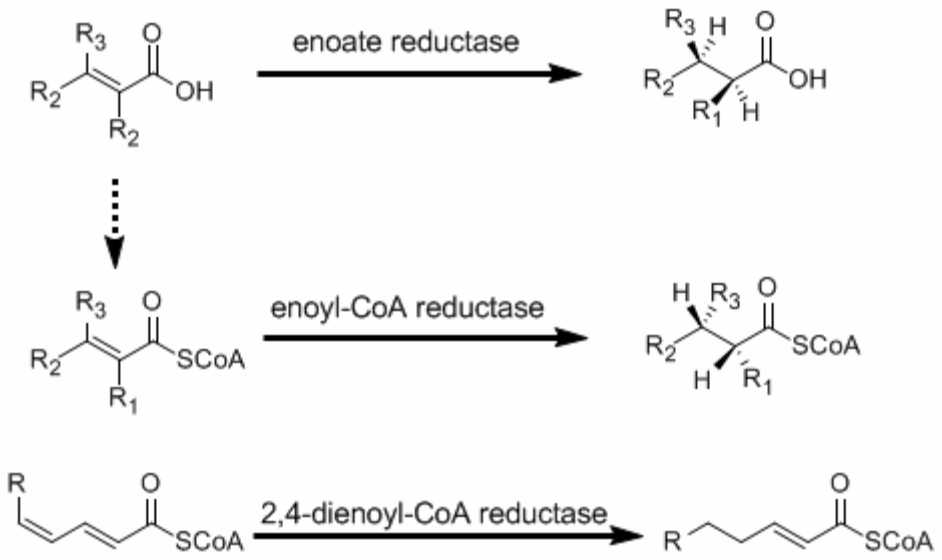

Figure 4-26. Biohydrogenation of unsaturated carboxylic acids from three different types of enzymes.

In 1975, Simon and coworkers observed that the hydrogenation of (*E*)-2-methyl-butenoate by some *Clostridia* species could occur even when the acid was not converted to corresponding CoA ester.[346] The key for this observation was the different stereochemical outcome of this reduction (2*R*) compared to what had been previously reported for the action of butyryl-CoA reductase on the corresponding CoA ester (2*S*).[347] The enzyme responsible for the former transformation would be called 2-enoate reductase.

Interestingly, in the first 2-enoate reductase preparation from *Clostridium kluyveri*, the FMN cofactor was not found but catalytic activity was detected for the compounds listed in Table 4-5.[353] A shorter enzyme purification protocol developed in the same laboratory allowed the isolation of the most studied enoate reductase from *Clostridium tyrobutiricum*.[348] In that preparation, the 0.6-0.7 mol of FMN per mol of subunit found indicated labile binding of the FMN cofactor in these flavoproteins. In addition, the rapid deactivation of the catalyst in the presence of oxygen (1-2 min for the reduced form) renders its purification quite laborious since strictly anaerobic conditions are required in all steps. Attempts to express ER from *Clostridium tyrobutiricum* in *E. coli* have failed so far. However, a third ER from *Clostridium thermoaceticum* was successfully overexpressed in *E. coli*, but only when the engineered strain grew under anaerobic conditions.[341]

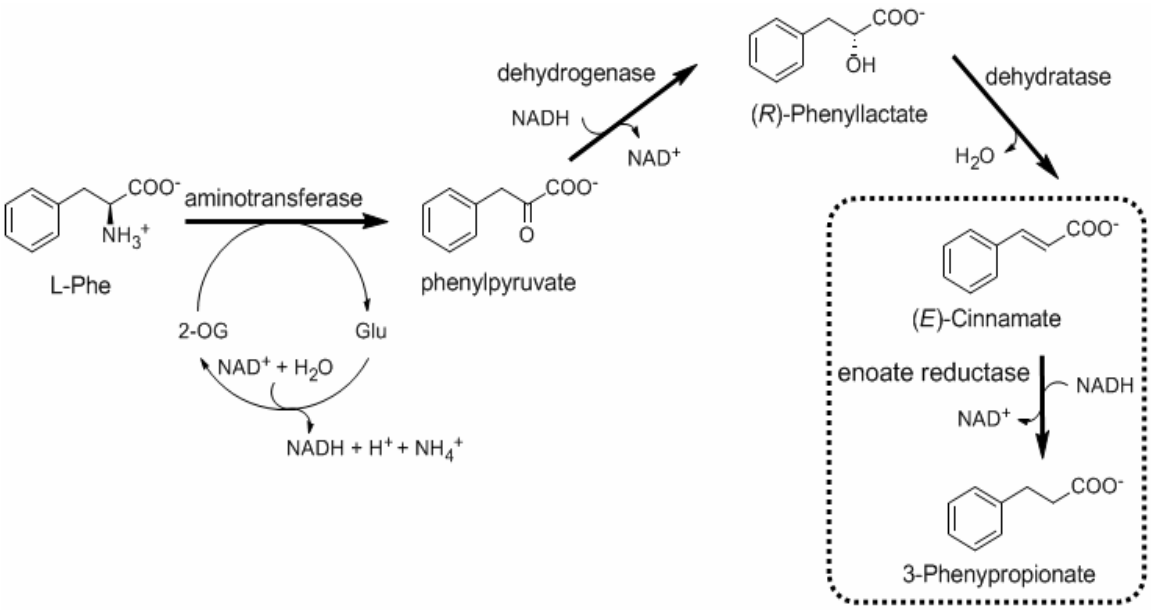

Figure 4-27. Reductive part of the phenylalanine fermentation pathway in *Clostridia sporogenes*. Glu, glutamate; 2-OG, 2-oxoglutarate (Adapted from ref. 350).

The physiological role for the ER from *Clostridium sporogenes* has been elucidated by Simon and coworkers.[349] It was found that certain Clostridia species ferment L-phenylalanine to phenylacetate and 3-phenylpropionate. Enoate reductase

catalyzed the last step in the formation of the latter compound (Figure 4-27). However, the substrate specificity for this particular reductase is narrow and limited to cinnamic acid. In contrast, ERs from *Clostridium tyrobutiricum* and *Clostridium kluyveri* could accept a broad range of enoates. A complete list of substrates is not included in Table 4-5 because in most cases whole cells or crude extracts have been employed and the subject has been reviewed elsewhere.[267]

General rules derived from biohydrogenations with whole cells, mentioned in the first part, regarding the substrate specificity (no bulky disubstitution at the β-position and different stereoisomers depending on the initial enoate *E* or *Z* stereochemistry) are also valid for the purified ERs. A complication, however, has been observed in the case of geraniate (Table 4-5). Hydrogenation of (*E*) and (*Z*) geraniate afforded 95% *ee* (*R*)- and 95% *ee* (*S*)-citronellate respectively, when purified ER was employed. When whole cells were used instead, a lower ee value (60-85%) was observed for the *Z* geraniate presumably due to isomerization of the (*Z*)-isomer to thermodynamically more stable (*E*)-geraniate by the cells.[267]

Enals could also be reduced easily by ERs. However, caution should be taken to remove simultaneously the obtained aldehyde product quickly from the reaction mixture, either by further enzymatic reduction to corresponding alcohol or by continuous extraction with an organic solvent, otherwise low ee values are observed.[351] It has been shown that this is due to a desaturation reaction catalyzed by ERs when aldehydes, but not when carboxylates are used, in the presence of an electon acceptor such as oxygen. Surprisingly under those conditions, the half life of ER was more than 20 h. Lastly β-halogenated enoates undergo an elimination reaction by ERs affording saturated, halogen-free carboxylates with concomitant consumption of 2 equivalents of NADH.[268]

Table 4-5. List of ERs and representative substrate specificity.

Year (Ref.)	**Organism**	**Protein(Swiss-Prot accession no.)**	**Gene**
Substrates			
1980 (352)	***Clostridium kluyveri*, 2-enoate reductase**	**2-enoate reductase (O52933)**	***enr***
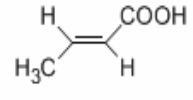 (*E*)-2-butanoate 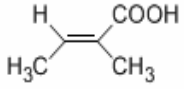 (*E*)-2-methyl-2-butanoate 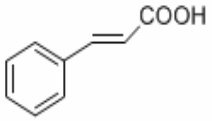 cinnamate			
1979 (353)	***Clostridium tyrobutiricum* (*Clostridium spec.* La1)**	**2-enoate reductase (Q52922)**	***enr***
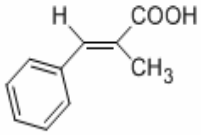 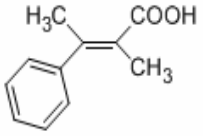 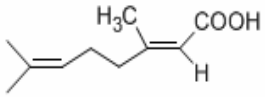 (E)-geraniate 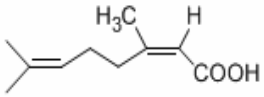 (Z)-geraniate 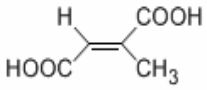 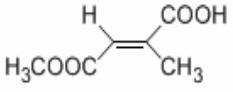 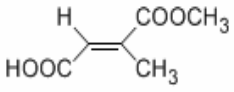			
2000 (350)	***Clostridium sporogenes***	**2-enoate reductase**	**unknown**
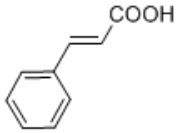			
2001 (344)	***Clostridium thermoaceticum***	**2-enoate reductase (O52935)**	***enr***
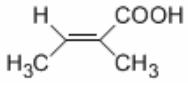			

Structure-Function Studies among Flavin-Containing En-Reductases

The extensive biochemical and biophysical analyses of old yellow enzyme family members aim mostly to shed light on the catalytic microenvironment (Figure 4-28) of these enzymes as well as to pinpoint subtle structural differences among them.

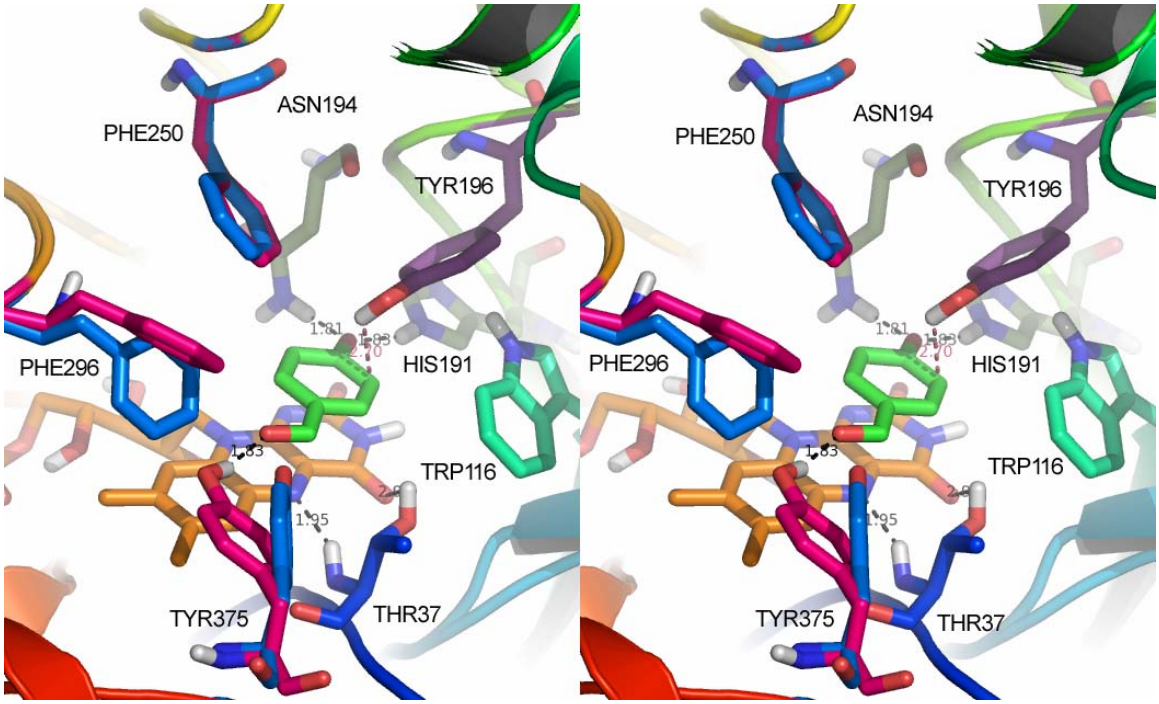

Figure 4-28. Close up view of the catalytic microenvironment of OYE1 before (1OYA) and after (1OYB) the binding of para-hydroxy-benzaldehyde.[290] Amino acid residues in distance equal of smaller of 4Å around the binding ligand are shown. Amino acid residues for which conformational changes are imposed before and after the binding of the ligand (i.e Phe250, Phe296, and Tyr375) are colored in blue and magenta respectively. The figure was rendered in PyMOL.

Tyrosine 196 was the first amino acid residue that was targeted by site-directed mutagenesis.[284] The observation that the Y196F mutation did not alter the ability of *S. carlsbergensis* OYE1 to bind phenol analogs suggested that no significant structural changes occurred in the catalytic site upon this mutation. However, the nearly complete loss of catalysis for the oxidative-half reaction step, with 2-cyclohexenone as a substrate, was consistent with the role of Tyr196 as an active site general acid in the reduction of unsaturated ketones. By contrast, the observation that the rate of enzyme oxidation was not significantly altered when nitrocyclohexene was used as a substrate by the Y196F mutant suggested that hydride transfer and substrate protonation are decoupled events for this type of compound. Further investigation of the OYE1-mediated reduction of nitro-alkenes revealed that the existence of Tyr196 may not be

necessary for the reduction of nitrocyclohexene (i.e formation of nitronate intermediate) but it still accelerates the protonation of the rapidly released into the medium intermediate nitronate. In case of Y196F mutant, the reaction was found to be a slow non-enzymatic process.[297] Interestingly, in the same study it was found that OYE1 catalyzed the non-redox deprotonation of nitrocyclohexane (pKa=8.65) forming a nitronate, the same intermediate formed as in the redox reaction, presumably via the Tyr196 side chain (pk_a=9.1).

A tyrosine residue is present in an analogous position in all well-studied isoenzymes of OYE1, with the only exception being the morphinone reductase, in which Cys191 aligns with Tyr196. Surprisingly, mutagenesis studies (i.e. C191A in the case of MR and Y186F in the case of PETN reductase) argued against a similar role for either Cys191 or Tyr186 as an active general site acid in this OYE homolog.[354] A water molecule has been suggested as the most likely proton donor in these enzymes.[355] In addition, the protonation of the nitronate intermediate during the MR-mediated reduction of nitrocyclohexene is not an enzymatic reaction even though this nitroalkene is a good substrate for MR.

In the crystal structure of OYE1 with *para*-hydroxybenzaldehyde, His191 and Asn194 are supposed to make hydrogen bonds with the hydroxy moiety of the ligand. Replacement of His191 with Asn reduced the ability of OYE1 to bind ligands or substrates whereas mutation of Asn194 to His resulted in a protein that did not bind FMN tightly. Surprisingly, a double OYE1 mutant H191N/N194H was reduced by NADPH much faster than the native enzyme.[356] This result indicates that OYE is not optimized for the reductive half reaction alone. In effort to alter the redox potential of the FNM by protein engineering, Thr37 was mutated to Ala.[357] This replacement lowered the redox potential of the bound FMN by 33mV and the rate of the oxidative half reaction

was accelerated. However, the reductive-half reaction was slowed down and thus the overall catalytic turnover number was decreased.

Mutagenesis of Trp102 (the corresponding Trp116 in Figure 4-28) to either Tyr or Phe in PETN reductase was designed to minimize steric clashes between the side chain of this amino acid and the C6 nitro group of picric acid and this resulted in tighter binding of the substrate by the mutant enzymes. The mutations altered also the chemical nature of products obtained upon the reduction of PETN reductase with picric acid.[358]

The X-ray crystal structure of *B. subtilis* YqjM has recently been solved.[359] The enzyme is a homotetramer in contrast to other OYE homologues which are monomeric (OPR1, SEY1, MR) or dimeric (OYE1, PETN). In addition, even though the superposition of the two crystal structures of YqjM and OYE1 with bound *para*-hydroxybenzaldehyde (p-HBA) places both flavin and ligand at almost the same position in both cases, only two amino acid residues (Tyr196 and His191, numbers are based on OYE1) are conserved (Figure 4-29). The most dramatic changes are the replacement of the amino acid residue Trp116 by Ala (not shown in Figure 4-29) and Thr37 by Cys26. Both Trp and Thr are well conserved amino-acids among other members of OYE family (Figure 4-30). The common replacement, Asn194 by His, found in other OYE members is also present in YqjM structure. The founding that an Arg residue from the C terminus of the second monomer participates in the catalytic environment of the first monomer may explain way a C terminus 6xHis-tagged YqjM is an almost completely inactive enzyme.[360] Last but not least, the aldehyde moiety of pHBA is rotated 180° in YqjM structure in order to be placed in appropriate position for a hydrogen bond with Tyr28, since an analogous toTyr375 residue of OYE1 is absent in the YqjM structure.

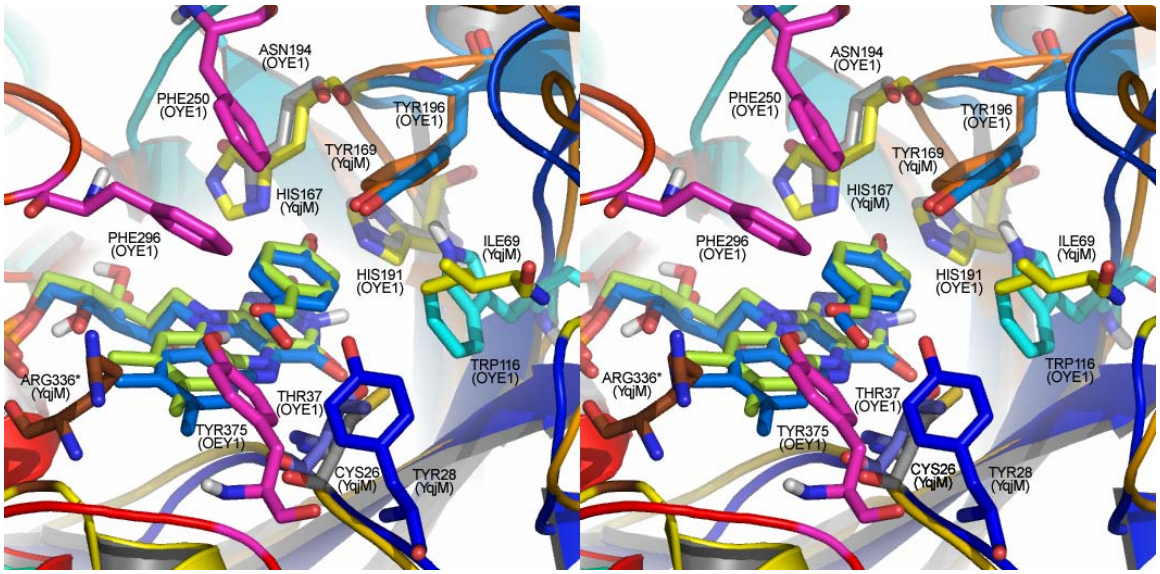

Figure 4-29. Superposition of OYE1 and YqjM structure. The flavin molecule as well as the p-HBA colored in yellow belongs to OYE1 structure. In blue are colored both flavin and p-HBA molecules belonging to YqjM structure. The Figure was rendered in PyMOL.

Structure-function correlations in between OPR1 and OPR3 subfamilies are under vigorous investigations in order to explain their different substrate stereospecificities. When the X-ray structure of Leopr1 with bound 9*R*,13*R* –OPDA[361] was compared to that of *S. carlsbergensis* OYE1, it became apparent that the catalytically important amino acids are highly structurally conserved. It was proposed for the first time that amino acid residues in longer distance from the catalytic center should probably interact with the non-reactive part of the substrates and cause the observed altered stereoselectivities. Specifically, attention was paid to the two loops surrounding the entrance of the OYE catalytic cavity (Figure 4-31). Both loops showed pronounced flexibility. In fact, certain amino acid residues in loop6 are not well defined in the Leopr1 structure (i.e., black dots in Figure 4-31) as well as in the subsequently released X-ray structures of AtOPR1[362] and AtOPR3.[363]

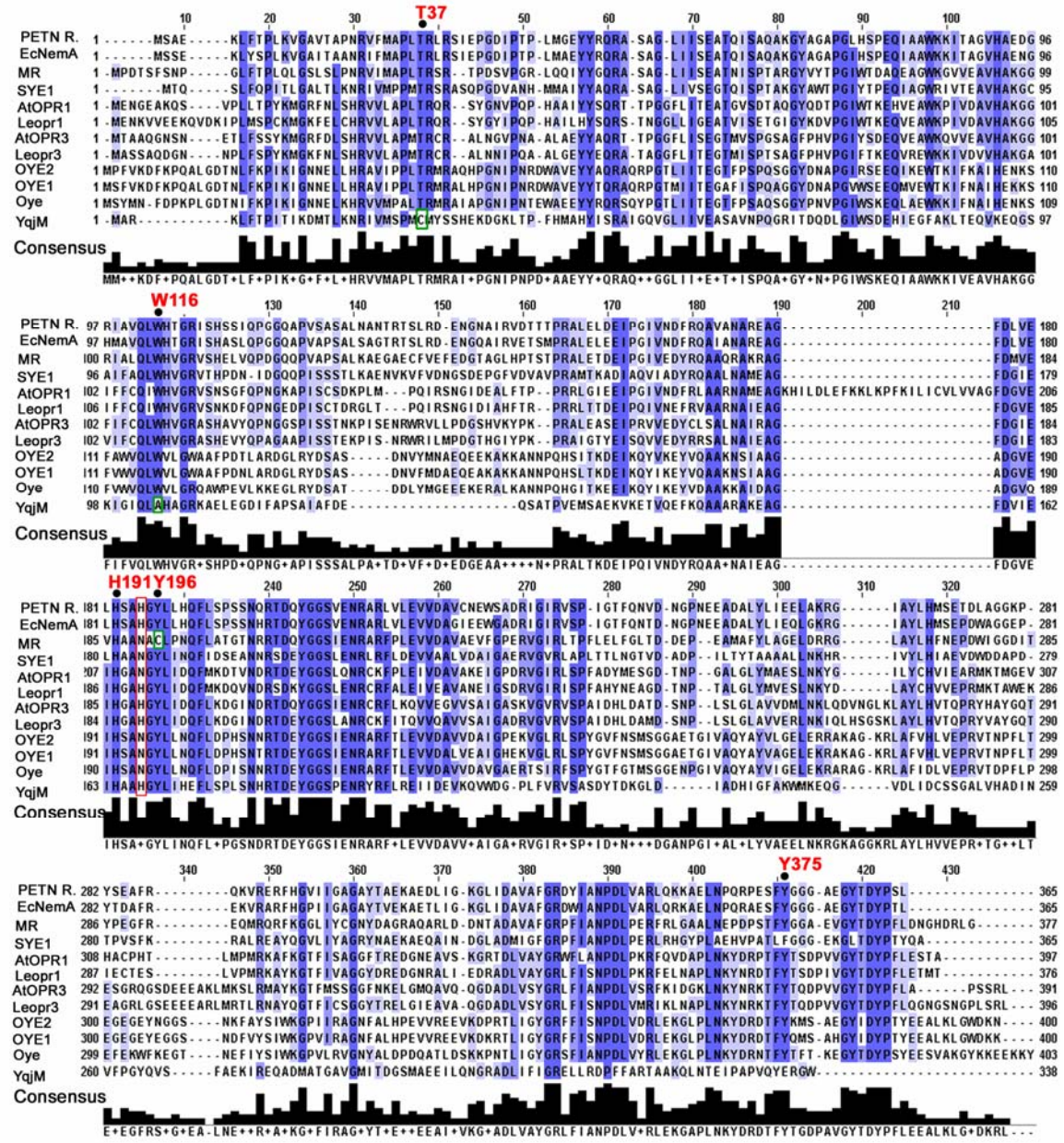

Figure 4-30. Multiple alignment of twelve en-reductases belonging to OYE family. Black dots indicate amino acid residues present in the catalytic site of OYE1 and conserved among other OYE homologs. The replacement of T37 by C26 and W116 with A104 in case of YqjM as well as the replacement of Y196 by C191 in case of PETN reductase, discussed in the text, are highlighted in green boxes. The red box shows the replacement of N194 (OYE1) with His in some OYEs. The alignment was generated using the ClustalW web server software.

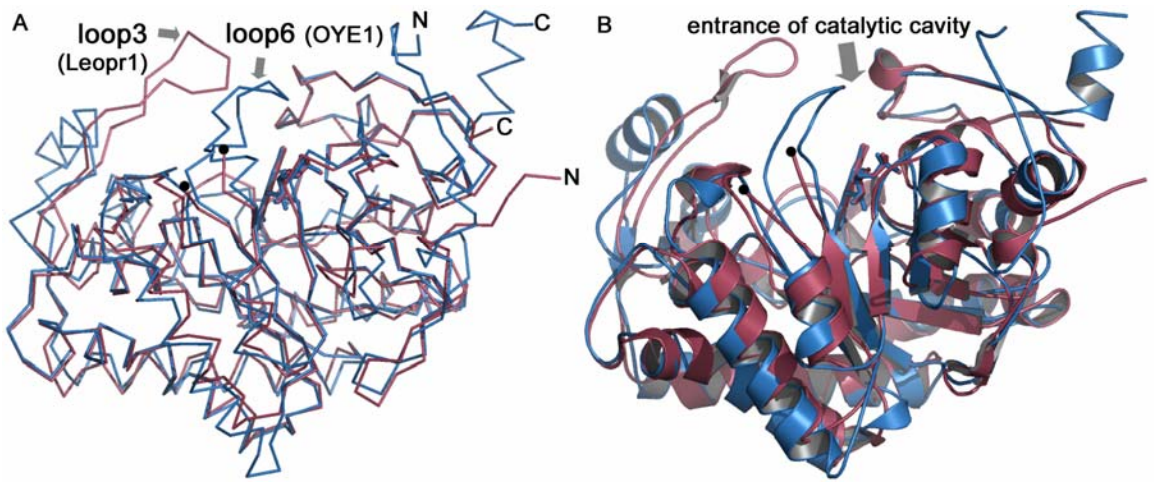

Figure 4-31. Superposition of OYE1 and Leopr1 structure. A. Ribbon structure of OYE1 (blue) and Leop1 (purple). Arrows indicate loop3 and loop6 in Leopr1 and OYE1 structure respectively. B. Cartoon of superimposed structures. Arrow indicates the entrance of the catalytic center in both enzymes. Black dots indicate the disorder of residues 283-288 in loop6 of Leopr1 structure. The Figure was rendered in PyMOL.

The accumulated X-ray structure data of OYEs from yeast, bacteria and plants clearly showed that the motif of loop3 is very similar in both bacterial and plant OYEs and consists of one parallel and one antiparallel beta strand (Figure 4-32). However, only the Leopr1 structure is the loop pointed toward the catalytic center. In the OYE1 structure, the loop3 is composed of two helices and two β sheets and it does not capping the catalytic cavity.

The crystallization of LeOPR3 uncovered an unprecedented property among flavoproteins.[364] Unexpectedly, LeOPR3 crystallized as a self-inhibited dimer. The loop6 of the one monomer was protruded into the catalytic cavity of the second unit and vice versa (Figure 4-33). Mutagenesis studies revealed that replacement of Glu291, which is found at the tip of loop6, by Lys prevented the dimerization. The dimerization was also detected in solution and lead to slower catalytic turnover numbers. The co-crystallization of the dimer with two sulfate ions (i.e., red dots in Figure 4-33) at a hydrogen bond distance with Tyr364 suggested a possible regulation of catalytic activity

in vivo by dimerization modulated by reversible phosphorylation. The observation that the Y364F mutant Leopr3 could not form a dimer supports this hypothesis.

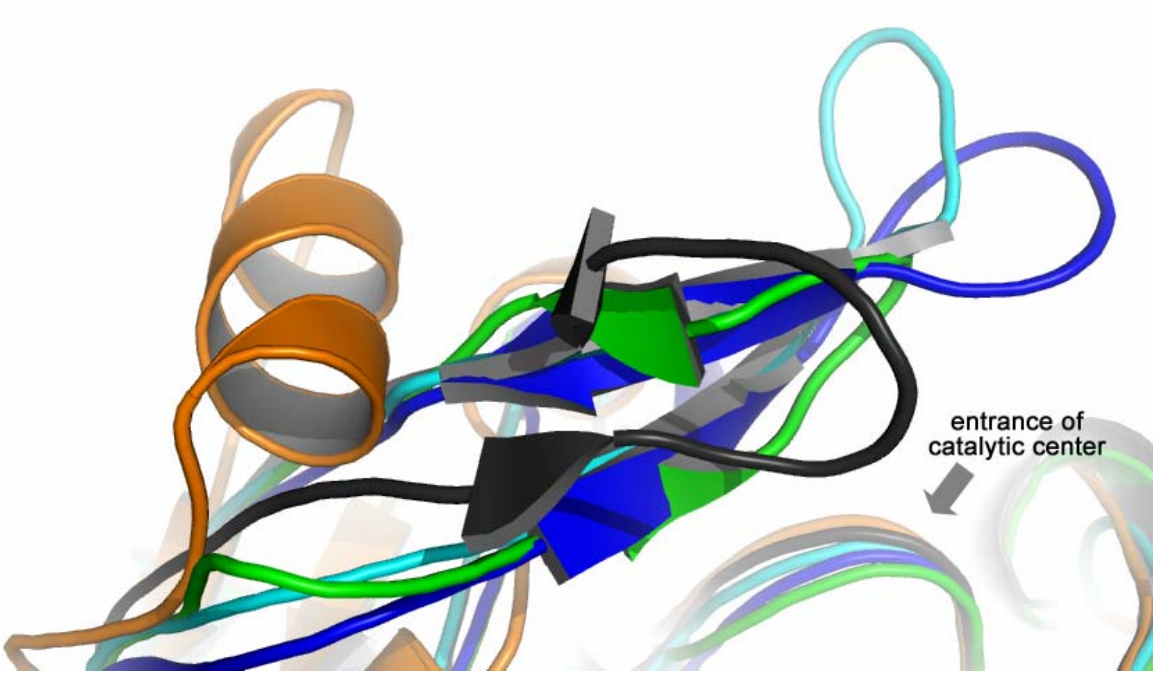

Figure 4-32. Close-up view of loop3 after superposition of five OYE crystal structures. Orange for OYE1 (1OYEA), black for Leopr1 (1ICP), green for AtOPR3 (1Q45), cyan for MR (1GWJ) and blue for SEY1 (2GOU).[365] The Figure was rendered in PyMOL.

Despite the accumulated knowledge regarding the structural details of OYE family members, the exact amino acid residues responsible for the differential stereoselectivities among OPRs have not yet identified. Further experimentation with compounds similar to OPDA as well as comparative studies among OYEs from fungi, bacteria and plants may provide useful and complementary data to augment crystallographic studies.

A preliminary, low resolution, crystal structure of the enoate reductase[340] from *Clostridium tyrobutyricum* revealed that the overall fold resembles that of *E. coli* 2,4-dienoyl-CoA Reductase (DCR).[366] It seems that these two flavoproteins have evolved so that the reductive and oxidative half reaction take place in two distinct domains, whereas a 4Fe-4S cluster plays the role of an electron mediator across the two centers. In

contrast, in the OYE family, both reduction and oxidation are carried out by the same FMN-bearing catalytic center (Figure 4-34).

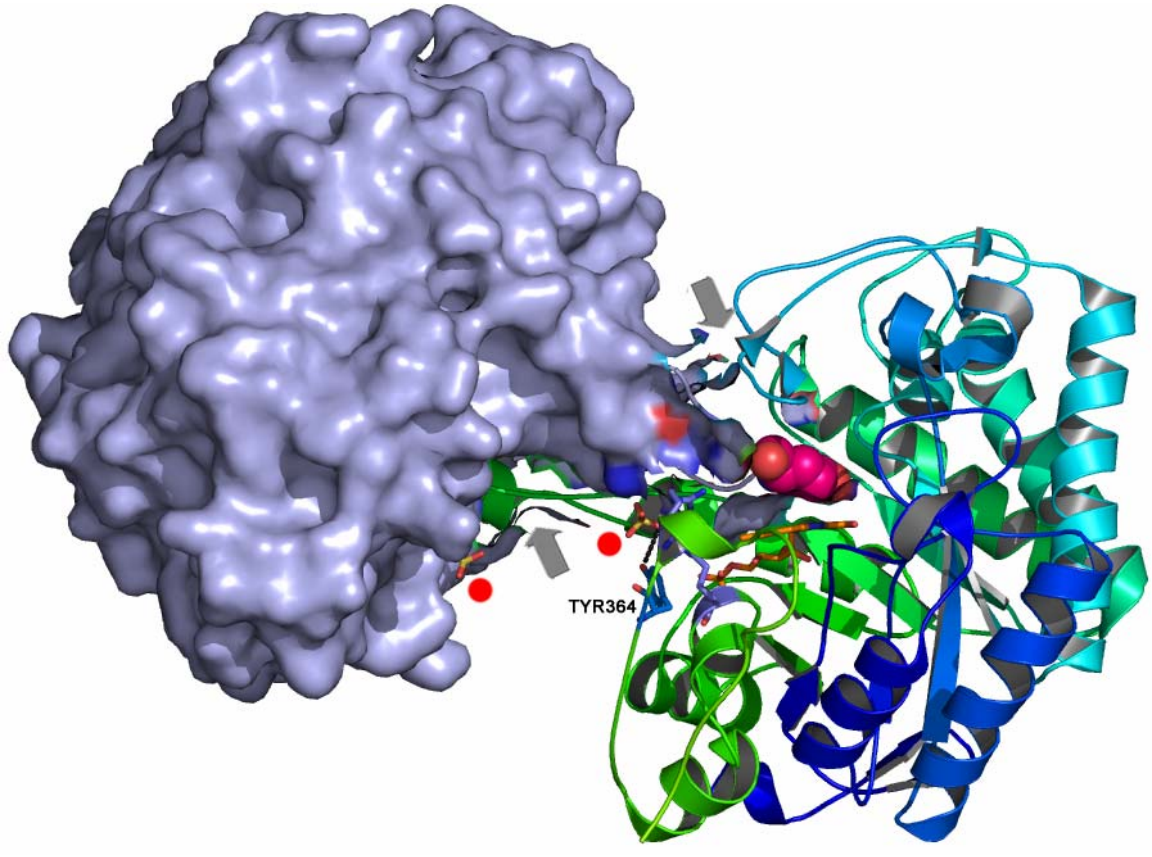

Figure 4-33. Bird's view of the overall structure of the self-inhibited Leopr3 dimer. Arrows indicate the direction of loop6 in each monomer. Glu291 is shown in red (space filled model) from the left-hand unit is stacking above the flavin (colored in orange) of the right-hand unit blocking the catalytic center. Red dots highlight the two sulfate ions in the proximity of Tyr364, colored in blue, in the right-hand unit only. The Figure was rendered in PyMOL.

Even though DCR and OYEs have been co-crystallized with their natural substrates or an analog, this is not the case for ER. In principle, DCR, OYEs, and ERs perform the same chemistry (reduction of a carbon-carbon double bond) in a similar TIM barrel domain; however, the substrate specificities are unique: enones/enals for OYE1, enoates and enones/enals for ER and CoA dienoyl esters for DCR) differs. Thus, determining which amino acids participate in substrate binding and catalysis for ER as well as additional experimentation with alternative substrates for OYEs and DCR will

help us understand the catalytic features controlling the different substrate specificities among these flavoproteins. Such studies may also serve as a platform for subsequent protein engineering projects.

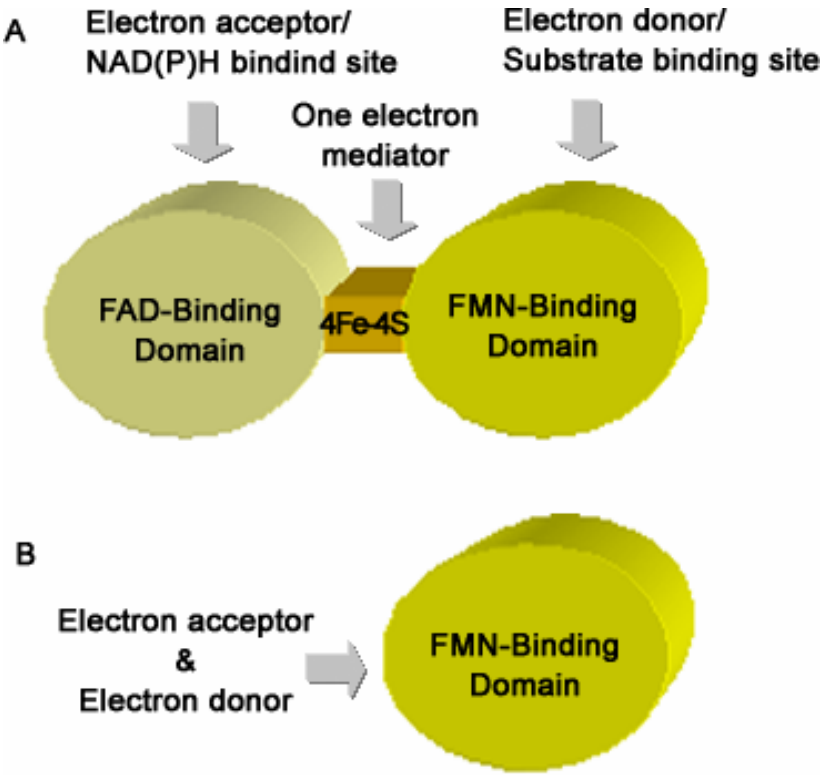

Figure 4-34. Structural differences in between the flavor-bearing en-reductases. A. Cartoon of multi-domain structure of enoate reductase. B. Cartoon of OYE family single domain.

Medium Chain Dehydrogenases Possessing En-Reductase Activity

Alkenal/one oxidoreductase (AOR) compromises by itself a distinct family in the medium chain dehydrogenase/reductase (MDR) superfamily, called the LTD family[367, 368] It is a key player in the inactivation of eicosanoids and can act either as an allylic alcohol dehydrogenase (leukotriene B_4 12-hydroxydehydrogenase) or as an enone reductase (15-oxo-prostaglandin 13-reductase) on major endogenous lipids mediators (Figure 4-35) such as leukotriene B_4 (LTB_4), lipoxin A_4 (LXA_4) and prostaglandin E (PGE_2).[369]

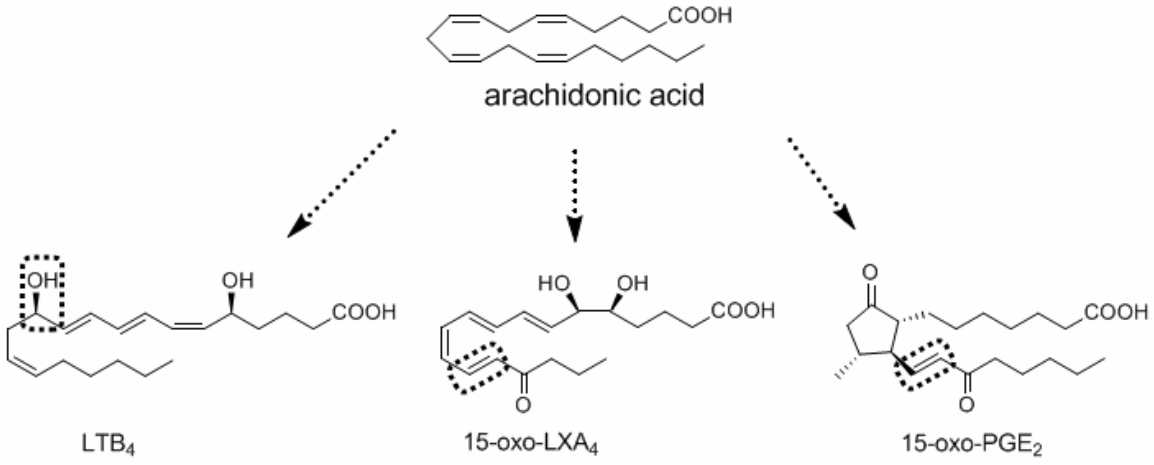

Figure 4-35. The bifunctional action of AOR. AOR catalyzes the first step in degradation metabolism of the highly biologically active compounds LTB_4, LXA_4 and PGE_2.

AOR is found in a number of mammalian species and in various tissues. It was first isolated by Yokomizo et al. from the cytosolic fraction of porcine kidney as LTB_4 12-hydroxydehydrogenase (LTB_4DH).[370] It showed 3.5 times higher activity for 6-*trans*-LTB_4 compared to the one for LTB_4, whereas its activity towards the 6-*trans*-12-*epi*-LTB_4 was four times lower. The cDNA for the human enzyme was also cloned and overexpressed in *E. coli* from the same laboratory and showed 84.7% identity at the nucleotide level with that from pig.[371]

In an independent study, Tai and coworkers purified a 15-oxoprostaglandin reductase (PGR) from pig lung.[372] Surprisingly, sequence homology analysis showed that the novel reductase differed from the LTB_4DH only in one amino acid. Moreover, the reductase function of PGR on 15-oxo PGE_2 was 300-fold higher compared to the dehydrogenase function on LTB_4. Subsequent work uncovered guinea pig PGR's role on inactivation of lipoxin A_4. The ternary complex structure of AOR for guinea pig with $NADP^+$ and the ω-chain of 15-oxo-PGE_2 (Figure 4-36) provided some insights for the possible mechanism of AOR as reductase (Figure 4-37).[373] On the other hand the mechanistic action of the same enzyme as LTB_4 dehydrogenase remains unclear.

The significant sequence homology of AOR with the quinone reductase from *E. coli*[374] forced Kensler and co-workers to postulate that the former enzyme possesses an additional role in chemoprotection by degrading toxic by-products of lipid peroxidation such as enones and enals.[375, 376] They evaluated their hypothesis by measuring spectrophotometrically the catalytic activity of recombinant AOR from rat with a number of enones and enals. They found that enones are better substrates for AOR as compared to enals, especially when they bear a long aliphatic chain (ca. 8-10 carbon atoms, Table 4-6). Substitution at either α or β-carbons of enones or enals was not tolerated by the enzyme, nor could it reduce endocyclic double bonds. Interestingly, the sequiterpenes illudin S and illudin M, as well as semisynthetic derivatives such as acylfulvene, which all well-known alkylating agents and promising chemotherapeutic agents, are bioactivated by AOR.[377, 378]

In plants, the P1-ζ-crystallin (P1ZCr) quinone oxidoreductase from *Arabidopsis thaliana*,[379] an oxidative-stess induced enzyme, and the alkenal dehydrogenase from barley possess substrate specificities similar to AOR (Table 4-6).[380] Due to this function, the alternative term 'NADPH: 2-alkenal/one α,β-hydrogenase (ALH)' has been proposed to describe of this family of enzymes.[381]

In addition, the pulegone reductase from peppermint[382] and the quinone oxidoreductase from strawberry[383] were found to reduce the exocyclic double bond of (+)-pulegone and 4-hydroxy-5-methyl-2methylene-3(2H)-furanone (HMMF), respectively (Table 4-6). It is interesting to note that pulegone reductase lacks strict facial stereoselectivity in the reduction of pulegone and affords a mixture of (-)-methone and (+)-isomethone in a 55:45. The catalytic activity of both enzymes on other enones has not been explored so far.

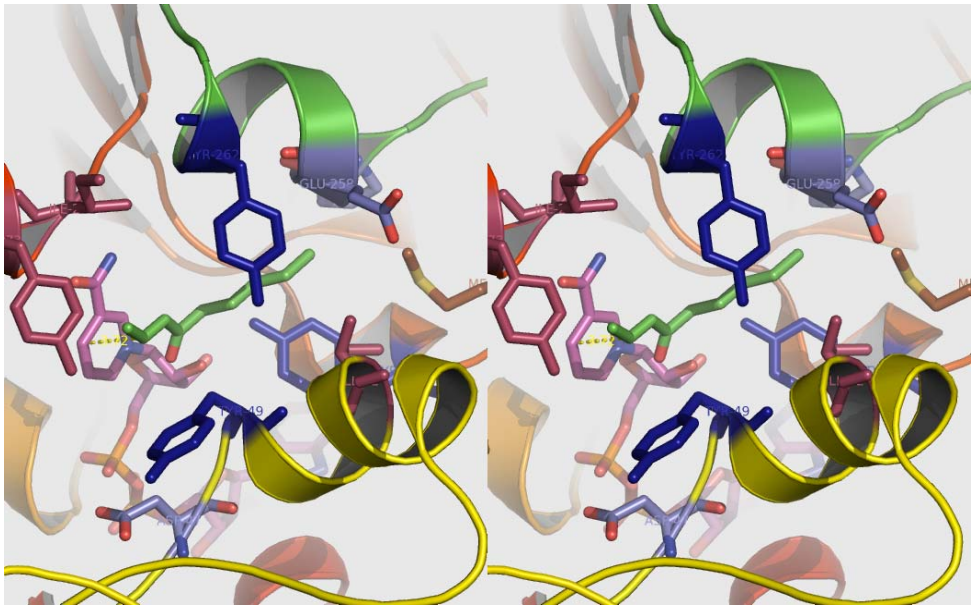

Figure 4-36. Close up view of the hydrophobic pocket of AOR from guinea pig (PDB, 1V3V). The ω chain of 15-oxo-PGE_2 bearing the double bond is colored in green. $NADP^+$ is colored in magenta. The three conserved Tyr residues (see Figure 4-38) are colored in blue. The Tyr residue 271, colored in purple, is replaced by Thr in rat and porcine AOR (See Figure 4-38).

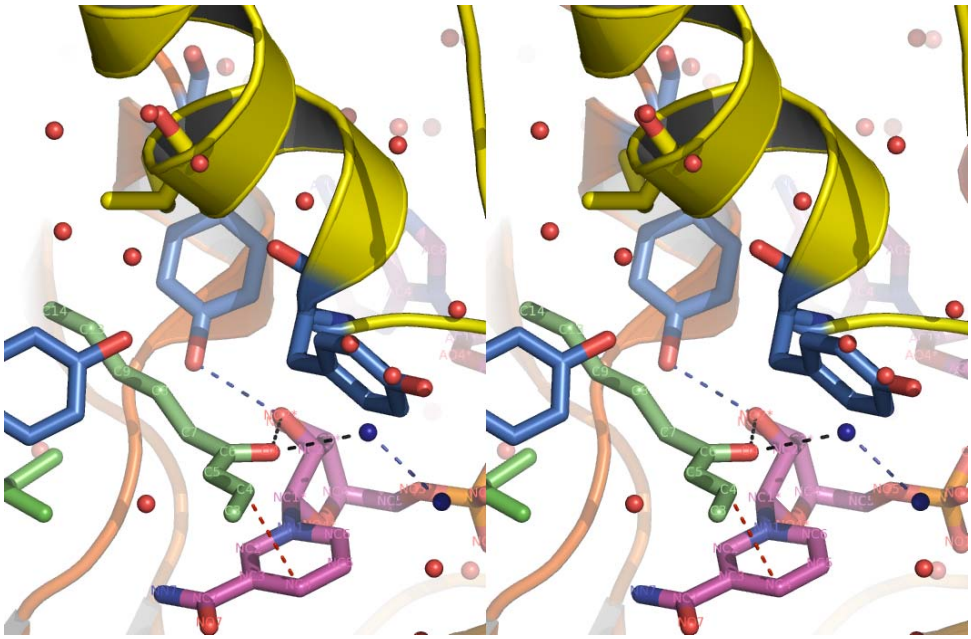

Figure 4-37. Proposed catalytic mechanism of the reductase activity of AOR from guinea pig. The enolate anion form of substrate is stabilized in the active site by making hydrogen bonds with the 2' hydroxyl group of nicotine amide ribose of NADPH and a water molecule (colored in blue). The pro-*R* hydrogen of NADPH as a hydride is attacking the electrophilic carbon C-13 of PGE_2 (numbered as C4 in this figure). The Figure was rendered in PyMOL.

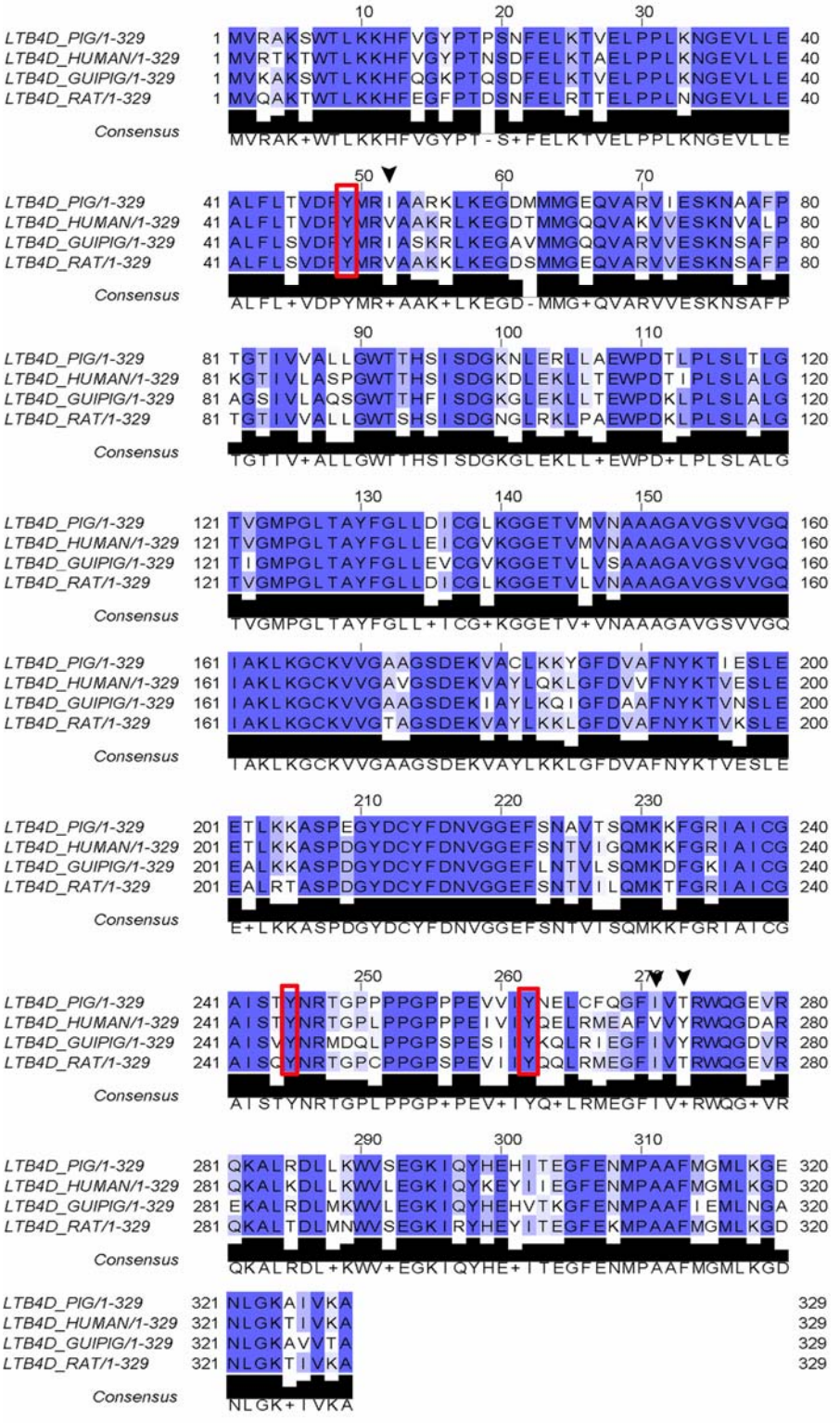

Figure 4-38. Multiple alignment of the four purified AORs. The alignment was generated using the ClustalW web server software. Within a red frame the 3 Tyr residues, colored in blue in Figure 4-37. Wedges are showing the Ile and Tyr residues colored in purple in Figure 4-37.

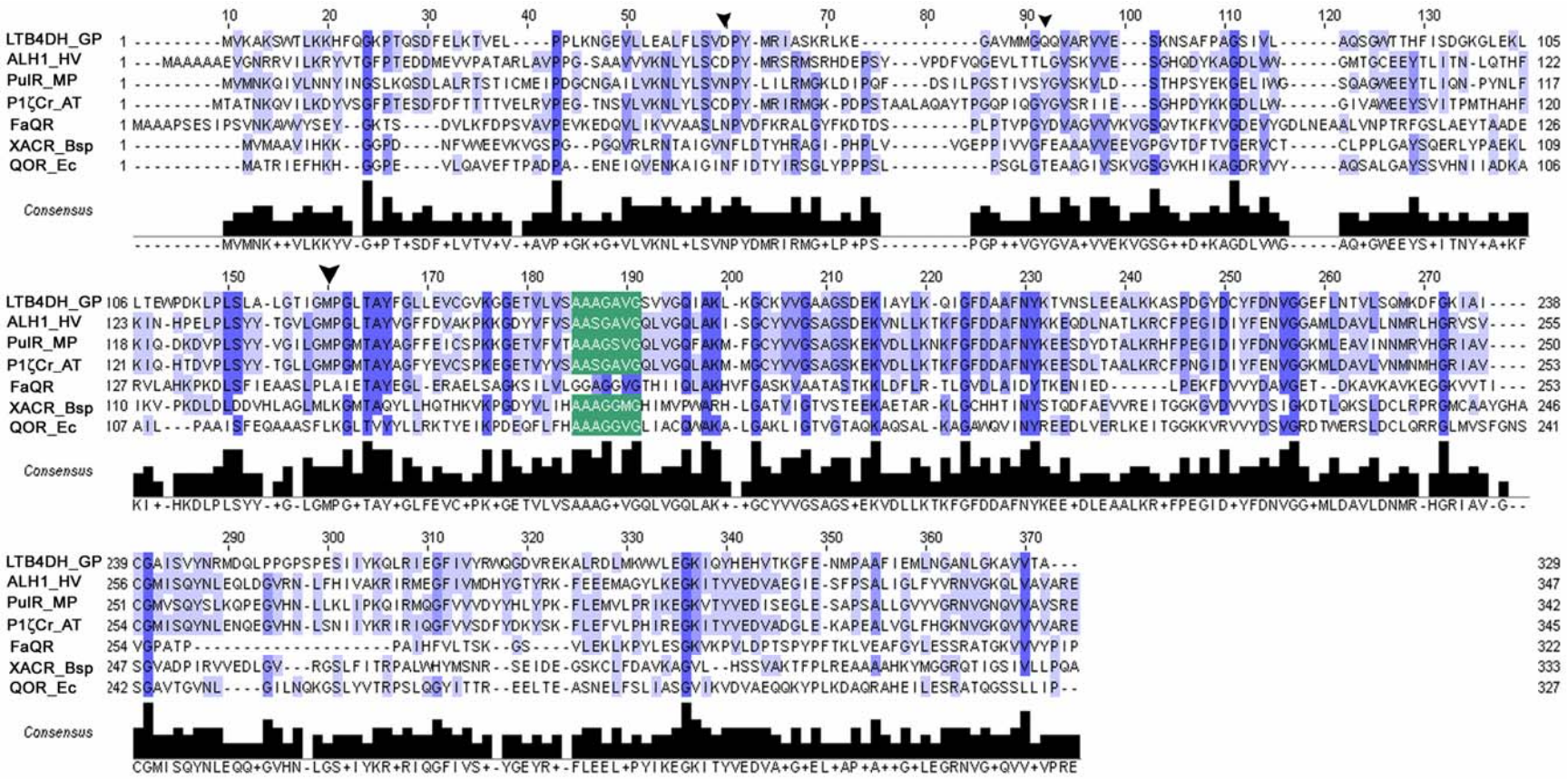

Figure 4-39. Multiple alignment of zinc independent en-reductases belonging to MDR superfamily. First row the AOR from guinea pig. Last row the Quinone Oxidoreductase (QOR) from *E. coli*. Alkenal hydrogenase from barley (ALH1), pulegenone reductase (PulR) from peppermint and P1-ζ-crystallin (P1ζCr) from *Arabidopsis thaliana* are supposed to belong to LTD family. Quinone reductase from strawberry (FaQR) and 2-haloacrylate reductase from *Burkholderia* sp. WS are supposed to belong to QOR family. The conserved NADPH binding motif AXXGXXG is highlighted in green. In FaQR the first residue (Ala) in this motif is replaced by Gly. Wedges are indicating where residues (Cys, His and Cys respectively) for binding the catalytic zinc atom were supposed to be but they are absent in these two subfamilies of MDR superfamily. The alignment was generated using the MUSLE web server software.

Lastly, an en-reductase from the soil bacterium *Burkholderia* sp. WS was inducibly synthesized when the cells were grown on 2-chloroacrylate.[384] The purified protein catalyzed the reduction of chloro- and bromo-acrylates to the corresponding (*S*)-halo acids and thus it was named 2-haloacrylate reductase. It is unknown if the quinone oxirdoreductase from *E. coli* with which the 2-haloacrylate shares a significant sequence similarity (38.2% identity) also possesses en-reductase activity; however, the reductase from *Burkholderia* sp. did not act on quinones.

In contrast to what is common for other oxidoreductases belonging to MDR superfamily, all the aforementioned en-reductases are metal independent and lack bound Zn^{+2}. (Figure 4-39).[345] The central cofactor-binding domain contains the characteristic *βαβαβ* Rossman fold. In the highly conversed, in this fold, Gly-X-Gly-X-X-Gly (where X any amino acid) motif found in this fold, the first Gly has been replaced by an Ala in all but FaQR reductase, whereas a single residue insertion (i.e. Ala or Gly for FaQR) is apparent in all sequences (Figure 4-39).[385] Thus, a nucleotide binding motif G/A-XX-G-XX-G is better description for this family of MDRs (Figure 4-40).[386]

Table 4-6. En-Reductases in MDR superfamily.

Year (Ref)	**Organism**	**Protein(Swiss-Prot accession no.)**	**Gene**
Substrates		Inhibitors	
1993 (370)	***Sus scrofa* (pig)**	**NADP-dependent leukotriene B4 12-hydroxydehydrogenase, 15-oxoprostaglandin 13-reductase, (Q29073)**	**LTB4DH**
1996 (371)	***Homo sapiens* (human)**	**NADP-dependent leukotriene B4 12-hydroxydehydrogenase, (Q14914)**	**LTB4DH**
2001 (387)	***Cavia porcellus* (guinea pig)**	**NADP-dependent leukotriene B4 12-hydroxydehydrogenase, (Q9EQZ5)**	**LTB4DH**
2001 (375)	***Rattus novergicus* (rat)**	**Alkenal/one Oxidoreductase, (P97584)**	**Ltb4dh**

Table 4-6. Continued.

Year (Ref)	**Organism**	**Protein (Swiss-Prot accession no.)**	**Gene**
Substrates			Inhibitors
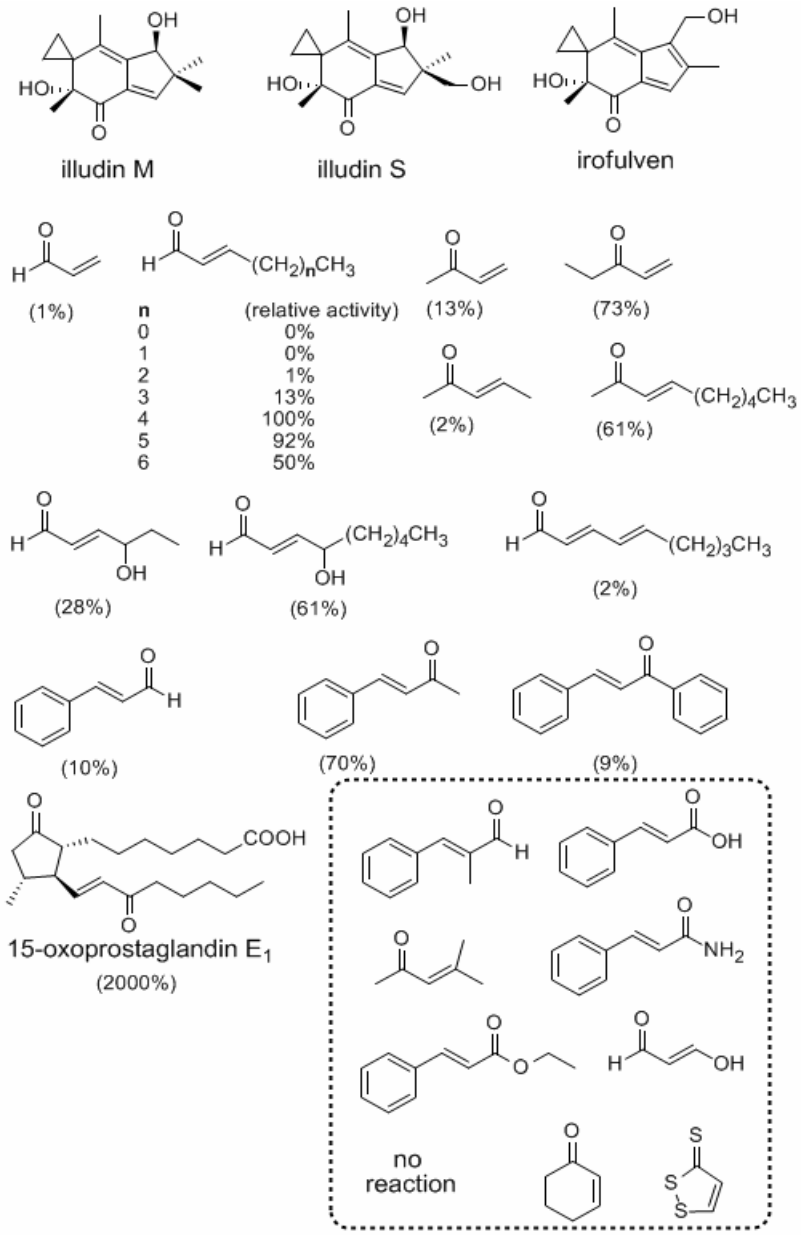			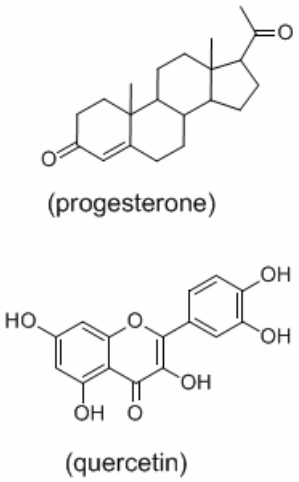
2003 (382)	***Mentha x Piperita* L. cv. Black Mitcham**	**(+)-pulegenone reductase (Q6WAU0)**	**AY300163**
			

Table 4-6. Continued.

Year	Organism	Protein (Swiss-Prot accession no.)	Gene
Substrates			
2000 (379, 381)	***Arabidopsis thaliana***	**P1-ζ-crystallin (Q39172)**	***P1* (At5g16970)**
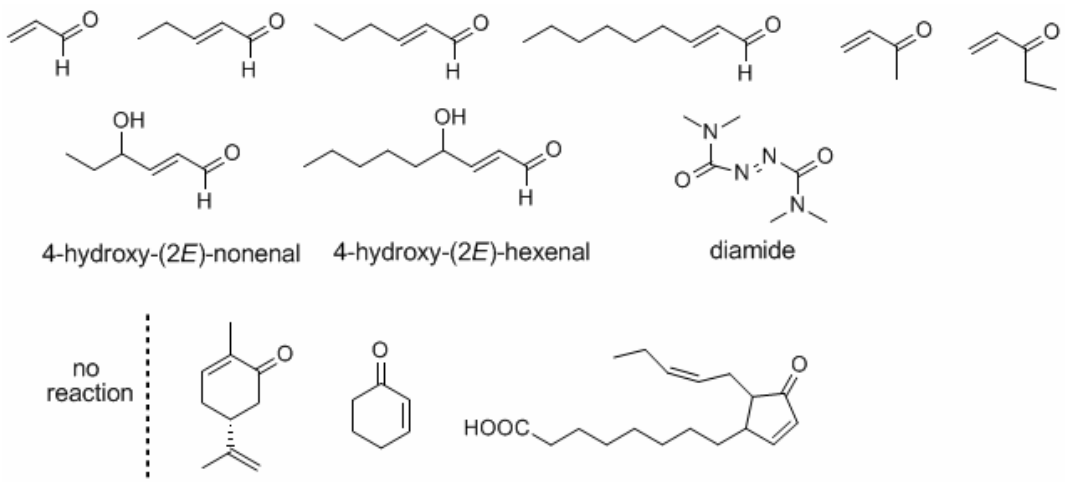			
2005 (380)	***Hordeum vulgare* cv. (barley), alkenal hydrogenase**	**alkenal hydrogenase, ALH1 (Q2KM86)**	***ALH***
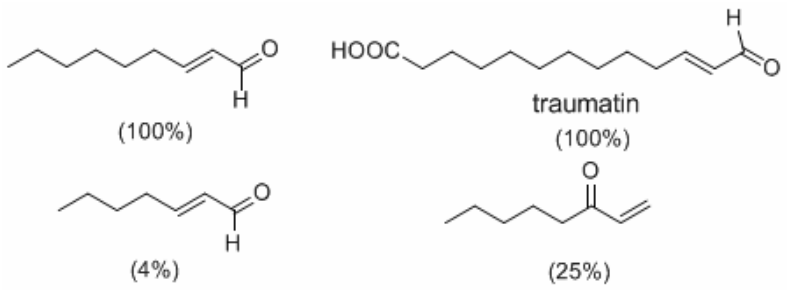			
2006 (385)	***Fragaria x ananassa* (strawberry)**	***Fragaria x ananassa* quinone oxidoreductase (Q84V25)**	***QR***
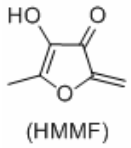			
2005 (384)	***Burkholderia* sp. WS**	**2-haloacrylate reductase (Q59I44)**	***caa43***
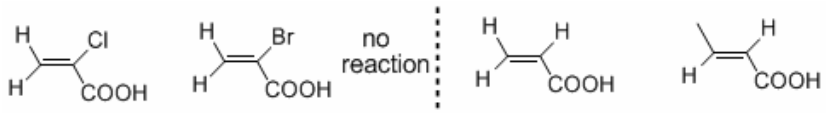			

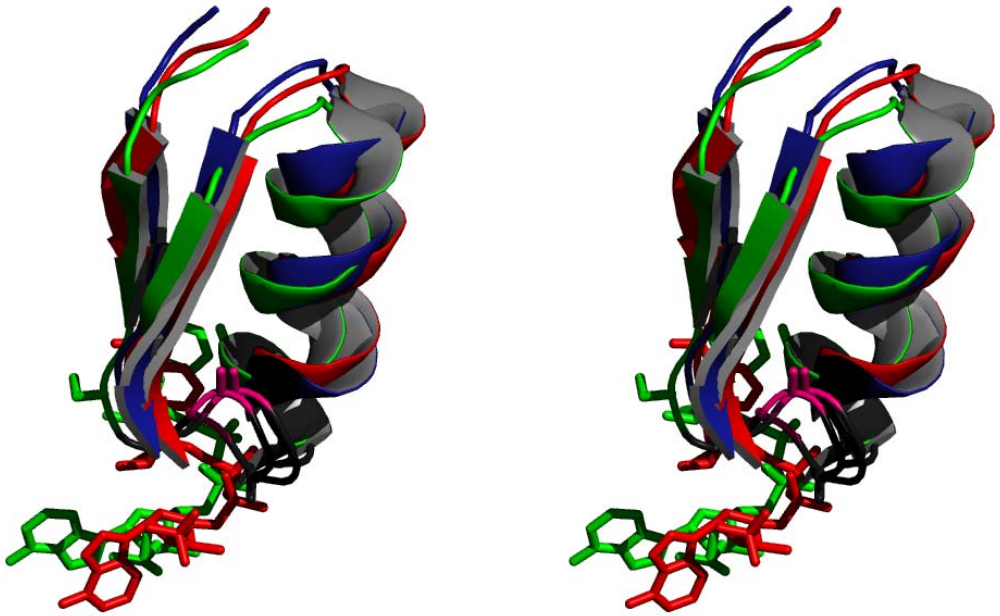

Figure 4-40. Superposition of two en-reductase structures belonging to the MDR superfamily (green for LTB_4DH from puinea pig; 1V3V, blue for 2-haloacrylate reductase;1WLY) with quinone oxidoreductase from *E. coli* (1QOR, red). Only the *βαβ* nucleotide binding motif is shown. Black loops, at the bottom, are part of the AAXGXXG motif, whereas the second inserted Ala residue is colored in magenta. The nicotinamide cofactor is shown only for QOR (red) and LTB_4DH (green). The Figure was rendered in PyMOL.

Short Chain Dehydrogenases Possessing En-Reductase Activity

The Croteau laboratory's long efforts to understand monoterpenes metabolism in plants lead to the isolation of (-)-isopiperitone reductase (IspR) from peppermint[382] (Table 4-7). A BLAST sequence analysis and identification of conserved motifs placed IspR in the short chain dehydrogenase/reductase superfamily (Figure 4-41). More interesting was the finding that the human carbonyl reductase (CR), a classical short chain dehydrogenase, showed 33% identity with the reductase from peppermint. Indeed, a year later the first experimental evidence for the dual action of CR on the same substrate (Table 4-7) would be published by Doorn et al.[388] Previous work had demonstrated that this ubiquitous in nature enzyme catalyzes the NADPH-dependent reduction of many endogenous and xenobiotic carbonyl compounds and quinones.[389] Its action on carbon-carbon double bonds has been explored so far only for 4-oxonon-2-

enal (4ONE). It was found that the two carbonyl groups are prerequisite for the enone/al activity of human CR. If the one of the two carbonyl groups is reduced first, by the same enzyme, the obtained product is no longer a substrate for CR. Molecular modeling of 4ONE in porcine CR active site revealed no specific or consistent contacts between the enzyme and substrate suggesting conformational freedom in the binding of 4ONE.[388]

Table 4-7. En-Reductases in SDR superfamily.

Year	**Organism**	**Protein**	**Gene**
Substrates			
2004 (388)	***Homo sapiens***	**Human carbonyl reductase (P16152)**	**CBR1**
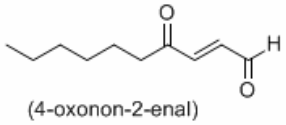 (4-oxonon-2-enal)			
2003 (382)	***Mentha x Piperita* L. cv. Black Mitcham,**	**(-)-isopiperitenone reductase (Q6WAU1)**	**AY300162**
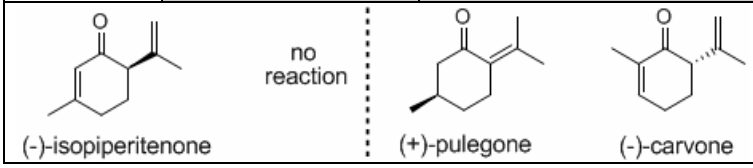 (-)-isopiperitenone; no reaction; (+)-pulegone; (-)-carvone			

CR and IspR possess classic characteristics of the SDR superfamily NAD(P)H binding motif Gly-XXX-Gly-X-Gly (Figure 4-41).[390, 391] On the other hand, in the catalytic motif Tyr-XXX-Lys, the Tyr residue has been replaced by Glu in the case of IspR. A Tyr residue at this position has been shown to participate in catalysis by making a critical hydrogen bond with the carbonyl group (Figure 4-42).[392]

Unclassified En-Reductases

The last decade, at least eight 'novel' en-reductases have been isolated from different organisms unfortunately with no amino acid sequence information. Half of these enzymes have been purified from bakers' yeast and their substrate specificities are listed in Table 4-8. Only the purification protocols for the two enone reductases EI and EII, have been reported in detail.[393]

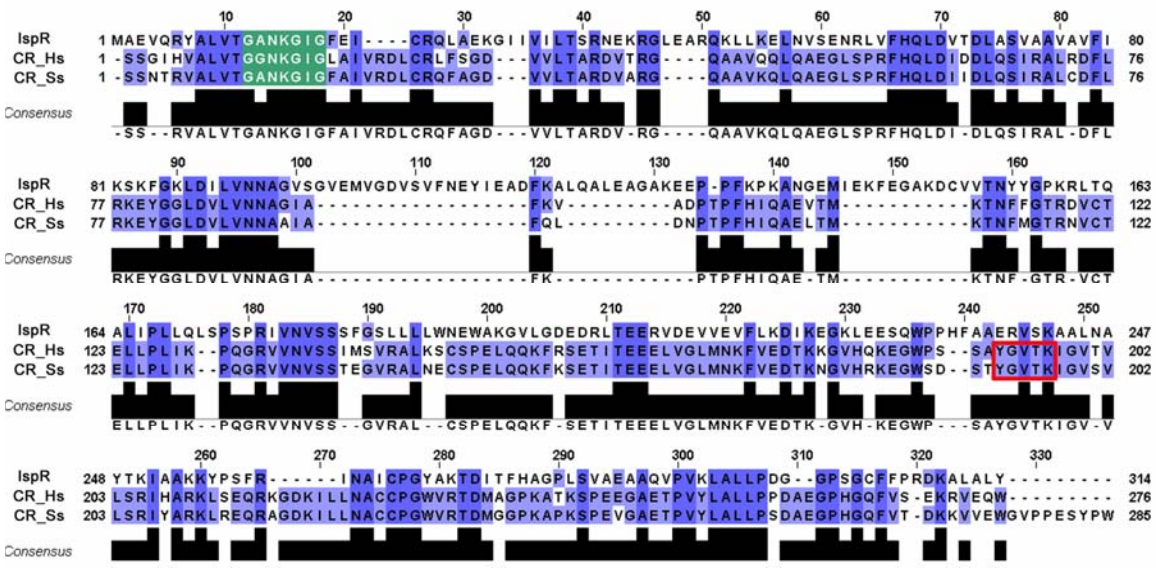

Figure 4-41. Multiple alignment of the two known short chain en-reductases (isopiperitenone reductase, IspR; and human carbonyl reductase, CR_Hs) with the porcine CR (CR_Ss) The conserved NAD(P)H binding motif GXXXGXG is highlighted in green. Within the red frame the catalytic motif YXXK. The alignment was generated using the Muscle web server software.

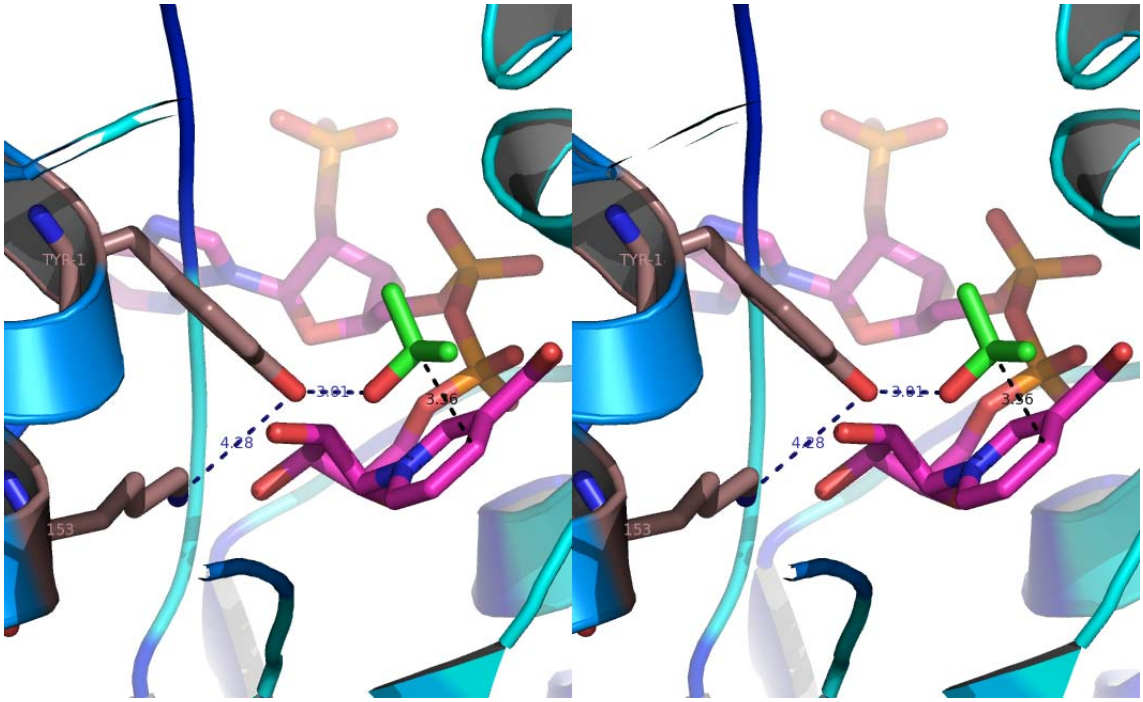

Figure 4-42. Stereoview of the catalytic active site of porcine carbonyl reductase (1CYD) with the nicotinamide cofactor in magenta and isopropanol in green. The key for the catalysis residues Tyr and Lys are colored in purple.

Both the EI and EII reductases have the same substrate specificities but possess very distinct biophysical properties. EI was found to be an NADPH-dependent heterodimer which was decomposed under denaturing electrophoresis into two subunits of 34 kDa and 37 kDa. The second enzyme, EII, was also decomposed into two subunits of 56 kDa and 64 kDa but it was NADH-dependent. Both enzymes showed high enantioselectivity towards the reduction of *cis* and *trans*-phenyl-2-butenal, producing (*R*)-2-phenylbutanal in >97% *ee*.

Interestingly the three en-reductases isolated from *Nicotiana tabacum* show divergent substrate specificities (Table 4-8).[394] The 44 kDa reductase (p44) is only reduces α-substituted cyclohexenones to corresponding (*R*)-ketones, while the reduction of β-alkylated–enones by the 90 kDa reductase (p90) affords (*S*)-ketones. In contrast, the 74 kDa reductase (p74) was found to reduce only exocyclic double bonds. Unfortunately, even though detailed purification protocols have been reported for the abovementioned enzymes, their complete amino acid sequences have not been revealed. In case of the p74 reductase, the sequence of a small stretch of amino acids produced after digestion of p74 with lysylendopeptidase showed significant similarity with the isovaleryl-CoA dehydrogenase from potato that has desaturase activity and with other putative homologs in *Arabidopsis thaliana*.[395]

Lastly, the three en-reductases isolated from the protozoa in genus *Euglena*, showed narrow substrate specificity with strongest preference for α-substituted cyclohexenones.

Table 4-8. List of unclassified en-reductases.

Year (Ref.)	**Organism**	**Protein**	**M_r**
Substrates			
1998 (393)	**Bakers' yeast**	**EI**	**34 kDa and 37 kDa**
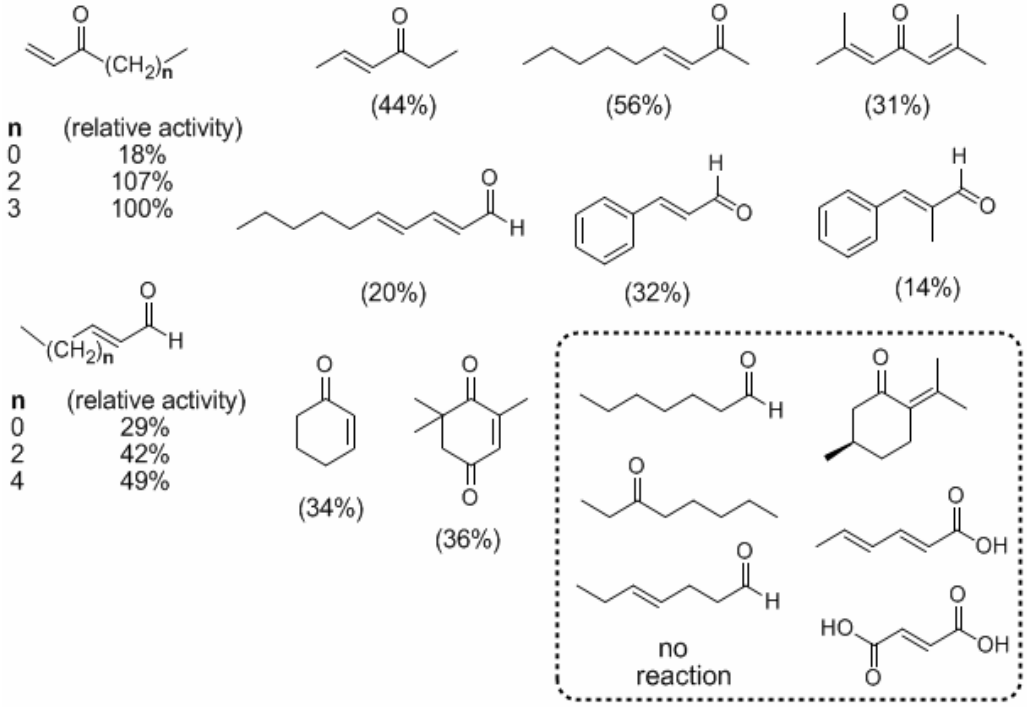			
1998 (393)	**Bakers' yeast**	**EII**	**56kDa and 64 kDa**
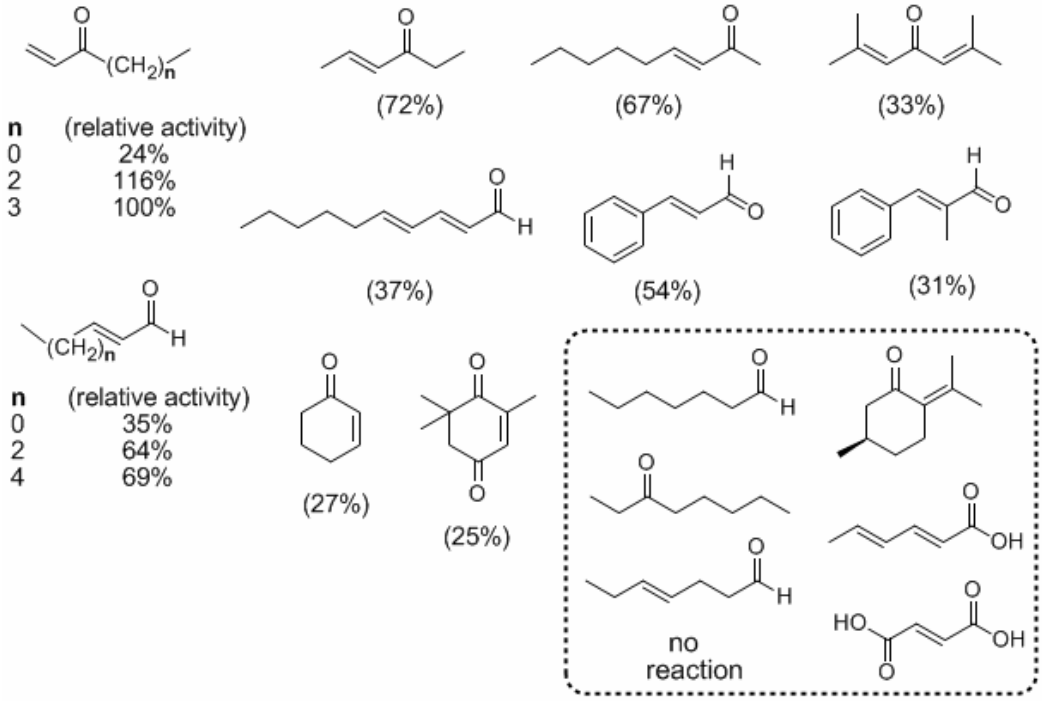			

Table 4-8. Continued.

Year	Organism	Protein	M_r
Substrates			
1998 (396)	**Bakers' yeast**	**Carbon-carbon double bond reductase**	**unknown**
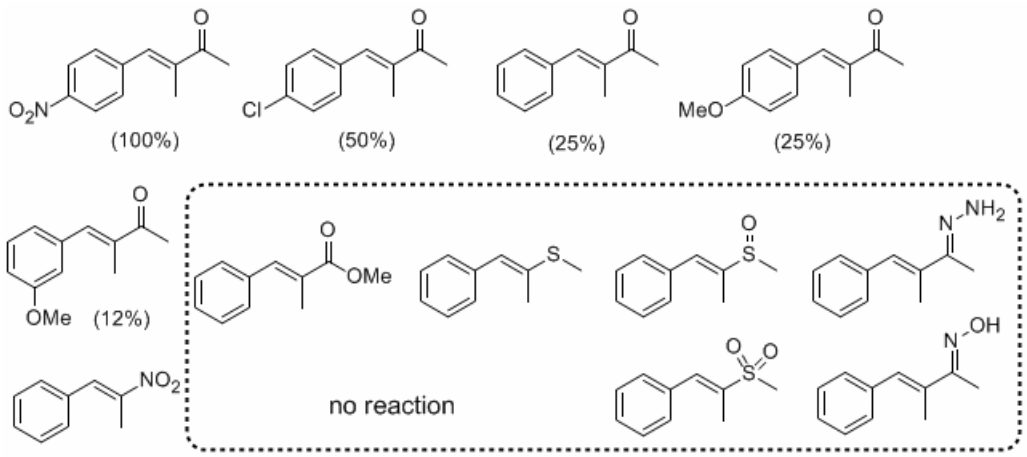			
2001 (397)	**Bakers' yeast, Nitroalkene reductases**	**Nitroalkene reductases: YNAR-I, YNAR-II,**	**unknown**
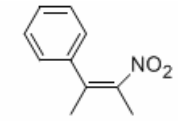 (Z)-3-phenyl-2-nitro-2-butene			
1996 (398)	***Nicotiana tabacum***	**verbenone reductase (p90)**	**90 kDa (2 subunits)**
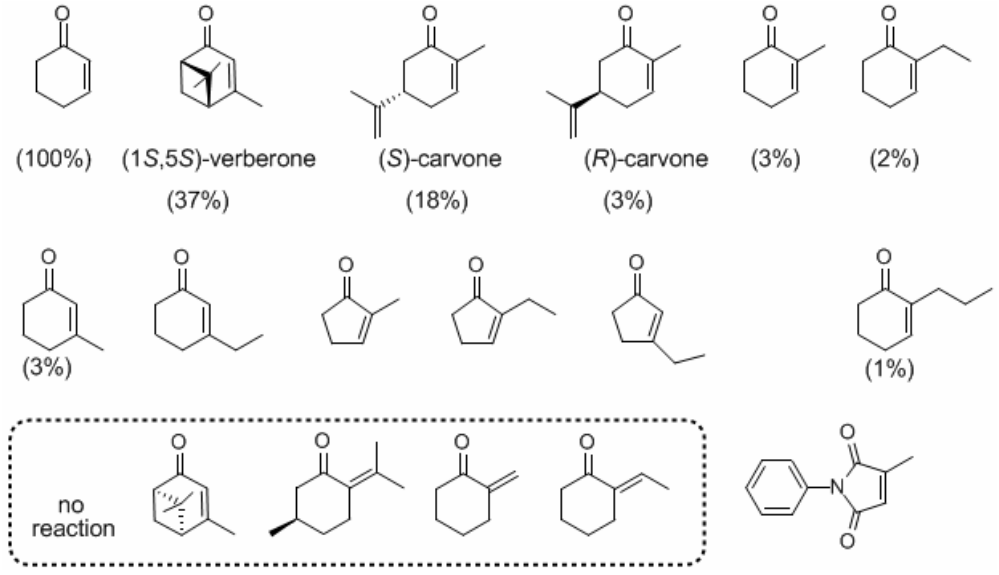			

Table 4-8. Continued.

Year	Organism	Protein	M_r
Substrates			
1989 (399)	***Nicotiana tabacum***	**carvone reductase (p44)**	**44 kDa (2 subunits)**
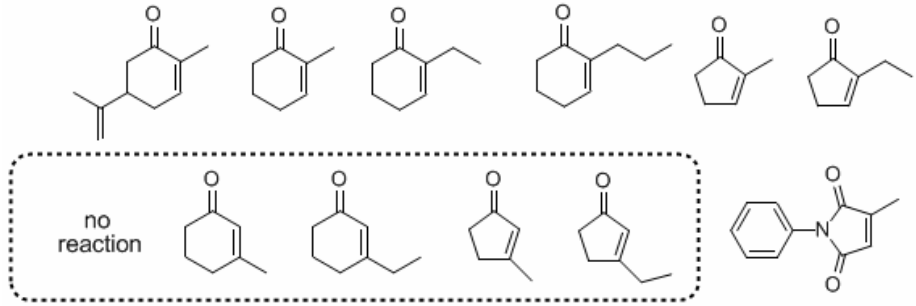			
2002 (395)	***Nicotiana tabacum***	**pulegone reductase (p74)**	**74 kDa (2 subunits)**
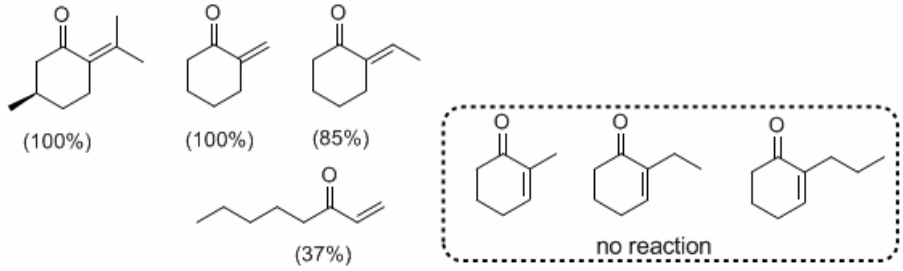			
1998 (400)	***Euglena gracilis***	**enone reductase**	**55 kDa**
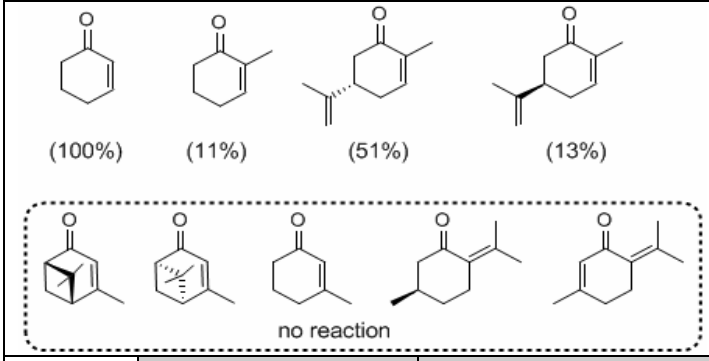			
2000 (401)	***Astasia longa***	**Reductase-I, Reductase-II**	**35 kDa, 36 kDa**
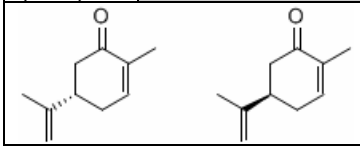			

Cofactor Specificity of En-Reductases

The cofactor specificity of the en-reductases presented in the previous sections is listed in Table 23. En-reductases belonging to the Old Yellow Enzyme family are A-type

enzymes and possess more or less stronger preference for the NADPH instead of NADH cofactor with only exception being the morphinone reductase (MorR) which is a NADH-dependent enzyme. In contrast, enoate reductases are B-type, NADH-dependent enzymes. For the non-flavin containing enzymes, experimental data exist only for the alkenal/one oxidoreductase, which is an A-type enzyme and the human carbonyl reductase, which is a B-type enzyme.

Table 4-9. Cofactor specificity of En-Reductases.

Entry	Enzyme	NADPH	NADH	Stereospecificity
1	OYE1	Yes (strongly preferred)	Yes	A (pro-R)
2	OYE2	Yes (preferred)	Yes	---[c]
3	OYE3	Yes (preferred)	Yes	---
4	EBP1	Yes	nd	---
5	N-Ethylmaleimide Reductase of *Y.lipolytica*	Yes	nd	A (pro-R)
6	oye	Yes	Yes	---
7	MorB	No	Yes	---
8	NemA	Yes (slightly preferred)	Yes	---
9	PB2 PETN reductase	Yes (strongly preferred)	Yes	A (pro-R)
10	Type strain PETN reductase	Yes (slightly preferred)	Yes	---
11	Glycerol trinitrate reductase	---	Yes	---
12	2-cyclohexen-1-one reductase	Yes (preferred)	Yes	---
13	YqjM	Yes (slightly preferred)	Yes	---
14	SYE1	Yes	Yes (preferred)	---
15	SYE3	Yes (preferred)[a]	Yes (preferred)[b]	---
16	SYE4	Yes (preferred)	Yes	---
17	enoate reductase	No	Yes	B (pro-S)
18	Alkenal/one oixidoreductase	Yes	No	A (pro-R)

Table 4-9. Continued.

Entry	Enzyme	NADPH	NADH	Stereospecificity
19	FaQR	Yes	Yes	---
20	P1-ζ-crystallin	Yes (strongly preferred)	Yes	---
21	2-haloacrylate Reductase	Yes	No	---
22	(+)-pulegenone reductase	Yes	No	---
23	(-)-isopiperitenone reductase	Yes (preferred)	Yes	---
24	Carbonyl Reductase	Yes (strongly preferred)	Yes	B (pro-S)
25	YNAR-I	Yes (preferred)	Yes	---
26	YNAR-II	Yes (preferred)	Yes	---
27	EI	Yes	No	---
28	EII	No	Yes	---
29	Enone reductase	No	Yes	A (pro-R)
30	Pulegone reductase	Yes (preferred)	Yes	---
31	Verbenone reductase	Yes (strongly preferred)	Yes	B (pro-S)
32	Reductase-I	Yes	Yes (preferred)	A (pro-R)
33	Reductase-II	Yes	Yes	B (pro-S)

[a] Preferred with oxygen as substrate. [b] Preferred with NEM as substrate. [c] not determined.

Concluding Remarks

Where should we look for en-reductases useful in biocatalysis? In an attempt to answer the above question in this chapter, it became apparent that with the exception of enzymes belonging to enoate reductase family, no serious efforts have been made towards the utilization of en-reductases from other families in the field of biocatalysis. Unfortunately, functional heterologous ERs could not be easily produced in *E. coli*, therefore problems related to overexpression and stabilization of these biocatalysts should be first solved before we envision their use in preparative scale biotransformations. On the other hand, more than 30 isoenzymes form the OYE family have been successfully overexpressed in *E. coli* but a systematic study regarding their substrate specificity is missing.

Also, the characterization of flavin-free en-reductases is still in its infancy. A sequence similarity search in databases returns a large number of proteins in this category, albeit with unknown function. It would be interesting to learn if those enzymes could act as reductases, as well as if there are any specific features that discriminate them from the alcohol dehydrogenases and/or the quinone reductases. Also, the possibility that the 'orphan' en-reductases may belong to any of the abovementioned families or they may uncover new en-reductase families remains open.

To this end, we will present in the next chapter our efforts in answering the above questions as well as a comparative substrate specificity study among different en-reductase subfamilies.

CHAPTER 5
IN VIVO RECOMBINATIONAL CLONING OF OLD AND NEW EN-REDUCTASES: A COMPARATIVE SUBSTRATE SPECIFICITY STUDY

> By three methods we may learn wisdom: first, by reflection, which is the noblest; second by imitation, which is the easiest; and third, by experience, which is the most bitter.
>
> -Confucius Quotes, Confucius[402]

Introduction

Several studies have shown that the ‘’burning issue’’ in the field of biocatalysis is the lack of a broad enzyme platform.[403] Difficulties identifying the most appropriate biocatalyst for a particular biotransformation, in a short time-frame, usually render the bio-based technology a second choice in the manufacturing of pharmaceutical intermediates. The traditional approach to solving this problem is the perpetual screening of strain collections in hopes of identifying a suitable enzyme for the desired transformation. Unfortunately, this method is time consuming and unable to cover the estimated 99% of the ‘’unculturable’’ microorganisms. Alternatively, different strategies (Figure 5-1) have been developed the recent years in an effort to create the desired diversity *in vitro*, by means of directed evolution,[404] or to gain access to the existed biodiversity. In the latter case, the metagenome approach and the sequence-based strategy have been recognized.[405] While in the former, the entire genomic DNA from soil samples must be cloned and expressed in a heterologous host such as *E. coli*, in the sequence-based approach, only a small number of protein sequences are required to act as baits for mining novel biocatalysts from the constantly increasing whole genome sequence databases.

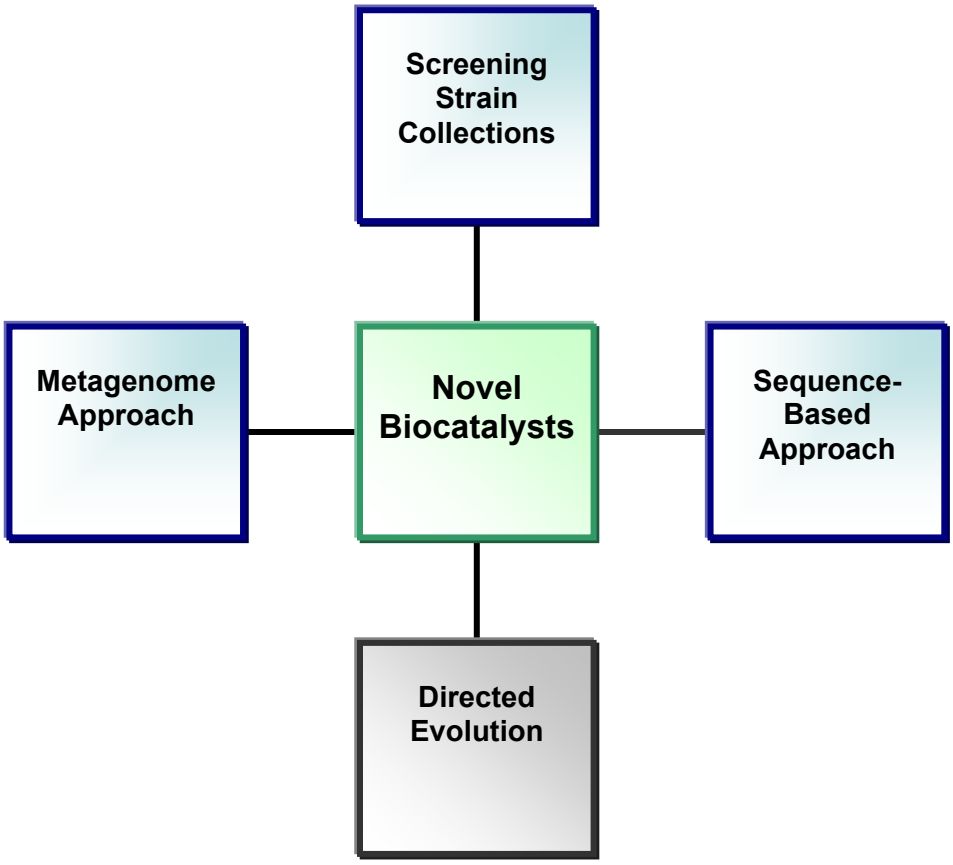

Figure 5-1. Different approaches towards the identification of novel biocatalysts.

The concept of the sequence-based discovery for biocatalysis was beautifully demonstrated by Stewart and coworkers using the bakers' yeast genome database for mining putative ketone reductases. Sequence similarity searches using a small number of known reductases as probes revealed the presence of ca. 50 putative ketone reductases in the *S. cerevisiae* genome. Eighteen out of twenty two selected were successfully cloned and overproduced in *E. coli* as glutathione S-transferase fusion proteins. A small scale screening of this collection towards various β-keto esters not only uncovered biocatalysts with distinct and in some cases opposing stereopreferences but also provide the basis for the production of synthetically useful building blocks in gram scale quantities. The powerful features of this methodology were immediately

recognized by other research groups, which applied the same concept in order to build libraries of: i) ketoreductases from modular polyketide synthases,[406] ii) epoxide hydrolases from bacteria[407] and iii) Bayer-Villiger monooxygenases from *Mycobacterium tuberculosis* H37Rv.[408]

In this work, the abovementioned principle was applied in an expanded and improved form for the construction and evaluation of a collection of fifteen known and putative alkene reductases.

Experimental Strategy

Our experimental strategy is schematically depicted in Figure 5-2 and each step will be described more completely below.

Selection of Alkene Reductases Clones

Our first concern in selecting the alkene reductases genes was to include the highest possible diversity based on two constraints: i) the availability of the genomic DNA from which the desired gene will be amplified and ii) the available time for completion of the project.

Our analysis of the different alkene reductases families, in the previous chapter, indicated that the Old Yellow Enzyme family is the wealthiest source of putative alkene reductases. We used the well-studied OYE1 from *Saccharomyces carlsbergensis* as a probe in order to select OYEs from other yeasts, as well as from bacteria and plants (Table 5-1). All of our plant targets have been overexpressed before in *E. coli*, but their substrate specificities are the least studied. From bacteria, only NemA has been studied before and we felt that we should include this particular enzyme in our list since it is derived from a host that we routinely use to overexpress the rest of biocatalysts. Among the OYEs from fungi, the catalytic activities of OYEA and OYEB from *Schizosaccharomyces pombe* has not been tested before. Nonetheless the percent identity among the selected OYEs spans from 91 to 28 percent (Table 5-2).

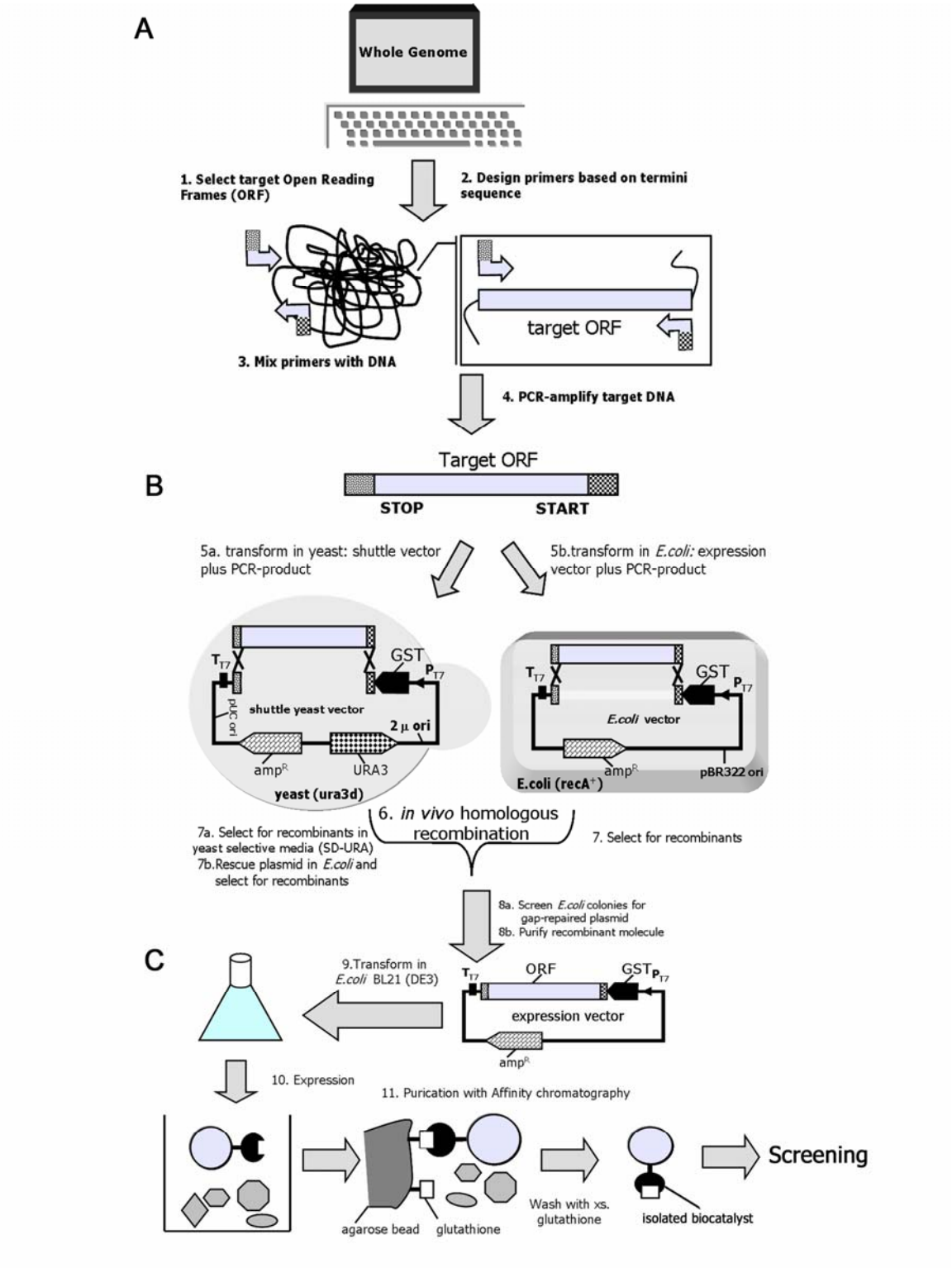

Figure 5-2. Construction of the alkene reductase library. A. Selection of target genes. B. *In vivo* recombinational cloning. C. Overexpression and purification of GST-En-Reductases.

Table 5-1. List of alkene reductases cloned in this study.

Entry	Organism	Gene (GI)	Protein (Swiss Prot. Acc. #)	Purified before? (mg/L)[a]
1	*Saccharomyces carlsbergensis* or *Saccharomyces pastorianus*	OYE1 (4092)	OYE1 (Q02899)	Yes (32)
2	*S. cerevisiae*	YHR179W (172029)	OYE2 (Q03558)	Yes (24)
3	*S. cerevisiae*	YPL171C (460038)	OYE3 (P41816)	Yes (48)
4	*Candida macedoniensis* or *Kluyveromyces marxianus* or *Candida kefyr*	oye (49387279)	Oye (Q6I7B7)	Yes (36)
5	*Schizosaccharomyces pombe*	SPAC5H10.04 (854599)	OYEA (Q09670)	No (12)
6	*S. pombe*	SPAC5H10.10 (854599)	OYEB (Q09671)	No (48)
7	*E. coli* BL21(DE3)	nemA (1711243)	NemA (P77258)	Yes (44)
8	*Pseudomonas Putida* KT2440	PP2486 (24987239)	ppOYE (Q88K07)	No (48)
9	*P. putida* KT2440	nemA (24987239)	ppNEMA (Q88I29)	No (22)
10	*Synechococcus elongatus* PCC 7942	Synpcc7942_0473 (81167692)	SeOYE (Q31R14)	No (60)
11	*Arabidopsis thaliana*	At1g76680 (2765082)	OPR1 (Q8LAH7)	Yes (32)
12	*Arabidopsis thaliana*	At1g76690 (26450548)	OPR2 (Q8GYB8)	Yes (0)
13	*Arabidopsis thaliana*	At2g06050 (5059114)	OPR3 (Q9FUP0)	Yes (34)
14	*Lycopersicon esculentum* (tomato)	OPR1 (4894181)	Leopr (Q9XG54)	Yes (48)
15	*Rattus norvegicus* (rat)	Ltb4dh (6012070)	Ltb4dh (P97584)	Yes (14)
16	*S. cerevisiae*	YNL134C (45269933)	YNL134c (P53912)	No[b] (30)

[a] Amount of protein obtained in this study. [b] The protein has been cloned and overexpressed in *E. coli* and tested for its catalytic activity as a crude extract.

Table 5-2. Percent identity in between OYEs cloned in this study.

Ind. (%)[a]	OYE1	OYE2	OYE3	oye	OYEA	OYEB	NemA	ppNemA	ppOYE	SeOYE	OPR1	OPR2	OPR3	Leopr
OYE1	100	91	80	69	36	35	37	34	33	41	35	36	37	37
OYE2	91	100	81	71	37	36	37	35	35	40	31	36	38	38
OYE3	80	81	100	68	37	36	39	37	34	41	37	38	36	39
Oye	69	71	68	100	37	35	38	36	34	38	34	35	35	37
OYEA	36	37	37	37	100	57	32	32	30	36	35	37	35	38
OYEB	35	36	36	35	57	100	30	31	28	36	35	34	34	36
NemA	37	37	39	38	32	30	100	69	46	49	41	43	37	42
PpNEMA	34	35	37	36	32	31	69	100	44	50	39	41	38	42
PpOYE	33	35	34	34	30	28	46	44	100	47	38	38	35	39
SeOYE	41	40	41	38	36	36	49	50	47	100	45	49	44	49
OPR1	35	31	37	34	35	35	41	39	38	45	100	84	47	68
OPR2	36	36	38	35	37	34	43	41	38	49	84	100	51	72
OPR3	37	38	36	35	35	34	37	38	35	44	47	51	100	50
Leopr	37	38	39	37	38	36	42	42	39	49	68	72	50	100

[a]The different OYE family subgroups: fungi, bacteria and plants are highlighted with yellow, blue and green respectively.

From the medium-chain reductase family, we selected the well-studied Ltb4dh from rat mainly because the cDNA was commercially available. In addition, its demonstrated broad substrate specificity, its enantioselectivity towards prochiral substrates had never been explored. Members from the short chain reductase family were not included in this collection. The reported sensitivity of the enoate reductases to oxygen as well as their poor expression in *E. coli* discouraged our including this family in collection.

We also made an effort to answer the following question: Besides the two known alkene reductases, namely OYE2 and OYE3 characterized in Massey's laboratory, do other genes in the bakers' yeast genome encode proteins responsible for reducing activated alkenes? Based on our discussion in the last part of chapter 4, four out of eight reported 'orphan' alkene reductases have been purified from this microorganism. We decided to repeat the purification protocol for the EI and EII enone reductases described by Wanner and Tressl in 1998, for following reasons:

- Both the EI and EII reductases showed broad substrate specificity, albeit similar to one another and to OYE1.
- this is the only report for which detailed experimental protocol is given and the published SDS-PAGE analysis is clearly shown that these two enzymes have different molecular weights from the OYE2 or OYE3.
- it is intriguing that even though this report was published three years after Massey's characterization of OYE2 and two years after the release of the *S. cerevisiae* genome, the authors neither commented about the existence of the OYE2 and its catalytic activity towards enones nor explained why they did not determine the N-terminal amino acid sequence of their isolated proteins.

Cloning and Expression of Alkene-Reductases

The methodology for constructing of the yeast GST-reductase library by Kaluzna et al.[409] was inspired by the seminal work of Phizicky and coworkers.[410] In the latter, a genomic library of yeast strains expressing GST-ORF fusion proteins was constructed and used to link enzymatic activity to gene function. Their approach was rapid and sensitive mainly because:

- cloning and overexpression of the whole proteome were achieved in same host (i.e. yeast) and in a single step, taking advantage of the very efficient recombinational machinery of *S. cerevisiae*.
- detection of 10^{-17} moles of product from a substrate with a single ^{32}P-label was achieved with an enzyme concentration as little as 0.02 μM
- side-reactions, by-products and catalysts' inactivation or degradation were minimized due to the fact that contaminant proteins were eliminated during the protein affinity-chromatography purification step introduced before the screening of the yeast lysate.

Since 1999 numerous improvements have been introduced to the original protocol;[411, 412] however, whenever we attempt to implement biochemical and enzyme genomic approaches in the field of biocatalysis we should always keep in mind that:

- we are looking for enzymes capable of successfully transforming nonnatural substrates, which usually means lower turnover numbers and the requirement of higher amounts of protein, typically in a range of 0.5-5 μM
- most of the compounds for which an organic chemist may show an interest do not possess a radio-labeled atom or a chromophore. As a consequence, higher amounts are required for their detection, typically in a range of 1-5x10^{-6} moles for 1 ml scale biotransformations.

Driven by the need to produce sufficient amounts of yeast reductases, Stewart and co-workers had to switch to *E. coli* overproduction. Although the fusion protein library approach permits the rapid purification and screening of a number of biocatalysts, it suffers in terms of the time required to clone the target genes into the appropriate bacterial expression vector. In order to break the cloning bottleneck step, we introduced a one step recombination-mediated cloning method into our overall strategy. This modification allowed us, with appropriately designed primers, to PCR-amplify and fuse the target cassettes to the C-terminus of the GST-tag directly, thereby bypassing otherwise laborious sub-cloning steps. We evaluated two pathways: i) the well-established[413] yeast *in vivo* cloning via homologous recombination (HR) ii) and the RecA mediated *in vivo* recombination cloning in *E. coli*, which was introduced recently by Finley and co-workers.[414] Even though a number of kits are commercially available for *in vitro*, site specific HR cloning[415] the *in vivo* HR strategy is much cheaper and convenient

since no purchase of recombinase is required and any in-home modified vector could be used without the restrictions that the site-specific HR imposed.

Experimental Procedures

Purification of YNL134c

Preliminary efforts in YNL134c isolation were performed in collaboration with Erin Hanlin in our laboratory and started from commercially available bakers' yeast, as described by Tressl and Wanner. Our inability to reproduce the results obtained in the original published protocol lead us to the modified purification protocol described below.

All enzyme purification steps were carried out at 4 °C. Phenylmethylsulphonylfluoride (PMSF) and 2-mercaptoethanol were added to the standard buffer immediately before use. SDS-PAGE analyses were carried out according to Laemmli[416] and protein concentration was estimated by a Bradford assay using bovin serum albumin (BSA) as a protein standard.[417]

Materials and supplies

The yeast strain DAY128 (oye2Δ oye3Δ) used for protein isolation was generously provided by Dr. David Amberg. DEAE CL-6B was purchased from Sigma. Pre-packed HiLoad Q Sepharose, Mono Q anion exchange, Sephacryl S-300 Hi Prep 16/60 and fast desalting columns were all purchased from Pharmacia, Dyematrex Gel Blue A matrix was purchased from Millipore. Superdex 200 and Sephadex G-25 matrix were purchased from Pharmacia.

Enzyme activity assays

Enzyme activity was determined spectrophotometrically at 25 °C by following the decrease in absorbance of NAD(P)H at 340 nm. The standard assay mixture contained 0.2 mM NAD(P)H (10 µL of 20 mM stock solution prepared immediately before use in 0.1 mM KP_i, pH 7.0), 2.5 mM 1-octen-3-one (100 µL of 25 mM stock solution made in acetate buffer, pH 4.8 containing 0.1 % Triton X-100) and the appropriate amount of the

enzyme preparation in a final volume of 1 mL of acetate buffer pH 4.8. The above solution was passed through a 0.45-µm filter before being placed in a 1.00 cm cuvette. The background NAD(P)H oxidation was measured using an identical mixture in which the enone substrate was replaced by acetate buffer. One unit of enzyme activity was defined as the quantity sufficient to oxidize 1 µmol of NAD(P)H per minute in the mixture described above. Unit per mL of enzyme preparation were calculated based on the following equation:

$$Units/mL = dA/dt * 1000 / \in_{340} * l * V_{assay}/V_{enzyme} * Dilution$$, where dA/dt the slope in AU/min, ϵ^{340}= 6270 mol^{-1} L cm^{-1}, l=1 cm, V_{assay} = 1 mL, V_{enzyme} = volume of enzyme added in mL, Dilution= dilution factor.

Cell growth for protein isolation

Day128 cells were pre-cultured in double strength, non-selective yeast growth medium (2 x YPD: 20 g Bacto-Yeast Extract, 40 g Bacto-Peptone, 40 g Dextrose per liter) overnight at 30 °C and then diluted 1:100 into 500 mL of the same medium in eight 2 L baffled flasks. The cultures were grown at 30 °C for 24 h and the cell harvested by centrifugation (5000x g for 10 min at 4 °C) and stored at -20 °C.

Preparation of crude extract

Cells (53 g wet mass) were thawed, washed twice with three volumes of deionized water, resuspended in 200 ml Tris-HCl pH 7.5 containing 0.1 mM phenylmethylsulphonylfluoride (PMSF) and 5 mM 2-mercaptoethanol (standard buffer) and disrupted in a French pressure cell at 16,000 psi. The process was repeated twice. Debris was removed by ultracentrifugation at 70000x g (30,000 rpm, 45 Ti rotor) for 30 min and the pellet was discarded.

Streptomycin sulfate purification

Streptomycin sulfate solution was added to the clarified cell extract (5.7 mL of 25% solution) dropwise over 20 min. The protein solution was stirred for additional 2.5 h and the pellet collected by ultracentrifugation at 70000x g for 20 min was discarded. The supernatant was concentrated overnight by ultrafiltration using an Amicon ultrafiltration cell fitted with a PM-10 membrane under nitrogen at 20 psi.

Desalting by Sephadex G-25

The supernatant (~ 25 ml) was applied to a Sephadex G-25 column (40 cm x 3.5 cm) via a peristaltic pump at a rate of 1 ml/min equilibrated with standard buffer. The column was eluted with the same buffer at the same rate and 8 ml fractions were collected. All fractions bearing an absorbance at 280 nm >0.2 AU were pooled together and concentrated by ultrafiltration, as described above.

DEAE CL-6B anion exchange chromatography

The ultrafiltrate (~ 15 ml) was ultracentrifuged and applied to a DEAE CL-6B anion exchange column (18 cm x 3 cm) equilibrated with standard buffer. After the column was loaded and washed with 2 bed volumes of standard buffer, a NaCl gradient was applied from 0.0 to 0.5 M over 5 bed volumes. When the elution was completed, the column was further washed (1 bed volume) with the same buffer containing 0.5 M NaCl followed by 60 ml of standard buffer with 2 M NaCl. The proteins were eluted at a flow rate of 1 ml/min and fractions of 8 ml were collected. Fractions 31-38, having NADPH and NADH activity, were combined, concentrated to a final volume of 35 ml and dialyzed overnight against 4 L (2 x 2L) of standard buffer.

HiLoad Q sepharose anion exchange chromatography

The desalted protein solution was centrifuged as before and loaded on a 10 cm x 1.6 cm Q Sepharose anion exchange column using a Pharmacia FPLC system. After the column was loaded and washed with 2 bed volumes of standard buffer, a NaCl

gradient was applied from 0.0 to 0.5 M over five bed volumes. When the elution was completed, the column was further washed (1 bed volume) with the same buffer containing 0.5 M NaCl. The proteins were eluted at a flow rate of 1 ml/min and fractions of 5 ml were collected. Fractions 26-34, having NADPH and NADH activity, were combined, concentrated to a final volume of 12 ml and dialyzed overnight against 4 L (2 x 2L) of standard buffer.

Dyematrex gel blue A affinity chromatography

The desalted protein solution was loaded onto a Dyematrex gel blue A column (20 x 1.6 cm) at a flow rate of 0.3 ml/min. The elution was stopped for ~ 1.5 h in order to maximize interactions between the dye and the proteins. Then, the column was washed with 100 ml standard buffer until A_{280} of the eluant was ca. 0.2, and then it was eluted with 0.5 M NaCl in standard buffer at a flow rate of 0.5 ml/min. Fractions of 5 ml were collected. Fractions 6-12 (fraction FI), having NADPH and NADH activity, were combined, concentrated to a final volume of 10 ml and dialyzed overnight against 4 L (2 x 2L) of standard buffer. Fractions 22-28 (fraction FII), bearing absorbance at 280nm > 0.2 AU, were also collected, concentrated and desalted in the same manner. Both fractions, FI and FII, were further concentrated to a final volume of 1 ml.

Superdex 200 filtration chromatography

The fraction FI, from the previous step, was centrifuged and loaded onto a Superdex 200 filtration column (25 cm x 1.4 cm) at a flow rate of 0.5 ml/min equilibrated with 0.15 M NaCl in standard buffer. The proteins were eluted in the same buffer. Fractions of 2 ml were collected and NAD(P)H activity was found in fractions 5-8. The latter fractions were pooled together, dialyzed overnight against 2 L standard buffer, concentrated to final volume of 1 ml and desalted further using a Pharmacia fast desalting column. The desalted fractions were combined and concentrated to a final volume of 1 ml.

HiLoad Q Sepharose anion exchange chromatography

The desalted protein preparation from the previous step was loaded onto a Mono Q anion exchange column (5 cm x 0.5 cm) at a flow rate of 1 ml/ min. After the column was loaded and eluted with 10 ml of standard buffer, a 50 ml NaCl gradient was applied from 0.0 to 0.5 M NaCl in standard buffer. The column was further washed with 10 ml of 0.5 M NaCl in standard buffer. Fractions of 1 ml were collected and NAD(P)H activity was found in fractions 29-34. The latter fractions were combined and desalted as before.

Sephacryl S-300 Hi Prep filtration chromatography

The fraction from the previous step was concentrated to a final volume of 0.5 ml and was loaded onto a 60 cm x 1.6 cm Sephacryl S-300 Hi Prep filtration column at flow rate of 1 ml/min equilibrated with 0.15 M NaCl in standard buffer. The proteins were eluted in the same buffer. Fractions of 1 ml were collected and NAD(P)H activity was found in fractions 72-82. Fractions 74-78 were 10 fold concentrated individually with a centrifugal filter device (Microcon YM-3, 3,000 molecular weight cut off) before loading on a SDS-PAGE gel and submitted for LC-MS analysis.

Protein Sequencing

N-terminal sequencing and LC-MS analysis of the YNL134c were performed by the University of Florida-ICBR-Protein Core and sample preparation followed their recommended protocols. Protein digestion and LC-MS analysis was carried out by Dr. Scott McClung.

Cloning and Purification of GST-Alkene Reductases

Biochemicals, plasmids and strains

Restriction endonuclucleases were purchased from New England Biolabs or Fermentas. T4 DNA ligase, *Taq* and *Vent* polymerases were obtained from New England Biolabs. Glutathione uniflow resin was purchased fron Clontech. cDNA from

rat (normal tissue: liver) was obtained from BioChain. DNA from *Synechococcus elongatus* PCC 7942 and a cosmid containing the SeOYE gene were kindly provided by Dr Susan S. Golden.

E. coli expression vector pET22b(+) was obtained from Novagen. pET-OYE was a gift from V. Massey's laboratory. Yeast shuttle vector pYEX4T-1-Rec. DOM. was a gift from Dr M. Martzen. Plasmids, pIK1(-) and pIK2 were constructed by Dr Iwona Kaluzna in our laboratory. Clones cTOF30K9, cLEY12J2 and cTOD19I19 for amplification of Leopr gene were obtained from sol genomics network, Cornell University. Clones pda07378, pda10767 and pdx20368 for amplification of OPR1, OPR2 and OPR3 genes respectively, were purchased from RIKEN Tsukuba Institute.

S. cerevisiae strain, BY4742 used for homologous recombination and DNA isolation was a gift from Dr. Thomas Lyons. Strains *Kluyveromyces marxianus* (ATCC 200965), *Schizosaccharomyces pombe* (ATTC 16979) and *Pseudomonas pudida* (ATCC2440) used from DNA isolation were purchased from American Type Culture Collection. *E. coli* KC8 competent cells, used for homologous recombination, were purchased from Clontech.

Cloning of alkene reductases.

Recombinant DNA techniques were carried out as described by Maniatis et al.[418] DNA used as a template in PCR reactions, was isolated from different yeasts and bacteria as described elsewhere.[419] Genes were PCR-amplified using a Perkin-Elmer Geneamp PCR system 2400. Clone cTOD was used for amplification of Leopr gene (restriction analysis showed that cLEY clone contains only a part of the Leopr gene and DNA sequencing of cTOF clone revealed a single nucleotide deletion in the Leopr gene). When an amp^R plasmid was used as a template for PCR, linearization of the template-plasmid after PCR was found necessary for eliminating of false positives after the *in vivo* homologous recombination in *E. coli* KC8 strain. All PCR products and the linearized

universal vectors pDJB2(3) were purified by agarose gel electrophoresis prior to recombinational cloning. As a rule, ca. 150 ng of purified PCR product and linearized vector were used for the homologous recombination.

Routine *E. coli* transformations were performed by electroporation. Yeast transformations utilized the high efficiency LiAc/SS-DNA/PEG protocol.[420] *E. coli* KC8 chemically competent cells were transformed according to the manufacture's instructions or they were prepared using a PEG-DMSO protocol.[414] Yeast recombinants were plated on the appropriate selective media. Total yeast DNA was prepared and used to transform *E. coli* TOP10 cells in order to screen for recombinant molecules by restriction digestion analysis. *E. coli* KC8 recombinants were screened by colony-PCR.

Purified plasmid DNA for sequencing was obtained by density gradient ultracentrifugation with CsCl in presence of ethidium bromide.

Isolation of GST-fusion proteins

An overnight culture of the appropriate overexpression strain grown in LB medium containing 100 µg/ml amp.(40 µg/mL kan was used for GST-OYE1) was diluted 1 : 100 into 500 mL of the same medium in a 2 L baffled flask. The culture was shaken at 37°C until the optical density at 600 nm reached 0.5-1.0, then isopropylthio-β-D-galactoside (IPTG) was added to a final concentration of 100 µM and the culture was shaken for an additional 6 hours at room temperature. The cells were collected by centrifugation, washed twice with cold sterile water and then resuspended in 30 mL loading buffer (50 mM Tris-Cl, 4 mM $MgCl_2$, 1 mM DTT (added immediately before use), 1 mM PMSF (added immediately before use), 10% glycerol, pH 7.5). All purification steps were carried out at 4°C. The cells were lysed by passage through a French pressure cell and debris was removed by centrifugation at 15,000 x g for 20 min at 4°C. The supernatant was passed through a 0.45 µm filter and loaded rapidly onto a column containing 10 mL of glutathione-uniflow resin. The resin was thoroughly mixed with the lysate and then

allowed to settle in the column. The protein sample was continuously circulated through the column for 3-5 h via a peristaltic pump at a flow rate of ~0.5 ml/min. Then, the nonadsorbed lysate was drained and the resin was washed, without disturbing it, twice with 20ml of loading buffer. GST-fusion proteins were eluted with 40 ml of freshly prepared elution buffer (Loading buffer (39.6 ml), 0.40 ml NaOH (2 M) and solid reduced glutathione (0.31 g)). The eluant was concentrated and dialyzed overnight against 1 L of dialysis buffer (20 mM Tris-Cl, 4 mM $MgCl_2$, 55 mM NaCl, 2 mM EDTA, 1 mM DTT, 50% glycerol, pH 7.5) prior to storage at -20°C.

Regeneration of glutathione resin

The glutathione resin was regenerated by washing (3 x 200 mL) with regeneration buffer A (0.1 M Tris-Cl, 0.5 M NaCl, pH 8.5) and the same volume of regeneration buffer B (0.1 M Sodium acetate; 0.5 M NaCl, pH 4.5). After regeneration, the resin was equilibrated with loading buffer.

Screening of Alkene Reductases

Chemicals were purchased from Acros, Aldrich, Alpha Aesar or Lancaster and used without further purification.

Preparation of 6-alkyl-2-cyclohexen-1-ones

The methyl substituted cyclohexenones were prepared via tandem Michael addition-aldol condensation of the corresponding β-ketoesters to conjugated enals[421] (Table 5-3).

To a stirred solution of β-keto ester (7 mmol) and acrolein (7 mmol) in 7 ml of t-BuOH was added a catalytic amount of t-BuOK at 4 °C. The reaction mixture was stirred at that temperature for 30 min and then 1.75 mmol of t-BuOK were added and the mixture was held at for 20 h. After cooling to room temperature, the mixture was quenched with 10 ml of 1M HCl, diluted with a 1:1 mixture of ether and benzene (80 mL) washed with 1 M NaOH (20 mL x 3) and brine (20 mL x 2). The organic layer was dried

over magnesium sulfate and concentrated under reduced pressure. The crude 6-substituted 2-cyclohexenones were purified by flash column chromatography (SiO_2, 10-20 % ethyl acetate in hexanes). The yield did not exceed the 10-12% in any case.

Table 5-3. Starting materials for preparation of 6-substituted cyclohexenones.

β-ketoesters	enals	Product	Name
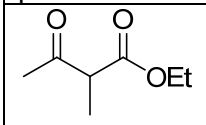	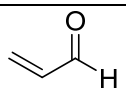	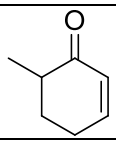	6-methyl-2-cyclohexenone
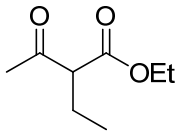	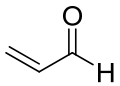	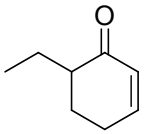	6-ethyl-2-cyclohexenone
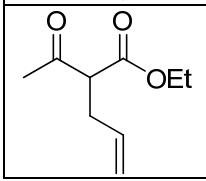	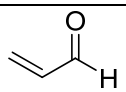	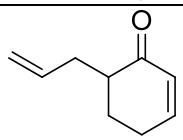	6-allyl-2-cyclohexenone

6-methyl-2-cyclohexenone ^{1}H NMR (300 MHz, $CDCl_3$) δ: 1.14, (td, 3H *J* = 6.9), 1.69-1.80, (m, 1H), 2.03-2.10 (m, 1H), 2.38-2.40 (m, 3H), 5.98 (td, 1H, *J* = 10.5), 6.89-6.95 (m, 1H).

6-ethyl-2-cyclohexenone ^{1}H NMR (300 MHz, $CDCl_3$) δ: 0.92 (t, 3H *J* = 7.5), 1,37-1,47 (m, 1H), 1.72-1.88 (m, 2H), 2.06-2.24 (m, 2H), 2.36-2.38 (m, 2H), 5.98 (td, *J* = 10. 2, 1H), 6.86-6.92 (m, 1H)

6-allyl-2-cyclohexenone ^{1}H NMR (300 MHz, $CDCl_3$) δ:1.22-1.26 (m, 1H), 1.71-.175 (m, 1H), 2.05-2.14 (m, 2H), 2.36-2.38 (m, 2H), 2.58-2.65 (m, 1H), 5.07 (t, *J* = 8.4, 2H), 5.73-5.82 (m, 1H), 6.00 (dd, *J* = 9.9, 1H) 6.90-6.95 (m, 1H).

Preparation of neral and geranial

Nerol or geraniol was oxidized to corresponding neral and citral with iodosobenzene diacetate (IBD) and catalytic amount of TEMPO.[422]

To a stirred solution of allylic alcohol (3.2 mmol) in 3 ml CH_3CN and 1 ml of 100 mM KP_i, pH 7.0 was added 3.6 mmol IBD and a catalytic amount of TEMPO (0.3 mmol)

at 0 °C. The reaction mixture was stirred at that temperature until alcohol was no longer detectable by GC-MS analysis (in 1-2h). The reaction mixture was diluted with diethyl ether (30 ml) and extracted with saturated aqueous sodium thiosulfate (3 x 30 ml). The aqueous phase was separated and extracted once with 40 ml of diethyl ether. The combined organic layers were washed with saturated aqueous sodium hydrogen carbonate (50 ml) and then with brine (50 ml). The organic layer was dried over magnesium sulfate and concentrated under reduced pressure. The crude product was purified by column chromatography starting with hexanes and finishing with 5% diethyl ether in hexanes. The yield was 50 % in case of neral and 25% in case of geranial. Traces (2-3 %) of the opposite alkene isomer were detected in both cases by GC analysis.

Neral ^{1}H NMR (300 MHz, $CDCl_3$) δ: 1.59 (s, 3H), 1.68 (s, 3H), 1.98 (d, 2H, *J* = 1.5 Hz), 2.20-2.27 (m, 1H), 2.58 (t, 2H, *J* = 6 Hz), 5.08-5.13 (m, 1H), 5.87 (d, *J* = 8.1 Hz, 1H), 9.90 (d, *J* = 8.1, 1H)

Geranial ^{1}H NMR (300 MHz, $CDCl_3$) δ: 1.61 (s, 3H), 1.69 (s, 3H), 2.17 (d, 2H, *J* = 1.3 Hz), 2.22 (m, 3H), 5.06 (m, 1H), 5.88 (td, 1H, *J* = 8.1), 10.0 (d, *J* = 7.2, 1H)

Biotransformations

A typical 1ml-scale biotransformations contained $NADP^+$ (0.20 μmoles), glucose-6-phosphate (14 μmoles),and glucose-6-phosphate dehydrogenase (5 μg) as an NADPH regeneration system, the appropriate amount of GST-En reductase (50-150 μg) and 5 μmoles of functionalized alkene in 100 mM KP_i, pH 7.0. Reaction mixtures were incubated at 30 °C and sampled, by extraction with ethyl-acetate, for GC analysis, typically after 18-20 h.

Detection of reduced activated alkenes

Biotransformations were monitored by GC-MS (EI) using a DB-17 column (0.25 mm x 25 m, 0.25 μm film thickness) and the following conditions: 60 °C (2 min) to 180 °C

(5 min) at 10°C/min. Chiral phase GC analyses were performed on a Chirasil-Dex CB column (0.25 mm x 25 m, 0.25 µm film thickness) using one of the following conditions: i) 80 °C (2 min) to 95 °C (0.5 °C/min, 1 min) followed by a 12°C/min gradient to 180 °C (7.00 min), ii) 60 °C (2 min) to 115 °C (0.5°C/min, 5 min) followed by a 2.5°C/min gradient to 180 °C (5.00 min). Other analyses utilized a Beta DEX column (0.25 mm x 30 m, 0.25 µm film thickness) using one of the followed programs: i) 95 °C (35 min) to 160 °C (5.0 °C/min, 2 min) followed by a 10.0 °C/min gradient to 200 °C (5.00 min) ii) 95 °C (35 min) to 160 (5.0 °C/min, 2 min) followed by a 5.0 °C/min gradient to 200 °C (5.00 min).

For the compounds, 2-cyclohexen-1-one, 2-cyclopenten-1-one, 2-methyl-2-cyclohexen-1-one, carvone, 3-methyl-2-cyclohexen-1-one, 1-octen-3-one, *trans*-2-decenal, *trans*, *trans*-2,4-decadienal, phorone, citral and 1-nitro-1-cyclohexene, the reduced products were compared with commercially available authentic standards. The reduced products of 6-substituted 2-cyclohexenones had been previously characterized in our laboratory.[423] The reduced products of *trans*-β-nitrostyrene and 2-nitro-1-phenylpropene were prepared by reduction with sodium borohydride as described elsewhere.[424] For the rest of the compounds tested in this study, the reduction of the double bond was inferred by GC-MS analysis.

Results and Discussion

Isolation of YNL134c

In our preliminary attempts to isolate the EI and EII enone reductases, we used commercially available bakers' yeast and we followed the purification protocol described by Wanner and Tressl with two major modifications: i) a strong anion exchange column (Q Sepharose Fast Flow) was used instead of the weak anion DEAE Sepharose CL-6B, which was employed in the original protocol, ii) a shorter gel filtration column (25 cm

instead of 60 cm) was available for the last purification step. Our observations are summarized below:

- at the first and the most crucial step of the anion exchange chromatography we never succeeded in separating two fractions, EI at the beginning of the NaCl gradient and EII by the end of the gradient, one with NADPH activity and a second with NADH activity towards the reduction of 1-octen-3-one, as described in the published procedure. Even though the exact gradient of NaCl is not reported, we tried different gradients and in any case we always obtained one active fraction that accepted both NADPH and NADH.

- at the affinity chromatography step, activity observed was mainly in the flow through and not in the protein fraction that it was bound to the dye. Even though it is not quite clear from the description given by Wanner and Tressl in which fraction they observed activity, it is more likely that active fractions were detected during the NaCl elution.

- after the last purification step (i.e. the gel filtration column), the most intense band on the SDS-PAGE gel had a molecular weight at 40-45 kDa and a number of other bands were also visible (data not shown).

- when the purification procedure lasted more that 10 days, loss of activity was observed as we reached the final purification step. But in those cases that we completed the procedure and obtained active fractions, GC-MS analysis of reduced 1-octen-3-one revealed that the carbonyl moiety remained intact and only the double bond was reduced.

To the above remarks we should add the following:

- OYE2 and OYE3 from bakers' yeast, cloned and purified by us as GST-fusion proteins, were also found active towards the reduction of 1-octen-3-one under identical to the protein purification assay conditions, despite the nicotinamide cofactor used.
- Both OYE2 and OYE3 have a molecular weight of ~45kDa.

To this end, we decided that it would be wiser to repeat the published purification protocol starting from a yeast strain missing the two genes encoding OYE2 and OYE3 (i.e., DAY1228). To confirm that the double knock-out strain still possesses enone reductase activity, we carried out whole-cell biotransformations using either 1-octen-3-one or 2-cyclohexenone as a substrate. After incubating yeast cells for one day at 30 °C with the appropriate substrate, reactions were analyzed by GC-MS (Table 5-4). To our

surprise, the *oye*Δ strain was unable to reduce the 2-cyclohexenone, whereas it still transformed 1-octen-3-one to the corresponding saturated ketone.

Table 5-4. Observed reduction of 1-octen-3-one or 2-cyclohexenone.

Strain	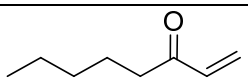	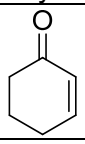
BY[a]	Yes	not determined
DAY111[b]	Yes	Yes
DAY128	Yes	No
EI enone reductase[c]	Yes	Yes
EII enone reductase[c]	Yes	Yes

[a] bakers' yeast from grocery store. [b] background strain used by David Amberg for construction of DAY128 strain. [c] data reported by Wanner and Tresll.

Only one explanation can accommodate both our data and Wanner and Tressl's reported observations (last two entries in Table 5-4): the YHR179w (OYE2) and YPL171c (OYE3) are the only two genes in *S. cerevisiae* genome encode enone reductases able to reduce 2-cyclohexenone.The EI and EII protein samples prepared Wanner and Tressl must be contaminated by OYE2 and/or OYE3, even though these proteins are not visible in their SDS-PAGE gel. The possibility that an enone reductase different from OYE2 or OYE3, but also distinct from the one responsible for reducing the 1-octen-3-one in the DAY128 strain, was present in the yeast strain used by Wanner and Tressl but not expressed in DAY128 strain can be easily excluded since the parent DAY111 strain does reduce the 2-cyclohexenone. Based on these results, it was apparent to us that a third enone reductase (in addition to OYE2 and OYE3) is also responsible for the reduction of 1-octen-3-one.

Convinced that a third enone reductase is present in DAY128 strain, we followed the purification procedure described in detail in the experimental section, which is still based on the reported protocol for the EI and EII enone reductases. In fact, in this case, we also prepared a weak anion exchange column using the matrix that Wanner and Tressl have been utilized before. However, neither this column nor the strong anion

exchange column that we have used before afforded two different active fractions. In any case, only one NADH- and NADPH-active fraction was detected closer to the end of the NaCl gradient (data not shown). In addition, as we had observed before, the most active fractions after the affinity column were found in the flow through (fraction FI in Table 5-5) whereas the activity in the fractions bound to the blue dye was negligible (fraction FII in Table 5-5). After the Superdex 200 filtration column, the last step in Wanner and Tressl's purification protocol, the picture of the SDS-PAGE gel was quite similar to the pattern we had observed in all our previous attempts: an intense protein band with molecular weight ~44kDa in presence of numerous other bands (Figure 5-3). In addition only 15-20-fold purification had been accomplished after this step compared to 165-257-fold purification accomplished by Wanner and Tressl.

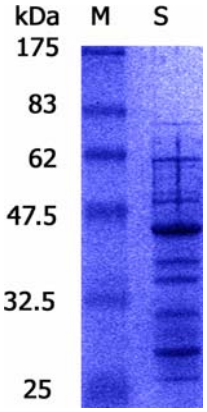

Figure 5-3. Protein gel after the Superdex 200 filtration column. Abbreviations: M :protein markers S: protein sample bearing NAD(P)H activity.

We therefore desalted the active protein fraction and loaded it onto a third strong anion exchange column. To our satisfaction, this step afforded a 60-78-fold purification and two major bands in the SDS-PAGE (Figure 5-4). Unfortunately, when the protein sample was electroblotted onto a PVDF membrane, a number of additional protein bands became visible (data not shown).

Table 5-5. Purification table for YNL134c.

Fraction	Volume (mL)	Protein (mg)	Total Units (NADPH)	Total Units (NADH)	Specific Activity in mU/mg (NADPH)	Specific Activity in mU/mg (NADH)	Purification Factor (NADPH)	Purification Factor (NADH)
Crude extract	220	2860	---[a]	---	---	---	---	---
Streptomycin sulfate precipitation	220	1626	31.9	31.1	19.6	19.1	---	---
Sephadex G-25	70	1050	18.2	16.2	17.3	15.5	1	1
DEAE CL-6B	62	371	20.5	16.5	55.2	44.2	3.2	2.8
HiLoad Q Sepharose	45	261	12.6	12.6	49	49	2.8	3.2
DyeMatrex Gel Blue A (Fraction FI)	50	54	4	8.8	74	163	4.3	10.5
DyeMatrex Gel Blue A (Fraction FII)	50	50	0.3	0.5	6	10	---	---
Superdex 200	20	20	5	6.5	252	324	14.6	20.9
MONO Q	5	5	2.5	2.9	1042	1217	60.2	78.5
Sephacryl S-300	0.7	0.17	0.08	0.05	470	294[b]	---	---

[a] We were unable to measure the specific activity in the crude extract and the protein solution after the streptomycin precipitation because of a strong precipitate formed in the enzyme assay solution even when it was passed through a 0.45 µm filter. [b]Specific activity is lowed in this step compared to the previous one mainly because it was performed 2 weeks latter and enzyme activity was lost during the storage at 4 °C.

Nonetheless, an N-terminal analysis by Edman degradation chemistry attempted for the most intense in Figure 5-4 protein band (~40kDa).No amino acid signal was obtained, suggesting that most likely, the N-terminus amino acid was blocked. In order to further enrich the protein sample for the enone reductase of interest, we loaded the mixture on a Sephacryl S-300 Hi Prep filtration column. Three peaks were detected during the protein elution (Figure 5-5), but only the last one (fractions 72-82) showed NAD(P)H-dependent activity towards 1-octen-3-one reduction as confirmed by both spectrophotometric assays and GS-MS analysis. Active fractions were individually concentrated and subjected to trichloroacetic acid (TCA) precipitation before being loaded onto an SDS-PAGE gel. Even though only the electrophoresis analysis of the fraction 76 is shown in Figure 5-5, all active fractions possessed the same composition with one major and one minor band. Both protein bands were excised from the gel, treated with a protease (trypsin) and subjected to LC-MS analysis, separately. The MASCOT search engine was used for correlation of the experimental MS data with proteins from primary sequences databases. In both cases, the major hit (score> 500) was the product of the YNL134c gene. Peptides found to match with the original sequence are highlighted in red and blue in Figure 5-6. Therefore, the minor band with a lower molecular weight is most likely derived from the major after proteolysis. Two additional hits were derived from this analysis: i) the cytoplasmic alanyl-tRNA synthetase (major band, score=185, 4 peptides matched the subject) ii) the phosphoribosylaminoimidazole-succinocarboxamide synthase (minor band, score=157, 5 peptides matched the subject).

The results from the Mascot search engine strongly suggested that the gene encoding the third unknown enone reductase in DAY128 strain is YNL134c. Indeed, an independent study Yamamoto and Kimoto[425] reached a similar conclusion by following a different approach. They purified and sequenced an enone reductase (MW ~ 42 kDa)

from the fungus *Kluyveromyces lactis* using methyl vinyl ketone as a screening substrate. Then, based on a BLAST search and using the *S. cerevisiae* genome as a query, they identified three hypothetical proteins: YNN4 (YNL134c), YL460 (YLR460c), and YCZ2 (YCR102c) with high similarity (i.e. ~68%) to the isolated one. They cloned and overexpressed the three putative reductases in *E. coli* and they verified their enone reductase activity using *E. coli* crude extracts based on the calculated specific activity for reducing methyl vinyl ketone. Higher activity was observed in the crude extract containing the overexpessesd YNL134c.

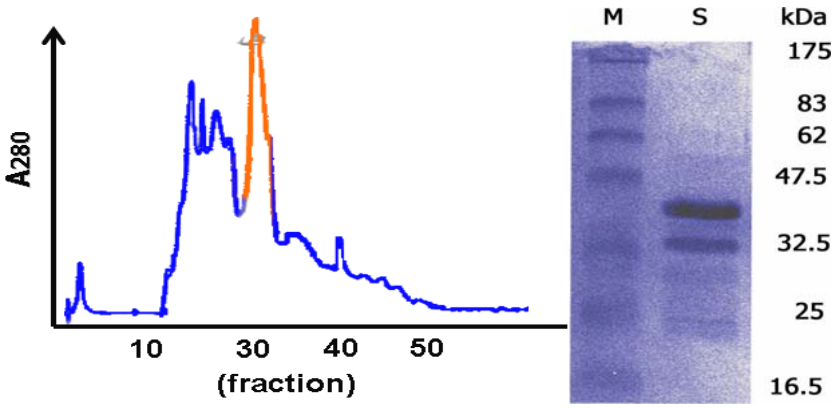

Figure 5-4. Protein elution pattern from Mono Q column during the NaCl gradient (fractions 10-50) and protein gel for active fractions (29-34). Abbreviations: M: protein markers, S: protein sample bearing NAD(P)H activity.

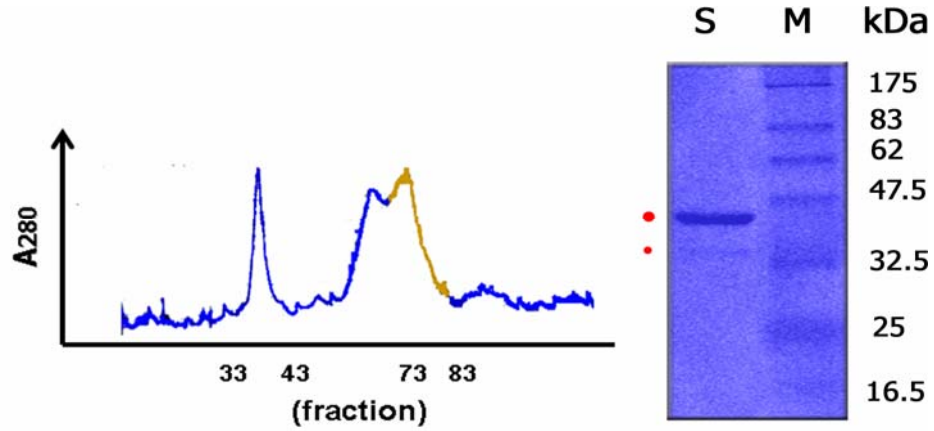

Figure 5-5. Protein elution pattern from Sephacryl S-300 Hi Prep filtration column and protein gel for active fractions (72-82). Abbreviations: M: protein markers, S: protein sample bearing NAD(P)H activity. Red dots indicate the major (big dot) and the minor (small dot) protein bands submitted for LC-MS analysis.

>YNL134c (major band)
MSASIPETMKAVVIENGKAVVKQDIPIPELEEGFVLIKTVAVAGNPTDWKHIDFKIGPQ
GALLGCDAAGQIVKLGPNVDAARFAIGDYIYGVIHGASVRFPSNGAFAEYSAISSETAY
KPAREFRLCGKDKLPEGPVKSLEGAVSLPVSLTTAGMILTHSFGLDMTWKPSKAQRDQP
ILFWGGATAVGQMLIQLAKKLNGFSKIIVVASRKHEKLLKEYGADELFDYHDADVIEQI
KKKYNNIPYLVDCVSNTETIQQVYKCAADDLDATVVQLTVLTEKDIKEEDRRQNVSIEG
TLLYLIGGNDVPFGTFTLPADPEYKEAAIKFIKFINPKINDGEIHHIPVKVYKNGLDDI
PQLLDDIKHGRNSGEKLVAVLK

>YNL134c (minor band)
MSASIPETMKAVVIENGKAVVKQDIPIPELEEGFVLIKTVAVAGNPTDWKHIDFKIGPQ
GALLGCDAAGQIVKLGPNVDAARFAIGDYIYGVIHGASVRFPSNGAFAEYSAISSETAY
KPAREFRLCGKDKLPEGPVKSLEGAVSLPVSLTTAGMILTHSFGLDMTWKPSKAQRDQP
ILFWGGATAVGQMLIQLAKKLNGFSKIIVVASRKHEKLLKEYGADELFDYHDADVIEQI
KKKYNNIPYLVDCVSNTETIQQVYKCAADDLDATVVQLTVLTEKDIKEEDRRQNVSIEG
TLLYLIGGNDVPFGTFTLPADPEYKEAAIKFIKFINPKINDGEIHHIPVKVYKNGLDDI
PQLLDDIKHGRNSGEKLVAVLK

Figure 5-6. Sequence of YLN134c. Peptides found to match with the subject are highlighted either by red or blue color.

It is probably not a surprise that the YLR460c was not detected in our sample since the Expasy database reveals that the later is present only at 799 molecules/ cell whereas the YNL134c is present at 3490 molecules/ yeast cell. The fact that OYE2 is at much higher level (15100 molecules/cell) virtually assures that it would be difficult to isolate pure YNL134c from a wild type yeast strain, especially if we consider that both are NAD(P)H dependent enzymes with high activity for the screening substrate.

Interestingly, during the purification of Gre2p, an NADPH-dependent methylglyoxal reductase, Chen et al. observed on a SDS-PAGE that the protein band corresponding to YNL134c was also enriched but it did not possess catalytic activity towards the screening substate.[426] Other physical interactions studies revealed that YNL134c interacts with its homolog YCR102c,[427] with the ribonucleotide-diphosphate reductase[428] and with a domain of vacuolar ATPase.[429] Nonetheless, YNL134c is listed as an uncharacterized ORF with unknown function in *S. cerevisiae* database. Our results for

the substrate specificity of YNL134c will be discussed later in comparison with the other enone reductases.

Amino acid sequence similarity search reveals a number of homologs in other fungi species with high identity to YNL134c. Most of them are annotated as putative zinc-binding dehydrogenases and/or NADPH quinone reductases. The most interesting finding is that YNL134c possesses a low but significant percent identity with FAQR, the enone oxidoreductase from strawberries described in the previous chapter. For comparison, a multiple sequence alignment of YNL134c, YCR102c, YLR460c and FAQR is depicted in Figure 5-7. We also noticed an unusual NAD(P)H binding motif in all three yeast sequences shown: instead of (G/A)-XX-G-XX-G the underlined glycine residue has been replaced by a threonine.

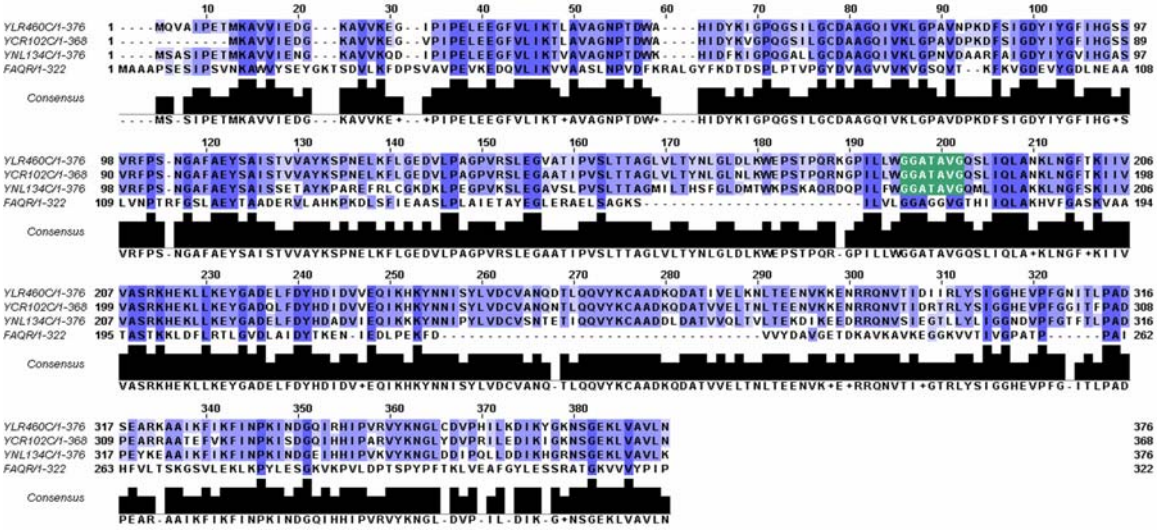

Figure 5-7. Multiple alignment of YNL134c subfamily with FAQR amino acid sequence. The G-XX-T-XX-G is highlighted in green.

Cloning and Expression of Alkene reductases

Construction of universal *E.coli* expression vector

The glutathione S-transferase gene was excised from pIK1 (-) vector as an *AseI*, *NcoI* fragment and cloned between the *NdeI* and *NcoI* sites of pET22b (-) to yield the expression vector pDJB3 (Figure 5-8).

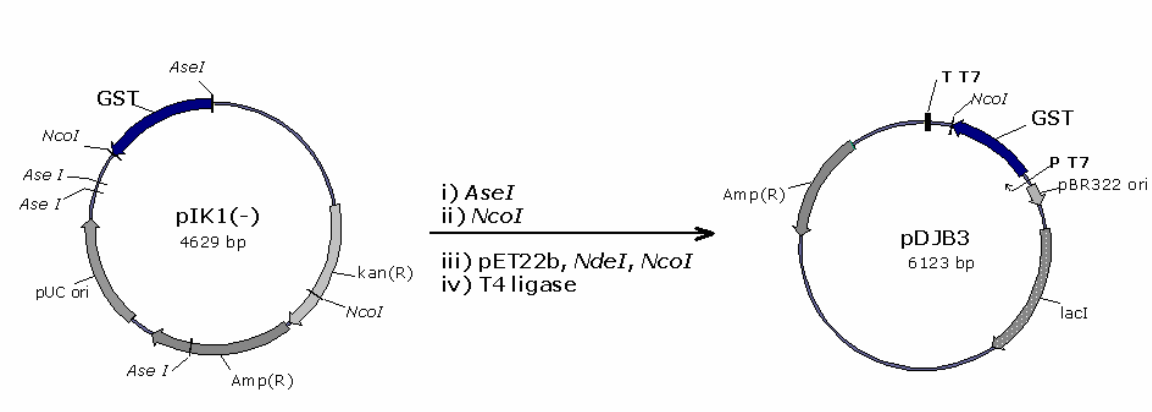

Figure 5-8. Construction of *E. coli* expression vector pDJB3.

Construction of a yeast shuttle universal *E.coli* expression vector

A fragment bearing the T7 terminator, the GST gene, the T7 promoter and the lacI gene (T_{T7}-GST-P_{T7}-lacI) was amplified from the pIK2 vector using appropriate primers that included sequences homologous to *BstEII*/*HindIII*-linearized pYEX4T-1-Rec. DOM. vector. The oligonucleotide primer for the 5' d (**TTTCACACAGGAAAC AGCTATGACCATGATTACGCC**TTTCAGCAAAAAACCCCTCAAGACC) included 36 residues homologous to *Hind III* end of the linearized pYEX4T-1-Rec. DOM. vector. The reverse oligonucleotide sequence 5' d(**GTAATGTCTGCCCCTAAGAAGATCGTCCTTTTGCCA**GCTTTCCAGTCG GGAAACCTGTCG) included 36 residues homologous to *BstEII* end of the linearized vector. Co-transformation of the PCR-amplified product flanked by the homologous regions with the *BstEII*/*HindIII*-linearized pYEX4T-1-Rec. DOM. vector into *S. cerevisiae* BY4742 strain or into *E. coli* KC8 ($recA^+$) strain was successful and afforded the yeast shuttle *E.coli* expression vector pDJB2 (Figure 5-9). Both *E.coli* expression vectors (pDJB2 and pDJB3) possess features for propagation and selection in *E.coli* BL21 (DE3) strain and facilitate the cloning of the desired gene at the C-terminus edge of the GST with the same set of primers. It is noteworthy that the pDJB2 is a higher copy plasmid

(pUC ori) compared to pDJB3 (pBR322 ori). Moreover, the pDJB2 bears features for propagation (2 micron origin) and selection (URA3 marker) in yeast.

Cloning of GST-alkene reductases

The gene encoding the OYE1 from *S. carlsbergensis* was excised from pET-OYE as an *NdeI* fragment and cloned at this site in pIK2 to afford pDJB5. (Figure 5-10) The appropriate orientation of the gene was confirmed by restriction enzyme digestion analysis.

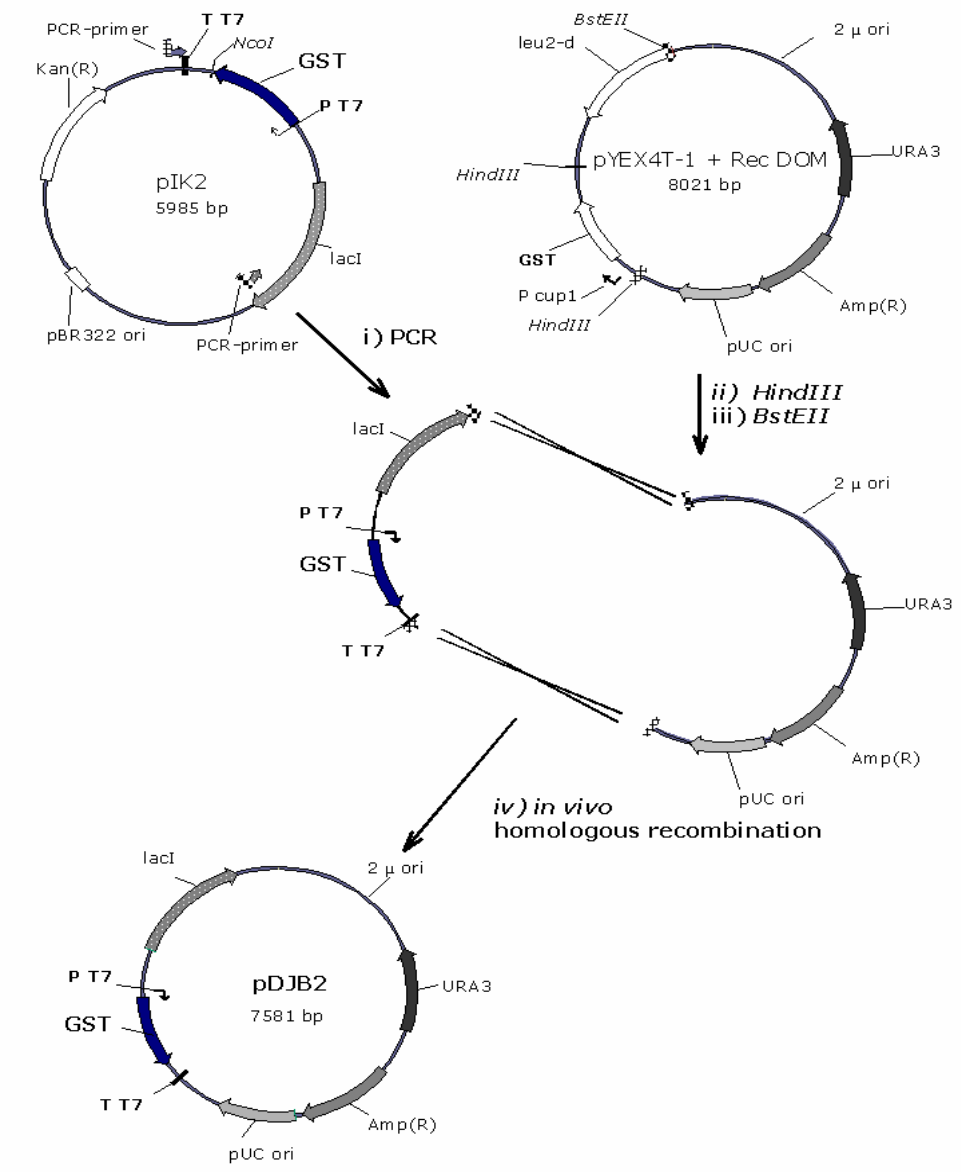

Figure 5-9. Construction of the *E. coli* expression *vector* pDJB2.

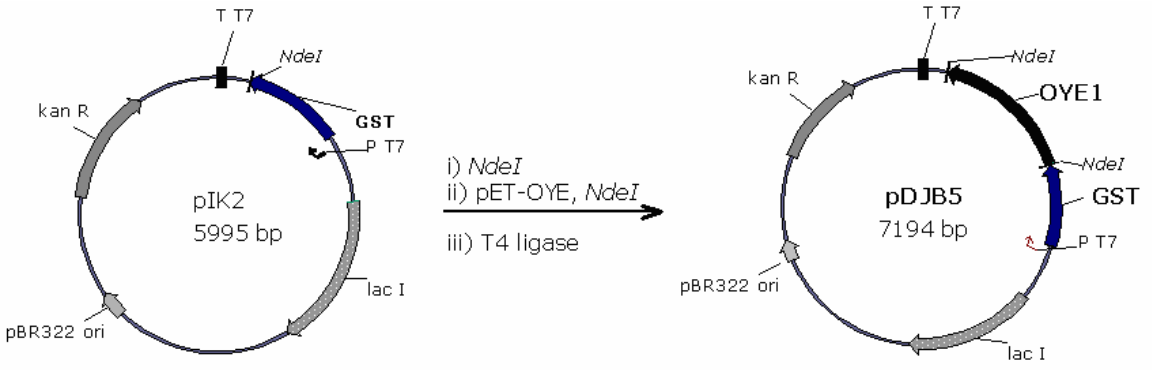

Figure 5-10. Construction of pDJB5.

The homologous recombination approach that we followed in order to clone the rest of alkene reductases is depicted in Figure 5-11. The pDJB3 vector was linearized using the *HindIII* and *NcoI* restriction enzymes. In case of pDJB2, the pair of *HindIII* and *Ecl136II* (*M. SacI* in Figure 5-11) was used instead, since both the *NcoI* and *NdeI* restriction sites are also present in the backbone of this plasmid. Co-transformation of the PCR-amplified product flanked by the homologous regions of pDJB2(3) in either yeast *or E. coli* KC8 strain afforded the final construct pDJBX. The overhand region between the *Ecl136II* and the *NcoI* was eliminated during the *in vivo* homologous recombination in yeast. The expression vector directed the synthesis of fused polypeptide in *E. coli* under control of the T7 promoter.

The HR in yeast led typically to thousands of recombinants whereas after the HR in *E. coli* KC8 strain, we observed any number in between 1-100 of recombinants. We never failed in obtained recombinants in *E. coli* and four to six out of the six colonies typically screened, by colony PCR had the desired structure. The bacterial procedure is much faster: two to three days are required for yeast colonies to grow in minimal media compared to 16 h in for *E. coli* cells and no additional steps (i.e. plasmid rescue) other than a plasmid preparation for sequencing and transformation into *E. coli* BL21 (DE3) are required. Because of these advantages, the *in vivo* HR in *E. coli* was the method of choice for the remainder of the project.

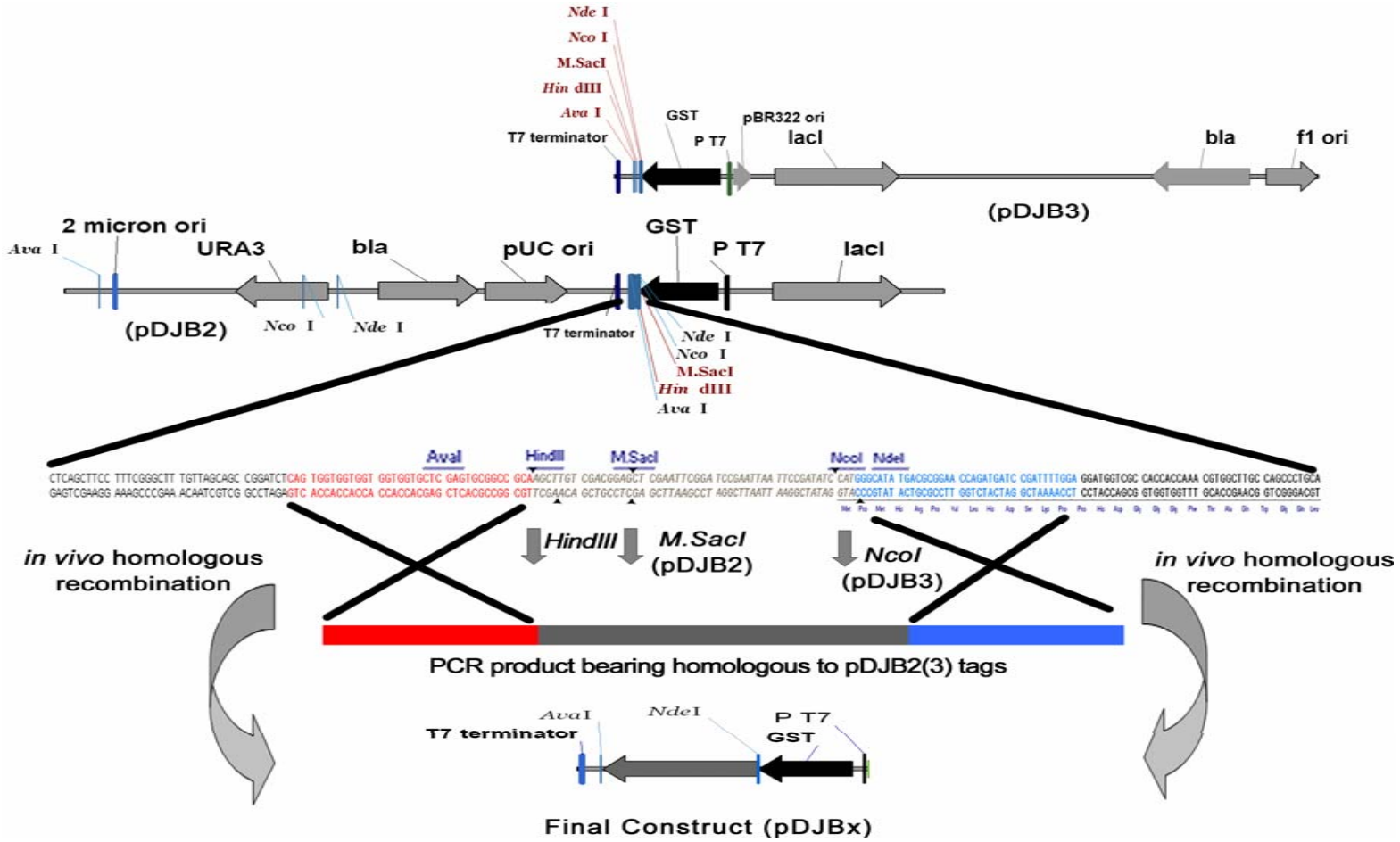

Figure 5-11. Homologous recombinational cloning into universal vectors pDJB2 and pDJB3. Only part of the final construct is shown in this figure.

Primers used for amplification of target genes are listed in Appendix C and the final plasmid constructs, in linear format, are listed in Table 5-6.

Table 5-6. Final plasmid constructs of akene reductases.

Plasmid	Plasmid construct in lineal format
pDJB8	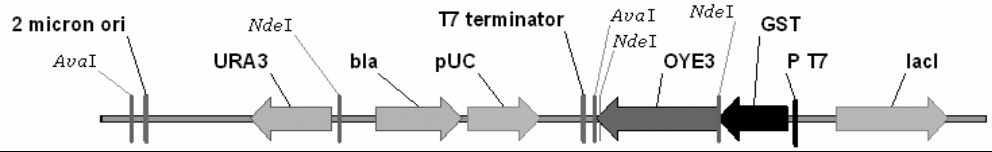
pDJB9	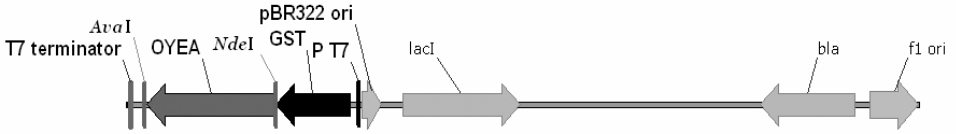
pDJB11	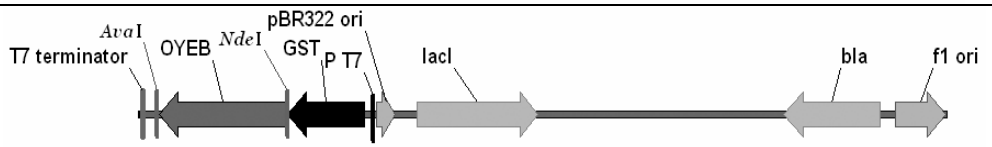
pDJB13	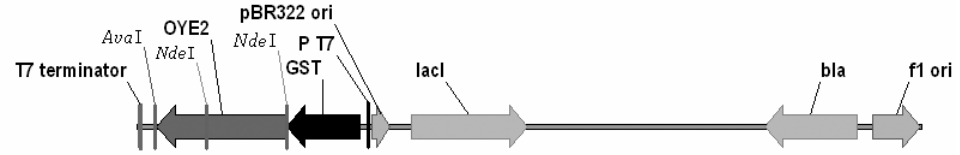
pDJB15	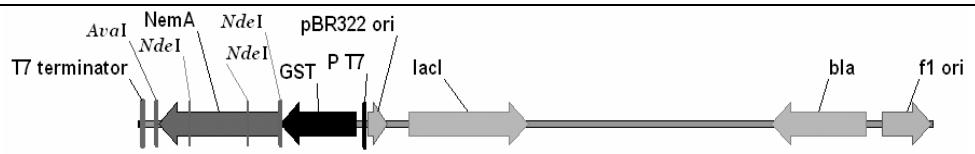
pDJB17	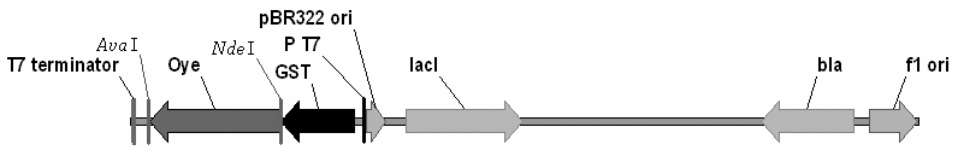
pDJB19	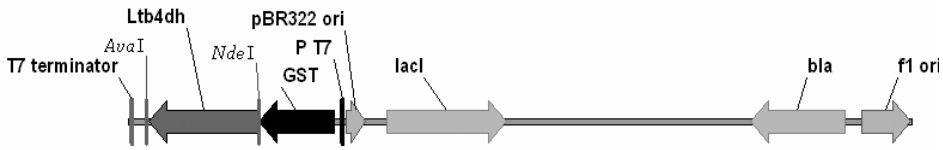
pDJB21	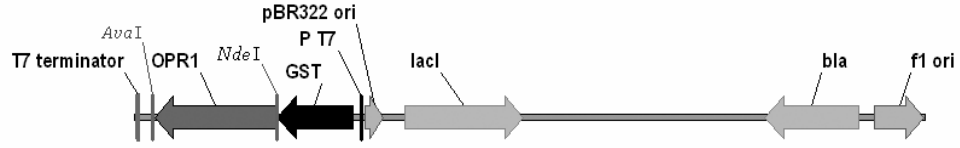
pDJB22	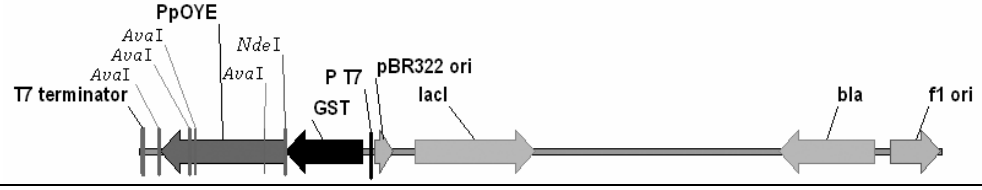

Table 5-6. Continued.

Plasmid	Plasmid constructs in lineal format
pDJB23	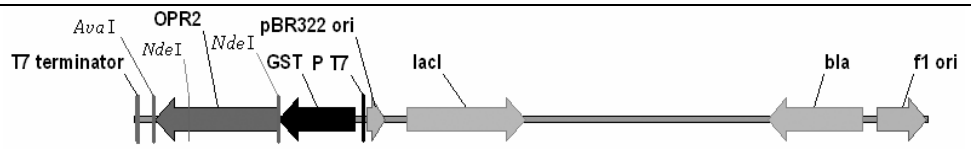
pDJB24	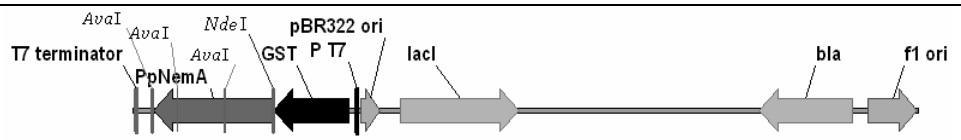
pDJB25	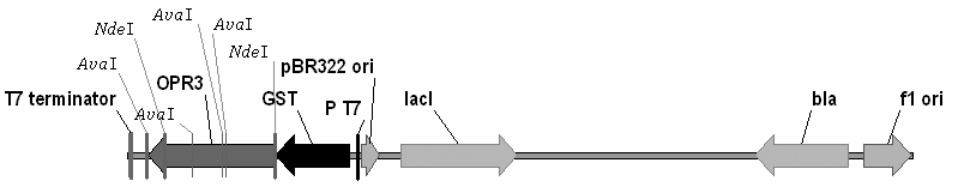
pDJB26	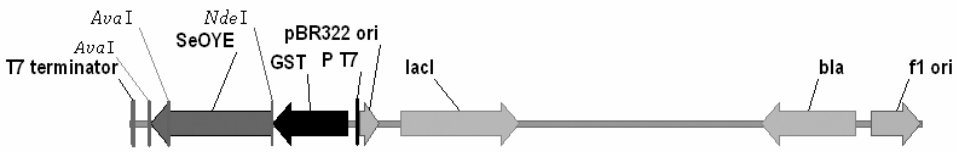
pDJB27	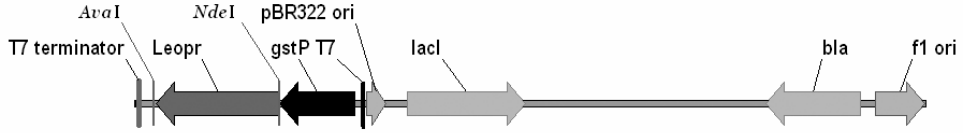
pDJB29	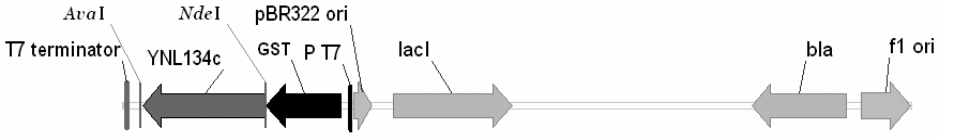

Expression of GST-alkene reductases

The expression and purification protocol for the GST fusion proteins is described in the experimental section and no additional effort was made to optimize these conditions for individual proteins. We failed to express only the OPR2 gene (Figure 5-12) and the lowest purification yield was obtained for OYEA. In two cases (OYE1 and SeOYE), a second protein band at the size of free glutathione transferase (26-28 kDa) is also co-purified. The SDS-PAGE for the partially purified, GST-fusion alkene reductases is depicted in Figure 5-13. Sample used for preparation of this protein gel have been purified six to eighteen months before and kept at -20 °C as 50 % glycerol solutions. Therefore a partial degradation in some cases could not be excluded and may explain

the other lower molecular weight, proteins bands which are visible in some cases. We also noticed that the YNL134c was co-purified with another protein with higher molecular weight.

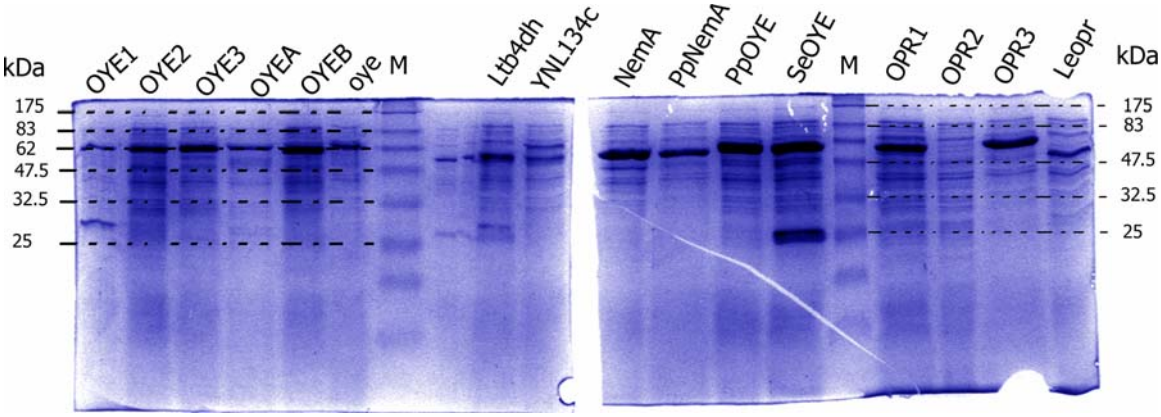

Figure 5-12. SDS-PAGE analysis of total cell extracts overexpressing (8h post-induction) alkene reductases. Abbreviations: M, protein markers.

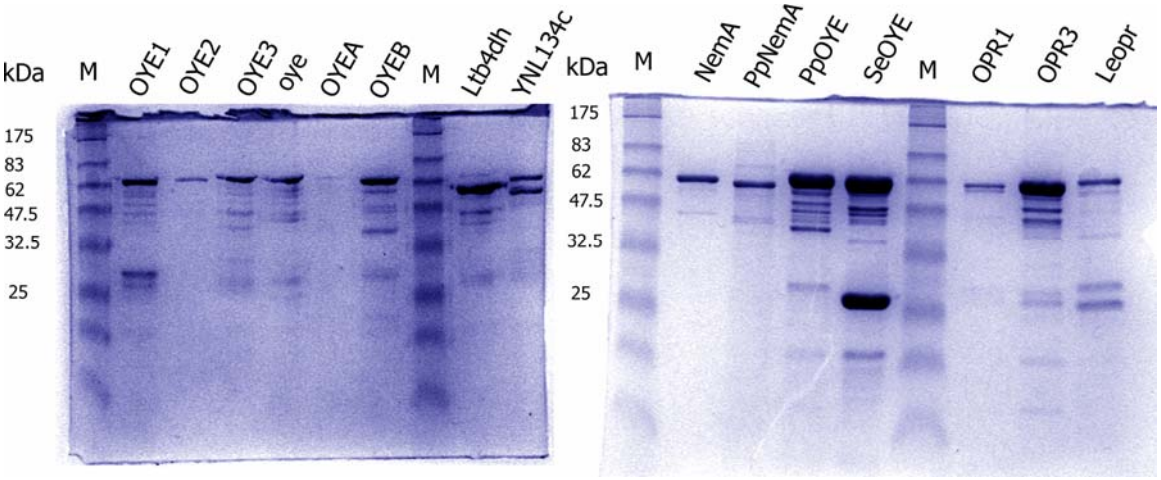

Figure 5-13. SDS-PAGE analysis of alkene reductases after the affinity column.

Screening of Alkene Reductases

In principle, upon the completion of the cloning step, the obtained biocatalysts could be screened either as pure GST-fusion enzymes or as small scale (3-5 ml) whole-cells biotransformations. Even though the latter approach is more convenient and faster, since the protein purification step could be omitted, side reactions from other enzymes

present in *E. coli* or production of other metabolites[408] may complicate the analysis of the data. In fact, it was the lack of stability of both substrate and enzyme in the crude yeast lysate that forced Phizicky and co-workers to include the affinity column chromatography step in their strategy before the screening. Nonetheless, we evaluated this approach for two substrates: the 2-cyclohexen-1-one and 2-phenyl-2-butenal. For the former substrate, even though reduction of the carbonyl group was not detected, reduction of double bond was detected even in an *E. coli* strain overexpressing an enzyme that in a pure form did not possess catalytic activity. When the unsaturated aldehyde was employed, reduction of the double bond as well as reduction of carbonyl moiety was observed, which in some cases led to formation of three products (data not shown). Those observations suggest that an alkene reductase as well as an aldehyde reductase present in *E. coli* may compete with some overexpressed alkene reductases for the same substrate, at least in these small scale reactions. Therefore, we switched to 1 ml screening reactions with partially purified GST-alkene reductases, and 5 mM of substrate as a more reliable method for evaluating new biocatalysts. In most cases, the biotransformations were carried out at 30 °C with gentle mixing, extracted with ethyl acetate and analyzed periodically.

Our results from ca. 600 small scale reactions are summarized in the following tables. Colored bars indicate conversion, usually after 18-24 h incubation. In all cases, the conversion is related to the reduction of the carbon-carbon double; reduction of carbonyl moiety was not observed in these reactions. Black and white bars indicate enantiomeric or diastereomeric excess values. In all bar graphs, the alkene reductases are presented with the same order (yellow bars for: OYE1, OYE2, OYE3, OYEA, and oye, blue bars for: NemA, PpNemA, PpOYE, SeOYE, green bars for: OPR1, OPR3 and Leopr, purple bar for Ltb4dh and orange bar for YNL134c). OYEB was not included since, with only one exception, did not show any catalytic activity under the reaction

conditions described in the experimental part with any of the substrates used in this study.

The reduction of the 2-cyclohexen-1-one, a generic substrate for the OYE family, and 2-cyclopentenone from the OYEs presented in Table 5-7 clearly indicated that all the GST-tagged proteins are catalytically active. A small but measurable conversion was also detected for the same substrates with Ltb4dh, previously reported as non-reactive. Lower conversion was observed with OYEs from plants for 2-cyclopentenone compared to 2-cyclohexenone even though the former is the core skeleton of the OPDA, their known physiological substrate. This suggests that the longer alkyl substituents in OPDA enhance the catalysis. Mostly yeast OYEs are capable of reducing the two lactones listed in Table 5-7 whereas bacteria-OYEs showed diminished activity, if any.

In Table 5-8, most of cyclo-enones listed bear a methyl group at the α-position. The stereochemical outcome of this biotransformation, for all the OYEs tested here, followed the mode described by Swiderska and Stewart for OYE1, with no exception. A crystal structure of OYE with 2-cyclohexenone exists only for pentaerythritol tetranitrate reductase (PETN). We built a methyl group at C-2 in order to visualize this transformation. In the proposed model (no energy minimization has been applied), depicted in Figure 5-14, protonation by the Tyr residue should afford the *R*-enantiomer in any of the relevant substrates listed in Table 5-8. In contrast, reduction of 3-methyl-2-cyclohexenone should afford the *S*-enantiomer (Figure 5-15). Unfortunately, the constraints implied by the planar flavin structure, the strong requirement for a proper alignment of the carbon-carbon above and in close proximity with the N-5 atom of flavin and the orientation of the carbonyl moiety in such a way that hydrogen bonds could be made with the conserved Asp (or His) and His amino acid residues diminished our chances to observe diversity among the OYE family members for these type of compounds.

Table 5-7.Unsubstituted cyclo-alkenes.

Substrate (name)	% Conversion
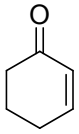 2-Cyclohexen-1-one	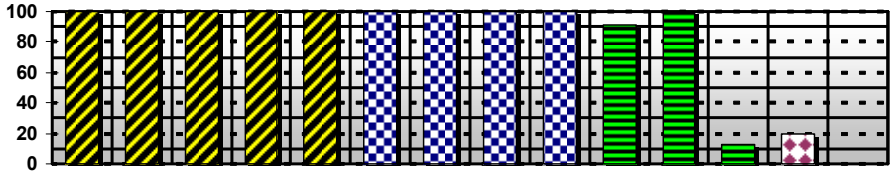
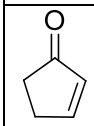 2-Cyclopenten-1-one	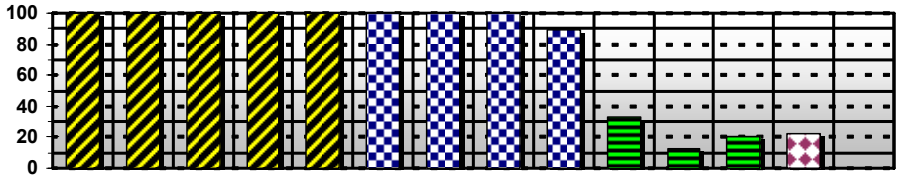
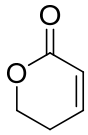 5,6-Dihydro-2H-pyran-2-one	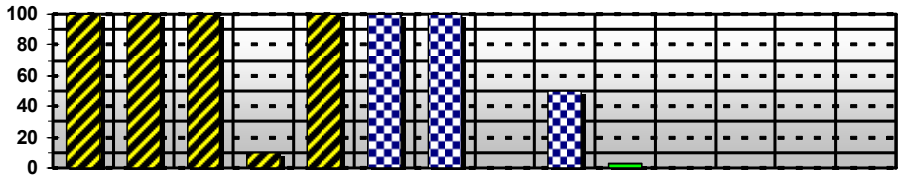
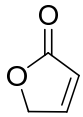 (2(5H)-Furanone)	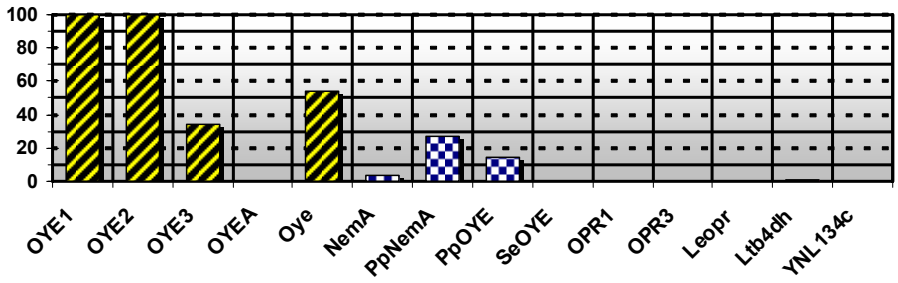

Table 5-8. α-substituted cyclo-alkenes.

Substrate	% Conversion
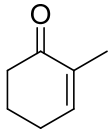 2-methyl-2-cyclohexen-1-one	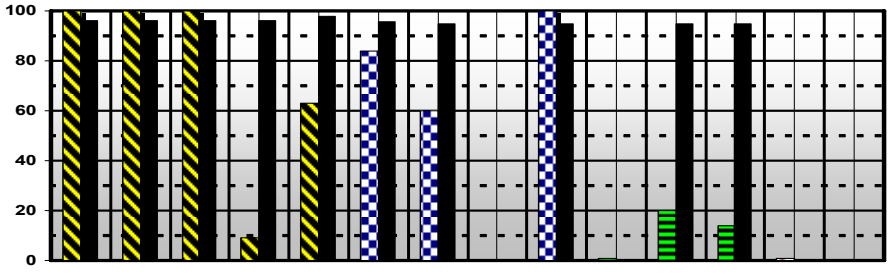

Table 5-8. Continued.

Substrate	% Conversion
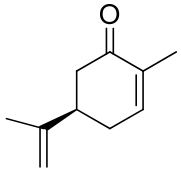 (*R*)-(+)-Carvone	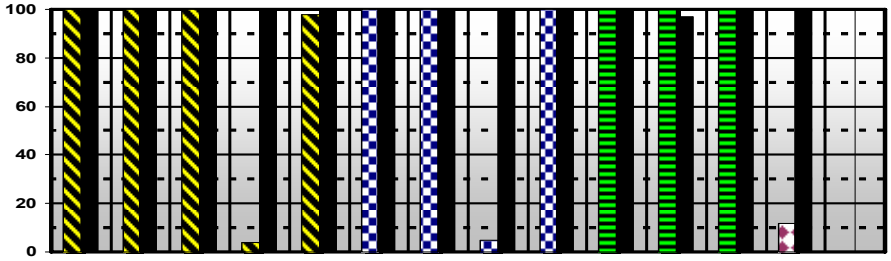
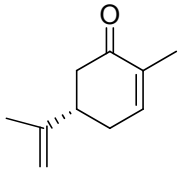 (*S*)-(-)-Carvone	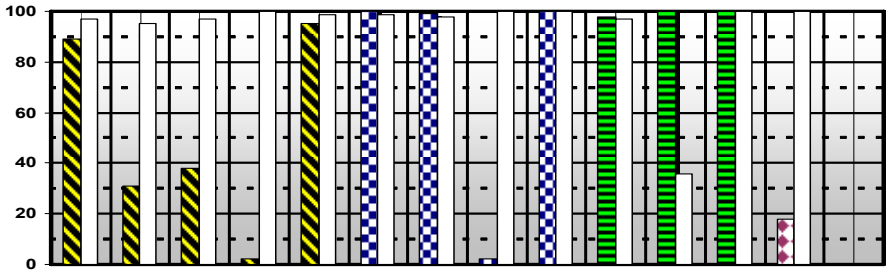
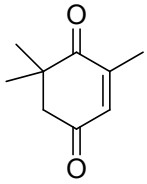 oxoisophorone	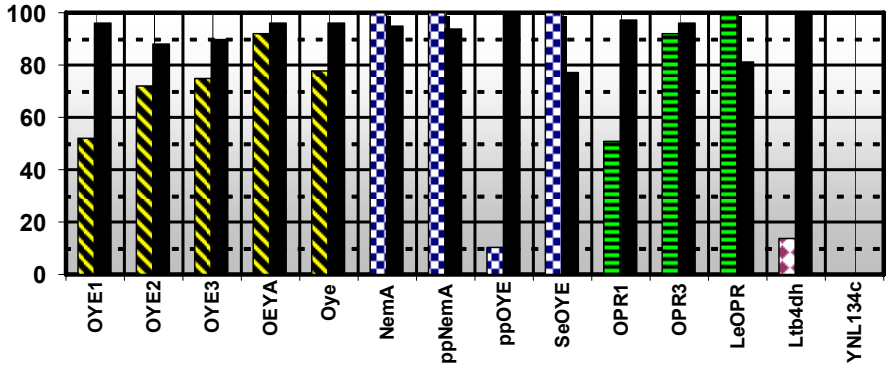
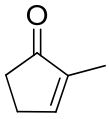 2-Methyl-2-cyclopenten-1-one	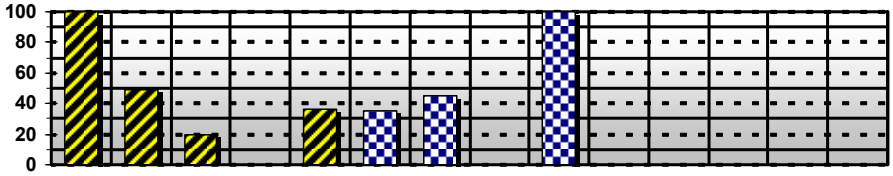
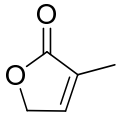 3-Methyl-2(5H)-furanone	no conversion
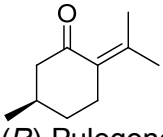 (*R*)-Pulegone	no conversion

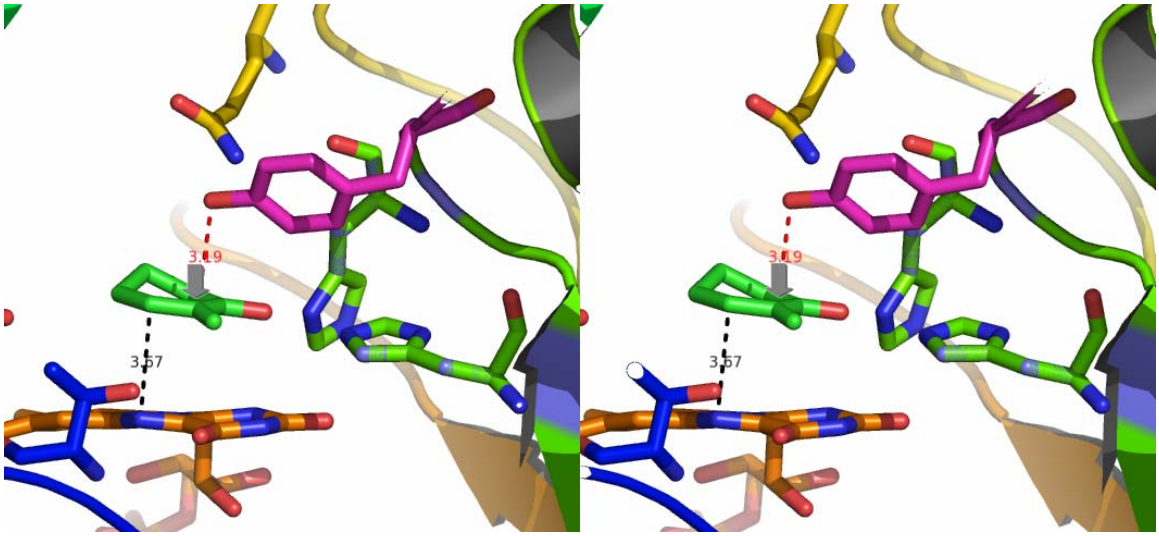

Figure 5-14. Predicted stereochemical outcome for 2-methyl-2-cyclohexenone. Figure was rendered in Pymol.

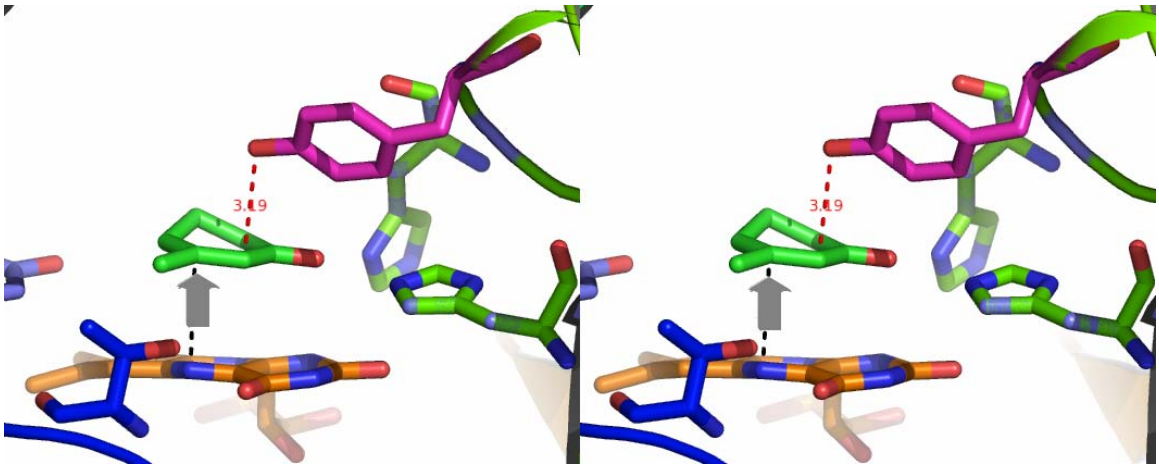

Figure 5-15. Predicted stereochemical outcome for 3-methyl-2-cyclohexenone. Figure was rendered in Pymol.

Asymmetric transformations of α-substituted cyclohexenones with whole cells of *Synechococcus elongatus* strain PCC 7942 were reported to afford the opposite enantiomer from the one we obtained with the purified OYE from the same microorganism.[432] Most likely, another enone reductase, which does not belong to OYE family, was responsible for those biotransformations. Ltb4dh showed a small but measurable conversion with certain compounds but with the same stereoselectivity as the OYEs. The results reported for oxoisophorone, in Table 5-8, are after 3 h incubation

since prolonged reaction-time lead to product racemization under the reaction conditions.

The exocyclic double bond, in s-*cis* conformation to carbonyl group, in pulegone was not reduced by any of the alkene reductases tested.

The dramatic decline in the catalytic activity of OYE1, when 3-methyl-2-cyclohexenone was used as substrate, had been pinpointed by Massey. Unfortunately, this situation is the same or even worse is the case for all additional OYEs screened in this work (Table 5-9). Massey hypothesized that this compound somehow interfered with the NADPH reduction of the flavin. His studies on manipulating the redox potential of the flavin by site-directed mutagenesis (T27A, Thr residue is shown in blue in Figure 120) revealed that by lowering the redox potential, the rate of oxidative-half reaction of OYE1 with this substrate was increased by 3-fold (over the wild type rate, 0.062 s^{-1}).The same fold increment was observed for 2-cyclohexenone (102 s^{-1} for the wild type) Considering also his measurements about the rate of reductive-half reaction for this mutant (0.43 s^{-1}) we may predict that the T27A mutation should accelerate the overall reaction since for this particular substrate the oxidative-step is the rate-limited. However, even with this acceleration, the total turnover number will remain low compared to other substrates. Based on the above observations, Massey concluded that steric hindrance during the hydride transfer should also account for the overall phenomenon.

We also explored substitution at the 6 position of cyclohexenones (Table 5-10). In this case, we are asking for a kinetic resolution of the racemic 6-substituted cyclohexenones and therefore in the best case the yield of reaction should not exceed 50%. Nonetheless, this is the first and the only example for which some diversity observed among the OYEs for cyclo-alkenes. In fact, the yeast-OYEs showed the opposite stereopreference from the one observed for bacteria and plants-OYEs.

Unfortunately, the enantiomeric ratio (E) derived from the calculated *ee* of the product and the corresponding conversion was <10 in all cases examined. An E >15 is considered as respectable value for further applications.

Table 5-9. β-substituted cycloalkenes.

Substrate	% Conversion
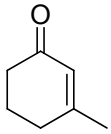 3-Methyl-2-cyclohexen-1-one	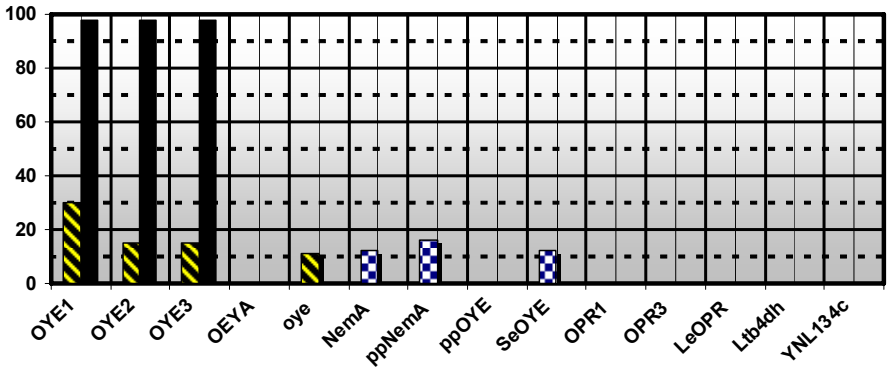
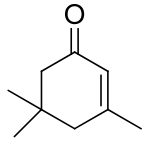 Isophorone	no conversion
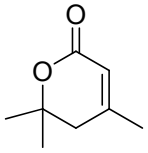 5,6-dihydro-4,6,6-trimetyl-pyranone	no conversion

Table 5-10. 6-substituted cyclohexenones.

Substrate	% Conversion[a,b]
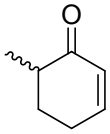 6-methyl-2-cyclohexen-1-one	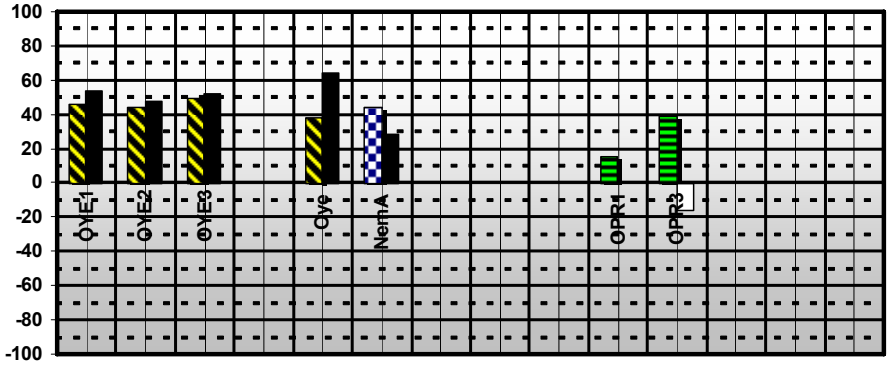

Table 5-10. Continued.

Substrate	% Conversion
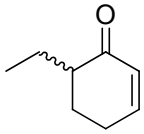 6-ethyl-2-cyclohexen-1-one	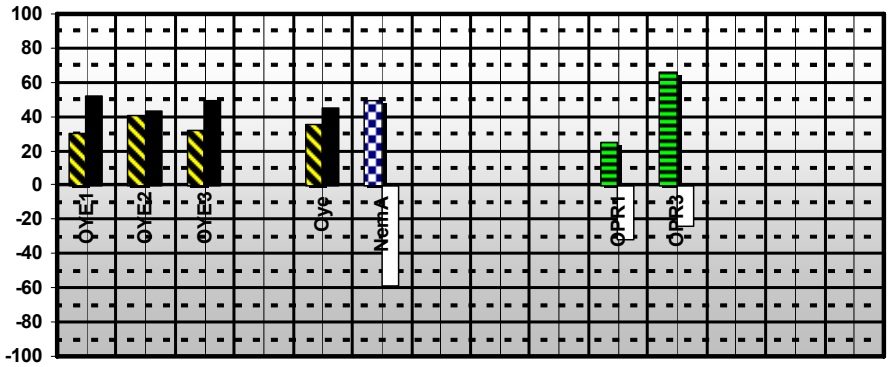
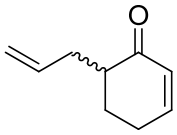 6-allyl-2-cyclohexen-1-one	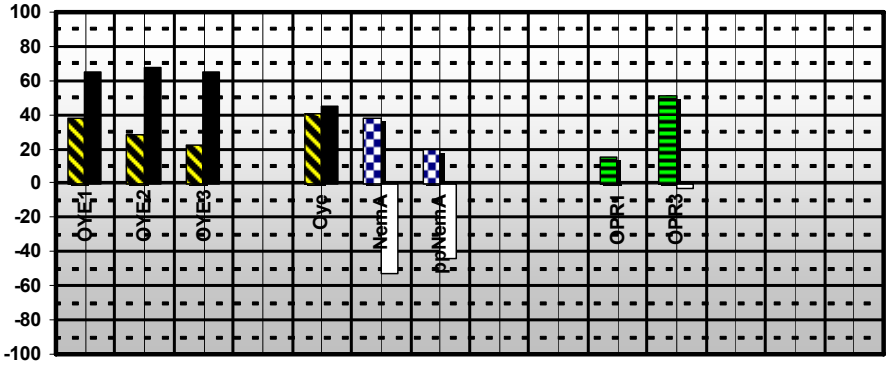

[a] Black bars indicate the %ee of product for the (*S*) enantiomer in case of methyl and ethyl substituent and (*R*) enantiomer for the allylic substituent. The opposite is true for the white bars. [b]Enzymes not listed, were not screened.

In the compounds listed in Table 5-11, the exocyclic carbonyl group is more flexible and can adopt an s-*trans* or an s-*cis* configuration. Even though an s-*trans* conformation is more likely preferred from OYEs, a favorable s-*cis* configuration in case of Ltb4dh could explain its high activity towards those compounds. From the conversion values, observed in the first and second entry, we may conclude that enals are more reactive with OYEs in contrast to what it was observed for the Ltb4dh. In addition, an enhanced reactivity observed in all cases when the cyclohexene ring was substituted at 4 position, but only in case of (*S*)-perillaldehyde for the OYEs, in contrast both enantiomers were proved excellent substrates for Ltb4dh.

Table 5-11. Perillaldehyde and derivatives.

Substrate	% Conversion
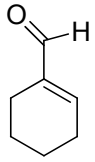 1-Cyclohexene-1-carboxaldehyde	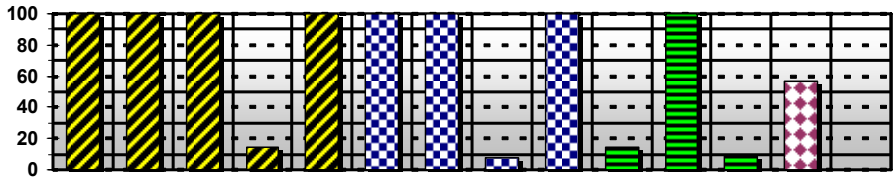
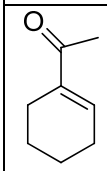 1-Acetyl-1-cyclohexene	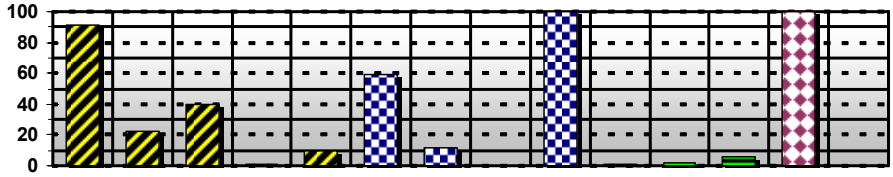
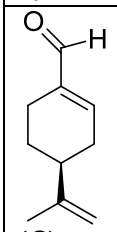 (*S*)-Perillaldehyde	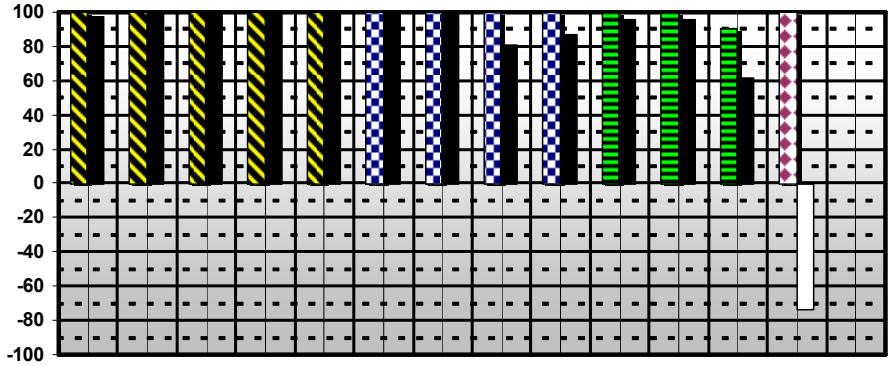
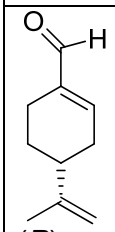 (*R*)-Perillaldehyde	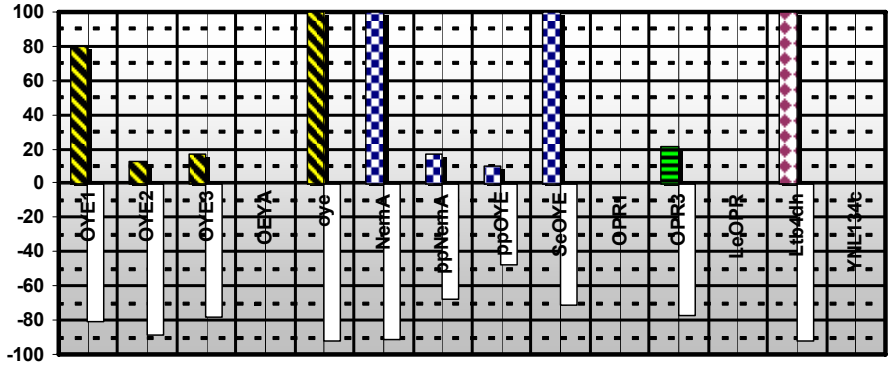
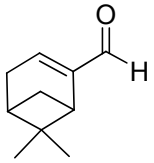 (-)-Myrtenal	no conversion

The two enantiomers of perillaldehyde allowed us to trace the stereopreference of the alkene reductases, since the obtained products are diastereoisomers. Bioreduction of perillaldehyde with bakers' yeast afforded the *trans* saturated alcohol for the natural (*S*)-perillaldehyde in 78% *de* and the *cis* saturated alcohol for the synthetic (*R*)-perillaldehyde in 60% *de*.[431] We also observed the same pattern for all the OYE family members. The stereochemical outcome of this biotransformation can be also rationalized as before (Figure 5-16 and 5-17). Building the perillaldehyde structure on the core of cyclohexenone in the crystal structure of PETR (no energy minimization was applied) we can easily predict that the stereochemistry of the obtained products should be that reported by Serra and co workers. The major differences in our case are that only the carbon-carbon double bond is reduced and higher *de* values obtained for both *trans* and *cis* products. However, lower conversion and % *de* observed for the synthetic (*R*)-perillaldehyde compared to (*S*) natural compound in almost all cases. It also apparent from the graph that the lower conversion values are linked with lower *de* numbers. The loss of stereocontrol for the *R* enantiomer may be due to steric hindrance with the planar flavin cofactor and this may explain both the lower *de* and the lower conversion. The explanation provided by Serra for the lower *de* values obtained with bakers' yeast was that more than one enone reductase compete for the same substrate. We cannot exclude this possibility but definitely this 'other' reductase is not the YNL134c, which did not show any catalytic activity with this substrate under our screening conditions. A flipped geometry of (*S*) perillaldehyde in the catalytic center of the OYE as it is depicted in Figure 5-18 should lead to the *cis* diastereroisomer and therefore should be excluded at least for this enantiomer, but it may be an alternative explanation for the low de values observed for the (*R*) enantiomer.

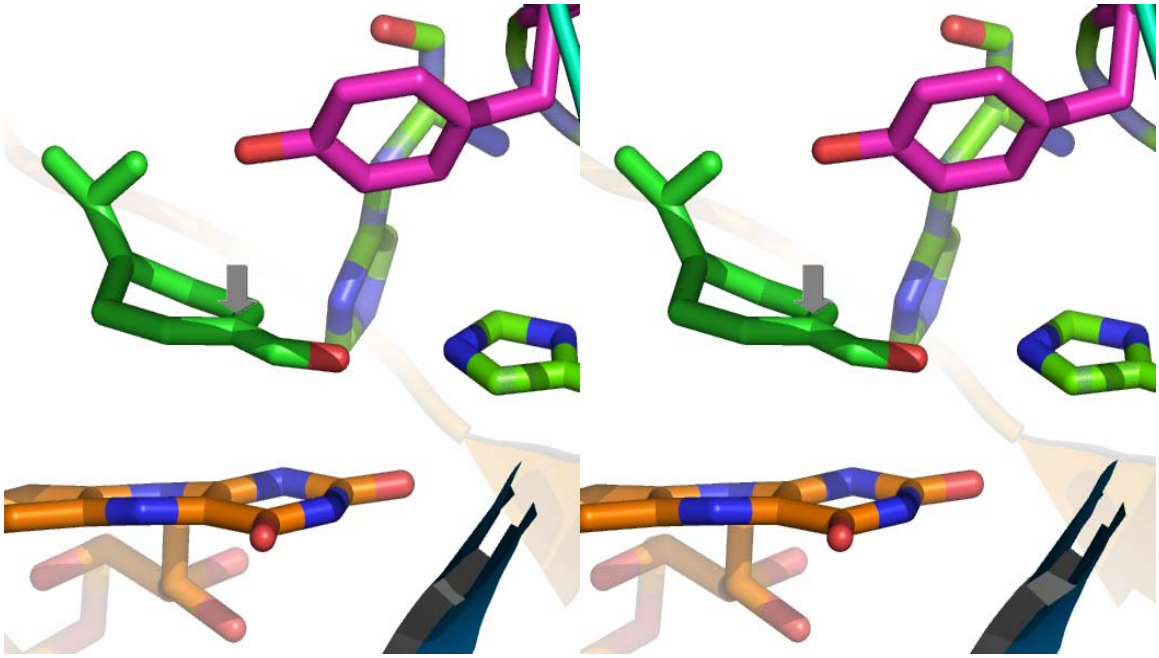

Figure 5-16. Predicted stereochemical outcome for (*S*)-perillaldehyde. Figure was rendered in Pymol.

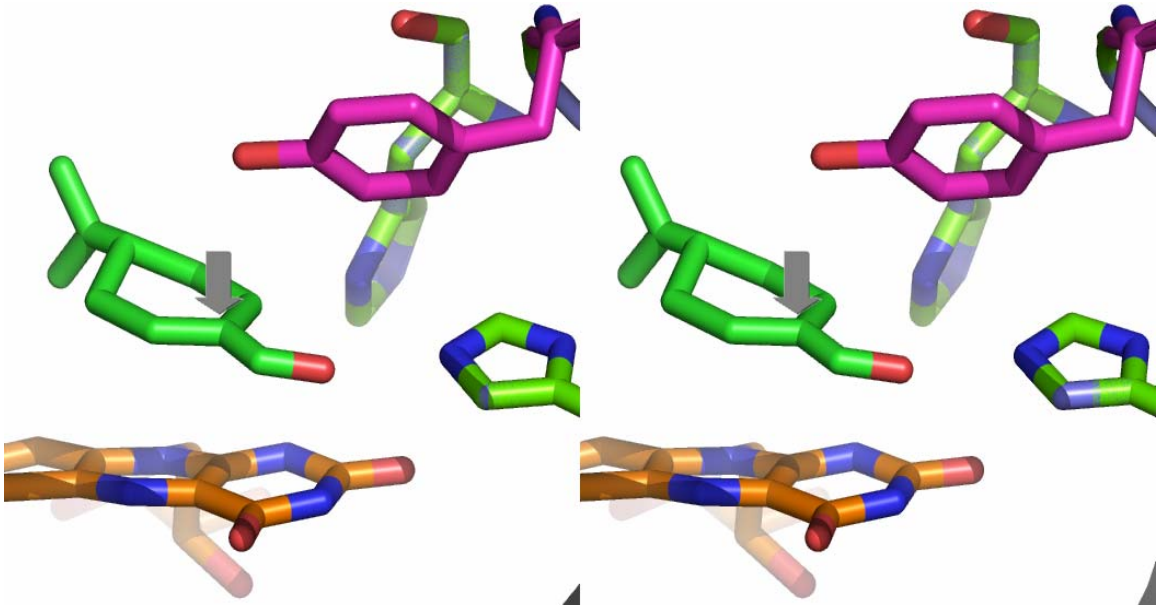

Figure 5-17. Predicted stereochemical outcome for (*R*)-perillaldehyde. Figure was rendered in Pymol.

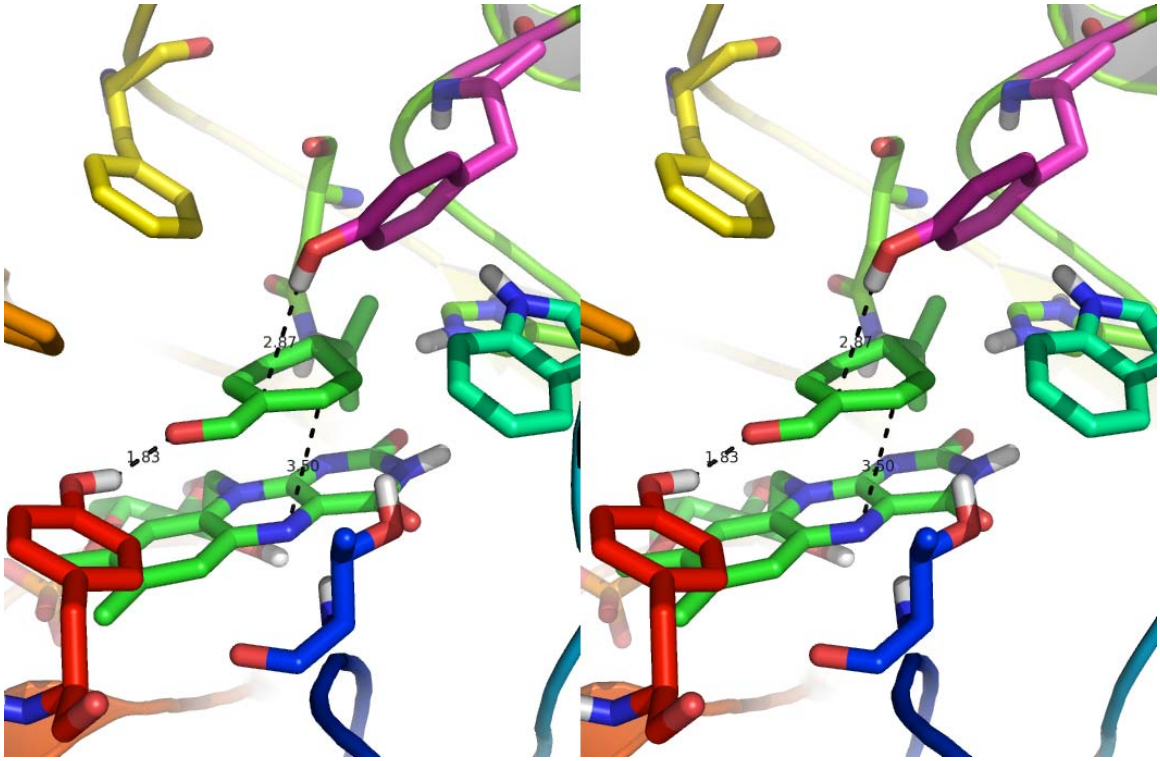

Figure 5-18. An alternative, flipped geometry of (*S*)-perillaldehyde in the catalytic center of OYE built based on the crystal structure of OYE1 with para-hydroxy-benzaldehyde. Tyr375, colored in red, could serve as a hydrogen donor. Figure was rendered in Pymol. No energy minimization was applied.

More interesting are the results obtained for perillaldehyde with Ltb4dh. Stereoselectivity studies with alkenal/one oxidoreductase (AOR) and with most of medium-chain reductases have not been reported so far. Unfortunately, the crystal structure of AOR from rat has not been solved and therefore we will try to explain our data based on the structure of AOR from guinea pig with 15-oxo-prostaglandin E (Figure 5-19A). This structure suggested an s-*cis* conformation of the carbonyl group and a hydride attack from the *re* face of perillaldehyde. It is less clear, however, from where the α-protonation occurred. The *cis*-1,2 dihydroperillaldehyde obtained, when the *R*-perillaldehyde was utilized, suggested a *trans*-addition across the double bond (Figure 5-19B). In contrast, for the same product, a *syn* addition must be hypothesized for the *S*-enantiomer (Figure 5-19C), if we assume a similar conformation for both enantiomers in the catalytic center of AOR. The possibility that a different amino acid (or a water

molecule) acts as a proton donor, depending on the substrate used, is open and in any case additional experiments are required for the elucidation of this mechanism.

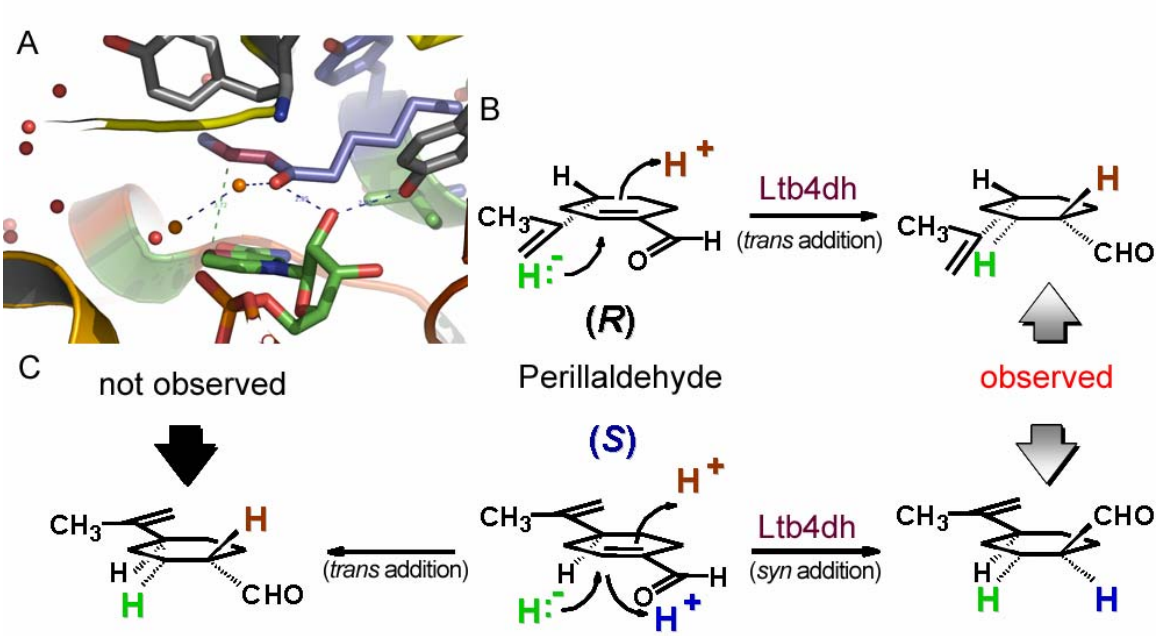

Figure 5-19. Proposed mechanism for the Ltb4dh-mediated reduction of perillaldehyde. A. Close-up view of Ltb4dh from guinea pig with 15-oxo-PGE_2. B. Proposed hydrogen addition for the *R*-enantiomer. C. Proposed hydrogen addition for the *S*-enantiomer.

The last group of cycloalkenes examined in the present study is listed in Table 5-12. All three maleimides were good substrates for the OYEs and even the Ltb4dh possesses some activity, especially with the two more hydrophobic compounds.

Table 5-12. N-substituted maleimides.

Substrate	% Conversion
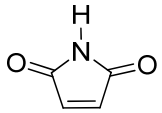 maleimide	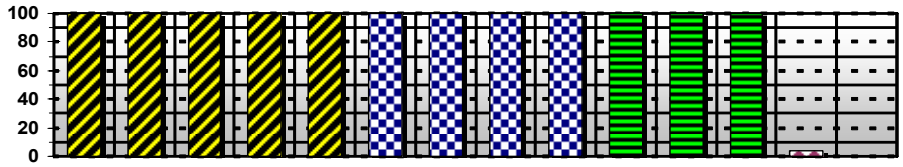
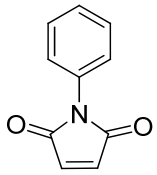 N-Phenylmaleimide	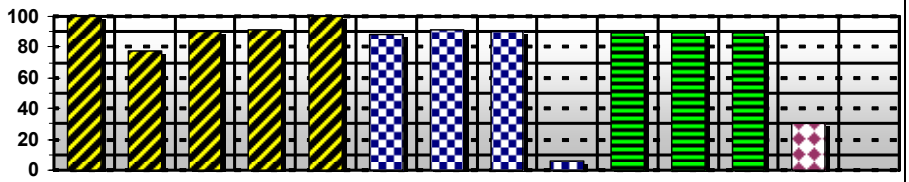

Table 5-12. Continued.

Substrate	% Conversion
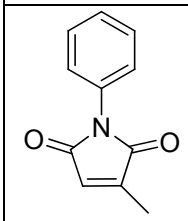 2-Methyl-N-phenylmaleimide	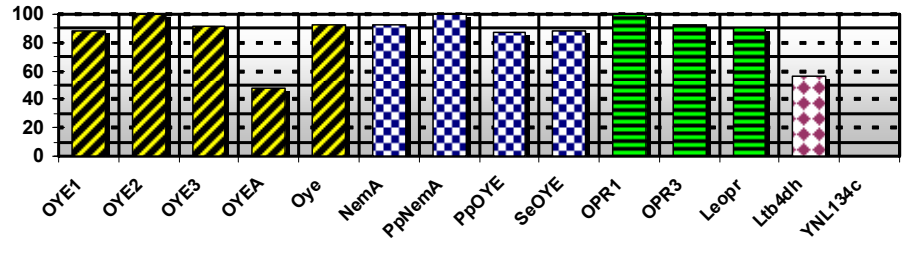

YNL134c, unreactive with all cyclo-alkenes presented above, was able to reduce most of the acyclic alkenes listed in Table 5-13. *Trans* dienals were not good substrates for the OYEs from plants and their reactivity was modest towards *trans*-2-decenal. Methyl *trans*-4-oxo-2-pentenoate, and 1-octen-3-one were proved to be the two universal substrates for this alkene reductase library. In fact, the former was the only substrate for which a small conversion was detected (~12%) even with the OYEB. Interestingly, all reductases, except YNL134c showed high activity towards the dimethyl maleate. Lastly, both double bonds of phorone were reduced by Ltb4dh whereas no activity was observed from any of the OYEs. The conversion reported for the same compound for the YNL134c corresponds to a product in which only the one double bond was reduced.

Table 5-13. Straight chain alkenes.

Substrate	% Conversion
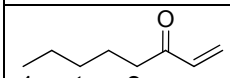 1-octen-3-one	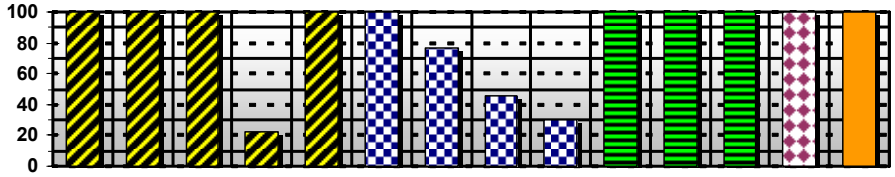
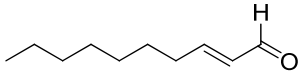 *trans*-2-decenal	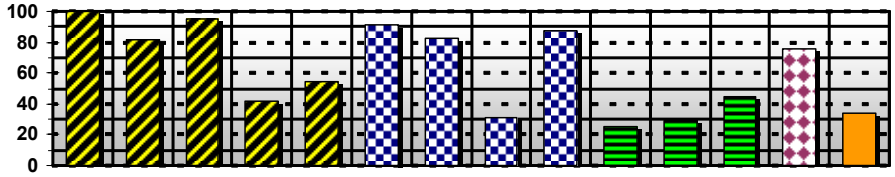

Table 5-13. Continued.

Substrate	% Conversion
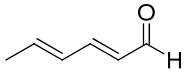 *trans*,*trans*-2,4-hexadienal[a]	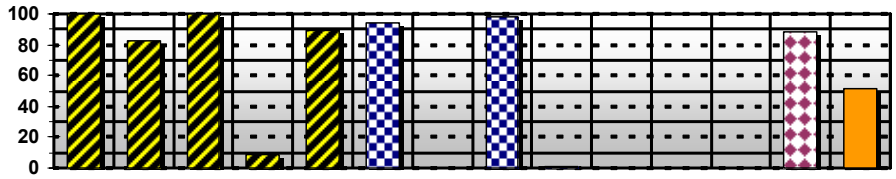
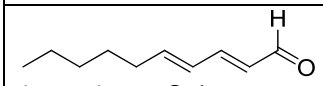 *trans*,*trans*-2,4-Decadienal[a]	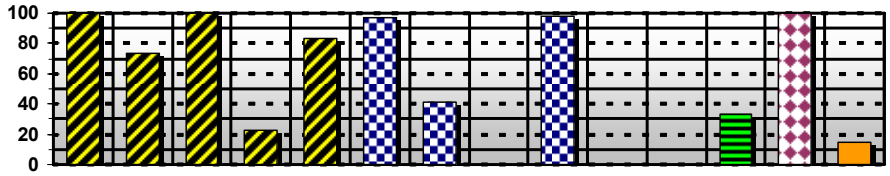
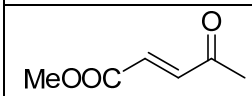 methyl *trans*-4-oxo-2-pentenoate	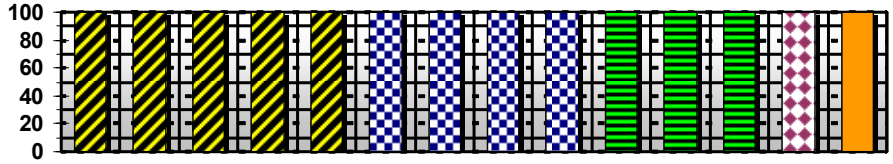
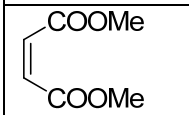 dimethyl maleate	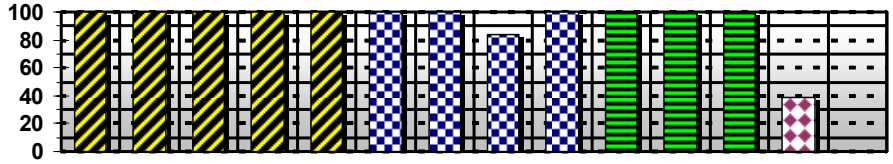
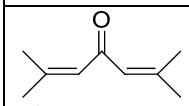 phorone	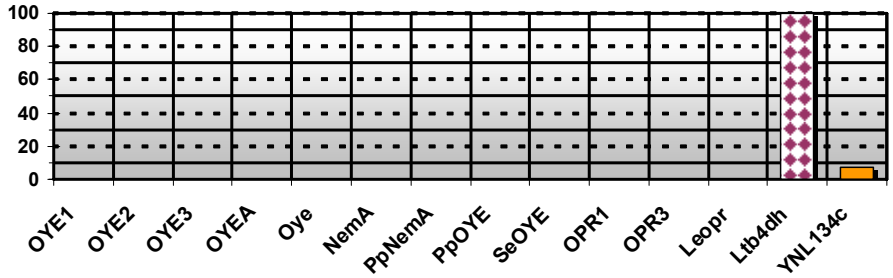

[a]Only the double bond conjugated to carbonyl group was reduced.

The reduction of the two geometric isomers of citral, geranial (*trans*) and neral (*cis*), allowed us to examine the stereo- and enantio-specificity of the reductases under study. Citral is a 60:40 mixture of *trans* and *cis* isomers, which, separately, are not commercially available.

Table 5-14. Substituted enals.

Substrate	% Conversion
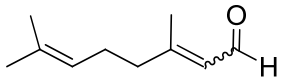 citral[a]	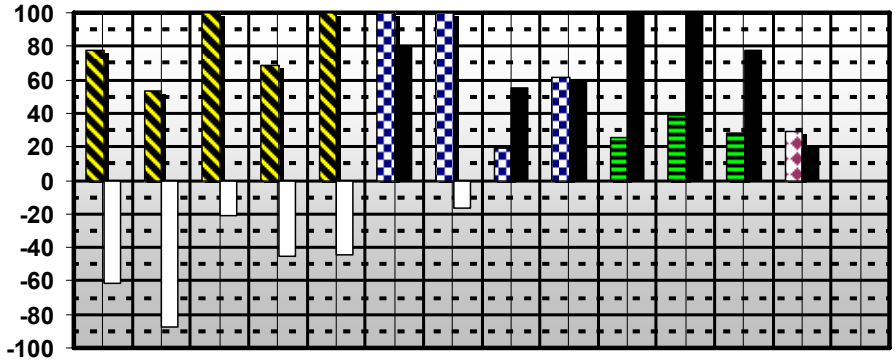
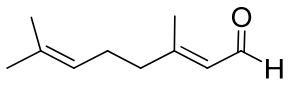 geranial[b]	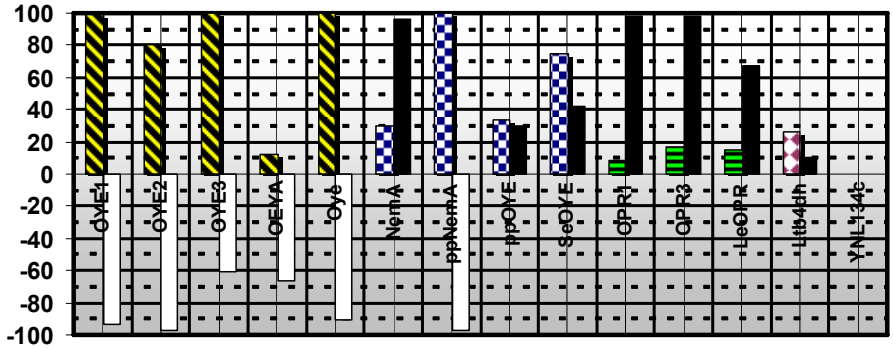
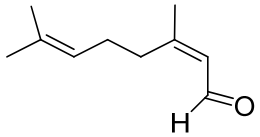 neral[b]	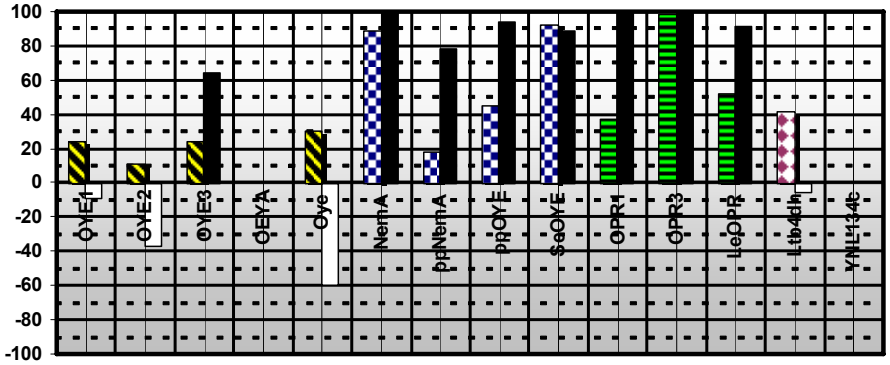

[a]Black bars indicate % *ee* for (*R*) enantiomer and white bars % *ee* for (*S*) enantiomer . [b]For OYE2 and SeOYE twice more enzyme was used compared to what was used for citral. For ppOYE, OPR1, OPR3, LeOPR and Ltb4dh the amount of each was increased 3 fold compared to what was used for citral.

Table 5-14. Continued.

Substrate	% Conversion
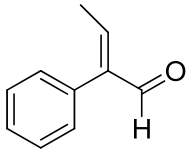 2-phenyl-2-butenal[c]	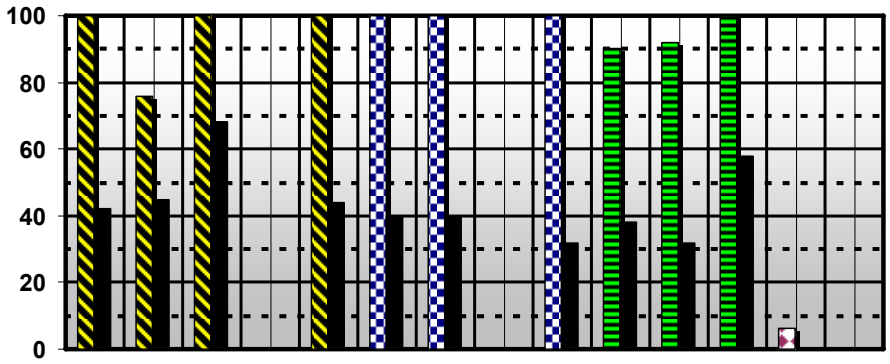
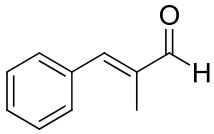 α methyl-cinnamaldehyde	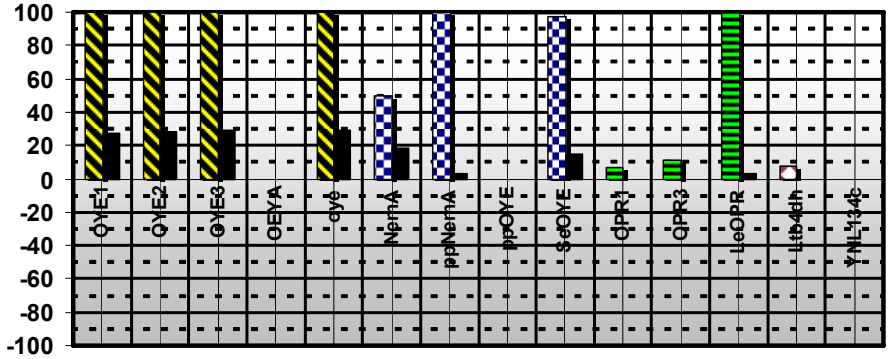

[c]Conversion values reported after 20 h incubation and % *ee* after 6h.

Our results with the mixture of two isomers (first entry of Table 5-14), indicated a divergent behavior among the OYEs. To a first approximation, yeast OYEs afforded (*R*)-citronellal with good (OYE2) to moderate (OYE3) enantiomeric excess whereas OYEs from bacteria and plants afford the opposite enantiomer with a broad range (60-99%) of *ee*. The only exception was the ppNemA. If we applied the proposed *trans* addition of hydrogen across the double bond of citral, as we did before for the cyclohexenones it would become apparent (Figure 5-20) that the *trans* isomer should lead to (*R*)-citronellal and the cis isomer to (*S*)-citronellal. If we assume no isomerization of starting compounds and no preference from the OYEs from the one or the other isomer then we should observed a ~20% ee (*R*)-enantiomer in all cases. Clearly this is not the case. Our results with pure *trans* or *cis* enantiomer suggested that the OYEs from plants have

a strong preference for neral whereas yeast-OYEs a strong preference for geranial. Bacterial-OYEs did not follow a consistent pattern: NemA followed the same patern as the OYEs from plants whereas ppNemA followed a similar to OYE3 patter. In all cases, an enhanced enantioselectivity was observed when the 'correct' isomer was employed with the preferred enzyme. This is probably due to fact that when the isomer presented in the reaction mixture is not utilized immediately from the enzyme under study, alkene isomerization yielded the opposite, 'correct' isomer which in turn was converted to the appropriate enantiomer. The amino acid- mediated isomerization of pure neral or pure geranial to citral is a well-documented phenomenon[432] and isomerization of the unreacted starting material was observed in our case too. Loss of stereocontrol, when the 'wrong' isomer is reduced by OYEs, is also possible. With the existent experimental data and with the lack of a crystal structure of an OYE in presence of a straight-chain alkene it is hard to explain the observed distinct stereopreference among OYEs.

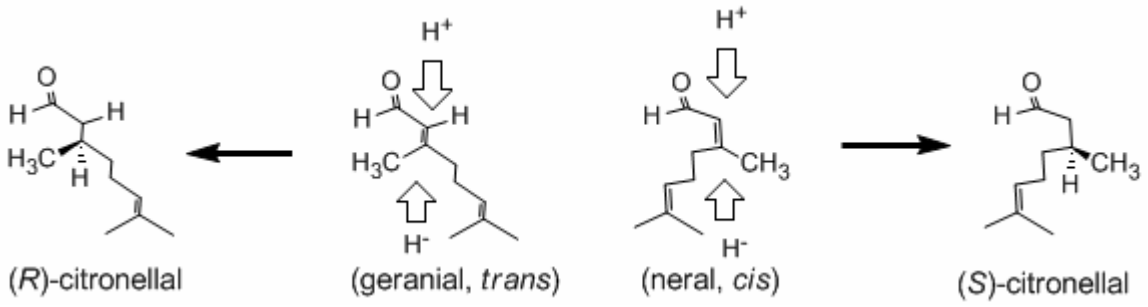

Figure 5-20. Proposed mechanism for the reduction of geranial or neral by OYEs.

A key substrate for the EI and EII enone reductases was the 2-phenyl-2-butenal, since both purified enzymes afforded the corresponding (*R*) 2-phenyl-butanal in 97% *ee*. In our hands, prolonged incubation of the above enal with all the enzymes tested led to a racemic product. We never succeeded in obtaining only one enantiomer, even at a lower pH (i.e. 4.8). Also, we did not observe any conversion with YNL234c. The observed enantioselectivity for α-methyl-cinnamaldehyde was also low (Table 5-14).

Nitro-alkenes were excellent substrates for OYEs as well as for Ltb4dh (Table 5-15). Unfortunately, a racemic mixture of 2-nitro-1-phenyl propane was obtained in both pH 7.0 and pH 4.8 for the last entry. Rapid release of the intermediate nitronate before protonation in the catalytic center, or enzyme-mediated racemization of the obtained chiral nitro-alkane, are two possible explanations that we did not investigate further in this work.

Table 5-15. Nitro-akenes.

Substrate	% Conversion
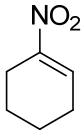 1-Nitro-1-cyclohexene	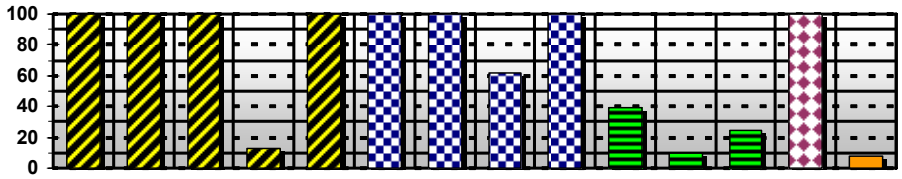
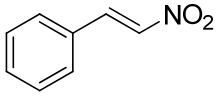 trans-β-nitrostyrene	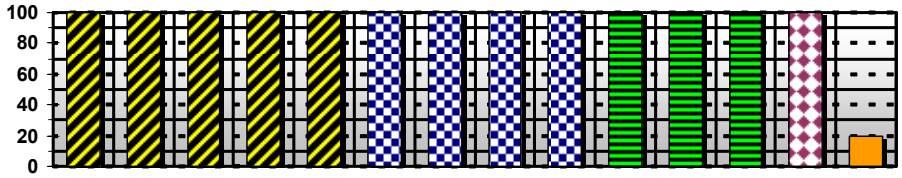
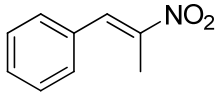 2-Nitro-1-phenylpropene	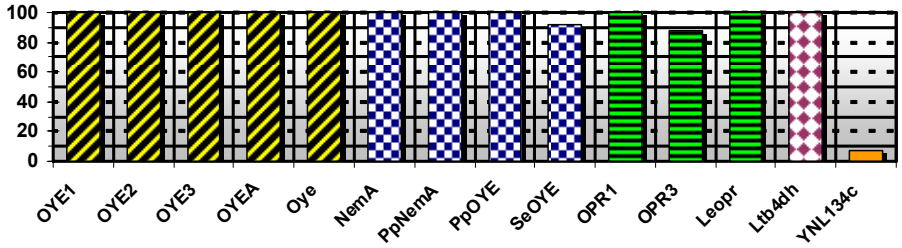

Concluding Remarks and Future Work

The aim of this study was dual: production of previously uncharacterized alkene reductases and investigation of their substrate specificity. We successfully created a collection of sixteen clones out of which only one failed to overexpress in *E. coli*. One of these clones encodes a yeast enzyme with previously uncharacterized function. Our efforts towards the purification of YNL134c from its native host suggested that OYE2 and

OYE3 are the key players for the majority of biotransformation with enones and enals in bakers' yeast since the YNL134c showed narrow substrate specificity. Therefore, whenever low stereoselectivities are observed with this microorganism, the most reasonable explanation is racemization of the obtained product or inherent incapability of the OYEs to produce a single enantiomer. The possibility of 'another' alkene-reductase with opposite stereopreference is limited, if any.

Our substrate specificity studies among OYEs uncovered:

- an extremely rigid action mode of all OYEs with α or β-substituted cyclohexenones probably due to the constraints that the planar of flavin imposes.
- a promising flexibility when straight chain alkenes were employed.

The case of citral is important for two reasons. First and foremost, it underlines the necessity of more than one biocatalyst able to perform a similar transformation. For example, from this collection of OYEs, OYE2 appeared the more suitable biocatalyst for production of (*R*)-citronellal and NemA for the production of the (*S*) enantiomer. In principle, after this rapid screening, the next logical step is the scale-up of the process. Microbial transformations that have been explored so far suffer from low yields, mainly because of concomitant reduction of the carbonyl group.[433] Gene deletions in *E. coli* can be easily constructed, as we already discussed in Chapter 3, and thus this bacterium is a promising workhorse for the production of both enantiomers of citronellal in a pure form.

Secondly, citral may be proved useful probe for further structure-function studies among the old yellow enzyme family members. In fact, citral is the only natural product after the 12-oxophytodienoic acid for which divergent activity has been observed in this family. Considering the constantly increasing number of crystal structures from OYE members the last few years, a co-crystallization of any OYE with neral or geranial seems a feasible task and probably useful since none of the available structures contains a

straight chain activated alkene. In parallel, compounds with similar to citral structures may help us to discover the limits of the observed diversity.

In this work, for the first time, the stereoselectivity of Ltb4dh was examined. Even though the substrate specificity of this medium chain reductase is narrower compared to that of OYEs, it is also less predictable. An important mechanistic detail, the proton donor during the reduction of the perillaldehyde, is missing and therefore experiments with labeled NADPH and site-directed mutagenesis based on the existed crystal structure may clarify this point. It will also be of great interest to explore whether the other AOR homologues possess the same substrate specificity.

In conclusion, our decision to analyze genomes from fungi, bacteria, plants and mammals and not to limit ourselves to one species was proved very useful. For example, we could not have observed any diversity in this library if we limited to *S. cerevisiae*'s genome. For the expansion of the current library the most challenging task is prediction of putative alkene reductases from the medium chain reductase family.

APPENDIX A
ILLUSTRATION OF CONSTRUCTION OF GENE KNOCK-OUTS IN *E.COLI*

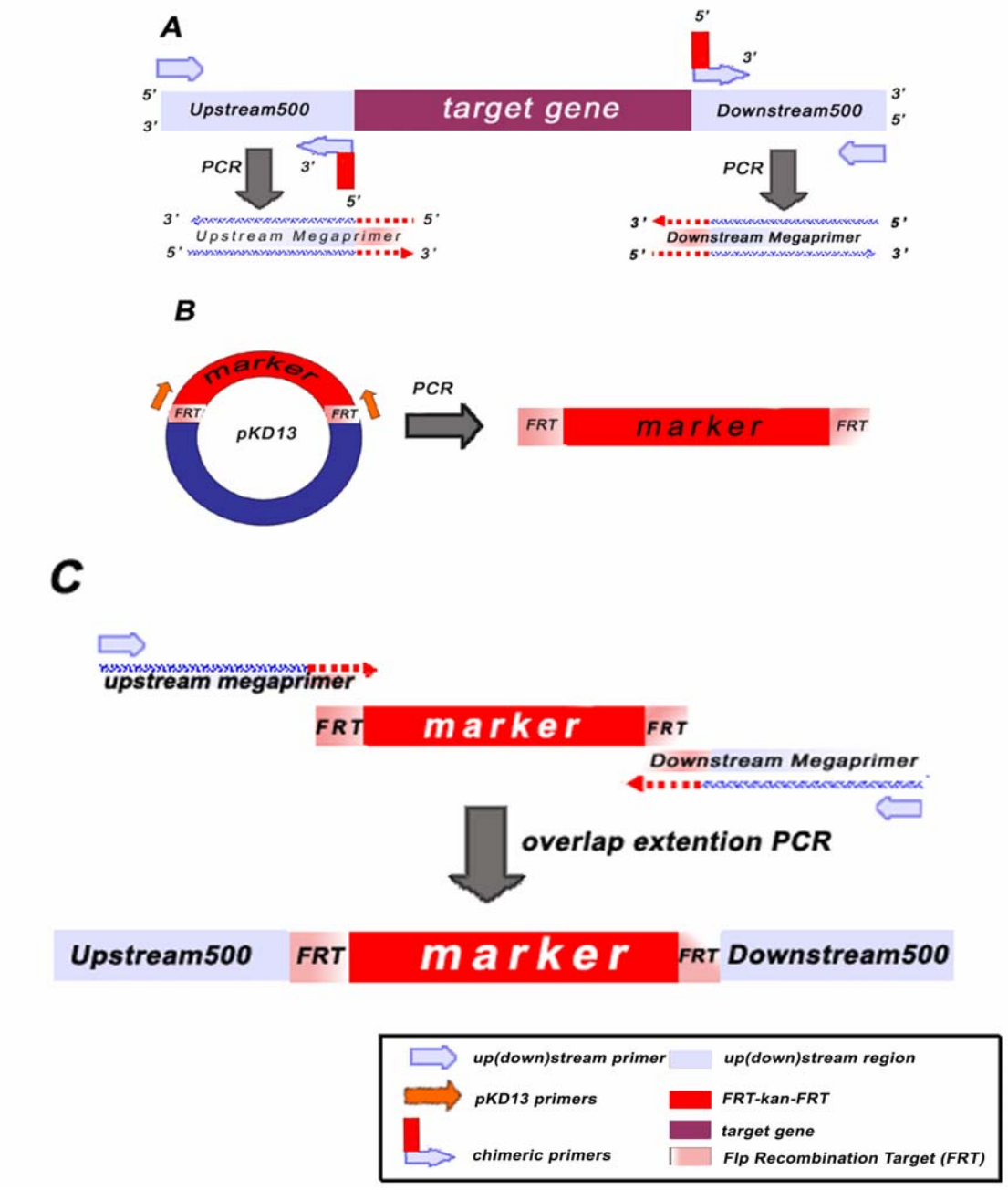

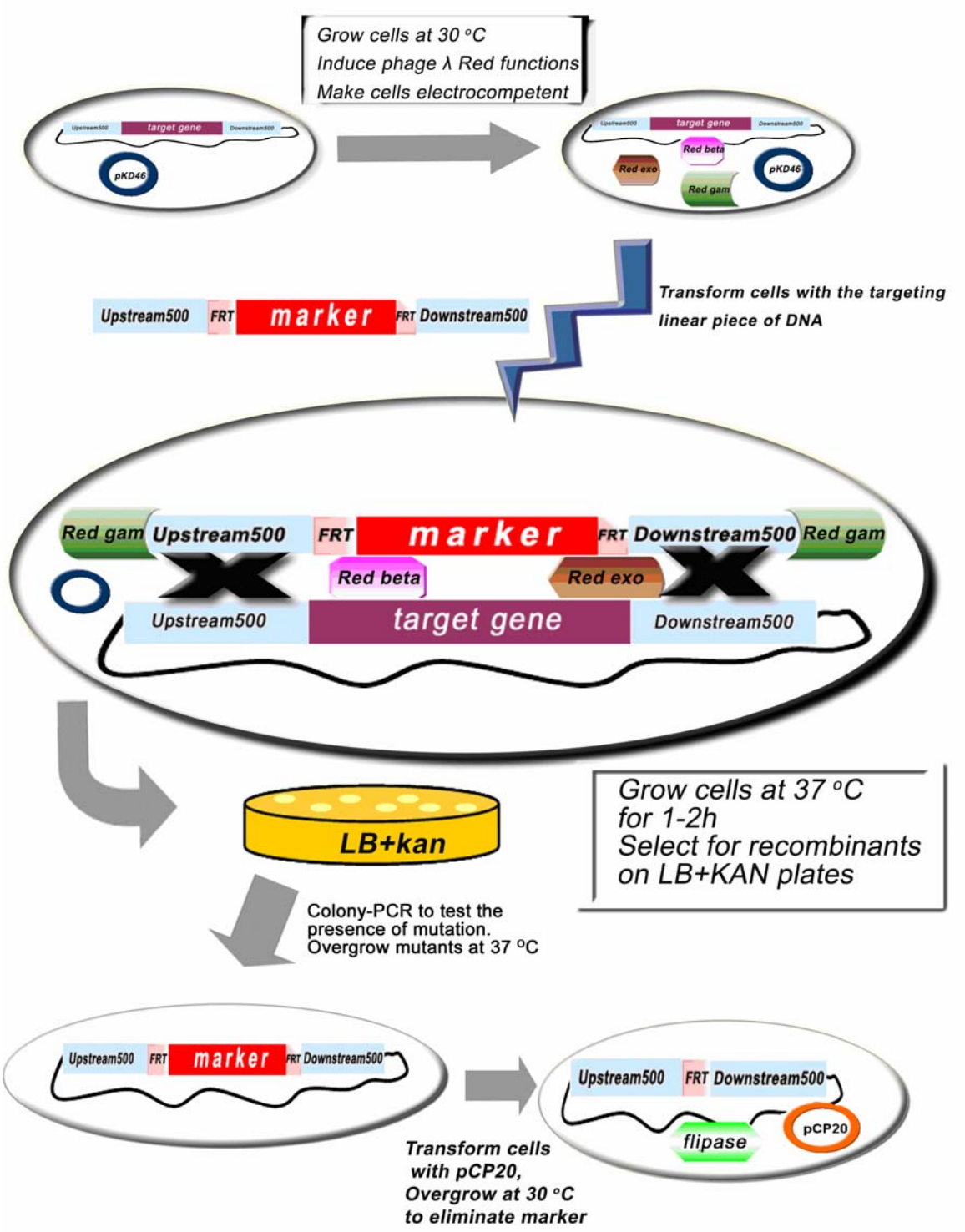
Grow cells at 30 °C
Induce phage λ Red functions
Make cells electrocompetent
Upstream500
target gene
Downstream500
pKD46
Red beta
Red exo
Red gam
Upstream500 FRT marker FRT Downstream500
Transform cells with the targeting linear piece of DNA
Red gam
Upstream500
FRT
marker
FRT
Downstream500
Red gam
Red beta
Red exo
Upstream500
target gene
Downstream500
LB+kan
Grow cells at 37 °C
for 1-2h
Select for recombinants
on LB+KAN plates
Colony-PCR to test the presence of mutation.
Overgrow mutants at 37 °C
Upstream500 FRT marker FRT Downstream500
Upstream500 FRT Downstream500
flipase
pCP20
Transform cells with pCP20,
Overgrow at 30 °C
to eliminate marker

APPENDIX B
LIST OF STRAINS AND PLASMIDS

Strain or Plasmid	Description	Source
BW25113 (pKD46)	*lacI*^{q} *rrnB*$_{T14}$ Δ *lacZ*$_{WJ16}$ *hsdR514* Δ *araBAD*$_{AH33}$ Δ *rhaBAD*$_{LD78}$	CGSC#: 7630
BW25141 (pKD13)	*lacI*^{q} *rrnB*$_{T14}$ Δ *lacZ*$_{WJ16}$ Δ *phoBR580 hsdR514* Δ *araBAD*$_{AH33}$ Δ *rhaBAD*$_{LD78}$ *galU95 endA*$_{BT333}$ *uidA* Δ (*Mlu*I)::*pir*$^+$ *recA1*	CGSC#: 7633
BT340 (pCP20)	F$^-$ λ$^-$ (Φ80*lac*ZΔM15) *end*A1 *recA*1 *sup*E44 *thi*-1 *gyrA*96*hsdr*17 *rel*A1? Δ(*lacZYA*-*argF*)U169	CGSC#: 7629
BL21(DE3)	F$^-$, *omp*T, *hsd*S$_B$(r$_B^-$m$_B^-$), *dcm*$^+$, *gal*, λ(DE3) *ton*A	Invitrogen
TOP10	F´ *mcr*A Δ*(mrr-hsd*RMS-*mcr*BC) Φ80*lac*ZΔM15 Δ*lac*X74 *rec*A1 *deo*R *ara*D139 Δ*(ara-leu)*7697 *gal*U *gal*K *rps*L (StrR) *end*A1 *nup*G	Invitrogen
KC8	*hsd*R, *leu*B600, *trp*C9830, *pyr*F::Tn5, *his*B463, *lac*ΔX74, *str*A, galU, K	Clontech
BY4742	MATα, *leu*2, *ura*3, *his*3, *lys*2	Dr. Thomas Lyons
DAY128	*MAT*a *ura3-52 leu2Δ1 trp1Δ63 his3Δ200 oye2-Δ2::HIS3 oye3-Δ2::TRP1*	Dr. David Amberg

APPENDIX C
LIST OF PRIMERS

Table C-1. Oligonucleotides used to create *pgi* mutant.

Name (length)	5' to 3' primer sequence	Application
pKD13F (20nt)	**GTGTAGGCTGGAGCTGCTTC**[a]	pKD13 specific primer used to amplify FRT-kan-FRT cassette
pKD13R (20nt)	**ATTCCGGGGATCCGTCGACC**	pKD13 specific primer used to amplify FRT-kan-FRT cassette
pgiUpF500 (24nt)	TTTTCAGCCTTGGCACAAGGGAAG	*E.coli* specific primer used to amplify Upstream500 region
pgiDownR500 (23nt)	TTTCCCTTCATTGAATGAATGGAG	*E.coli* specific primer used to amplify Downstream500 region
pgiDownF-pKD13R (45nt)	**GGTCGACGGATCCCCGGAAT** TCATCGTCGATATGTAGGCCGGAT	Long chimeric primer used to join FRT-kan-FRT fragment with Upstream 500 region
pgiUpR-pKD13F (44nt)	**GAAGCAGCTCCAGCCTACAC**[b] TAGCAATACTCTTCTGATTTTGAG	Long chimeric primer used to join FRT-kan-FRT fragment with Downstream 500 region
PgiF (24nt)	AACATCAATCCAACGCAGACCGCT	*E.coli* specific primer used to detect pgi mutants
PgiR (24nt)	TTAACCGCGCCACGCTTTATAGCG	*E.coli* specific primer used to detect pgi mutants
pgi550F (24nt)	CAGACATAACTACCTCGTGTCAGG	*E.coli* specific primer used to detect pgi mutants
pgi550R (24nt)	AAGTCGCCGCAAGCGCAGATATGG	*E.coli* specific primer used to detect pgi mutants
k1 (20nt)	CAGTCATAGCCGAATAGCCT	*kan* specific primer used to detect the FRT-kan-FRT insertion
k2 (20nt)	CGGTGCCCTGAATGAACTGC	*kan* specific primer used to detect the FRT-kan-FRT insertion

[a] Bolding indicates regions of complementarity between oligonucleotides pairs. [b]Italics indicates reverse complementarity

Table C-2. Oligonucleotides used to create *zwf* mutant.

Name (length)	5' to 3' primer sequence	Application
pKD13F (20nt)	GTGTAGGCTGGAGCTGCTTC	pKD13 specific primer used to amplify FRT-kan-FRT cassette
pKD13R (20nt)	ATTCCGGGGATCCGTCGACC	pKD13 specific primer used to amplify FRT-kan-FRT cassette
zwfUp500F (24nt)	ACAGAAACGATTCACCGTCGGTT C	*E. coli* specific primer used to amplify Upstream500 region
zwfDown500R (24nt)	TGGATAGTGTTCATAAGGCTGGT G	*E. coli* specific primer used to amplify Downstream500 region
zwfUp570F (23nt)	ATAGGGAGTGCCATTCGCCAGAC	*E. coli* specific primer used to amplify Upstream570 region
zwfDown570R (22nt)	CATCACACATGCCCGGAA CACC	*E. coli* specific primer used to amplify Upstream570 region
zwfDownF-pKD13R (45nt)	GGTCGACGGATCCCCGGAATTAA TATCTGCGCTTATCCTTTATGG	Long chimeric primer used to join FRT-kan-FRT fragment with Upstream 550 region
zwfUpR-pKD13F (45nt)	GAAGCAGCTCCAGCCTACACGTC ATTCTCCTTAAGTTAA CTAACCC	Long chimeric primer used to join FRT-kan-FRT fragment with Downstream 550 region
zwfF (24nt)	ATGCGGTAACGCAAACAGCCCAG	*E. coli* specific primer used to detect zwf mutants
zwfR (26nt)	TTACTCAAACTCATTCAAGGAACG AC	*E. coli* specific primer used to detect zwf mutants
zwf550F (24nt)	TGCCAGATGAAGTTTAAAATCAG G	*E. coli* specific primer used to amplify Upstream550 region
zwf550R (24nt)	AACCTGACCAACCGCATTCGCTT C	*E. coli* specific primer used to amplify Downstream550 region
k1 (20nt)	CAGTCATAGCCGAATAGCCT	kan specific primer used to detect the FRT-kan-FRT insertion
k2 (20nt)	CGGTGCCCTGAATGAACTGC	kan specific primer used to detect the FRT-kan-FRT insertion

Table C-3. Oligonucleotides used to create *pntAB* mutant.

Name (length)	5' to 3' primer sequence	Application
pKD13F (20nt)	GTGTAGGCTGGAGCTGCTTC	pKD13 specific primer used to amplify FRT-kan-FRT cassette
pKD13R (20nt)	ATTCCGGGGATCCGTCGACC	pKD13 specific primer used to amplify FRT-kan-FRT cassette
UpPntA510 (29nt)	CGCCTTGCGCAAACCAGGTACT GGTATTG	*E. coli* specific primer used to amplify Upstream510 region specific to *E. coli* BL21(DE3)
Down510PntBR (26nt)	GGCGATTCAACGTGCGATTGAC AGTG	*E. coli* specific primer used to amplify Downstream510 region specific to *E. coli* BL21(DE3)
PntAF (27nt)	GCATACCAAGAGAACGGTTAACC AATG	*E. coli* specific primer used to detect PntA region specific to *E. coli* BL21(DE3)
PntAR (27nt)	TTTGCGGAACATTTTCAGCATGC GCTG	*E. coli* specific primer used to detect PntA region specific to *E. coli* BL21(DE3)
PntBF (25nt)	ATGTCTGGAGGATTAGTTACAGC TG	*E. coli* specific primer used to detect PntB region specific to *E. coli* BL21(DE3)
PntBR (24nt)	TTACAGAGCTTTCAGGATTGCAT C	*E. coli* specific primer used to detect PntB region specific to *E. coli* BL21(DE3)
Up PntA R - pKD13F (52nt)	GAAGCAGCTCCAGCCTACACG ATATTCCCTTCCATCGGTTTTATT GATGATG	Long chimeric primer used to join FRT-kan-FRT fragment with Upstream 510 region specific to *E. coli* BL21(DE3)
Down pntB F- pKD13 R (50nt)	GGTCGACGGATCCCCGGAATC CCTGACGGCCTCTGCTGAGGC CGTCACTC	Long chimeric primer used to join FRT-kan-FRT fragment with Downstream 510 region specific to *E. coli* BL21(DE3)
k1 (20nt)	CAGTCATAGCCGAATAGCCT	kan specific primer used to detect the FRT-kan-FRT insertion
k2 (20nt)	CGGTGCCCTGAATGAACTGC	kan specific primer used to detect the FRT-kan-FRT insertion

Table C-4. Oligonucleotides used to create the library of En-Reductases

Name (length)	5' to 3' primer sequence	Application
pYEX4T-pIK2 UP (61)	TTTCACACAGGAAACAGCTATGACC ATGATTACGCCTTTCAGCAAAAAACC CCTCAAGACC	pYEX4T specific primer used for construction of pDJB2
pYEX4T-pIK2 Down (60)	GTAATGTCTGCCCCTAAGAAGATCG TCGTTTTGCCAGCTTTCCAGTCGGG AAACCTGTCG	pYEX4T specific primer used for construction of pDJB2
pDJB2Up-YPL171R (65)	CAGTGGTGGTGGTGGTGGTGCTCG AGTGCGGCCGCATCAGTTCTTGTTC CAACCTAAATCTACTG	pDJB2(3)-tagged Upstream primer used to amplify OYE3
pDJB2NcoI-YPL171F (62)	TCCAAAATCGGATCATCTGGTTCCG CGTCATATGCCCATGCCATTTGTAAA AGGTTTTGAGC	pDJB2(3)-tagged Downstream primer used to amplify OYE3
pDJB2NcoI-OYEAF (67)	TCCAAAATCGGATCATCTGGTTCCG CGTCATATGCCCATGGCTGTTCAAA AGTTATATGAATCGCAG	pDJB2(3)- tagged Upstream primer used to amplify OYEA
pDJB2Up-OYEAR (58)	CAGTGGTGGTGGTGGTGGTGCTCG AGTGCGGCCGCATCACTCAACCTTC TTGGTATCC	pDJB2(3)-tagged Downstream primer used to amplify OYEA
pDJB2NcoI-OYEBF (74)	TCCAAAATCGGATCATCTGGTTCCG CGTCATATGCCCATGAATGACCGAG GTGAATTGTTTAAACCCATCAAAG	pDJB2(3)- tagged Upstream primer used to amplify OYEB
pDJB2NcoI-OYEBF (64)	CAGTGGTGGTGGTGGTGGTGCTCG AGTGCGGCCGCATCACTTTGATTGA AGGAACTCTTTGCTA	pDJB2(3)-tagged Downstream primer used to amplify OYEB
pDJB2-NemAF (71)	TCCAAAATCGGATCATCTGGTTCCG CGTCATATGCCCATGTCATCTGAAAA ACTGTATTCCCCACTGAAAG	pDJB2(3)- tagged Upstream primer used to amplify NemA
pDJB2-NemAR (63)	CAGTGGTGGTGGTGGTGGTGCTCG AGTGCGGCCGCATTACAACGTCGG GTAATCGGTATAGCC	pDJB2(3)-tagged Downstream primer used to amplify NemA
pDJB2-OYE2F (69)	TCCAAAATCGGATCATCTGGTTCCG CGTCATATGCCCATGCCATTTGTTAA GGACTTTAAGCCACAAGC	pDJB2(3)- tagged Upstream primer used to amplify OYE2
pDJB2-OYE2R (57)	CAGTGGTGGTGGTGGTGGTGCTCG AGTGCGGCCGCATTAATTTTTGTCC CAACCGAG	pDJB2(3)-tagged Downstream primer used to amplify OYE2
pDJB2-oyeF (65)	TCCAAAATCGGATCATCTGGTTCCG CGTCATATGCCCATGTCGTACATGA ACTTTGACCCTAAGC	pDJB2(3)- tagged Upstream primer used to amplify oye
pDJB2-oyeR (72)	CAGTGGTGGTGGTGGTGGTGCTCG AGTGCGGCCGCATTAGTACTTCTTTT CCTCTTTCTTGTAACCCTTTGC	pDJB2(3)-tagged Downstream primer used to amplify oye
pDJB2-ltb4dhF (60)	TCCAAAATCGGATCATCTGGTTCCG CGTCATATGCCCATGGTACAAGCTA AGACCTGGAC	pDJB2(3)- tagged Upstream primer used to amplify Ltb4dh
pDJB2-ltb4dhR (63)	CAGTGGTGGTGGTGGTGGTGCTCG AGTGCGGCCGCATCACGCTTTCACT ATAGTCTTCCCCAG	pDJB2(3)-tagged Downstream primer used to amplify Ltb4dh

Table C-4. Continued.

pDJB2-OPR1F (65)	TCCAAAATCGGATCATCTGGTTCCG CGTCATATGCCCATGGAAAACGGAG AAGCAAAACAGAGTG	pDJB2(3)- tagged Upstream primer used to amplify OPR1
pDJB2-OPRR (63)	CAGTGGTGGTGGTGGTGGTGCTCG AGTGCGGCCGCATTAAGCTGTTGAT TCGAGGAAAGGGTA	pDJB2(3)- tagged Downstream primer used to amplify OPR1
pDJB2-OPR2F (60)	TCCAAAATCGGATCATCTGGTTCCG CGTCATATGCCCATGGAAATGGTAA ACGCAGAAGC	pDJB2(3)- tagged Upstream primer used to amplify OPR2
pDJB2-OPR2R (61)	CAGTGGTGGTGGTGGTGGTGCTCG AGTGCGGCCGCATTATGAAGGTATA ATGACTTAGAGT	pDJB2(3)- tagged Downstream primer used to amplify OPR2
pDJB2-OPR3F (64)	TCCAAAATCGGATCATCTGGTTCCG CGTCATATGCCCATGACGGCGGCAC AAGGGAACTCTAAC	pDJB2(3)- tagged Upstream primer used to amplify OPR3
pDJB2-OPR3R (61)	CAGTGGTGGTGGTGGTGGTGCTCG AGTGCGGCCGCATCAGAGGCGGGA AAAAGGAGCCAAG	pDJB2(3)- tagged Downstream primer used to amplify OPR3
pDJB2-PPOYEF (68)	TCCAAAATCGGATCATCTGGTTCCG CGTCATATGCCCATGACACAATCAG AACTTTTCAAAACCACTC	pDJB2(3)- tagged Upstream primer used to amplify PpOYE
pDJB2-PPOYER (64)	CAGTGGTGGTGGTGGTGGTGCTCG AGTGCGGCCGCATTAGGATTTGTAA GTCGGGTAGTCGGTG	pDJB2(3)- tagged Downstream primer used to amplify PpOYE
pDJB2-PPNemAF (65)	TCCAAAATCGGATCATCTGGTTCCG CGTCATATGCCCATGAAACTCTTGC AACCGCTGCAAATCG	pDJB2(3)- tagged Upstream primer used to amplify PpNemA
pDJB2-PPNemAR (63)	CAGTGGTGGTGGTGGTGGTGCTCG AGTGCGGCCGCATCAAGCCTGCTTC AGGAACGGATAATC	pDJB2(3)- tagged Downstream primer used to amplify PpNemA
pDJB2-seOYEF (63)	TCCAAAATCGGATCATCTGGTTCCG CGTCATATGCCCATGTCCGAATCGC TCAAACTGCTGAC	pDJB2(3)- tagged Upstream primer used to amplify SeOYE
pDJB2-seOYER (62)	AGTGGTGGTGGTGGTGGTGCTCGA GTGCGGCCGCATTAGACAGATGCTG CTTCCAAACTGG	pDJB2(3)- tagged Downstream primer used to amplify SeOYE
pDJB2-LeoprF (61)	TCCAAAATCGGATCATCTGGTTCCG CGTCATATGCCCATGGAAAATAAAG TCGTTGAAGAG	pDJB2(3)- tagged Upstream primer used to amplify Leopr
pDJB2-LeoprR (66)	CAGTGGTGGTGGTGGTGGTGCTCG AGTGCGGCCGCATCATGTCATGGTT TCTAGAAATGGATAATC	pDJB2(3)- tagged Downstream primer used to amplify Leopr

Table C-4. Continued.

pDJB2-orf14F (61)	TCCAAAATCGGATCATCTGGTTCCG CGTCATATGCCCATGTCCGCCTCGA TTCCAGAAACC	pDJB2(3)- tagged Upstream primer used to amplify YNL134c
pDJB2-orf14R (64)	CAGTGGTGGTGGTGGTGGTGCTCG AGTGCGGCCGCATTATTTCAAGACG GCAACCAACTTTTCG	pDJB2(3)- tagged Downstream primer used to amplify YNL134c
lacI-START (23)	GCGGGATCGAGATCTCGATCCTC	pDJB2 specific primer for sequencing lacI region
lacI-CONT (24)	CTCGCAATCAAATTCAGCCGATAG	pDJB2 specific primer for sequencing lacI region
GST-END (25)	ATGGACCCAATGTGCCTGGATG	pDJB2(3) specific primer for sequencing Upstream region of en-reductases genes

LIST OF REFERENCES

1. Horecker, B. L. *J. Biol. Chem.* **2002**, 277, 47965-47971.

2. Voet D.; Voet J.; *Biochemistry* 2nd ed.; Wiley, New York, 1995.

3. Encyclopedia of *Eschericia coli* K-12 Genes and Metabolism. Accessed on November 2006. http://ecocyc.org/

4. Sanchez, A. M.; Bennett, G. N.; San, K.-Y. *J. Biotechnol.* **2006**, *117*, 395-405.

5. Portais, J.-C.; Delort, A.-M. *FEMS Microbiol. Rev.* **2002**, *26*, 375-402.

6. Cohen, S. S. *Nature* **1951**, 168, 746-7.

7. Scott, D. B.; Cohen, S. S. *Biochem. J.* **1953**, 55, 33-6.

8. Wang, C. H.; Stern, I.; Gilmour, C. M.; Klungsoyr, S.; Reed, D. J.; Bialy, J. J.; Christensen, B. E.; Cheldelin, V. H. *J. Bacteriol.* **1958**, *76*, 207-16.

9. Rittenberg, D.; Ponticorvo, L. *J. Biol. Chem.* **1962**, *237*, C2709-10.

10. Model, P.; Rittenberg, D. *Biochemistry* **1967**, *6*, 69-80.

11. Zablotny, R.; Fraenkel, D. G. *J. Bacteriol.* **1967**, *93*, 1579-81.

12. Caprioli, R.; Rittenberg, D. *Proc. Natl. Acad. Sci. U S A.* **1968**, *60*, 1379-82.

13. Caprioli, R.; Rittenberg, D. *Biochemistry* **1969**, *8*, 3375-84.

14. Thomas, A. D.; Doelle, H. W.; Westwood, A. W.; Gordon, G. L. *J. Bacteriol.* **1972**, *112*, 1099-105.

15. Orthner, C. L.; Pizer, L. I. *J. Biol. Chem.* **1974**, *249*, 3750-5.

16. Csonka, L. N.; Fraenkel, D. G. *J. Biol. Chem.* **1977**, *252*, 3382-91.

17. Orozco de Silva, A.; Fraenkel, D. G. *J. Biol. Chem.* **1979**, *254*, 10237-42.

18. Wang, C. H. *Meth. Microbiol.* **1972**; 185-230.

19. Katz, J.; Wood, H. G. *J. Biol. Chem.* **1960**, *235*, 2165-77.

20. Katz, J.; Wood, H. G. *J. Biol. Chem.* **1963**, *238*, 517-23.

21. Katz, J.; Rognstad, R. *Biochemistry* **1967**, *6*, 2227-47.

22. Caprioli, R.; Rittenberg, D. *Proc. Natl. Acad. Sci. U S A.* **1968**, *61*, 1422-7.

23. Fraenkel, D. G.; Vinopal, R. T. *Annu. Rev. Microbiol.* **1973**, *27*, 69-100.

24. Csonka, L. N. *J. Biol. Chem.* **1977**, *252*, 3392-8.

25. Lowenstein, J. M. *J. Biol. Chem.* **1961**, *236*, 1213-6.

26. Rose, I. A. *J. Biol. Chem.* **1961**, *236*, 603-9.

27. Fraenkel, D. G.; Levisohn, S. R. *J. Bacteriol.* **1967**, *93*, 1571-8.

28. Wolf, R. E., Jr.; Prather, D. M.; Shea, F. M. *J. Bacteriol.* **1979**, *139*, 1093-6.

29. Baker, H. V., Wolf, R. E., Jr. *Proc. Natl. Acad. Sci. U S A.* **1984**, *81*, 7669-73.

30. Rowley, D. L.; Fawcett, W. P.; Wolf, R. E., Jr. *J. Bacteriol.* **1992**, *174*, 623-6.

31. Pease, A. J.; Wolf, R. E., Jr. *J. Bacteriol.* **1994**, *176*, 115-22.

32. Sanford, K.; Soucaille, P.; Whited, G.; Chotani, G. *Curr. Opin. Microbiol.* **2002**, *5*, 318-322.

33. Sauer, U. *Curr. Opin. Biotechnol.* **2004**, *15*, 58-63.

34. Ogino, T.; Arata, Y.; Fujiwara, S. *Biochemistry* **1980**, *19*, 3684-91.

35. Varma, A.; Palsson, B. O. *J. Theor. Biol.* **1993**, *165*, 503-522.

36. Varma, A.; Palsson, B. O. *J. Theor. Biol.* **1993**, *165*, 477-502.

37. Szyperski, T. *Eur. J. Biochem.* **1995**, *232*, 433-48.

38. Tsai, P. S.; Hatzimanikatis, V.; Bailey, J. E. *Biotechnol. Bioeng.* **1996**, *49*, 139-50.

39. Frey, A. D.; Fiaux, J.; Szyperski, T.; Wuthrich, K.; Bailey, J. E.; Kallio, P. T. *Appl. Environ. Microb.* **2001**, *67*, 680-687.

40. Szyperski, T.; Bailey, J. E.; Wuethrich, K. *Trends Biotechnol.* **1996**, *14*, 453-459.

41. Ponce, E.; Martinez, A.; Bolivar, F.; Valle, F. *Biotechnol. Bioeng.* **1998**, *58*, 292-295.

42. Follstad, B. D.; Stephanopoulos, G. *Eur. J. Biochem.* **1998**, *252*, 360-371.

43. Schmidt, K.; Nielsen, J.; Villadsen, J. *J. Biotechnol.* **1999**, *71*, 175-189.

44. Fiaux, J.; Andersson, C. I. J.; Holmberg, N.; Buelow, L.; Kallio, P. T.; Szyperski, T.; Bailey, J. E.; Wuethrich, K. *J. Am. Chem. Soc.* **1999**, *121*, 1407-1408.

45. Sauer, U.; Lasko, D. R.; Fiaux, J.; Hochuli, M.; Glaser, R.; Szyperski, T.; Wuthrich, K.; Bailey, J. E. *J. Bacteriol.* **1999**, *181*, 6679-6688.

46. Edwards, J. S.; Palsson, B. O. *Proc. Natl. Acad. Sci. U S A.* **2000**, *97*, 5528-5533.

47. Edwards, J. S.; Palsson, B. O. *BMC bioinformatics* **2000**, *1*, 1.

48. Edwards, J. S.; Palsson, B. O. *Biotechnol. Prog.* **2000**, *16*, 927-939.

49. Oh, M.-K.; Liao, J. C. *Biotechnol. Prog.* **2000**, *16*, 278-286.

50. Canonaco, F.; Hess, T. A.; Heri, S.; Wang, T.; Szyperski, T.; Sauer, U. *FEMS Microbiol. Lett.* **2001**, *204*, 247-252.

51. Emmerling, M.; Dauner, M.; Ponti, A.; Fiaux, J.; Hochuli, M.; Szyperski, T.; Wuthrich, K.; Bailey, J. E.; Sauer, U. *J. Bacteriol.* **2002**, *184*, 152-164.

52. Edwards, J. S.; Ibarra, R. U.; Palsson, B. O. *Nature Biotechnol.* **2001**, *19*, 125-130.

53. Edwards, J. S.; Ramakrishna, R.; Palsson, B. O. *Biotechnol. Bioeng.* **2002**, *77*, 27-36.

54. Flores, S.; Gosset, G.; Flores, N.; de Graaf, A. A.; Bolivar, F. *Metab. Eng.* **2002**, *4*, 124-137.

55. Fischer, E.; Sauer, U. *Eur. J. Biochem.* **2003**, *270*, 880-891.

56. Peng, L.; Shimizu, K. *Appl. Microbiol. Biotechnol.* **2003**, *61*, 163-178.

57. Kabir, M. M.; Shimizu, K. *J. Biotechnol.* **2003**, *105*, 11-31.

58. Kabir, M. M.; Shimizu, *Appl. Microbiol. Biotechnol.* **2003**, *62*, 244-255.

59. Brumaghim, J. L.; Li, Y.; Henle, E.; Linn, S. *J. Biol. Chem.* **2003**, *278*, 42495-42504.

60. Hua, Q.; Yang, C.; Baba, T.; Mori, H.; Shimizu, K. *J. Bacteriol.* **2003**, *185*, 7053-7067.

61. Zhao, J.; Shimizu, K. *J. Biotechnol.* **2003**, *101*, 101-117.

62. Jiao, Z.; Baba, T.; Mori, H.; Shimizu, K. *FEMS Microbiol. Lett.* **2003**, *220*, 295-301.

63. Jiao, Z.; Baba, T.; Mori, H.; Shimizu, K. *Appl. Microbiol. Biotechnol.* **2004**, *64*, 91-98.

64. Al Zaid Siddiquee, K.; Arauzo-Bravo, M. J.; Shimizu, K. *Appl. Microbiol. Biotechnol.* **2004**, *63*, 407-417.

65. Jiao, Z.; Baba, T.; Mori, H.; Shimizu, K. *Metab. Eng.* **2004**, *6*, 164-174.

66. Sauer, U.; Canonaco, F.; Heri, S.; Perrenoud, A.; Fischer, E. *J. Biol. Chem.* **2004**, *279*, 6613-6619.

67. Weber, J.; Kayser, A.; Rinas, U. *Microbiology*, **2005**, *151*, 707-716.

68. Stephanopoulos G. N., Aristidou A., Nielsen N. *Metabolic Engineering Principles and Methodologies*; Academic Press: San Diego, 1988.

69. Pramanik, J.; Keasling, J. D. *Biotechnol. Bioeng.* **1998**, *60*, 230-8.

70. Schuster, S.; Dandekar, T.; Fell, D. A. *Trends Biotechnol.* **1999**, *17*, 53-60.

71. Mahadevan, R.; Edwards, J. S.; Doyle, F. J., III *Biophys. J.* **2002**, *83*, 1331-1340.

72. Lee, S. Y.; Papoutsakis, E. T. *Metabolic Engineering*; Dekker: New York, 1999.

73. Eden E. Accessed on November 2006. http://www.cs.technion.ac.il/~eraneden/ .

74. Palsson B. Accessed on November 2006. http://gcrg.ucsd.edu/classes/2_10_fba.pdf

75. Kholodenko B. N., Westerhoff. H. V *Metabolic Engineering in the Post Genomic Era*; Horizon Bioscience: Norfolk, 2004.

76. Wiechert, W. *Metab. Eng.* **2001**, *3*, 195-206.

77. Wiechert, W.; Mollney, M.; Petersen, S.; de Graaf, A. A. *Metab. Eng.* **2001**, *3*, 265-283.

78. Szyperski, T. *Q. Rev. Biophys.* **1998**, *31*, 41-106.

79. Follstad, B. D.; Stephanopoulos, G. *Eur. J. Biochem.* **1998**, *252*, 360-371.

80. van Winden, W.; Verheijen, P.; Heijnen, S. *Metab. Eng.* **2001**, *3*, 151-162.

81. Edwards, J. S.; Ibarra, R. U.; Palsson, B. O. *Nature Biotechnol.* **2001**, *19*, 125-30.

82. Segre, D.; Vitkup, D.; Church, G. M. *Proc. Natl. Acad. Sci. U S A.* **2002**, *99*, 15112-15117.

83. Kelleher, J. K. *Metab. Eng.* **2001**, *3*, 100-110.

84. Boros L.G., Cascante M. and Lee W.-N.P., Eds. *Metabolic profiling. Its role in biomarker discovery and gene function analysis* Kruwer Academic Publishers, 2003;pp 141-169.

85. Neidhardt, F.C., Curtiss III, R., Ingraham, J.L., Lin, E.C.C., Brooks Low, K., Magasanik, B., Reznikoff, W.S., Riley, M., Schaechter, M., and Umbarger, H.E., Eds. *Escherichia coli and Salmonella typhimurium*. ASM Press, Washington, D.C. 1996

86. Schmidt, K.; Nielsen, J.; Villadsen, J. *J. Biotechnol.* **1999**, *71*, 175-189.

87. Szyperski, T. *Q. Rev. Biophys.* **1998**, *31*, 41-106.

88. Szyperski, T.; Bailey, J. E.; Wuethrich, K. *Trends Biotechnol.* **1996**, *14*, 453-459.

89. Szyperski, T.; Glaser, R. W.; Hochuli, M.; Fiaux, J.; Sauer, U.; Bailey, J. E.; Wuthrich, K. *Metab. Eng.* **1999**, *1*, 189-197.

90. Wittmann, C. *Adv. Biochem. Eng. Biotechnol.* **2002**, *74*, 39-64.

91. Dauner, M.; Sauer, U. *Biotechnol. Prog.* **2000**, *16*, 642-9.

92. Boonstra, B.; French, C. E.; Wainwright, I.; Bruce, N. C. *J. Bacteriol.* **1999**, *181*, 1030-1034.

93. Hanson, R. L.; Rose, C. *J. Bacteriol.* **1980**, *141*, 401-4.

94. Gosset, G. *Microb. Cell Fact.* **2005**, *4*, 14

95. Shimizu, K. *Adv. Biochem. Eng. Biotechnol.* **2004**, *91*, 1-49.

96. Cozzone, A. J.; El-Mansi, M. *J. Mol. Microbiol. Biotechnol.* **2005**, *9*, 132-146.

97. Kimata, K.; Tanaka, Y.; Inada, T.; Aiba, H. *EMBO J.* **2001**, *20*, 3587-3595.

98. van Winden, W.; Schipper, D.; Verheijen, P.; Heijnen, J. *Metab. Eng.* **2001**, *3*, 322-343.

99. Zamboni, N.; Fischer, E.; Sauer, U. *BMC Bioinformatics* **2005**, *6*, 209

100. van Winden, W.; Verheijen, P.; Heijnen, S. *Metab. Eng.* **2001**, *3*, 151-162.

101. Wiechert, W.; Mollney, M.; Petersen, S.; de Graaf, A. A. *Metab. Eng.* **2001**, *3*, 265-283.

102. Bailey, J. E. *Science* **1991**, *252*, 1668-75.

103. Mertens, R.; Greiner, L.; van den Ban, E. C. D.; Haaker, H. B. C. M.; Liese, A. *J. Mol. Catal. B* **2003**, *24-25*, 39-52.

104. Lundquist, R.; Olivera, B. M. *J. Biol. Chem.* **1971**, *246*, 1107-16.

105. Chenault, H. K.; Whitesides, G. M. *Appl. Biochem. Biotech.* **1987**, *14*, 147

106. Wichmann, R.; Vasic-Racki, D. *Adv. Biochem. Eng.Biotech.* **2005**, *92*, 225-260.

107. Sigma-Aldrich. Accessed on May 2006. www.sigmaaldrich.com.

108. Institute of Biomolecular Design. Accessed on November 2006. http://redpoll.pharmacy.ualberta.ca/CCDB/cgi-bin/STAT_NEW.cgi

109. Leonida, M. D. *Curr. Med. Chem.***2001**, *8*, 345-369.

110. Eckstein, M.; Daussmann, T.; Kragl, U. *Biocatal. Biotransfor.* **2004**, *22*, 89-96.

111. Wolberg, M.; Hummel, W.; Wandrey, C.; Muller, M. *Angew. Chem. Int. Ed.* **2000**, *39*, 4306-4308.

112. Wong, C.-H.; Whitesides, G. M. *J. Am. Chem. Soc.* **1981**, *103*, 4890-9.

113. Wolberg, M.; Kaluzna, I. A.; Mueller, M.; Stewart, J. D. *Tetrahedron: Asymmetry* **2004**, *15*, 2825-2828.

114. Kalaitzakis, D.; Rozzell, J. D.; Kambourakis, S.; Smonou, I. *Org. Lett.* **2005**, *7*, 4799-4801.

115. Seelbach, K.; Riebel, B.; Hummel, W.; Kula, M.-R.; Tishkov, V. I.; Egorov, A. M.; Wandrey, C.; Kragl, U. *Tetrahedron Lett.* **1996**, *37*, 1377-80.

116. Julich Chiral Solutions. Accessed on May 2006. www.julich.com/public/default.cfm.

117. Woodyer, R.; Zhao, H.; van der Donk, W. A. *FEBS J.* **2005**, *272*, 3816-3827.

118. Kataoka, M.; Rohani, L. P. S.; Wada, M.; Kita, K.; Yanase, H.; Urabe, I.; Shimizu, S. *Biosci. Biotechnol. Biochem.* **1998**, *62*, 167-169.

119. Ema, T.; Yagasaki, H.; Okita, N.; Takeda, M.; Sakai, T. *Tetrahedron* **2006**, *62*, 6143-6149.

120. Weckbecker, A.; Hummel, W. *Biotechnol. Lett.* **2004**, *26*, 1739-1744.

121. Xu, Z.; Liu, Y.; Fang, L.; Jiang, X.; Jing, K.; Cen, P. *Appl. Microbiol. Biotechnol.* **2006**, *70*, 40-46.

122. Walton, A. Z.; Stewart, J. D. *Biotechnol. Prog.* **2004**, *20*, 403-411.

123. Hanson, R. L.; Goldberg, S.; Goswami, A.; Tully, T. P.; Patel, R. N. *Adv. Synth. Catal.* **2005**, *347*, 1073-1080.

124. van der Donk, W. A.; Zhao, H. *Curr. Opin. Biotechnol.* **2003**, *14*, 421-426.

125. Zhao, H.; van der Donk, W. A. *Curr. Opin. Biotechnol.* **2003**, *14*, 583-589.

126. Biocatalytic, Inc. Accessed on May 2006. www.biocatalytics.com.

127. Kataoka, M.; Rohani, L. P. S.; Yamamoto, K.; Wada, M.; Kawabata, H.; Kita, K.; Yanase, H.; Shimizu, S. *Appl. Microbiol. Biotechnol.* **1997**, *48*, 699-703.

128. van Beilen, J. B.; Duetz, W. A.; Schmid, A.; Witholt, B. *Trends Biotechnol.* **2003**, *21*, 170-177.

129. Duetz, W. A.; Van Beilen, J. B.; Witholt, B. *Curr. Opin. Biotechnol.* **2001**, *12*, 419-425.

130. Straathof, A. J. J.; Panke, S.; Schmid, A. *Curr. Opin. Biotechnol.* **2002**, *13*, 548-556.

131. Hummel, W. *Trends Biotechnol.* **1999**, *17*, 487-492.

132. J.D. Stewart, in *Environmental Catalysis*; Grassian V.H., Ed.; CRC Press, Boca Raton, FL, 2004; pp 649-665.

133. Held, M.; Schmid, A.; Van Beilen, J. B.; Witholt, B. *Pure Appl. Chem.* **2000**, *72*, 1337-1343.

134. Poulsen, B. R.; Nohr, J.; Douthwaite, S.; Hansen, L. V.; Iversen, J. J. L.; Visser, J.; Ruijter, G. J. G. *FEBS J.* **2005**, *272*, 1313-1325.

135. Moritz, B.; Striegel, K.; de Graaf, A. A.; Sahm, H. *Metab. Eng.* **2002**, *4*, 295-305.

136. Moreira dos Santos, M.; Raghevendran, V.; Koetter, P.; Olsson, L.; Nielsen, J. *Metab. Eng.* **2004**, *6*, 352-363.

137. Moreira dos Santos, M.; Thygesen, G.; Kotter, P.; Olsson, L.; Nielsen, J. *FEMS Yeast Res.* **2003**, *4*, 59-68.

138. Sanchez, A. M.; Bennett, G. N.; San, K.-Y. *J. Biotechnol.* **2005**, *117*, 395-405.

139. San, K.-Y.; Bennett, G. N.; Berrios-Rivera, S. J.; Vadali, R. V.; Yang, Y.-T.; Horton, E.; Rudolph, F. B.; Sariyar, B.; Blackwood, K. *Metab. Eng.* **2002**, *4*, 182-192.

140. Flores, S.; de Anda-Herrera, R.; Gosset, G.; Bolivar Francisco, G. *Biotechnol. Bioeng.* **2004**, *87*, 485-94.

141. Lim, S.-J.; Jung, Y.-M.; Shin, H.-D.; Lee, Y.-H. *J. Biosc. Bioeng.* **2002**, *93*, 543-549.

142. Sanchez, A. M.; Bennett, G. N.; San, K.-Y. *J. Biotechnol.* **2006**, *117*, 395-405.

143. Monroe M.;Pharkya P.;Chris, J.;Cirino P College of Engineering Research Symposium 2006. Accessed on November 2006. http://www.engr.psu.edu/symposium2006/papers/Session%202A%20-%20Biological%20Systems/Monroe.pdf.

144. Doig, S. D.; Avenell, P. J.; Bird, P. A.; Gallati, P.; Lander, K. S.; Lye, G. J.; Wohlgemuth, R.; Woodley, J. M. *Biotechnol. Prog.* **2002**, *18*, 1039-1046.

145. Doig, S. D.; Simpson, H.; Alphand, V.; Furstoss, R.; Woodley, J. M. *Enz. Microb. Tech.* **2003**, *32*, 347-355.

146. Medical Isotopes, Inc. Accessed on November 2006. http://medicalisotopes.com/index.asp

147. Alexeeva, S.; Hellingwerf, K. J.; Teixeira de Mattos, M. J. *J. Bacteriol.* **2002**, *184*, 1402-1406.

148. Alexeeva, S.; de Kort, B.; Sawers, G.; Hellingwerf, K. J.; de Mattos, M. J. *J. Bacteriol.* **2000**, *182*, 4934-40.

149. Kaluzna I., A.; Matsuda, T.; Sewell A., K.; Stewart J. D. *J. Am. Chem. Soc.* **2004**, *126*, 12827-32.

150. Aoshima, M.; Ishii, M.; Yamagishi, A.; Oshima, T.; Igarashi, Y. *Biotechnol. Bioeng.* **2003**, 84, 732-737.

151. Birren B; Green E. D.; Klapholz S,; Myers R. M, Roskams J. *Analyzing DNA: A Laboratory Manual : Genome Analysis*, Cold Spring Harbor Laboratory Press,1997

152. Kaluzna, I.; Andrew, A. A.; Bonilla, M.; Martzen, M. R.; Stewart, J. D. *J. Mol. Catal. B* **2002**, *17*, 101-105.

153. Sambrook, J; Fritsch, E. F.; Maniatis, T. *Molecular Cloning A Laboratory Manual*; Cold Spring Harbor: Cold Spring Harbor, 1989

154. Derbise, A.; Lesic, B.; Dacheux, D.; Ghigo, J. M.; Carniel, E. *FEMS Immunol. Med. Microbiol.* **2003**, *38*, 113-116.

155. Colibri, Institute Pasteur. Accessed on November 2006. http://genolist.pasteur.fr/Colibri

156. Viola, R. E.; Cook, P. F.; Cleland, W. W. *Anal. Biochem.* **1979**, *96*, 334-40.

157. Orr, G. A.; Blanchard, J. S. *Anal. Biochem.* **1984**, *142*, 232-4.

158. Esaki, N.; Shimoi, H.; Nakajima, N.; Ohshima, T.; Tanaka, H.; Soda, K. *J. Biol. Chem.* **1989**, *264*, 9750-2.

159. Jeong, S.-S.; Gready, J. E. *Anal. Biochem.* **1994**, *221*, 273-7.

160. Wolfrom, M. L.; Thompson, A. *Meth. Carbohydr. Chem.* **1963**, *2*, 65-8.

161. Koch, H. J.; Stuart, R. S. *Carbohydr. Res.* **1978**, *64*, 127-34.

162. Hatcher, J. T.; Wilcox, L. V. *Anal. Chem.* **1950**, *22*, 567-9.

163. Datsenko, K. A.; Wanner, B. L *Proc. Natl. Acad. Sci. U.S.A.* **2000**, *97*, 6640-6645.

164. Csonka, L. N.; Fraenkel, D. G. *J. Biol. Chem.* **1977**, *252*, 3382-91.

165. Sauer, U.; Canonaco, F.; Heri, S.; Perrenoud, A.; Fischer, E. *J. Biol. Chem.* **2004**, *279*, 6613-6619.

166. Canonaco, F.; Hess, T. A.; Heri, S.; Wang, T.; Szyperski, T.; Sauer, U. *FEMS Microbiol. Lett.* **2001**, *204*, 247-252.

167. Pionnier, S.; Robins, R. J.; Zhang, B.-L. *J. Agr. Food Chem.* **2003**, *51*, 2076-2082.

168. Aoshima, M.; Ishii, M.; Yamagishi, A.; Oshima, T.; Igarashi, Y. *Biotechnol. Bioeng.* **2003**, 84, 732-737.

169. Dauner, M.; Sauer, U. *Biotechnol. Prog*. **2000**, *16*, 642-649

170. Northrop, D. B. *Ann. Rev. Biochem.* **1981**, *50*, 103-31.

171. Arnold, L. J., Jr.; You, K.-S. *Methods Enzymol.* **1978**, *54*, 223-32.

172. Arnold, L. J., Jr.; You, K.-S.; Allison, W. S.; Kaplan, N. O. *Biochemistry* **1976**, *15*, 4844-9.

173. You, K.-S. CRC *Crit. Rev. Biochem*. **1985**, *17*, 313-451

174. Csonka, L. N.; Fraenkel, D. G. *J. Biol. Chem.* **1977**, *252*, 3382-91.

175. Parag Parekh Masters Thesis 2006, University of Florida

176. Csonka, L. N.; Fraenkel, D. G. *J. Biol. Chem.* **1977**, *252*, 3382-91.

177. Sauer, U.; Canonaco, F.; Heri, S.; Perrenoud, A.; Fischer, E. *J. Biol. Chem.* **2004**, *279*, 6613-6619.

178. Sauer, U.; Fischer, E. *J. Biol. Chem.* **2003**, *278*, 46446-46451.

179. Verho, R.; Londesborough, J.; Penttilae, M.; Richard, P. *Appl. Environ. Microbiol.* **2003**, *69*, 5892-5897.

180. Verho, R.; Richard, P.; Jonson, P. H.; Sundqvist, L.; Londesborough, J.; Penttilae, M. *Biochemistry* **2002**, *41*, 13833-13838.

181. Sprenger, G. A.; Hammer, B. A.; Johnson, E. A.; Lin, E. C. C. *J. Gen. Microbiol.* **1989**, *135*, 1255-62.

182. Tong, I. T.; Liao, H. H.; Cameron, D. C. *Appl. Environ. Microbiol.* **1991**, *57*, 3541-6.

183. Fisher, E. Syntheses in the Purine and Sugar Group. Accessed on November 2006. http://nobelprize.org/nobel_prizes/chemistry/laureates/1902/fischer-lecture.pdf

184. Filmore, D. *Mod. Drug Discov.* **2003**, *6*, 35-36, 38-39.

185. Federsel, H.-J. *Nature Rev. Drug Discov.* **2005**, *4*, 685-697.

186. Garcia-Urdiales, E.; Alfonso, I.; Gotor, V. *Chem. Rev.* **2005**, *105*, 313-354.

187. Schoemaker Hans, E.; Mink, D.; Wubbolts Marcel, G. *Science* **2003**, *299*, 1694-7.

188. Breuer, M.; Ditrich, K.; Habicher, T.; Hauer, B.; Kesseler, M.; Stuermer, R.; Zelinski, T. *Angew. Chem. Int. Ed.* **2004**, *43*, 788-824.

189. Lorenz, P.; Eck, J. *Nature Rev. Microbiol.* **2005**, *3*, 510-516.

190. Johanson, T.; Katz, M.; Gorwa-Grauslund, M. F. *FEMS Yeast Res.* **2005**, *5*, 513-525.

191. Stewart, J. D. *Curr. Opin. Biotech.* **2000**, *11*, 363-368.

192. Rodriguez, S.; Kayser, M.; Stewart, J. D. *Org. Lett.* **1999**, *1*, 1153-1155.

193. Rodriguez, S.; Kayser, M. M.; Stewart, J. D. *J. Am. Chem. Soc.* **2001**, *123*, 1547-1555.

194. Rodriguez, S.; Schroeder, K. T.; Kayser, M. M.; Stewart, J. D. *J. Org. Chem.* **2000**, *65*, 2586-2587.

195. Kaluzna, I. A.; Matsuda, T.; Sewell, A. K.; Stewart, J. D. *J. Am. Chem. Soc.* **2004**, *126*, 12827-12832.

196. Stewart, J.D., Rodriguez, S. Kayser, M.M.,Cloning, Structure and Activity of Ketone Reductases from Baker's Yeast. in *Enzyme Technology for Pharmaceutical and Biotechnological Applications,* H.A. Kirst, W.-K. Yeh and M.J. Zmijewski, Eds, Marcel Dekker: New York, 2001, pp 175-207.

197. Miya, H.; Kawada, M.; Sugiyama, Y. *Biosci., Biotech., Biochem.* **1996**, *60*, 95-8.

198. Misra, Kanika; Banerjee, Arun B.; Ray, Subhankar; Ray, Manju.Mol. Cell. Biochem. **1996**, *156,* 117-24.

199. Yum, D.-Y.; Lee, B.-Y.; Pan, J.-G. *Appl. Environ. Microbiol.* **1999**, *65*, 3341-3346.

200. Habrych, M.; Rodriguez, S.; Stewart, J. D. *Biotechnol. Progr.* **2002**, *18*, 257-261.

201. The EcoGene Database of Eschericia coli Sequence and Function. Accessed on November 2006. http://www.ecogene.org

202. Ko, J.; Kim, I.; Yoo, S.; Min, B.; Kim, K.; Park, C. *J. Bacteriol.* **2005**, *187*, 5782-5789.

203. Bacterial Targets IGS-CNRS. Accessed on November 2006. http://igs-server.cnrs-mrs.fr/Str_gen/

204. Jeudy, S.; Monchois, V.; Maza, C.; Claverie, J.-M.; Abergel, C. *Proteins: Structure, Function, and Bioinformatics* **2005**, *62*, 302-307.

205. Ellis, E. M. *FEMS Microbiol. Lett.* **2002**, *216*, 123-131.

206. Protein Data Bank. Accessed on November 2006. http://www.rcsb.org/pdb/Welcome.do;jsessionid=h+qtwqwGy+UQu0-VyP1ixw**

207. Obmolova, G.; Teplyakov, A.; Khil Pavel, P.; Howard Andrew, J.; Camerini-Otero, R. D.; Gilliland Gary, L. *Proteins* **2003**, *53*, 323-5.

208. Grant, A. W.; Steel, G.; Waugh, H.; Ellis, E. M. *FEMS Microbiol. Lett.* **2003**, *218*, 93-99.

209. Information Genomique et Stracturale, TCoffee. Accessed on November 2006. http://www.igs.cnrs-mrs.fr/Tcoffee/tcoffee_cgi/index.cgi

210. Datsenko, K. A.; Wanner, B. L *Proc. Natl. Acad. Sci. U.S.A.* **2000**, *97*, 6640-6645

211. Yu, D.; Ellis, H. M.; Lee, E. C.; Jenkins, N. A.; Copeland, N. G.; Court, D. L. *Proc. Natl. Acad. Sci. U.S.A* **2000**, *97*, 5978-5983.

212. Kitazume, T.; Nakayama, Y. *J. Org. Chem.* **1986**, *51*, 2795-9.

213. Kaluzna, I. A.; Dascier, D.; Stewart, J. D. Unpublished data

214. Theorell, H. The nature and mode of action of oxidation enzymes. Accessed on November 2006. http://nobelprize.org/nobel_prizes/medicine/laureates/1955/theorell-lecture.pdf.

215. Brown J. M. Hydrogenation of Functionalized Carbon-Carbon Double Bonds In *Comprehensive Asymmetric Catalysis Vol I*, Jacobsen E.N; Pfaltz, A. ; Yamamoto H., Eds. Speinger-Verlag, New York, 1999.

216. Dobbs, D. A.; Vanhessche, K. P. M.; Brazi, E.; Rautenstrauch, V.; Lenoir, J.; Genet, J.; Wiles, J.; Bergens, S. H. *Angew. Chem. Int. Ed. Engl*. **2000**, *39*, 1992-1995.

217. Ohta, T.; Miyake, T.; Seido, N.; Kumobayashi, H.; Takaya, H. *J. Org. Chem.* **1995**, *60*, 357-63.

218. Lipshutz, B. H.; Servesko, J. M. *Angew. Chem. Int. Ed. Engl*. **2003**, *42*, 4789-4792.

219. Lipshutz, Br. H.; Servesko, J. M.; Petersen, T. B.; Papa, P. P.; Lover, A. A. *Org. Lett.* **2004**, *6*, 1273-1275.

220. Matzinger P. K.; Leuenberger H. G. W. Enzyme-Catalyzed Hydrogenation, In *Stereoselective Synthesis* Vol 7, 1997, Houben J;Weyl T, Eds. Houben-weyl, 1997.

221. Faber K. Biotransformations in organic chemistry, 3rd ed.; Springer-Verlag, 1997.

222. Servi S. Stereoselective Synthesis of Chiral Compounds Using Whole-cell Biocatalysts In *Stereoselective Biocatalysis* Patel R. N. Ed.; Marcel Dekker, 1999.

223. Santaniello, E.; Manzocchi, A. *Trends Org. Chem.* **2000**, *8*, 21-34.

224. D'Arrigo, P.; Pedrocchi-Fantoni, G.; Servi, S. *Adv. Appl. Microbiol.* **1997**, *44*, 81-123.

225. Csuk, R.; Glaenzer, B. I. *Chem. Rev.* **1991**, *91*, 49-97.

226. Servi, S. *Synthesis* **1990**, 1-25.

227. Gramatica, P.; Manitto, P.; Monti, D.; Speranza, G., *Tetrahedron* **1987**, *43*, 4481-6.

228. Leuenberger, H. G. W.; Boguth, W.; Barner, R.; Schmid, M.; Zell, *Helv. Chim. Acta* **1979**, *62*, 455-63.

229. Fuganti, C.; Grasselli, P. *Chem. Ind*. **1977**, *24*, 983.

230. Fuganti, C.; Grasselli, P.; Servi, S. *Perkin Trans. 1* **1983**, 241-4.

231. Gramatica, P.; Giardina, G.; Speranza, G.; Manitto, P. *Chem. Lett.* **1985**, *9*, 1395-8.

232. D'Arrigo, P.; Fuganti, C.; Fantoni, G. P.; Servi, S. *Tetrahedron* **1998**, *54*, 15017-15026.

233. Gramatica, P.; Manitto, P.; Monti, D.; Speranza, G. *Tetrahedron* **1988**, *44*, 1299-304.

234. Ferraboschi, P.; Casati, S.; Santaniello, E. *Tetrahedron: Asymmetry* **1994**, *5*, 19-20.

235. Ferraboschi, P.; Grisenti, P.; Casati, R.; Fiecchi, A.; Santaniello, E. *Perkin Trans. 1* **1987**, 1743-8.

236. Utaka, M.; Konishi, S.; Mizuoka, A.; Ohkubo, T.; Sakai, T.; Tsuboi, S.; Takeda, A. *J. Org. Chem.* **1989**, *54*, 4989-92.

237. Utaka, M.; Konishi, S.; Okubo, T.; Tsuboi, S.; Takeda, A. *Tetrahedron Lett.* **1987**, *28*, 1447-50.

238. Fuganti, C.; Pedrocchi-Fantoni, G.; Sarra, A.; Servi, S. *Tetrahedron: Asymmetry* **1994**, *5*, 1135-8.

239. Ohta, H.; Ozaki, K.; Tsuchihashi, G. *Chem. Lett.* **1987**, 191-2.

240. Kawai, Y.; Inaba, Y.; Tokitoh, N. *Tetrahedron: Asymmetry* **2001**, *12*, 309-318.

241. McAnda, A. F.; Roberts, K. D.; Smallridge, A. J.; Ten, A.; Trewhella, M. A. *Perkin Trans. 1* **1998**, 501-504.

242. Serra, S.; Fuganti, C.; Brenna, E. *Trends Biotechnol.* **2005**, *23*, 193-198.

243. Kosjek, B.; Stampfer, W.; Van Deursen, R.; Faber, K.; Kroutil, W. *Tetrahedron* **2003**, *59*, 9517-9521.

244. Fronza, G.; Fuganti, C.; Mendozza, M.; Rallo, R. S.; Ottolina, G.; Joulain, D. *Tetrahedron* **1996**, *52*, 4041-52.

245. Fronza, G.; Fuganti, C.; Mendozza, M.; Rigoni, R.; Servi, S.; Zucchi, G. *Pure Appl. Chem.* **1996**, *68*, 2065-2071.

246. Koul, S.; Crout, D. H. G.; Errington, W.; Tax, J. *Perkin Trans. 1* **1995**, 2969-88.

247. Jui J., *Adv. Biochem. Eng.* **1980**, *17*, 37

248. Gramatica, P.; Manitto, P.; Poli, L *J. Org. Chem.* **1985**, *50*, 4625-8

249. Fischer F.G.; Weidemann, O. *Leibigs Ann. Chem.* **1935**, *520*, 52-70

250. Buque-Taboada, E. M.; Straathof, A. J. J.; Heijnen, J. J.; Van Der Wielen, L. A. M. *Biotechnol. Bioeng.* **2004**, *86*, 795-800.

251. Pillai, U. R.; Sahle-Demessie, E. *Ind. Eng. Chem. Res.* **2003**, *42*, 6688-6696.

252. Brunner, H.; Fisch, K. *J. Organomet. Chem.* **1993**, *456*, 71-5.

253. von Arx, M.; Mallat, T.; Baiker, A. *J. Mol. Catal. Chem.* **1999**, *148*, 275-283.

254. Cheetham, P. S. J. *Adv. Biochem. Eng. Biotechnol.* **2004**, *86*, 83-158.

255. El-Sharkawy, S. H.; Abul-Hajj, Y. J. *J. Org. Chem.* **1988**, *53*, 515-19.

256. Kergomard, A.; Renard, M. F.; Veschambre, H. *J. Org. Chem.* **1982**, *47*, 792-8.

257. Fauve, A.; Renard, M. F.; Veschambre, H. *J. Org. Chem.* **1987**, *52*, 4893-7.

258. Matsumoto, K.; Kawabata, Y.; Takahashi, J.; Fujita, Y.; Hatanaka, M. *Chem. Lett.* **1998**, 283-284.

259. Sato, Y.; Oda, T.; Saito, H. *Chem. Comm.* **1977**, 415-17.

260. Arnone, A.; Cardillo, R.; Nasini, G.; Vajna de Pava, O. *Perkin Trans. 1* **1990**, 3061-3.

261. Hirata, T.; Takarada, A.; Matsushima, A.; Kondo, Y.; Hamada, H. *Tetrahedron: Asymmetry* **2004**, *15*, 15-16.

262. Shimoda, K.; Kubota, N.; Hamada, H.; Yamane, S.-y.; Hirata, T. *Bull. Chem. Soc. Jpn.* **2004**, *77*, 2269-2272.

263. Hamada, H.; Miyamoto, Y.; Ishihara, K.; Nakajima, N.; Hamada, H. *Plant Biotechnol.* **2002**, *19*, 203-205.

264. Shimoda, K.; Kubota, N.; Hamada, H.; Kaji, M.; Hirata, T. *Tetrahedron: Asymmetry* **2004**, *15*, 1677-1679.

265. Bader, J.; Guenther, H.; Rambeck, B.; Simon, H. *Hoppe-Seyler's Zeitschrift fuer Physiologische Chemie* **1978**, *359*, 19-27.

266. Simon, H.; Rambeck, B.; Hashimoto, H.; Guenther, H.; Nohynek, G.; Neumann, H. *Angew. Chem.* **1974**, *86*, 675.

267. Simon, H.; Bader, J.; Guenther, H.; Neumann, S.; Thanos, J. *Angew. Chem.* **1985**, *97*, 541-55.

268. Simon, H. *Pure Apll. Chem.* **1992**, *64*, 1181-1186

269. Thanos, I. C. G.; Simon, H. *J. Biotechnol.* **1987**, *6*, 13-29.

270. Thanos, I.; Bader, J.; Guenther, H.; Neumann, S.; Krauss, F.; Simon, H. *Methods. Enzymol.* **1987**, *136*, 302-17.

271. Warburg, O. ; Christian, W. *Naturwissenschaften* **1932**, 20, 688

272. Williams, R. E.; Bruce, N. C. *Microbiology* **2002**, 148, 1607-1614.

273. Trotter, E. W.; Collinson, E. J.; Dawes, I. W.; Grant, C. M. *Appl. Environ. Microbiol.* **2006**, *72*, 4885-4892.

274. Haarer, B. K.; Amberg, D. C. *Mol. Biol. Cell* **2004**, *15*, 4522-4531.

275. Saito, K.; Thiele, D. J.; Davio, M.; Lockridge, O.; Massey, V. *J. Biol. Chem.* **1991**, *266*, 20720-4.

276. Massey, V. *Biochem. Soc. Trans.* **2000**, *28*, 283-296.

277. Massey, V.; Schopfer, L. M. *J. Biol. Chem.* **1986**, *261*, 1215-22.

278. Schopfer, L. M.; Massey, V. Old yellow enzyme. In *A Study of Enzymes*, Kuby, S. A., CRC Press, Cleveland, Ohio,1991.

279. Matthews, R. G.; Massey, V.; Sweeley, C. C. *J. Biol. Chem.* **1975**, *250*, 9294-8.

280. Abramovitz, A. S.; Massey, V. *J. Biol. Chem.* **1976**, *251*, 5321-6.

281. Abramovitz, A. S.; Massey, V. *J. Biol. Chem.* **1976**, *251*, 5327-36.

282. Matthews, R. G.; Massey, V. *J. Biol. Chem.* **1969**, *244*, 1779-86.

283. Stott, K.; Saito, K.; Thiele, D. J.; Massey, V. *J. Biol. Chem.* **1993**, *268*, 6097-106

284. Kohli, R. M.; Massey, V. *J. Biol. Chem.* **1998**, *273*, 32763-32770.

285. Xu, D.; Kohli, R. M.; Massey, V. *Proc. Natl. Acad. Sci. U.S.A.* **1999**, *96*, 3556-3561.

286. Brown, B. J.; Hyun, J.; Duvvuri, S.; Karplus, P. A.; Massey, V. *J. Biol. Chem.* **2002**, *277*, 2138-2145.

287. Vaz, A. D. N.; Chakraborty, S.; Massey, V. *Biochemistry* **1995**, 34, 4246-56.

288. Swiderska, M. A.; Stewart, J. D. *J. Mol. Catal. B* **2006**, *42*, 52-54.

289. Karplus, P. A.; Fox, K. M.; Massey, V. *FASEB J.* **1995**, *9*, 1518-26.

290. Fox, K. M.; Karplus, P. A. *Structure* **1994**, *2*, 1089-105.

291. PyMOL, DeLano Scientific, LLC. Accessed on November 2006. www.pymol.org

292. Barna, T. M.; Khan, H.; Bruce, N. C.; Barsukov, I.; Scrutton, N. S.; Moody, P. C. E. *J. Mol. Biol.* **2001**, *310*, 433-447.

293. Murthy, Y. V. S. N.; Meah, Y.; Massey, V. *J. Am. Chem. Soc.* **1999**, *121*, 5344-5345.

294. Murthy, Y. V. S. N.; Massey, V. *J. Biol. Chem.* **1998**, *273*, 8975-8982.

295. Stewart, R. C.; Massey, V. *J. Biol. Chem.* **1985**, *260*, 13639-47.

296. Murthy, Y. V. S. N.; Massey, V. *Methods. Enzymol.* **1997**, *280*, 436-460.

297. Meah, Y.; Massey, V. *Proc. Natl. Acad. Sci. U.S.A.* **2000**, *97*, 10733-10738.

298. Meah, Y.; Brown, B. J.; Chakraborty, S.; Massey, V. *Proc. Natl. Acad. Sci. U.S.A.* **2001**, *98*, 8560-8565.

299. Niino, Y. S.; Chakraborty, S.; Brown, B. J.; Massey, V. *J. Biol. Chem.* **1995**, *270*, 1983-91.

300. Kataoka, M.; Kotaka, A.; Hasegawa, A.; Wada, M.; Yoshizumi, A.; Nakamori, S.; Shimizu, S. *Biosci. Biotechnol. Biochem.* **2002**, *66*, 2651-2657.

301. Madani, N. D.; Malloy, P. J.; Rodriguez-Pombo, P.; Krishnan, A. V.; Feldman, D. *Proc. Natl. Acad. Sci. U.S.A.* **1994**, *91*, 922-6.

302. Buckman, J.; Miller, S. M. *Biochemistry* **1998**, *37*, 14326-14336.

303. Komduur, J. A.; Leao, A. N.; Monastyrska, I.; Veenhuis, M.; Kiel, J. A. K. W. *Curr. Genet.* **2002**, *41*, 401-406.

304. Miura, K.; Tomioka, Y.; Suzuki, H.; Yonezawa, M.; Hishinuma, T.; Mizugaki, M. *Biol. Pharmaceut. Bull.* **1997**, *20*, 110-112.

305. Mizugaki, M.; Unuma, T.; Yamanaka, H. *Chem. Pharmaceut. Bull.* **1979**, *27*, 2334-7.

306. Mizugaki, M.; Nakazawa, M.; Yamamoto, H.; Yamanaka, H. *J. Biochem.* **1989**, *105*, 782-4.

307. Wada, M.; Yoshizumi, A.; Noda, Y.; Kataoka, M.; Shimizu, S.; Takagi, H.; Nakamori, S. *Appl. Environ. Microbiol.* **2003**, *69*, 933-937.

308. Kataoka, M.; Kotaka, A.; Thiwthong, R.; Wada, M.; Nakamori, S.; Shimizu, S. *J. Biotechnol.* **2004**, *114*, 1-9.

309. Mergler, M.; Wolf, K.; Zimmermann, M. *Appl. Microbiol. Biotechnol.* **2004**, *63*, 418-421.

310. Adachi, O.; Matsushita, K.; Shinagawa, E.; Ameyama, M. *J. Biochem.* **1979**, *86*, 699-709.

311. French, C. E.; Bruce, N. C. *Biochem. J.* **1994**, *301*, 97-103.

312. French, C. E.; Bruce, N. C. *Biochem. J.* **1995**, *312*, 671-8.

313. Boonstra, B.; Rathbone, D. A.; Bruce, N. C. *Biomol. Eng.* **2001**, *18*, 41-7.

314. Ramos, J. L.; Gonzalez-Perez, M. M.; Caballero, A.; van Dillewijn, P. *Curr. Opin. Biotechnol.* **2005**, *16*, 275-281.

315. Stenuit, B.; Eyers, L.; El Fantroussi, S.; Agathos, S. N. *Environ. Sci. Biotechnol.* **2005**, *4*, 39-60.

316. French, C. E.; Rosser, S. J.; Davies, G. J.; Nicklin, S.; Bruce, N. C. *Nature biotechnol.* **1999**, *17*, 491-4.

317. French, C. E.; Nicklin, S.; Bruce, N. C. *Appl. Environ. Microbiol.* **1998**, *64*, 2864-2868.

318. Messiha H. L.; Bruce N. C.; Sattelle B. M.; Sutcliffe M. J.; Munro A., W.; Scrutton N., S. *J. Biol. Chem.* **2005**, *280*, 27103-10.

319. Moody, P. C. E.; Shikotra, N.; French, C. E.; Bruce, N. C.; Scrutton, N. S. *Acta Crystallogr. Section D* **1998**, *D54*, 675-677.

320. Barna, T.; Messiha, H. L.; Petosa, C.; Bruce, N. C.; Scrutton, N. S.; Moody, P. C. E. *J. Biol. Chem.* **2002**, *277*, 30976-30983.

321. Blehert, D. S.; Knoke, K. L.; Fox, B. G.; Chambliss, G. H. *J. Bacteriol.* **1997**, *179*, 6912-6920.

322. Pak, J. W.; Knoke, K. L.; Noguera, D. R.; Fox, B. G.; Chambliss, G. H. *Appl. Environ. Microbiol.* **2000**, *66*, 4742-50.

323. Khan, H.; Harris, R. J.; Barna, T.; Craig, D. H.; Bruce, N. C.; Munro, A. W.; Moody, P. C. E.; Scrutton, N. S. *J. Biol. Chem.* **2002**, *277*, 21906-21912.

324. Blehert, D. S.; Fox, B. G.; Chambliss, G. H. *J. Bacteriol.* **1999**, *181*, 6254-6263.

325. Marshall, S. J.; Krause, D.; Blencowe, D. K.; White, G. F. *J. Bacteriol.* **2004**, *186*, 1802-1810.

326. French, C. E.; Nicklin, S.; Bruce, N. C. *J. Bacteriol.* **1996**, *178*, 6623-7.

327. Fitzpatrick, T. B.; Amrhein, N.; Macheroux, P. *J. Biol. Chem.* **2003**, *278*, 19891-19897.

328. Brige, A.; Van den Hemel, D.; Carpentier, W.; De Smet, L.; Van Beeumen, J. J. *Biochem. J.* **2006**, *394*, 335-344.

329. Williams, R. E.; Rathbone, D. A.; Scrutton, N. S.; Bruce, N. C. *Appl. Environ. Microbiol.* **2004**, *70*, 3566-3574.

330. Vick, B. A.; Zimmerman, D. C. *Plant Physiol.* **1986**, *80*, 202-5.

331. Schaller, F. *J. Exp. Bot.* **2001**, *52*, 11-23.

332. Schaller, F.; Weiler, E. W. *Eur. J. Biochem.* **1997**, *245*, 294-299.

333. Schaller, F.; Weiler, E. W. *J. Biol. Chem.* **1997**, *272*, 28066-28072.

334. Schaller, F.; Hennig, P.; Weiler, E. W. *Plant Physiol.* **1998**, *118*, 1345-1351.

335. Costa, C. L.; Arruda, P.; Benedetti, C. E. *Plant Mol. Biol.* **2000**, *44*, 61-71.

336. Schaller, F.; Biesgen, C.; Mussig, C.; Altmann, T.; Weiler, E. W. *Planta* **2000**, *210*, 979-984.

337. Sobajima, H.; Takeda, M.; Sugimori, M.; Kobashi, N.; Kiribuchi, K.; Cho, E.-M.; Akimoto, C.; Yamaguchi, T.; Minami, E.; Shibuya, N.; Schaller, F.; Weiler, E. W.; Yoshihara, T.; Nishida, H.; Nojiri, H.; Omori, T.; Nishiyama, M.; Yamane, H. *Planta* **2003**, *216*, 692-698.

338. Matsui, H.; Nakamura, G.; Ishiga, Y.; Toshima, H.; Inagaki, Y.; Toyoda, K.; Shiraishi, T.; Ichinose, Y. *Mol. Genet. Genom.* **2004**, *271*, 1-10.

339. Strassner, J.; Furholz, A.; Macheroux, P.; Amrhein, N.; Schaller, A. *J. Biol. Chem.* **1999**, *274*, 35067-35073.

340. Steinbacher, S.; Stumpf, M.; Weinkauf, S.; Rohdich, F.; Bacher, A.; Simon, H. Enoate Reductase in *Flavins and Flavoproteins* , Berlin, **2002**; p 941-949.

341. Caldeira, J.; Feicht, R.; White, H.; Teixeira, M.; Moura, J. J. G.; Simon, H.; Moura, I. *J. Biol. Chem.* **1996**, *271*, 18743-18748.

342. He, X.-Y.; Yang, S.-Y.; Schulz, H. *Eur. J. Biochem.* **1997**, *248*, 516-520.

343. Fillgrove, K. L.; Anderson, V. E. *Biochemistry* **2001**, *40*, 12412-12421.

344. Rohdich, F.; Wiese, A.; Feicht, R.; Simon, H.; Bacher, A. *J. Biol. Chem.* **2001**, *276*, 5779-5787.

345. Liang, X.; Thorpe, C.; Schulz, H. *Arch. Biochem. Biophys.* **2000**, *380*, 373-379.

346. Hashimoto, H.; Guenther, H.; Simon, H. *Hoppe-Seyler's Zeitschrift fuer Physiologische Chemie* **1975**, *356*, 1195-1201.

347. La Roche, H. J.; Kellner, M.; Guenther, H.; Simon, H. *Hoppe-Seyler's Zeitschrift fuer Physiologische Chemie* **1971**, *352*, 399-402.

348. Kuno, S.; Bacher, A.; Simon, H. *Biol. Chem. Hoppe-Seyler* **1985**, *366*, 463-72.

349. Buehler, M.; Simon, H. *Hoppe-Seyler's Zeitschrift fuer Physiologische Chemie* **1982**, *363*, 609-25.

350. Dickert, S.; Pierik, A. J.; Linder, D.; Buckel, W. *Eur. J. Biochem.* **2000**, *267*, 3874-84.

351. Thanos, I.; Deffner, A.; Simon, H. *Biol. Chem. Hoppe-Seyler* **1988**, *369*, 451-60.

352. Bader, J.; Simon, H. *Arch. Microbiol.* **1980**, *127*, 279-87.

353. Tischer, W.; Bader, J.; Simon, H. *Eur. J. Biochem.* **1979**, *97*, 103-12.

354. Messiha, H. L.; Bruce, N. C.; Sattelle, B. M.; Sutcliffe, M. J.; Munro, A. W.; Scrutton, N. S. *J. Biol. Chem.* **2005**, *280*, 27103-27110.

355. Khan, H.; Barna, T.; Bruce, N. C.; Munro, A. W.; Leys, D.; Scrutton, N. S. *FEBS Journal* **2005**, *272*, 4660-4671.

356. Brown, B. J.; Deng, Z.; Karplus, P. A.; Massey, V. *J. Biol. Chem.* **1998**, *273*, 32753-32762.

357. Xu, D.; Kohli, R. M.; Massey, V. *Proc. Natl. Acad. Sci. U.S.A.* **1999**, *96*, 3556-3561.

358. Khan, H.; Barna, T.; Harris, R. J.; Bruce, N. C.; Barsukov, I.; Munro, A. W.; Moody, P. C. E.; Scrutton, N. S. *J. Biol. Chem.* **2004**, *279*, 30563-30572.

359. Kitzing, K.; Fitzpatrick, T. B.; Wilken, C.; Sawa, J.; Bourenkov, G. P.; Macheroux, P.; Clausen, T. *J. Biol. Chem.* **2005**, *280*, 27904-27913.

360. Fitzpatrick Teresa, B.; Auweter, S.; Kitzing, K.; Clausen, T.; Amrhein, N.; Macheroux, P. *Protein Expr. Purif.* **2004**, *36*, 280-91.

361. Breithaupt, C.; Strassner, J.; Breitinger, U.; Huber, R.; Macheroux, P.; Schaller, A.; Clausen, T. *Structure* **2001**, *9*, 419-429.

362. Fox Brian, G.; Malone Thomas, E.; Johnson Kenneth, A.; Madson Stacey, E.; Aceti, D.; Bingman Craig, A.; Blommel Paul, G.; Buchan, B.; Burns, B.; Cao, J.; Cornilescu, C.; Doreleijers, J.; Ellefson, J.; Frederick, R.; Geetha, H.; Hruby, D.; Jeon Won, B.; Kimball, T.; Kunert, J.; Markley John, L.; Newman, C.; Olson, A.; Peterson Francis, C.; Phillips George, N., Jr.; Primm, J.; Ramirez, B.; Rosenberg Nathan, S.; Runnels, M.; Seder, K.; Shaw, J.; Smith David, W.; Sreenath, H.; Song, J.; Sussman Michael, R.; Thao, S.; Troestler, D.; Tyler, E.; Tyler, R.; Ulrich, E.; Vinarov, D.; Vojtik, F.; Volkman Brian, F.; Wesenberg, G.; Wrobel Russell, L.; Zhang, J.; Zhao, Q.; Zolnai, Z. *Proteins* **2005**, *61*, 206-8.

363. Malone, T. E.; Madson, S. E.; Wrobel, R. L.; Jeon, W. B.; Rosenberg, N. S.; Johnson, K. A.; Bingman, C. A.; Smith, D. W.; Phillips, G. N., Jr.; Markley, J. L.; Fox, B. G. *Proteins* **2004**, *58*, 243-245.

364. Breithaupt, C.; Kurzbauer, R.; Lilie H.; Schaller, A.; Strassner, J.; Huber, R.; Macheroux, P.; Clausen T. *Proc. Natl. Acad. Sci. U.S.A.* **2006**, *103,* ;14337-14342

365. van den Hemel, D.; Brige, A.; Savvides, S. N.; Van Beeumen, J. *J. Biol. Chem.* **2006**, *281*, 28152-28161.

366. Hubbard, P. A.; Liang, X.; Schulz, H.; Kim, J.-J. P. *J. Biol. Chem.* **2003**, *278*, 37553-37560.

367. Nordling, E.; Jornvall, H.; Persson, B. *Eur. J. Biochem.* **2002**, *269*, 4267-4276.

368. Riveros-Rosas, H.; Julian-Sanchez, A.; Villalobos-Molina, R.; Pardo Juan, P.; Pina, E. *Eur. J. Biochem.* **2003**, *270*, 3309-34.

369. Hori, T.; Yokomizo, T.; Ago, H.; Sugahara, M.; Ueno, G.; Yamamoto, M.; Kumasaka, T.; Shimizu, T.; Miyano, M. *J. Biol. Chem.* **2004**, *279*, 22615-22623.

370. Yokomizo, T.; Izumi, T.; Takahashi, T.; Kasama, T.; Kobayashi, Y.; Sato, F.; Taketani, Y.; Shimizu, T. *J. Biol. Chem.* **1993**, *268*, 18128-35.

371. Yokomizo, T.; Ogawa, Y.; Uozumi, N.; Kume, K.; Izumi, T.; Shimizu, T. *J. Biol. Chem.* **1996**, *271*, 2844-50.

372. Ensor, C. M.; Zhang, H.; Tai, H.-H. *Biochem. J.* **1998**, *330*, 103-108.

373. Hori, T.; Yokomizo, T.; Ago, H.; Sugahara, M.; Ueno, G.; Yamamoto, M.; Kumasaka, T.; Shimizu, T.; Miyano, M. *J. Biol. Chem.* **2004**, *279*, 22615-22623.

374. Thorn, J. M.; Barton, J. D.; Dixon, N. E.; Ollis, D. L.; Edwards, K. J. *J. Mol. Biol.* **1995**, *249*, 785-99.

375. Dick, R. A.; Kwak, M.-K.; Sutter, T. R.; Kensler, T. W. *J. Biol. Chem.* **2001**, *276*, 40803-40810.

376. Dick R., A.; Kensler Thomas, W. *J. Biol. Chem.* **2004**, *279*, 17269-77.

377. Dick, R. A.; Yu, X.; Kensler, T. W. *Clin. Cancer. Res.* **2004**, *10*, 1492-1499.

378. Gong, J.; Neels, J. F.; Yu, X.; Kensler, T. W.; Peterson, L. A.; Sturla, S. J. *J. Med. Chem.* **2006**, *49*, 2593-2599.

379. Mano, J. i.; Babiychuk, E.; Belles-Boix, E.; Hiratake, J.; Kimura, A.; Inze, D.; Kushnir, S.; Asada, K. *Eur. J. Biochem.* **2000**, *267*, 3661-3671.

380. Hambraeus, G.; Nyberg, N. *J. Agr. Food Chem.* **2005**, *53*, 8714-8721.

381. Mano, J. i.; Torii, Y.; Hayashi, S.-i.; Takimoto, K.; Matsui, K.; Nakamura, K.; Inze, D.; Babiychuk, E.; Kushnir, S.; Asada, K. *Plant Cell Physiol.* **2002**, *43*, 1445-1455.

382. Ringer, K. L.; McConkey, M. E.; Davis, E. M.; Rushing, G. W.; Croteau, R. *Arch. Biochem. Biophys.* **2003**, *418*, 80-92.

383. Raab, T.; Lopez-Raez, J. A.; Klein, D.; Caballero, J. L.; Moyano, E.; Schwab, W.; Munoz-Blanco, J. *Plant Cell* **2006**, *18*, 1023-1037.

384. Kurata, A.; Kurihara, T.; Kamachi, H.; Esaki, N. *J. Biol. Chem.* **2005**, *280*, 20286-20291.

385. Raab, T.; Lopez-Raez, J. A.; Klein, D.; Caballero, J. L.; Moyano, E.; Schwab, W.; Munoz-Blanco, J. *Plant Cell* **2006**, *18*, 1023-1037.

386. Edwards, K. J.; Barton, J. D.; Rossjohn, J.; Thorn, J. M.; Taylor, G. L.; Ollis, D. L. *Arch. Biochem Biophys.* **1996**, *328*, 173-83.

387. Yamamoto, T.; Yokomizo, T.; Nakao, A.; Izumi, T.; Shimizu, T. *Eur. J. Biochem.* **2001**, *268*, 6105-6113.

388. Doorn, J. A.; Maser, E.; Blum, A.; Claffey, D. J.; Petersen, D. R. *Biochemistry* **2004**, *43*, 13106-13114.

389. Forrest, G. L.; Gonzalez, B. *Chemico-Biological Interactions* **2000**, *129*, 21-40.

390. Joernvall, H.; Persson, B.; Krook, M.; Atrian, S.; Gonzalez-Duarte, R.; Jeffery, J.; Ghosh, D. *Biochemistry* **1995**, *34*, 6003-13.

391. Tanaka, N.; Nonaka, T.; Nakamura, K. T.; Hara, A. *Curr. Org. Chem.* **2001**, *5*, 89-111.

392. Ghosh, D.; Sawicki, M.; Pletnev, V.; Erman, M.; Ohno, S.; Nakajin, S.; Duax, W. L. *J. Biol. Chem.* **2001**, *276*, 18457-18463.

393. Wanner, P.; Tressl, R. *Eur. J. Biochem.* **1998**, *255*, 271-278.

394. Hirata, T.; Shimoda, K.; Gondai, T. *Chem. Lett.* **2000**, 850-851.

395. Shimoda, K.; Izumi, S.; Hirata, T. *Bull. Chem. Soc. Jpn.* **2002**, *75*, 813-816.

396. Kawai, Y.; Hayashi, M.; Inaba, Y.; Saitou, K.; Ohno, A. *Tetrahedron Lett.* **1998**, *39*, 5225-5228.

397. Kawai, Y.; Inaba, Y.; Hayashi, M.; Tokitoh, N. *Tetrahedron Lett.* **2001**, *42*, 3367-3368.

398. Shimoda, K.; Ito, D. I.; Izumi, S.; Hirata, T. *Perkin Trans. 1* **1996**, 355-8.

399. Hirata, T.; Tang, Y.; Okano, K.; Suga, T. *Phytochemistry* **1989**, *28*, 3331-3.

400. Shimoda, K.; Ito, D. I.; Izumi, S.; Hirata, T. *Perkin Trans. 1* **1996**, 355-8.

401. Shimoda, K.; Hirata, T. *J. Mol. Catal. B* **2000**, *8*, 255-264.

402. Zaadz, Inc. Accessed on November 2006. http://quotes.zaadz.com/Confucius?page=16

403. Leresche, J. E.; Meyer, H.-P. *Org. Process Res. Dev.* **2006**, *10*, 572-580.

404. Kaur, J.; Sharma, R. *Crit. Rev. Biotech.* **2006**, *26*, 165-199.

405. Bornscheuer, U. T. *Adv. Biochem. Engin. Biotechn.* **2005**, *100*, 181-203.

406. Bali, S.; O'Hare Helen, M.; Weissman Kira, J. *Chembiochem* **2006**, *7*, 478-84.

407. van Loo, B.; Kingma, J.; Arand, M.; Wubbolts, M. G.; Janssen, D. B. *Appl. Environ. Microbiol.* **2006**, *72*, 2905-2917.

408. Bonsor, D.; Butz, S. F.; Solomons, J.; Grant, S.; Fairlamb, I. J. S.; Fogg, M. J.; Grogan, G. *Org. Biomol. Chem.* **2006**, *4*, 1252-1260.

409. Kaluzna, I. A.; Matsuda, T.; Sewell, A. K.; Stewart, J. D. *J. Am. Chem. Soc.* **2004**, *126*, 12827-12832.

410. Martzen, M. R.; McCraith, S. M.; Spinelli, S. L.; Torres, F. M.; Fields, S.; Grayhack, E. J.; Phizicky, E. M. *Science* **1999**, *286*, 1153-1155

411. Phizicky, E. M.; Grayhack, E. J. *Crit. Rev. Biochem. Mol. Biol.* **2006**, *41*, 315-327.

412. Kuznetsova, E.; Proudfoot, M.; Sanders, S. A.; Reinking, J.; Savchenko, A.; Arrowsmith, C. H.; Edwards, A. M.; Yakunin, A. F. *FEMS Microbiol. Rev.* **2005**, *29*, 263-279.

413. Hudson, J. R., Jr.; Dawson, E. P.; Rushing, K., L.; Jackson, C. H.; Lockshon, D.; Conover, D.; Lanciault, C.; Harris, J. R.; Simmons, S. J.; Rothstein, R.; Fields, S. *Genome Res.* **1997**, *7*, 1169-1173.

414. Parrish, J. R.; Limjindaporn, T.; Hines, J. A.; Liu, J.; Liu, G.; Finley, R. L., Jr. *J. Proteome Res.* **2004**, *3*, 582-586.

415. Lu, Q. *Trends Biotech.* **2005**, *23*, 199-207.

416. Lammli, U. K. *Nature*, **1970**, 227, 680-685

417. Bradford M. M *Anal. Biochem.* **1976**, *72*, 248-254

418. Sambrook, J; Fritsch, E. F.; Maniatis, T. *Molecular Cloning A Laboratory Manual*; Cold Spring Harbor: Cold Spring Harbor, 1989

419. Birren B; Green E. D.; Klapholz S,; Myers R. M, Roskams J. *Analyzing DNA: A Laboratory Manual : Genome Analysis*, Cold Spring Harbor Laboratory Press,1997

420. Gietz, R.D. and R.A. Woods. *Methods Enzymol*. **2002** *350*: 87-96.

421. Chong, B.-D.; Ji, Y.-I.; Oh, S.-S.; Yang, J.-D.; Baik, W.; Koo, S. *J. Org. Chem.* **1997**, *62*, 9323-9325.

422. Piancatelli, G.; Leonelli, F.; Do, N.; Ragan, J. *Org. Syntheses* **2006**, *83*, 18-23.

423. Kyte, B. G.; Rouviere, P.; Cheng, Q.; Stewart, J. D. *J. Org. Chem.* **2004**, *69*, 12-17.

424. McAnda, A. F.; Roberts, K. D.; Smallridge, A. J.; Ten, A.; Trewhella, M. A. *J. Chem. Soc. Perk. T 1***1998**, 501-504.

425. Yamamoto, H.; Kimoto, K. ; (Daicel Chemical Industries, Ltd., Japan).: US-6780976

426. Chen, C.-N.; Porubleva, L.; Shearer, G.; Svrakic, M.; Holden, L. G.; Dover, J. L.; Johnston, M.; Chitnis, P. R.; Kohl, D. H. *Yeast* **2003**, *20*, 545-554.

427. Krogan, N. J.; Cagney, G.; Yu, H.; Zhong, G.; Guo, X.; Ignatchenko, A.; Li, J.; Pu, S.; Datta, N.; Tikuisis, A. P.; Punna, T.; Peregrin-Alvarez, J. M.; Shales, M.; Zhang, X.; Davey, M.; Robinson, M. D.; Paccanaro, A.; Bray, J. E.; Sheung, A.; Beattie, B.; Richards, D. P.; Canadien, V.; Lalev, A.; Mena, F.; Wong, P.; Starostine, A.; Canete, M. M.; Vlasblom, J.; Wu, S.; Orsi, C.; Collins, S. R.; Chandran, S.; Haw, R.; Rilstone, J. J.; Gandi, K.; Thompson, N. J.; Musso, G.; St. Onge, P.; Ghanny, S.; Lam, M. H. Y.; Butland, G.; Altaf-Ul, A. M.; Kanaya, S.; Shilatifard, A.; O'Shea, E.; Weissman, J. S.; Ingles, C. J.; Hughes, T. R.; Parkinson, J.; Gerstein, M.; Wodak, S. J.; Emili, A.; Greenblatt, J. F. *Nature* **2006**, *440*, 637-643.

428. Ho, Y.; Gruhler, A.; Heilbut, A.; Bader Gary, D.; Moore, L.; Adams, S.-L.; Millar, A.; Taylor, P.; Bennett, K.; Boutilier, K.; Yang, L.; Wolting, C.; Donaldson, I.; Schandorff, S.; Shewnarane, J.; Vo, M.; Taggart, J.; Goudreault, M.; Muskat, B.; Alfarano, C.; Dewar, D.; Lin, Z.; Michalickova, K.; Willems Andrew, R.; Sassi, H.; Nielsen Peter, A.; Rasmussen Karina, J.; Andersen Jens, R.; Johansen Lene, E.; Hansen Lykke, H.; Jespersen, H.; Podtelejnikov, A.; Nielsen, E.; Crawford, J.; Poulsen, V.; Sorensen Birgitte, D.; Matthiesen, J.; Hendrickson Ronald, C.; Gleeson, F.; Pawson, T.; Moran Michael, F.; Durocher, D.; Mann, M.; Hogue Christopher, W. V.; Figeys, D.; Tyers, M. *Nature* **2002**, *415*, 180-3.

429. Ito, T.; Chiba, T.; Ozawa, R.; Yoshida, M.; Hattori, M.; Sakaki, Y *Proc. Natl. Acad. Sci. U.S.A.* **2001**, *98*, 4569-4574.

430. Shimoda, K.; Kubota, N.; Hamada, H.; Yamane, S.-y.; Hirata, T. *Bull. Chem. Soc. Japan* **2004**, *77*, 2269-2272.

431. Fronza, G.; Fuganti, C.; Pinciroli, M.; Serra, S. *Tetrahedron: Asymmetry* **2004**, *15*, 3073-3077.

432. Wolken, W. A. M.; ten Have, R.; van der Werf, M. J. *J. Agric. Food Chem.* **2000**, *48*, 5401-5405.

433. Mueller, A.; Hauer, B.; Rosche, B. *J. Mol. Catal. B* **2006**, *38*, 126-130.

BIOGRAPHICAL SKETCH

Despina Bougioukou was born in Athens, Greece, on May 26th, 1974. She received a 1998 BS and a 2001 MS from the University of Crete, Greece. In 2002 she started her doctoral studies at University of Florida, working for Dr J. Stewart. Her research interests are in the field of biocatalysis. She expects to earn her PhD by the end of 2006.